

Solomon I. Khmelnik

Gravitomagnetism:

Nature's Phenomenas, Experiments,
Mathematical Models

Israel

2017

Solomon I. Khmelnik

Gravitomagnetism: Nature's Phenomenas, Experiments, Mathematical Models

Copyright © 2017 by Solomon I. Khmelnik

All right reserved. No portion of this book may be reproduced or transmitted in any form or by any means, electronic or mechanical, without written permission of the author.

Published by "MiC" - Mathematics in Computer Comp.

BOX 15302, Bene-Ayish, Israel, 0060860

E-mail: solik@netvision.net.il

Printed in United States of America, Lulu Inc.,

ID 20912835

ISBN 978-1- 365-95647



Israel 2017

Annotation

Some large-scale natural phenomena and unexpected experiments are analyzed. It is proved that they can be explained by gravitomagnetism existence and significant gravitomagnetic forces. On the same basis it is proved that a generator using the gravitational conservative forces source energy for work performance can exist and this does not contradict the energy conservation law.

A new solution of Maxwell's equations for gravitomagnetism, used in order to create the various models of phenomena (sand-devil, sea current, rotary stream, funnel, water soliton, water and sand tsunami, turbulent flows, additional (non-Newtonian) forces of celestial bodies' interaction) is proposed.

A detailed proof for interested reader is given.

Experimental validations of the theory are considered.

Explanations of experiments that have not been justified until now are proposed.

Contents

- Chapter 1. Gravitomagnetism \ 5
- Chapter 2. Equations of a stationary gravitomagnetic field \ 24
- Chapter 3. On the possibility of using gravitational forces to perform work \ 32
- Chapter 4. Natural phenomena \ 37
 - 4.1. Dust Whirl \ 38
 - 4.1a. Clouds \ 50
 - 4.2. Water Soliton \ 54
 - 4.3. Whirlpool \ 59
 - 4.4. Saturn's Hexagon \ 71
 - 4.4a. Active field of honeycombs \ 86
 - 4.5. Funnel and jet from the pipe \ 96
 - 4.6. Sea currents \ 104
 - 4.7. Water and sand tsunami \ 115
 - 4.8. Additional forces of celestial bodies interaction (co-author Khmelnik M.I.) \ 126
 - 4.9. Turbulent flows \ 139
- Chapter 5. Experiments \ 149
 - 5.1. Samokhvalov's Experiments \ 150
 - 5.2. Aldo Costa's Gravity Motor \ 160
 - 5.3. Tolchin's Inertioid \ 182
 - 5.4. Unusual Fountain \ 195
 - 5.5. Taylor Vortex \ 198
 - 5.6. Ranque Effect \ 205
 - 5.7. Sound and Gravity \ 214
- Chapter 6. Experiment Projects \ 224
 - 6.1. Gravitomagnetic induction detection \ 225
 - 6.2. Gravitational Wheel \ 231
 - 6.3. Gravitational waves detection \ 242
 - 6.4. The theory of dowsing \ 246
 - 6.5. Projects of experiments, considered in previous chap \ 253

Chapter 1. Gravitomagnetism

Contents

- 1. Introduction \ 5
- 2. Certain Analogies and Consequences \ 8
 - 2.1. The Induction of Circular Mass Current \ 8
 - 2.2. Gravitational Excitation of Electric Current \ 8
 - 2.4. Induction of a Moving Body \ 10
 - 2.5. Gravitomagnetic law the Biot-Savart-Laplace \ 10
 - 2.6. Gravitomagnetic Ampere Force \ 10
 - 2.7. Density of Magnetic Wave Energy \ 11
 - 2.8. Induction of Current-carrying Conductor \ 12
- 3. Certain Experimental Estimates \ 12
- 4. More about the Lorentz forces \ 13
- 5. About gravity force propagation velocity \ 14
- Appendix 1. The Equations of Electro-magnetism and Gravitomagnetism \ 15
- Appendix 2. Some formulas in the CGS system \ 17
- Appendix 3. Transformation of a vector product \ 18
- Appendix 4. Interaction of moving electric charges and efficiency of Lorentz electromagnetic forces. \ 20
- Appendix 5. Gravitomagnetic interaction of moving masses and the efficiency of Lorentz gravitomagnetic forces. \ 20
- References \ 22

1. Introduction

There are widely known Maxwell's equations for the electromagnetic field in the form (1), suggested by Heaviside [1] (the formulas are given in Appendix 1). Heaviside is also the author of gravitation theory [2], in which the gravitational field is described by equations of similar form (3). Later it has been shown [3], that in a weak gravitational field at low velocity it is possible to derive from the basic equations of general relativity the gravitational analogs of the electromagnetic field (3).

“The idea of the similarity of the gravitation laws to the laws of electromagnetism was discussed by J.K. Maxwell, Brillouin, Bridgman, O. Heaviside, G. Bondi (1962), E. Braginsky and others. R. Forward (1961) derived gravitational relations, which are similar to Maxwell's

equations based on A. Einstein's general theory of relativity. J. Karstua (1969) derived the same system of the "gyrofield" equations based on the isomorphism of the electromagnetism and gravitation basic laws." [12]

Next, we will consider the gravitation equations presented by Maxwell's equations and call them the Maxwell's equations of gravitomagnetism or the MGM-equations. Below we consider the MGM-equations and Samokhvalov's experiments. It is noted that the effects observed in these experiments are so significant that in order to explain them within the framework of these Maxwell-like gravitational equations it is necessary to supplement these equations with a certain empirical coefficient, which can be called the gravitational permeability of the medium. It is further shown that with such an addition the results of the experiments are in good agreement with the equations of gravitation such modified. A rough estimate of this coefficient is given. Some results of these equations are considered, in particular, the gravitational excitation of electric current, the effect of gravitomagnetic induction on electric current, etc.

Some phenomena and experiments that can be explained with the help of these equations are considered in detail. Further, the solutions of the indicated equations are proposed explaining the observed phenomena and experiments. In other words, it is shown that there are solutions adequate to many phenomena and experiments. Therefore, one can assert for certain that the proposed theory describes the observed reality.

Thus, in the weak gravitation field of the Earth the Maxwell-like equations may be used for the description of gravitational interactions. It means that there exist gravitational waves having a gravitoelectrical component with intensity E_g and gravitomagnetic component with induction B_g . On a mass m , moving in a magnetic field with a velocity \mathbf{v} , gravitomagnetic Lorentz force (an analog of the known Lorentz force) is acting in form (GHS system)

$$F = \zeta \frac{m}{c} [\mathbf{v} \times B_g], \quad (1)$$

where ζ is a coefficient equal to 1 by Heaviside and equal to 2 by general relativity.

Samokhvalov [4-9] had conceived and carried out a series of unexpected and surprising experiments, which presumably can be explained by interaction of irregular mass currents. Irregular mass currents J_g create variable gravito-electrical intensity E_g and gravito-

magnetic induction B_g . At the interaction of this induction with the masses m , moving with speed v there arises gravito-magnetic Lorentz force. It is important to note that the effect are so significant, that in order to explain them within the said Maxwell-similar equations these equations should be supplemented by a certain empirical coefficient ξ . (similar to the coefficient of the magnetic permeability μ of the medium in electromagnetism). Further it is shown that with such modification the results of experiments are in good agreement with the modified gravitation equations. The value of the coefficient ξ from these experiments is determined for a reduced pressure. Its value at atmospheric pressure can be estimated very approximately.

Thus, based on the Samokhvalov's experiments the Maxwell-similar equations should be rewritten in the form

$$\operatorname{div} E_g = 4\pi G m, \quad (2)$$

$$\operatorname{div} B_g = 0, \quad (3)$$

$$\operatorname{rot} E_g = -\frac{1}{c} \frac{\partial B_g}{\partial t}, \quad (4)$$

$$\operatorname{rot} B_g = \frac{4\pi G \xi}{c} J_g + \frac{1}{c} \frac{\partial E_g}{\partial t}. \quad (5)$$

where the value of coefficient ξ will be determined below from the said experiments. This coefficient can be called the gravitational permeability of the medium.

Lorentz force for mass

$$F = m E_g + \zeta \frac{m}{c} [v \times B_g], \quad (6)$$

2. Certain Analogies and Consequences

Here we shall consider certain analogies between electrodynamics and gravito-electrodynamics, and some consequences of the above examined equations.

2.1. The Induction of Circular Mass Current

Magnetic flow Φ , passing through the area S of the coil with the length L , carrying alternated current J , in CGS system

$$\Phi = \frac{4\pi}{c} \cdot \frac{SJ}{L}. \quad (1)$$

The induction average for the area S is

$$B = \frac{4\pi J}{cL}. \quad (2)$$

If the coil is a ring of diameter R , then

$$B = \frac{2J}{cR}. \quad (3)$$

Let us assume now that the ring is carrying alternated mass current J_g .

Then, without considering the technical realization, by analogy with (1.5) we shall get

$$B_g = \frac{2G\xi J_g}{cR}. \quad (4)$$

Comparing these formulas, we find the gravimagnetic flow Φ_g passing through the area S of the ring in length L , along which the alternating mass current flows J_g :

$$\Phi_g = \frac{4\pi G\xi}{c} \cdot \frac{SJ_g}{L}. \quad (4a)$$

2.2. Gravitational Excitation of Electric Current

From (1.4) follows that gravitational moving force created by gravito-magnetic flow in the circuit of mass current is

$$\varepsilon_g = \frac{1}{c} \cdot \frac{d\Phi_g}{dt}. \quad (5)$$

The force of induced electric current in a closed-loop (in the CGS system) is:

$$J = \frac{1}{cR_e} \cdot \frac{d\Phi}{dt}, \quad (5a)$$

where R_e - the resistance to these electrons motion. This current in the metal is created by free electrons with the charge e_0 . By analogy, taking into account (5), we find that variable gravito-magnetic flow Φ_g also creates vortex induced mass current

$$J_g = \frac{\xi}{cR_m} \cdot \frac{d\Phi_g}{dt}, \quad (6)$$

where R_m is the resistance to mass particles motion. This current in the metal is created by free electrons of the mass m_e . Then $R_m = R_e$ - resistance to the electrons motion. In this case mass current J_g corresponds to electric current

$$J_{ge} = J_g \frac{e_o}{m_e}. \quad (7)$$

It is known that

$$m_e \approx 9.1 \cdot 10^{-34} \text{ г}, \quad e_o \approx 1.6 \cdot 10^{-19} \text{ Кл},$$

$$\eta = \frac{e_o}{m_e} \approx 1.8 \cdot 10^{14} \frac{\text{Кл}}{\text{г}}. \quad (8)$$

Thus, the strength of the induced current created by variable gravito-magnetic flow Φ_g is

$$J_{ge} = \frac{\eta}{cR_e} \cdot \frac{d\Phi_g}{dt}. \quad (9)$$

Similarly to (7), the mass current J corresponds to mass current

$$J_{gm} = J \frac{m_e}{e_o}. \quad (9a)$$

Thus, the strength of mass current created by variable magnetic flow Φ is

$$J_{gm} = \frac{1}{cR_e\eta} \cdot \frac{d\Phi}{dt}. \quad (9b)$$

2.4. Induction of a Moving Body

It is known that the induction of field in a medium with permeability μ , created by a charge q , moving with speed \bar{v} , in a certain point, is

$$\bar{B} = \mu q (\bar{v} \times \bar{r}) cr^3. \quad (16)$$

The vector \bar{r} is directed from the point, where the moving charge q_1 is located, to the referred point. Similarly, the gravito-magnetic induction of the field created by the mass m , moving with a speed \bar{v} , in a certain point, is

$$\overline{B}_g = \xi Gm(\overline{v} \times \overline{r}) cr^3, \quad (17)$$

Because, as shown in the Section 2.2, the electronic current is at the same time also the mass current, the gravito-magnetic induction can create the Lorentz force, affecting the electric current.

2.5. Gravitomagnetic law the Biot-Savart-Laplace

It is known that an electric current creates a magnetic flux density, determined by the Biot-Savart-Laplace law as

$$\overline{dB} = \frac{\mu \cdot J}{r^3 c} [\overline{dL} \times \overline{r}] \quad (18a)$$

where \overline{dL} - vector element conductor with current, \overline{r} - vector between it and the point where, it is determined of induction. This law is currently being considered as a consequence of Maxwell's equations. Therefore, it can be argued that a similar law for gravitomagnetic induction, generated of mass current. In this case, the Biot-Savart-Laplace law is written as follows:

$$\overline{dB}_g = \frac{\xi Gm}{r^3 c} [\overline{v} \times \overline{r}], \quad (18b)$$

where \overline{v} - the speed vector of the mass m .

2.6. Gravitomagnetic Ampere Force

It is known that a conductor carrying electric current \overline{J} in a magnetic field with induction \overline{B} is affected by Ampere force (per a length unit

$$\overline{F}_a = \frac{1}{c} (\overline{J} \times \overline{B}) \quad (19)$$

Similarly, a conductor carrying mass current \overline{J}_g in a gravito-magnetic field with induction \overline{B}_g is affected by Ampere force

$$\overline{F}_{ag} = \frac{\xi}{c} [\overline{J}_g \times \overline{B}_g], \quad (20)$$

Let us consider the case when mass current is a consequence of electric current, i.e. the particles carrying the charge form the mass current. Then

$$\overline{J}_g = J\eta_2, \quad (21)$$

$$\eta_2 = m/q, \quad (22)$$

where m , q – mass and charge of the particle. Then a conductor carrying electric current \bar{J} in a gravito-magnetic field with induction \bar{B}_g is affected by Ampere force

$$F_{age} = \frac{\zeta \eta_2}{c} [\bar{J} \times \bar{B}_g]. \quad (23)$$

For example, if the charged particle is an electron, then

$$m_e \approx 9.1 \cdot 10^{-34} \text{ r}, \quad e_o \approx 1.6 \cdot 10^{-19} \text{ Kl}, \quad (24)$$

$$\eta_2 = \frac{m_e}{e_o} \approx 0.6 \cdot 10^{-14} \frac{\text{g}}{\text{Kl}}.$$

But if the charged particle is an ion with mass $m = h \cdot m_e$, then

$$\eta_2 = \frac{h \cdot m_e}{e_o} \approx 0.6 h \cdot 10^{-14} \frac{\text{g}}{\text{Kl}}. \quad (25)$$

and for complex molecules $\eta_2 \Rightarrow 1$. So, at the interaction of gravito-magnetic induction with electrical current significant Ampere forces are likely to act.

2.7. Density of Magnetic Wave Energy

It is known that the density of electromagnetic wave energy [10], is

$$W = \frac{B^2}{8\pi} \left[\frac{\text{g}}{\text{cm} \cdot \text{sec}^2} \right] \quad (26)$$

By applying the derivation shown there for the equations (1.2-1.5) of gravito-electromagnetic wave, we find

$$W_g = \frac{B_g^2}{8\pi G}. \quad (27)$$

2.8. Induction of Current-carrying Conductor

It is known that the magnetic induction of infinite conductor carrying electric current is:

$$B = 2J / (cd), \quad (28)$$

where d - is the distance from the conductor to the point of measurement. Similarly, the gravito-magnetic induction of infinite conductor with mass current is

$$B_g = 2\xi G J_g / (cd). \quad (29)$$

3. Certain Experimental Estimates

The analysis of Samokhvalov's experiments [4-9], performed in Chapter 51, permits to obtain a crude estimate of the coefficient ξ of gravitational permeability. There it was shown that for vacuum

$$\xi \approx 10^{12}. \quad (30)$$

This value can be greatly understated, as the experiments were carried out at an average vacuum, but ξ increases with decreasing pressure. For atmospheric pressure $\xi \Rightarrow 0$, which explains the absence of visible effects of gravitational interaction of moving masses.

The gravitational permeability of the medium is now introduced into the equation for the gravitomagnetic induction rotor in the same way as the magnetic permeability of the medium is introduced into the equation for the magnetic induction rotor.

In order to discover the phenomenon of the decrease in the air gravitational permeability compared to vacuum gravitational permeability we should point out that the magnetic permeability of electrically conductive materials sharply decreases with increasing of current frequency which forms the magnetic field (due to the appearance of Foucault currents shielding the magnetic induction). It can be assumed that being influenced by alternating gravimagnetic field the moving air molecules behave similarly to free electrons in a conductor under the action of an alternating magnetic field – “Foucault mass currents” screening the gravimagnetic induction arise in the air. In this case, it can be assumed that at low velocity of mass motion the significant effects can be observed even in the atmosphere.

Further, it is shown that there are natural phenomena and experiments that do not have universally accepted explanations and mathematical models, but can be explained with the use of the equations considered above.

4. More about the Lorentz forces

The interaction between moving masses is described by gravitomagnetic Lorentz forces (hereinafter GL forces), analogous to the Lorentz forces in electrodynamics, acting between moving electric charges. It follows from (2.20) that the GL-force (its gravitomagnetic component) has the form

$$F_L = J \times B, \quad (1)$$

where, as follows from (2.4), the gravitomagnetic induction B_{GL} ,

$$B = G\xi H. \quad (2)$$

Here G is the gravitational constant, ξ is gravitomagnetic permeability of the medium.

Thus, the Lorentz forces (1, 2) act or

$$F_L = G\xi(\mathbf{J} \times \mathbf{H}). \quad (3)$$

or

$$F_L = G \cdot \xi \cdot S_o, \quad (4)$$

while

$$S_o = (\mathbf{J} \times \mathbf{H}). \quad (5)$$

This vector product is the density of the gravitomagnetic energy flux.

The Lorentz force and the gravitomagnetic induction are defined above in (1.6, 2.18c), respectively, in the form

$$F = \zeta \frac{m}{c} [\mathbf{v} \times B_g], \quad (6)$$

$$B_g = \frac{\xi G m}{r^3 c} [\mathbf{v} \times \mathbf{r}]. \quad (7)$$

Consequently, the Lorentz gravitomagnetic force, acting from the first body to the second,

$$F = \frac{\xi \zeta \cdot G m_1 m_2}{r^3 c^2} [\mathbf{v} \times \mathbf{v} \times \mathbf{r}]. \quad (8)$$

Chapter 3 shows that due to the GL-forces the gravitating body spends its energy to create and maintain mass currents. The analogy between Maxwell's equations for electrodynamics and MGM-equations proves the existence of a flow of S gravitational energy.

Further, some large-scale natural phenomena and unexpected experiments are analyzed. It is proved that they can be explained by the existence of gravitomagnetism and significant gravitomagnetic interaction forces. These gravitomagnetic forces are significant in a vacuum.

For the weak gravitational field of the Earth the MGM-equations can be used. As already noted, GL-forces are significant in vacuum. The moving molecules of a fluid flow are separated by vacuum. Therefore, their gravitomagnetic interaction forces can be significant and affect the nature of the flow.

5. About gravity force propagation velocity

Fedulaev's book [1] provides a calculation of the gravity force propagation velocity and a number of references to the works of well-known scientists (Lesage, Laplace, Poincare, van Flandern, Atsiukovsky) who had previously performed the same calculations. All of the

mentioned calculations are based on completely different methods, but their result is approximately the same: the velocity

$$\mathbf{g} = \boldsymbol{\beta} \cdot \mathbf{c}, \quad (1)$$

where \mathbf{c} - light velocity in vacuum, $\boldsymbol{\beta} \approx 10^{13}$. The author shows that the same result can be obtained directly from experiments on earth.

In electrodynamics, the Lorentz force acting on electric charge q moving in a magnetic field with \mathbf{B} induction was determined,

$$\mathbf{F} = \frac{q}{c} [\mathbf{v} \times \mathbf{B}], \quad (2)$$

The gravitomagnetic Lorentz force affecting m mass moving with \mathbf{v} velocity in gravitational field with gravitomagnetic induction \mathbf{B}_g , was determined above

$$\mathbf{F}_g = \xi \frac{m}{c} [\mathbf{v} \times \mathbf{B}_g], \quad (3)$$

where ξ - gravitational permeability. Section 3 shows that in vacuum

$$\xi \approx 10^{12}. \quad (3a)$$

Now let us derive (2) for medium as following

$$\mathbf{F} = c_e \frac{q}{\gamma} [\mathbf{v} \times \mathbf{B}], \quad (4)$$

where $\gamma = c^2$ - known coefficient, c_e - light velocity in some medium. By analogy (like in other cases when comparing the laws of gravitation to the laws of electromagnetism) we rederive (3) as following

$$\mathbf{F}_g = c_e \xi \frac{m}{\gamma} [\mathbf{v} \times \mathbf{B}_g] \quad (5)$$

or

$$\mathbf{F}_g = g_e \frac{m}{\gamma} [\mathbf{v} \times \mathbf{B}_g] \quad (6)$$

where

$$\mathbf{g}_e = c_e \xi. \quad (7)$$

Again, the value (7) is in the same way naturally considered as the velocity of gravity propagation in medium. We have obtained formula (1) from which we began. Consequently, we have obtained approximately the same result as the well-known scientists mentioned at the beginning (see (3a)). Thus, we can assume that this coincidence is yet another

confirmation of the estimate (3a) for the gravitational permeability value ξ .

Appendix 1. The Equations of Electro-magnetism and Gravito-magnetism

Further we shall use the following notations:

- q - electric charge $[\sqrt{\text{g} \cdot \text{cm}}]$;
- ρ - electric charge density $[\sqrt{\text{g} \cdot \text{cm}}/\text{cm}^3]$;
- J - electric current density $\left[\frac{1}{\text{cm} \cdot \text{sec}} \sqrt{\frac{\text{g}}{\text{cm}}}\right]$;
- c - speed of light in vacuum $c \approx 3 \cdot 10^{10}$ [cm/sec];
- E - electric field intensity $[\sqrt{\text{g} \cdot \text{cm}}/\text{sec}^2 = 3 \cdot 10^4 \text{ V/m}]$;
- B - magnetic induction $\left[\frac{1}{\text{sec}} \sqrt{\frac{\text{g}}{\text{cm}}} = \text{Gs}\right]$;
- \mathcal{E} - permittivity of the medium is equal to 1 for the vacuum in the CGS system;
- μ - permeability of the medium is equal to 1 for the vacuum in the CGS system;
- v - speed [cm/sec];
- F - force [dyn = g · cm/sec²];
- m - mass [g];
- ρ_g - mass density [g/cm³];
- J_g - mass current density [g/cm²sec];
- G - gravitational constant, $G \approx 7 \cdot 10^{-8} \left[\frac{\text{dyn} \cdot \text{cm}^2}{\text{g}^2} = \frac{\text{cm}^3}{\text{g} \cdot \text{sec}^2}\right]$;
- E_g - gravito-electric field intensity [cm/sec²];
- B_g - gravito-magnetic induction [cm/sec²];
- ξ - gravito-magnetic permeability of the medium.

The Maxwell equations for electromagnetism in CGS system are as follows [1]:

$$\text{div}E = 4\pi\rho, \quad (1)$$

$$\text{div}B = 0, \quad (2)$$

$$\text{rot}E = -\frac{1}{c} \frac{\partial B}{\partial t}, \quad (3)$$

$$\text{rot}B = \frac{4\pi \cdot \mu}{c} J + \frac{\varepsilon}{c} \frac{\partial E}{\partial t}. \quad (4)$$

The Lorentz force for the electric charge is

$$F = qE + \frac{q}{c} [v \times B]. \quad (5)$$

The Maxwell equations for gravito-electromagnetism in CGS system [3], supplemented by analogy with equations (1-4) permeability ξ , are as follows:

$$\text{div}E_g = 4\pi G\rho_g, \quad (6)$$

$$\text{div}B_g = 0, \quad (7)$$

$$\text{rot}E_g = -\frac{1}{c} \frac{\partial B_g}{\partial t}, \quad (8)$$

$$\text{rot}B_g = \frac{4\pi G\xi}{c} J_g + \frac{1}{c} \frac{\partial E_g}{\partial t}. \quad (9)$$

The Lorentz force for the mass is

$$F = mE_g + \zeta \frac{m}{c} [v \times B_g], \quad (10)$$

where ζ - is a coefficient equal to 1 by Heaviside and equal to 2 in general relativity theory.

Appendix 2. Some formulas in the CGS system

| Name | Electromagnetism | Gravitomagnetizm |
|---------------------|---|--|
| Maxwell's equations | $\text{div}E = 4\pi\rho/\varepsilon$ | $\text{div}E_g = 4\pi G\rho_g$ |
| | $\text{div}B = 0$ | $\text{div}B_g = 0$ |
| | $\text{rot}E = -\frac{1}{c} \frac{\partial B}{\partial t}$ | $\text{rot}E_g = -\frac{1}{c} \frac{\partial B_g}{\partial t}$ |
| | $\text{rot}B = \left(\begin{array}{c} \frac{4\pi \cdot \mu}{c} J \\ + \frac{\varepsilon}{c} \frac{\partial E}{\partial t} \end{array} \right)$ | $\text{rot}B_g = \left(\begin{array}{c} \frac{4\pi G\xi}{c} J_g \\ + \frac{1}{c} \frac{\partial E_g}{\partial t} \end{array} \right)$ |

| | | |
|---|---|---|
| Lorentz force | $F = qE + \frac{q}{c} [\mathbf{v} \times \mathbf{B}]$ | $F = mE_g + \zeta \frac{m}{c} [\mathbf{v} \times \mathbf{B}_g]$ |
| The magnetic Lorentz force, acting from the first body to the second | $F_{12} = \mu \frac{q_1 q_2}{r^3 c^2} \bullet [\bar{\mathbf{v}}_2 \times [\bar{\mathbf{v}}_1 \times \bar{\mathbf{r}}]]$ | $F_{12} = \zeta \xi G \frac{m_1 m_2}{r^3 c^2} \bullet [\bar{\mathbf{v}}_2 \times [\bar{\mathbf{v}}_1 \times \bar{\mathbf{r}}]]$ |
| Magnetic flow passing through the area of coil with a current (p.2.1) | $\Phi = \frac{4\pi\mu}{c} \cdot \frac{SJ}{L}$ | $\Phi_g = \frac{4\pi G \xi}{c} \cdot \frac{SJ_g}{L}$ |
| Induction of the ring current (p.2.1) | $B = \frac{2\mu J}{cR}$ | $B_g = \frac{2G \xi J_g}{cR}$ |
| The moving force (p.2.2) | $\varepsilon = \frac{1}{c} \cdot \frac{d\Phi}{dt}$ | $\varepsilon_g = \frac{1}{c} \cdot \frac{d\Phi_g}{dt}$ |
| The strength of the induced current (p.2.2) | $J = \frac{1}{cR_e} \cdot \frac{d\Phi}{dt}$ | $J_g = \frac{1}{cR_m} \cdot \frac{d\Phi_g}{dt}$ |
| Induction of a moving body (p.2.4) | $\bar{B} = \mu q (\bar{\mathbf{v}} \times \bar{\mathbf{r}}) cr^3$ | $\bar{B}_g = \xi Gm (\bar{\mathbf{v}} \times \bar{\mathbf{r}}) cr^3$ |
| Biot-Savart-Laplace law (p.2.5) | $\bar{d\mathbf{B}} = \frac{\mu \cdot J}{r^3 c} [\bar{d\mathbf{L}} \times \bar{\mathbf{r}}]$ | $\bar{d\mathbf{B}}_g = \frac{\xi Gm}{r^3 c} [\bar{\mathbf{v}} \times \bar{\mathbf{r}}]$ |
| Ampere Force (p.2.6) | $\bar{F}_a = \frac{1}{c} (\bar{\mathbf{J}} \times \bar{\mathbf{B}})$ | $F_{ag} = \frac{1}{c} [\bar{\mathbf{J}}_g \times \bar{\mathbf{B}}_g]$ |
| The energy density of a magnetic wave (p.2.7) | $W = \frac{B^2}{8\pi}$ | $W_g = \frac{B_g^2}{8\pi G}$ |
| Induction of current conductor (p.2.8) | $B = 2J / (cd)$ | $B_g = 2\xi GJ_g / (cd)$ |

Appendix 3. Transformation of a vector product.

Consider an expression with vectors of the form

$$\bar{\mathbf{f}} = (\bar{\mathbf{a}} \times (\bar{\mathbf{b}} \times \bar{\mathbf{r}})). \quad (1)$$

In the right-hand Cartesian coordinate system, this expression takes the form

$$\bar{f} = \begin{bmatrix} a_y (b_x r_y - b_y r_x) - a_z (b_z r_x - b_x r_z) \\ a_z (b_y r_z - b_z r_y) - a_x (b_x r_y - b_y r_x) \\ a_x (b_z r_x - b_x r_z) - a_y (b_y r_z - b_z r_y) \end{bmatrix}. \quad (2)$$

Suppose that the projections of these vectors on the z axis are zero. Then

$$\bar{f} = (b_x r_y - b_y r_x) \begin{bmatrix} a_y \\ -a_x \\ 0 \end{bmatrix}. \quad (2a)$$

Assume also that $r_y = 0$, i.e. $r = r_x$. Then

$$\bar{f} = r b_y \begin{bmatrix} -a_y \\ a_x \\ 0 \end{bmatrix}. \quad (3)$$

So, under the specified conditions

$$\bar{f}_{ab} = (\bar{a} \times (\bar{b} \times \bar{r})) = r b_y \begin{vmatrix} -a_y \\ a_x \end{vmatrix}. \quad (3a)$$

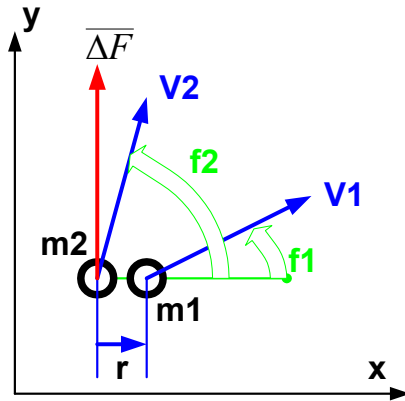


Fig. 1

Similarly,

$$\bar{f}_{ba} = (\bar{b} \times (\bar{a} \times (-r))) = -r a_y \begin{vmatrix} -b_y \\ b_x \end{vmatrix}.$$

We have

$$\overline{\Delta f} = \overline{f}_{ab} + \overline{f}_{ba} = r \left(\begin{array}{c} 0 \\ a_x b_y - a_y b_x \end{array} \right) \quad (4)$$

or

$$\overline{\Delta f}_y = r(a_x b_y - a_y b_x) = rab(\cos \varphi_a \sin \varphi_b - \sin \varphi_a \cos \varphi_b), \quad (5)$$

where φ_a , φ_b are the angles of the vectors a , b with the x axis Ox .

Thus, the vector $\overline{\Delta f}$ lies in the same plane as the initial vectors, is directed along the axis oy and has a value (see Fig. 1)

$$\Delta f = rab \sin(\varphi_b - \varphi_a). \quad (6)$$

Appendix 4. Interaction of moving electric charges and efficiency of Lorentz electromagnetic forces.

Let us consider two charges q_1 and q_2 moving with velocities v_1 and v_2 , respectively. The induction of the field created by the charge q_1 at the point where the charge q_2 is currently at (here and later the CGS system is used) is known [13] to be

$$\overline{B}_1 = q_1 (\overline{v}_1 \times \overline{r}) / cr^3. \quad (1)$$

The vector \overline{r} is directed from the point where the moving charge q_1 is.

The Lorentz force affecting the charge q_2 is

$$\overline{F}_{12} = q_2 (\overline{v}_2 \times \overline{B}_1) / c. \quad (2)$$

Similarly,

$$\overline{B}_2 = q_2 (\overline{v}_2 \times \overline{r}) / cr^3, \quad (3)$$

$$\overline{F}_{21} = q_1 (\overline{v}_1 \times \overline{B}_2) / c. \quad (4)$$

In the general case $\overline{F}_{12} \neq \overline{F}_{21}$, i.e. the third Newton's law is not observed as there are unbalanced forces acting on the charges q_1 and q_2 distorting the trajectories of these charges motion.

Let us consider the relationship between the Lorentz force and the attraction force of charges. In the simplest case, the Lorentz force found from (1, 2) can be presented as the following

$$F = \frac{q_1 q_2 v_1 v_2}{r^2 c^2}. \quad (5)$$

The force of attraction of two charges
 Consequently,

$$P = \frac{q_1 q_2}{r^2}. \quad (6)$$

Consequently,

$$\phi_e = \frac{F}{P} = \frac{v_1 v_2}{c^2}. \quad (7)$$

Let us consider this value as the efficiency of the electromagnetic Lorentz forces.

Appendix 5. Gravitomagnetic interaction of moving masses and the efficiency of Lorentz gravitomagnetic forces

By analogy with the interaction of electric charges (see Appendix 4), two masses m_1 and m_2 moving with velocities v_1 and v_2 , respectively, also interact with each other. In Section 2.4 it is shown that gravitomagnetic inductions are found as the following:

$$\overline{B_{g1}} = G m_1 (\overline{v_1} \times \overline{r}) / c r^3, \quad (1)$$

$$\overline{B_{g2}} = G m_2 (\overline{v_2} \times \overline{r}) / c r^3, \quad (2)$$

where

c — speed of light in vacuum, $c \approx 3 \cdot 10^{10}$ cm/sec;

G - gravitational constant, $G \approx 7 \cdot 10^{-8}$ dyne*cm²*g⁻².

The gravitomagnetic Lorentz forces also affect the masses, which can be presented as the following (see Figure 1 in Appendix 3):

$$\overline{F_{12}} = \zeta \xi m_2 (\overline{v_2} \times \overline{B_{g1}}) c, \quad (3)$$

$$\overline{F_{21}} = \zeta \xi m_1 (\overline{v_1} \times \overline{B_{g2}}) c, \quad (4)$$

where

$\zeta = 2$, which follows from general relativity,

$\xi \approx 10^{12}$ - coefficient of gravity permeability of vacuum.

In the general case we find from (2, 4)

$$\overline{F_{21}} = \frac{\zeta \xi G m_1 m_2}{c^2 r^3} (\overline{v_1} \times (\overline{v_2} \times \overline{r})). \quad (5)$$

Let us consider the unit vectors marking them with chain-dotted line. Then we obtain the following from (5):

$$\overline{F_{21}} = \sigma \overline{f_{21}}, \quad (6)$$

where

$$\overline{f_{21}} = (\overline{v'_1} \times (\overline{v'_2} \times \overline{r'})). \quad (7)$$

$$\sigma = \frac{\zeta \xi G \cdot m_1 m_2 v_1 v_2}{c^2 r^2}. \quad (8)$$

Similarly,

$$\overline{F_{12}} = \sigma \overline{f_{12}}, \quad (9)$$

where

$$\overline{f_{12}} = (\overline{v'_2} \times (\overline{v'_1} \times \overline{r'})), \quad (10)$$

or

$$\overline{\Delta F} = \sigma \overline{\Delta f}, \quad (11)$$

where

$$\overline{\Delta F} = \overline{F_{21}} + \overline{F_{12}}, \quad (12)$$

$$\overline{\Delta f} = \overline{f_{21}} + \overline{f_{12}}. \quad (13)$$

In Appendix 3 (see (6)) it is shown that value of the vector (13) is calculated by the formula

$$\Delta f = r \sin(\varphi_2 - \varphi_1). \quad (14)$$

Taking into account (13, 11) we obtain:

$$\Delta F = \sigma \sin(\varphi_2 - \varphi_1). \quad (15)$$

We find the relationship between the Lorentz gravitomagnetic force and the attraction force of the masses. The attraction force of two masses is

$$P = \frac{G m_1 m_2}{r^2}. \quad (16)$$

Consequently,

$$\phi_g = \frac{F}{P} = \zeta \xi \cdot \frac{v_1 v_2}{c^2}. \quad (17)$$

Let us designate this value as the efficiency of the Lorentz gravitomagnetic forces. Comparing (17) with the efficiency of the Lorentz electromagnetic forces (see (7) in Appendix 4) we can observe the following:

$$\phi_g = \phi_e \zeta \xi. \quad (18)$$

Consequently, the efficiency of the Lorentz gravitomagnetic forces exceeds the efficiency of the Lorentz electromagnetic forces at comparable velocities.

Combining (8, 17) we obtain

$$F = \phi_g P. \quad (19)$$

References

Note: **DNA-№.срп** – The Papers of independent Authors,
ISSN 2225-6717, <http://izdatelstwo.com/>

1. Maxwell's equations,
https://en.wikipedia.org/wiki/Maxwell%27s_equations
2. Oliver Heaviside. A Gravitational and Electromagnetic Analogy. Part I, The Electrician, 31, 281-282 (1893),
<http://serg.fedosin.ru/Heavisid.htm>
3. Gravitoelectromagnetism,
<https://en.wikipedia.org/wiki/Gravitoelectromagnetism>
4. Samokhvalov V.N. Mass-dynamic and Mass-variational interaction of moving masses. **DNA-13**, 2009 – C. 110-159.
5. Samokhvalov V.N. Quadrupole radiation of the rotating masses. **DNA-14**, 2010 – C. 112-145.
6. Samokhvalov V.N. Forceful action of mass-variational radiation on solids. **DNA-15**, 2010 – C. 175-195.
7. Samokhvalov V.N. The study of the forceful action and reflection of rotating mass quadrupole radiation from solids. **DNA-18**, 2011 – C. 165-187.
8. Samokhvalov V.N. Force effects at mass-dynamic interaction on the average vacuum. **DNA-19**, 2011 – C. 170-181.
9. Samokhvalov V.N. Investigation and measurement of force effects during mass-dynamic interaction. **DNA-24**, 2013 - C. 113-131.
10. Savelyev I.V. Fundamentals of theoretical physics. Volume 1 - mechanics, electrodynamics. Moscow, Fizmatgiz, 1991 (in Russian).
11. Andre Ango. Mathematics for Electrical and Radio Engineers, publ. "Nauka", Moscow, 1964, 772 p. (in Russian).
12. Schultz E.O. On the issue of global vortex radiation. The Journal of the Forming Directions of Science, No. 12 (4), p. 184-185, 2016, <http://www.unconv-science.org/n12>
13. Zilberman G.E. Electricity and magnetism, Moscow, publ. "Science", 1970.

14. Fedulaev L.E. Fedulaev, L.E. Physical form of gravity: The dialectics of nature. M., publ. "KomKniga", 2006, http://www.vixri.com/d/Fedulova%20L.E%20_Fizicheskaja%20forma%20gravitacii.pdf
15. Khmelnik S.I. On the speed of propagation of gravitational action, **DNA-23**, 2013

Chapter 2. Equations of a stationary gravitomagnetic field

Contents

1. Equations of gravitomagnetism in a stationary gravitomagnetic field \ 24
 2. Equations of gravitomagnetism in cylindrical coordinates (system B) \ 25
 3. Helical motion (system B) \ 28
 4. Flows of gravitomagnetic energy (system B) \ 29
 5. Equations of gravitomagnetism in Cartesian coordinates (system B) \ 30
- References \ 31

1. Equations of gravitomagnetism in a stationary gravitomagnetic field

Further, the experiments described by Maxwell's equations for gravitomagnetism in a stationary gravitomagnetic field will often be considered. In order to obtain these equations, let us recall, first of all, the equations (6-9) from Appendix 1 in Chapter 1:

$$\operatorname{div} E_g = 4\pi G \rho_g, \quad (1)$$

$$\operatorname{div} B_g = 0, \quad (2)$$

$$\operatorname{rot} E_g = -\frac{1}{c} \frac{\partial B_g}{\partial t}, \quad (3)$$

$$\operatorname{rot} B_g = \frac{4\pi G \xi}{c} J_g + \frac{1}{c} \frac{\partial E_g}{\partial t}. \quad (4)$$

where variables have the following meanings:

B_g - gravitomagnetic induction,

E_g - gravitoelectric tension,

J_g - mass currents density,

ρ_g - mass density.

If we do not consider the time-dependent summands and mass density, not interested in future for the stationary case, we obtain the following in SI system:

$$\operatorname{div}E_g = 0, \quad (5)$$

$$\operatorname{div}B_g = 0, \quad (6)$$

$$\operatorname{rot}E_g = 0, \quad (7)$$

$$\operatorname{rot}H_g = J_g, \quad (8)$$

where H_g - gravitomagnetic tension. In addition, the currents must also comply with continuity condition.

$$\operatorname{div}(J) = 0. \quad (9)$$

Considering only the tensions and currents, we obtain a system of equations (for further we reject the indices):

$$\operatorname{div}J = 0, \quad (10)$$

$$\operatorname{div}H = 0, \quad (11)$$

$$\operatorname{rot}H = J, \quad (12)$$

$$\operatorname{rot}J = 0. \quad (13)$$

For a stationary gravitomagnetic field, we will use an abridges system of equations (10-12), which is usually used for a stationary magnetic field. These equations link up H gravitomagnetic tensions and J mass currents density.

Next, this system will be designated as (10-12) - **system B**.

Interaction between moving masses is described by gravitomagnetic Lorentz forces (hereinafter GL-forces), similar to Lorentz forces in electrodynamics, acting between the moving electric charges.

Below it will be shown that system B has a lot of solutions. Our task is to find solutions that explain the observed phenomena and experiments. In other words, it is necessary to prove that there is a solution adequate to this phenomenon. If such phenomena and experiments will be multipally discovered, it will be possible to confirm with a certain sureness that the proposed theory describes an observed reality.

2. Equations of gravitomagnetism in cylindrical coordinates (system B)

In r, φ, z cylindrical coordinates, [2], the divergence and curl of H vector are known[2] to have the form of

$$\operatorname{div}(H) = \left(\frac{H_r}{r} + \frac{\partial H_r}{\partial r} + \frac{1}{r} \cdot \frac{\partial H_\varphi}{\partial \varphi} + \frac{\partial H_z}{\partial z} \right), \quad (\text{a})$$

$$\operatorname{rot}_r(H) = \left(\frac{1}{r} \cdot \frac{\partial H_z}{\partial \varphi} - \frac{\partial H_\varphi}{\partial z} \right), \quad (\text{b})$$

$$\operatorname{rot}_\varphi(H) = \left(\frac{\partial H_r}{\partial z} - \frac{\partial H_z}{\partial r} \right), \quad (\text{c})$$

$$\operatorname{rot}_z(H) = \left(\frac{H_\varphi}{r} + \frac{\partial H_\varphi}{\partial r} - \frac{1}{r} \cdot \frac{\partial H_r}{\partial \varphi} \right). \quad (\text{d})$$

Considering equations (a-d), we rewrite equations (1.10-1.12) in the following form:

$$\frac{H_r}{r} + \frac{\partial H_r}{\partial r} + \frac{1}{r} \cdot \frac{\partial H_\varphi}{\partial \varphi} + \frac{\partial H_z}{\partial z} = 0, \quad (1)$$

$$\frac{1}{r} \cdot \frac{\partial H_z}{\partial \varphi} - \frac{\partial H_\varphi}{\partial z} = J_r, \quad (2)$$

$$\frac{\partial H_r}{\partial z} - \frac{\partial H_z}{\partial r} = J_\varphi, \quad (3)$$

$$\frac{H_\varphi}{r} + \frac{\partial H_\varphi}{\partial r} - \frac{1}{r} \cdot \frac{\partial H_r}{\partial \varphi} = J_z, \quad (4)$$

$$\frac{J_r}{r} + \frac{\partial J_r}{\partial r} + \frac{1}{r} \cdot \frac{\partial J_\varphi}{\partial \varphi} + \frac{\partial J_z}{\partial z} = 0 \quad (5)$$

Equations (1-5) describe, in fact, the processes of currents, tensions and gravitational Lorentz forces (GL-forces) interaction, namely, gravitational field tension is directed along z axis,

1. it generates J_z vertical mass flow-mass current,
2. J_z vertical mass current forms a circular gravitomagnetic magnetic field with H_φ tension and H_r radial gravitomagnetic magnetic field - see (4),
3. H_φ gravitomagnetic magnetic field rejects the masses of vertical flow in radial direction by GL-forces, creating a radial current of mass - J_r radial mass current,
4. H_φ gravitomagnetic field rejects the radial current mass perpendicular to radii by GL-forces, creating J_z vertical current,

5. H_r gravitomagnetic magnetic field rejects the mass of vertical flow perpendicular to radii by GL-forces, creating J_φ ring mass current,
6. H_r gravitomagnetic magnetic field rejects the mass of ring current along radii by GL-forces, creating J_z vertical current,
7. J_r mass current forms a vertical gravitomagnetic field and H_φ ring gravitomagnetic field - see (2),
8. J_φ mass current forms H_z vertical gravitomagnetic field and H_r radial gravitomagnetic field - see (3).
9. J_z mass current forms H_φ ring gravitomagnetic field and H_r radial gravitomagnetic field - see (4); etc.

The system of 5 equations (1-5) with respect to 6 ($H_r, H_\varphi, H_z, J_r, J_\varphi, J_z$) unknowns is newly defined and can have a lot of solutions. Below it is shown that such solutions exist and for some cases some of possible solutions are determined.

At first let us search for solution of this system of equations (1-5) in the form of functions which are separable with respect to coordinates. These functions are the following:

$$H_r = h_r(r) \cdot \cos(\chi z), \quad (1)$$

$$H_\varphi = h_\varphi(r) \cdot \sin(\chi z), \quad (2)$$

$$H_z = h_z(r) \cdot \sin(\chi z), \quad (3)$$

$$J_r = j_r(r) \cdot \cos(\chi z), \quad (4)$$

$$J_\varphi = j_\varphi(r) \cdot \sin(\chi z), \quad (5)$$

$$J_z = j_z(r) \cdot \sin(\chi z). \quad (6)$$

where χ - a constant, and $h_r(r), h_\varphi(r), h_z(r), j_r(r), j_\varphi(r), j_z(r)$ - functions of r coordinate; the derivatives of these functions will be indicated by dash marks.

Substituting (6-11) in (1-5), we obtain:

$$\frac{h_r}{r} + h_r' + \eta h_z = 0, \quad (12)$$

$$-\eta h_\varphi = j_r, \quad (13)$$

$$-\eta h_r - h_z' = j_\varphi \quad (14)$$

$$\frac{h_\varphi}{r} + h_\varphi' = j_z, \quad (15)$$

$$\frac{j_r}{r} + j'_r + \eta j_z = 0. \quad (16)$$

Substituting (13) and (15) in (16). Then we obtain:

$$\frac{-\eta h_\varphi}{r} - \eta h'_\varphi + \eta \left(\frac{h_\varphi}{r} + h'_\varphi \right) = 0. \quad (17)$$

An expression (17) is an identity of $0 = 0$. Therefore (16) follows from (13, 15) and can be excluded from the system of equations (12-16). The remaining equations should be rewritten in the form of:

$$h_z = -\frac{1}{\eta} \left(\frac{h_r}{r} + h'_r \right), \quad (18)$$

$$j_z = \frac{h_\varphi}{r} + h'_\varphi, \quad (19)$$

$$j_r = -\eta h_\varphi, \quad (20)$$

$$j_\varphi = -\eta h_r - h'_z \quad (21)$$

In this system of 4 differential equations with 6 unknown functions, two functions can be defined at random. This definition will be made in the following chapters.

3. Helical motion (system B)

It can be assumed that the mass current is a flow of elementary masses - EM. Let us consider the case when EM average velocity does not depend on mass current direction. In particular, for a fixed radius, the distance covered per EM time unit full circle, and the distance covered by it in vertical direction, will be equal. Consequently, in this case, for a fixed radius, we can assume that

$$\Delta\varphi \equiv \Delta z. \quad (1)$$

In the system considered above, EM trajectory is described by formulas

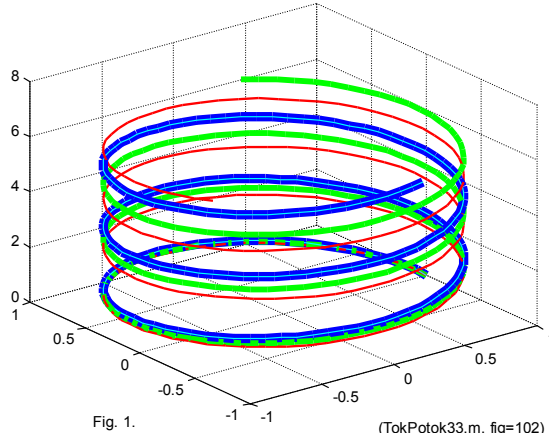
$$co = \cos(\chi z), \quad (2)$$

$$si = \sin(\chi z). \quad (3)$$

Thus, in such a system a trajectory of particle described by formulas (1-3) is on r constant radius cylinder. Such a trajectory is a helix line. On this trajectory, all the current tensions and densities don't depend on φ .

Based on this assumption, it is possible to construct the trajectory of EM motion in accordance with functions (1-3). Fig. 1 shows three helix lines at $\Delta\varphi = \Delta z$, described by $j_r(r)$ and $j_z(r)$ functions of

current: thick line at $\chi = 0.8$, middle line at $\chi = 1.2$ and thin line at $\chi = 1.6$.



4. Flows of gravitomagnetic energy (system B)

In [1] a structure of electromagnetic energy flows of direct current in a cylindrical wire with a constant current was described. The electromagnetic energy flow density is shown as:

$$S = \rho(J \times H), \quad (1)$$

where ρ - specific electrical resistivity. By analogy, let us determine the gravitomagnetic energy flow density in mass current

$$S = \sigma \cdot (J \times H), \quad (2)$$

where σ - specific resistance to mass current. Consequently,

$$S = \sigma \cdot S_o, \quad (3)$$

where

$$S_o = (J \times H), \quad (4)$$

Let us note once again that interaction between the moving masses is described by gravitomagnetic Lorentz forces (hereinafter GL-forces), similar to Lorentz forces in electrodynamics, acting between the moving electric charges. In (1.4.4), it is shown that the following GL-forces act between the moving masses

$$F_L = G \cdot \xi \cdot S_o. \quad (5)$$

Gravitomagnetic energy flow density (4) in r, φ, z cylindrical coordinates has three S_r, S_φ, S_z components directed along the radius, full circle, along the axis, respectively, i.e.

$$S_o = \begin{bmatrix} S_r \\ S_\varphi \\ S_z \end{bmatrix} = \begin{bmatrix} J_\varphi H_z - J_z H_\varphi \\ J_z H_r - J_r H_z \\ J_r H_\varphi - J_\varphi H_r \end{bmatrix}. \quad (6)$$

Thus, for a known solution of the system of equations (3.1-3.8), GL-forces can be found from (3).

From (3.1-3.6, 3) it follows that the total energy flow is

$$S = \begin{bmatrix} S_r \\ S_\varphi \\ S_z \end{bmatrix} = \iiint_{r,\varphi,z} \begin{bmatrix} (j_\varphi h_z - j_z h_\varphi) \sin^2(\chi z) \\ (j_z h_r - j_r h_z) \sin(\chi z) \cdot \cos(\chi z) \\ (j_r h_\varphi - j_\varphi h_r) \sin(\chi z) \cdot \cos(\chi z) \end{bmatrix} dr \cdot d\varphi \cdot dz.$$

or

$$\begin{bmatrix} S_r \\ S_\varphi \\ S_z \end{bmatrix} = \iiint_{r,\varphi,z} \begin{bmatrix} (j_\varphi h_z - j_z h_\varphi) \sin^2(\chi z) \\ (j_z h_r - j_r h_z) \cdot 0.5 \sin(2\chi z) \\ (j_r h_\varphi - j_\varphi h_r) \cdot 0.5 \sin(2\chi z) \end{bmatrix} dr \cdot d\varphi \cdot dz. \quad (7)$$

Fig. 3.1. in the right column shows the following functions

$$\begin{bmatrix} \overline{S_r}(r) \\ \overline{S_\varphi}(r) \\ \overline{S_z}(r) \end{bmatrix} = \begin{bmatrix} (j_\varphi h_z - j_z h_\varphi) \\ (j_z h_r - j_r h_z) \\ (j_r h_\varphi - j_\varphi h_r) \end{bmatrix}. \quad (8)$$

From (4, 5) we obtain:

$$S = \left(\int_r \begin{bmatrix} \overline{S_r}(r) \\ \overline{S_\varphi}(r) \\ \overline{S_z}(r) \end{bmatrix} dr \right) \cdot \begin{bmatrix} D_3 \\ D_2 \\ D_2 \end{bmatrix}, \quad (9)$$

where

$$\begin{bmatrix} D_3 \\ D_2 \\ D_2 \end{bmatrix} = \iiint_{\varphi,z} \begin{bmatrix} \sin^2(\chi z) \\ 0.5 \sin(2\chi z) \\ 0.5 \sin(2\chi z) \end{bmatrix} d\varphi \cdot dz = 2\pi \int_z \begin{bmatrix} \sin^2(\chi z) \\ 0.5 \sin(2\chi z) \\ 0.5 \sin(2\chi z) \end{bmatrix} dz. \quad (10)$$

5. Equations of gravitomagnetism in Cartesian coordinates (system B)

In Cartesian coordinates, equations (1.10-1.12) take the following form:

$$\frac{\partial H_z}{\partial y} - \frac{\partial H_y}{\partial z} = J_x, \quad (1)$$

$$\frac{\partial H_x}{\partial z} - \frac{\partial H_z}{\partial x} = J_y, \quad (2)$$

$$\frac{\partial H_y}{\partial x} - \frac{\partial H_x}{\partial y} = J_z, \quad (3)$$

$$\frac{\partial H_x}{\partial x} + \frac{\partial H_y}{\partial y} + \frac{\partial H_z}{\partial z} = 0, \quad (4)$$

$$\frac{\partial J_x}{\partial x} + \frac{\partial J_y}{\partial y} + \frac{\partial J_z}{\partial z} = 0. \quad (5)$$

References

1. Khmelnik S.I. Inconsistency Solution of Maxwell's Equations. Publisher by "MiC", printed in USA, Lulu Inc., ID 18555552, Israel, 2017, ISBN 978-1-365-23941-0, 180 c.
2. Andre Ango. Mathematics for Electrical and Radio Engineers, publ. "Nauka", Moscow, 1964, 772 p. (in Russian).

Chapter 3. On the possibility of using gravitational forces to perform work

Below it is proved that the power of conservative forces (including gravitational forces) performs work on **closed** trajectories of multiple body's motion, if these bodies are not rigidly connected and between them forces are acting, which depend on the speed of these bodies. A shortened version of this paper has been published in [1, 2] as an appendix.

We shall begin with considering some examples.

Example 1. There is an electrical charge Q and another charge much smaller by its size $q_1 \ll Q$. Coulomb forces acting of the q_1 from the side of the charge Q do not perform any work on a closed path of the motion of charge q_1 . Let there be another charge $q_2 \ll Q$, and both charges q_1 and q_2 are moving along near closed paths. Then between them Lorentz forces are acting. Let the medium in which the charges q_1 and q_2 are moving provides some resistance to their motion. Then under the influence of Lorentz forces a certain work will be performed. The energy for this work is provided from the electrical charge Q (this is similar to the fact that Lorentz forces acting as Ampere forces perform work by the energy of the power force). Thus, the source of Coulomb forces performs work on closed paths of the two charges motion.

Example 2. There is a DC motor with self-excitation (in which the armature winding and the electromagnetic field are connected in series or in parallel). In such a motor the energy source is a DC voltage source, i.e. a source of Coulomb forces. This source explicitly performs work.

In the general case from these examples it follows that the source of Coulomb forces performs work on closed trajectories of multiple unconnected charges motion. As the Coulomb forces are conservative, then the previous conclusion is equivalent to the following:

- 0) The source of conservative forces performs work along **closed** trajectories of multiple bodies motion, if

- a body – it is something, on which a conservative force is acting,
- The bodies are not connected rigidly,
- Between the bodies are acting forces that depend on the speed of these bodies motion.

Conservative forces (by definition) do not perform work on a closed trajectory. The force of gravity is a conservative force (which is proved mathematically). Hence the conclusion is reached that

- 1) there does not exist a motor using only conservative forces (specifically, the force of gravity) to perform work.

Next an *unproven* conclusion is made that

- 2) there **does not exist** a motor using **the energy** of conservative forces source (including the gravity forces), for performing the work.

Coulomb forces are also conservative. From this by analogy one can make the conclusion 1). However, the conclusion 2) is easily refuted by the previous assertion 0). Therefore, in the general case, the assertion 2) is incorrect, and the true statement is as follows:

- 3) **There can exist** a motor using **the energy** of conservative forces source for performing work.

Nevertheless, the existence of the motor that uses energy of the **electrical conservative** forces source (ECF) does not mean that there is a motor that uses the energy source of the **gravitational conservative** forces (GCF).

Electrical forces create the charges motion along a closed trajectory – *electric current* which forms a magnetic field. Due to this the energy of ECF turns into magnetic energy. It occurs even if the energy is not expended for the motion of the charges on the closed path. Thus, the energy of ECF exceeds the energy of the mechanical motion of the charges. This is the reason for the existence of a motor using the energy ECF.

Gravity forces also can create a mass motion on a closed trajectory – *mass current*. Let us assume that mass current also forms a *gravity magnetic* field (it is shown Chapter 1). Then by analogy with the previous we may assume that

Гравитационные силы также могут создать движение масс по замкнутой траектории – *массовый ток*. Массовый ток тоже формирует *гравитоманнитное поле* – см. главу 1. Тогда по аналогии с предыдущим, можно предположить, что

- 4) **there can exist** a motor using the **energy** of the source of **gravity** conservative forces for performing work.

This does not contradict the law of conservation of energy: it is the energy of GCF that is converted into work, and GCF power source loses some of its energy (it cannot be said that the energy of GCF may be used only for the movement of the masses).

Let us approach the subject on the other hand.

The gravity force is a conservative force, i.e. the gravitational work is not influenced by the motion trajectory and determined only by the initial and final position of the point of this force application. This statement does not consider the velocity of this point. As a rule, the gravitational work is not influenced by this velocity. For example, the gravitational work can be spent on friction and changing the velocity of the point. In this case, the spent potential energy of the body is equal to the work of the frictional force (directed **opposite to** the force of gravity) and the increase of the body kinetic energy does not depend on the trajectory and motion velocity.

Let us consider the gravitational work which is independent of velocity and trajectory as the **conservative** gravitational work. No example of the velocity of movement affecting the gravitational work, i.e. when the gravitational work is not conservative can be found in mechanics.

However, formally such an example can be found. Suppose that the shear force is directed **along** the force of gravity and depends on the velocity, and additionally this shear force is formed due to gravity work (as well as the force of ordinary friction). Then the increase in the kinetic energy of the body is equal to the sum of the conservative work and the work of shear force. However, the latter is also performed by gravity (on the assumption just adopted). Consequently, in this case the gravitational work is greater than the conservative work, i.e. the gravitational work is not conservative.

It appears that in mechanics one cannot find such case. However, in the electromechanical system such a case is possible. Let us consider the motion of charged bodies - heavy electric charges (HEC) in the field of gravity. Such charges are affected by gravity forces, electric attraction / repulsion forces and Lorentz forces. As it is known the Lorentz forces do not perform work, but they use the work of external forces, in this case these are gravity forces (electric forces can be neglected). Since the Lorentz force depends on the velocity, in this case the gravitational work depends on the velocity of motion (HEC) along the given trajectory.

Thus, **in the electromechanical system the forces of gravity are not conservative**. (Note that there is another case of fundamental

difference between the laws in mechanics and electromechanics: Newton's third law is observed in mechanics, and in electromechanics it is not observed because of the same Lorentz forces).

It follows from the basic equations of general relativity theory that in a weak gravitational field at low velocities, i.e. on the Earth, you can use the MGM equations to describe gravitational interactions. This means that there are gravitational waves, and the gravitomagnetic Lorentz force (GL force) affect the mass m moving in the gravitomagnetic field with velocity v .

So, in mechanical system (as well as in electromechanical system), Lorentz forces can arise, i.e. **in mechanical system the forces of gravity are not conservative if motion under the action of gravity causes the appearance of Lorentz gravitomagnetic forces.**

Thus, force of gravity can do work.

References

1. Khmelnik S.I. Mathematical Model of Dust Whirl, <http://vixra.org/abs/1505.0087.pdf>; see also <http://lib.izdatelstwo.com/Papers/33.141.pdf>; <http://vixra.org/pdf/1504.0169v3.pdf>.
2. Khmelnik S.I. The Equation of Whirlpool, <http://vixra.org/abs/1506.0157.pdf>

Chapter 4. Natural phenomena

A number of natural phenomena can be admittedly explained by significant intensity of gravitomagnetic forces. To the author's knowledge, many of them have no rigorous mathematical model and, therefore, quantitative estimates. These phenomena and their mathematical models are discussed below.

Chapter 4.1. Dust Whirl

Contents

1. Introduction \ 38
2. Mathematical Model \ 39
3. The Energy Flows \ 43
4. Vertical stability and height of vortex \ 44
5. The Motion of the Dust whirl \ 44
6. Retention of vortex shape \ 45
7. Mathematical model of non-cylindrical vortices \ 46
- References \ 49

1. Introduction

There exists a widely known dust dust whirl, which is an almost vertical cloud of dust – see Fig. 1.

Such a dust whirl has a vertical axis of rotation, height of a few tens of meters, diameter - a few meters, the time of existence - a few tens of seconds [1]. There are similar phenomena - water, air, ash dust whirls. The cause of their existence is assumed to be various atmospheric phenomena (wind, heating of the atmosphere). However, the very existence of the dust whirl – its shape retention and movement, - are difficult to explain by the same reasons. Furthermore, such dust whirls are also moving on Mars, where there is no atmosphere - see Fig. 2 [1]. Therefore, in the explanation of the dust whirls the main question is about the source of energy. Therefore, below we consider the source of energy in sandy vortex. Atmospheric phenomena cannot be the only source of energy, since such vortices exist also on Mars where the atmosphere is absent. Below it is shown that the energy source for the sand vortex is the energy of the gravitational field - see Chapter 3. In any case, it is difficult to find another source of energy on Mars. The mathematical model of the sand vortex is proposed which applies the system of MGM gravity equations. Some properties of the sandy vortex are explained, for example, retention of the cylindrical vertical form of the vortex, the motion of the vortex as a whole.



Fig. 1.



Fig. 2.

The model is based on the following assumptions. Sandy dust whirl is composed of material particles – sand grains. The movement of these particles is likened to mass currents. Mass currents in the gravitational field are described by MLG-equations. The interaction between the moving masses is described by the Lorentz gravity-magnetic (the GL-force) similar to the Lorentz forces in electrodynamics acting between moving electrical charges.

Currents arising in the dust whirl are circulating (as shown) in the cross section of the vortex and along the vertical (up and down). The kinetic energy of such circulation is spent on the losses from collisions of sand grains. It comes from a gravitating body. Potential energy of the dust whirl is not changed, and therefore is not consumed. I.e. in this case there is no conversion of potential energy into kinetic energy and vice versa. However, gravitating body expends its energy on creating and maintaining a mass current - see Chapter 3.

2. Mathematical Model

In Chapter 2, we solve the equations of gravitomagnetism in cylindrical coordinates (system B). In cylindrical coordinates r , φ , z these equations have the form:

$$\frac{J_r}{r} + \frac{\partial J_r}{\partial r} + \frac{1}{r} \cdot \frac{\partial J_\varphi}{\partial \varphi} + \frac{\partial J_z}{\partial z} = 0, \quad (1)$$

$$\frac{H_r}{r} + \frac{\partial H_r}{\partial r} + \frac{1}{r} \cdot \frac{\partial H_\varphi}{\partial \varphi} + \frac{\partial H_z}{\partial z} = 0, \quad (2)$$

$$\frac{1}{r} \cdot \frac{\partial H_z}{\partial \varphi} - \frac{\partial H_\varphi}{\partial z} = J_r, \quad (3)$$

$$\frac{\partial H_r}{\partial z} - \frac{\partial H_z}{\partial r} = J_\varphi, \quad (4)$$

$$\frac{H_\varphi}{r} + \frac{\partial H_\varphi}{\partial r} - \frac{1}{r} \cdot \frac{\partial H_r}{\partial \varphi} = J_z, \quad (5)$$

In Chapter 2 (Section 2) it is shown that for equations (1-5) there exists a solution in the form of functions having the following form:

$$H_r = h_r(r) \cdot \cos(\chi z), \quad (1)$$

$$H_\varphi = h_\varphi(r) \cdot \sin(\chi z), \quad (2)$$

$$H_z = h_z(r) \cdot \sin(\chi z), \quad (3)$$

$$J_r = j_r(r) \cdot \cos(\chi z), \quad (4)$$

$$J_\varphi = j_\varphi(r) \cdot \sin(\chi z), \quad (5)$$

$$J_z = j_z(r) \cdot \sin(\chi z), \quad (6)$$

where χ is a constant, and $h_r(r)$, $h_\varphi(r)$, $h_z(r)$, $j_r(r)$, $j_\varphi(r)$, $j_z(r)$ is a function of the coordinate; the derivatives of these functions will be denoted by primes.

In Chapter 2 it is shown that after substituting (9-14) into (1-5), the following system of equations is obtained:

$$h_z = -(h_r/r + h'_r)/\eta, \quad (18)$$

$$j_z = h_\varphi/r + h'_\varphi, \quad (19)$$

$$j_r = -\eta h_\varphi, \quad (20)$$

$$j_\varphi = -\eta h_r - h'_z. \quad (21)$$

In this system of 4-th differential equations with 6-th unknown functions, two functions can be defined in an arbitrary way. For the following we define the following two functions:

$$h_\varphi = q \cdot r \cdot \sin(\pi \cdot r/\eta), \quad (22)$$

$$h_r = h \cdot r \cdot \sin(\pi \cdot r/\eta), \quad (23)$$

where q , h are some constants. Then from (18-23) we find:

$$h'_\varphi = q \cdot \left(\sin(\pi \cdot r/\eta) + \frac{\pi \cdot r}{\eta} \cdot \cos(\pi \cdot r/\eta) \right), \quad (24)$$

$$h'_r = h \cdot \left(\sin(\pi \cdot r/\eta) + \frac{\pi \cdot r}{R} \cdot \cos(\pi \cdot r/\eta) \right), \quad (25)$$

$$h_z = -\frac{1}{\eta} \left(\left(h \cdot \sin(\pi \cdot r/\eta) + h \cdot \left(\sin(\pi \cdot r/\eta) + \frac{\pi \cdot r}{\eta} \cos(\pi \cdot r/\eta) \right) \right) \right) =$$

$$= -\frac{h}{\eta} \left(2 \sin(\pi \cdot r/\eta) + \frac{\pi \cdot r}{\eta} \cos(\pi \cdot r/\eta) \right)$$

$$h'_z = -\frac{h}{\eta} \left(2 \cos(\pi \cdot r/\eta) - \frac{\pi}{\eta} \left(\cos(\pi \cdot r/\eta) - \frac{\pi}{\eta} r \cdot \sin(\pi \cdot r/\eta) \right) \right) =$$

$$= -\frac{h}{\eta} \left(\left(2 - \frac{\pi}{\eta} \right) \cdot \cos(\pi \cdot r/\eta) + \frac{\pi^2}{\eta^2} r \cdot \sin(\pi \cdot r/\eta) \right)$$

$$j_z = q \sin(\pi \cdot r/\eta) + q \cdot \left(\sin(\pi \cdot r/\eta) + \frac{\pi \cdot r}{\eta} \cdot \cos(\pi \cdot r/\eta) \right) =$$

$$= q \left(2 \sin(\pi \cdot r/\eta) + \frac{\pi \cdot r}{\eta} \cdot \cos(\pi \cdot r/\eta) \right)$$

$$j_r = -\eta \cdot q \cdot r \cdot \sin(\pi \cdot r/\eta) \quad (29)$$

$$j_\phi = -\eta h \cdot r \cdot \sin(\pi \cdot r/\eta) + \frac{h}{\eta} \left(\left(2 - \frac{\pi}{\eta} \right) \cdot \cos(\pi \cdot r/\eta) + \frac{\pi^2}{\eta^2} r \cdot \sin(\pi \cdot r/\eta) \right) =$$

$$= h \cdot \left(\frac{\pi^2}{\eta R^2} - \eta \right) \cdot r \cdot \sin(\pi \cdot r/\eta) + \frac{h}{\eta} \left(2 - \frac{\pi}{\eta} \right) \cdot \cos(\pi \cdot r/\eta)$$

Thus, the functions $j_r(r)$, $j_\phi(r)$, $j_z(r)$, $h_r(r)$, $h_\phi(r)$, $h_z(r)$ are determined by (29, 30, 28, 23, 22, 26), respectively.

Example 1.

The graphs of functions $j_r(r)$, $j_\phi(r)$, $j_z(r)$, $h_r(r)$, $h_\phi(r)$, $h_z(r)$ are presented in Fig. 3. These functions are determined at given $R = 2$, $\chi = 2$, $h = 1$, $q = -1$. The first column shows $h_r(r)$, $h_\phi(r)$, $h_z(r)$ functions, the second column shows $j_r(r)$, $j_\phi(r)$, $j_z(r)$ functions and the functions in the third column will be considered further.

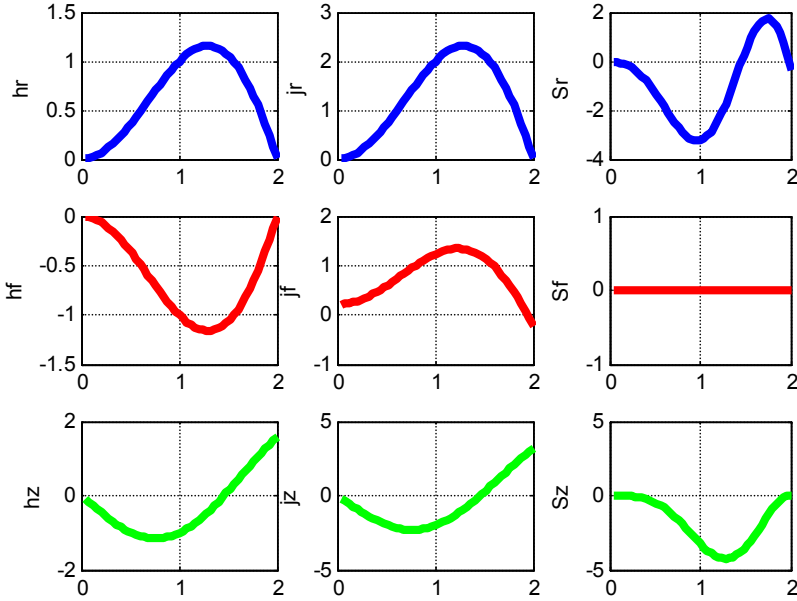


FIG. 1 fig-Pyl-10.m

Fig. 3.

It is important to note that there is a point on the graph of functions $j_r(r)$, $j_\phi(r)$ where $j_r(r)=0$ and $j_\phi(r)=0$. Physically this means that in the area of $r < \eta$ there are radial mass currents $J_r(r)$ directed from the center (at $\eta q < 0$). At point $r = \eta$ mass currents $J_r(r)$, $J_\phi(r)$ are absent. Therefore, the value $R = \eta$ is the radius of the vortex.

It is also important to note here that the vertical currents circulate in such a way that the sum of the currents J_z in each circle and in each section is zero (see (14)). This means that in each cylindrical layer of the vortex there are counter flows (up and down). Thus, the dust masses move along the closed trajectory and gravity forces do not work along this trajectory. Nevertheless, the work is done to overcome the frictional forces between dust particles when they are moved by GL forces. This work is carried out due to the energy of the gravitational field – see Chapter 3.

3. The Energy Flows

Chapter 2.5 shows that along with the mass currents and in the same physical volume, there are flows of gravitomagnetic energy. In the cylindrical coordinate system, these internal flows are directed.

- along the radius from periphery to center - S_r ;
- circumferentially - S_φ ;
- vertical down - S_z .

The densities of these flows are described by a formula of the form

$$\begin{bmatrix} S_{r0}(r, \varphi, z) \\ S_{\varphi0}(r, \varphi, z) \\ S_{z0}(r, \varphi, z) \end{bmatrix} = \begin{bmatrix} (j_\varphi h_z - j_z h_\varphi) \sin^2(\chi z) \\ (j_z h_r - j_r h_z) \cdot \sin(\chi z) \cdot \cos(\chi z) \\ (j_r h_\varphi - j_\varphi h_r) \sin(\chi z) \cdot \cos(\chi z) \end{bmatrix} . \quad (1)$$

The total fluxes are equal to the integrals of these densities:

$$S = \begin{bmatrix} S_r \\ S_\varphi \\ S_z \end{bmatrix} = \iiint_{r, \varphi, z} \begin{bmatrix} S_{r0}(r, \varphi, z) \\ S_{\varphi0}(r, \varphi, z) \\ S_{z0}(r, \varphi, z) \end{bmatrix} dr \cdot d\varphi \cdot dz . \quad (2)$$

or

$$S = \begin{bmatrix} S_r \\ S_\varphi \\ S_z \end{bmatrix} = \left(\int_r \begin{bmatrix} \overline{S_r}(r) \\ \overline{S_\varphi}(r) \\ \overline{S_z}(r) \end{bmatrix} dr \right) \cdot \begin{bmatrix} D_3 \\ D_2 \\ D_2 \end{bmatrix} , \quad (3)$$

where the densities of these flows

$$\begin{bmatrix} \overline{S_r}(r) \\ \overline{S_\varphi}(r) \\ \overline{S_z}(r) \end{bmatrix} = \begin{bmatrix} (j_\varphi h_z - j_z h_\varphi) \\ (j_z h_r - j_r h_z) \\ (j_r h_\varphi - j_\varphi h_r) \end{bmatrix} . \quad (4)$$

In Fig. 1 functions (4) are shown in the right column. The values

$$\begin{bmatrix} D_3 \\ D_2 \\ D_2 \end{bmatrix} = 2\pi \int_z \begin{bmatrix} \sin^2(\chi z) \\ 0.5 \sin(2\chi z) \\ 0.5 \sin(2\chi z) \end{bmatrix} dz . \quad (5)$$

So, there is no energy flow outside the body of the vortex. These internal energy flows provide

- a certain height of the vortex,
- vertical stability,
- movement of a vortex,
- retaining the shape of the vortex.

4. Vertical stability and height of vortex

At $\chi=0$ from (5) we have $D_3 \neq 0$, $D_2 = 0$. From this and (3) it follows that in this case there is no total vertical energy flow so the vortex cannot exist. At some $\chi \neq 0$ we have $D_3 \neq 0$, $D_2 \neq 0$. This means that the vertical energy flow exists. If the Lorentz force proportional to this flow is directed upwards and exceeds the force of gravity, then the vortex exists. We can always find the value χ at which this condition is met. This means that the existence of the vortex is necessarily associated with its rotation. The existence of motion along a helical line in the cylindrical vortex follows from the general solution of system B - see Section 3 in Chapter 2. In the case of variable radius of the vortex the motion along the conical helical line occurs (see Figure 4).

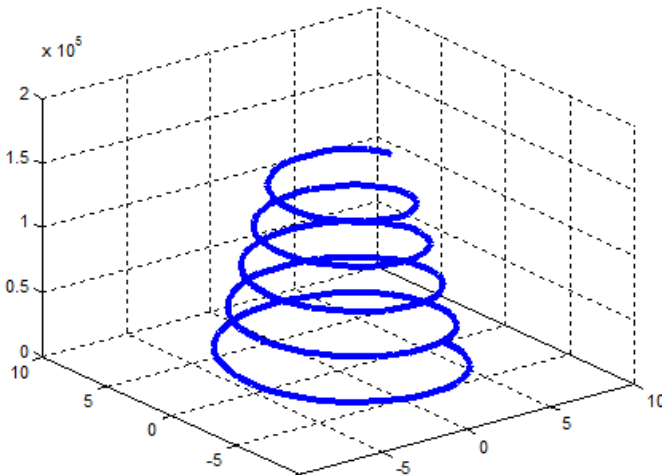


Рис. 4.

Therefore, this Lorentz force maintains the vortex in vertical position. It is counteracted and counterbalanced by its gravity increasing with height. At some height, the gravitational force of the vortex becomes equal to the Lorentz force. This condition determines the height of the vortex.

5. The Motion of the Dust whirl

The trajectory of the dust whirl is poorly predictable. We can say, that the dust whirl makes chaotic movement. In order to show that the motion of the dust whirl is accomplished by the internal energy (and not by the force of the wind) let us again turn to the consideration of the

internal flow of gravitomagnetic energy. Above it is shown that in the body of the dust whirl there is a flow of energy directed radially with density

$$\overline{S}_r = J_\varphi H_z - J_z H_\varphi. \quad (1)$$

Just as for a vertical energy flow, this flux corresponds to a force with a density

$$F_r \equiv S_r. \quad (2)$$

Let us find the total force acting in the dust whirl's body along the radius:

$$F_{ro} \equiv \int_0^R \overline{S}_r r \cdot dr. \quad (3)$$

For a symmetrical distribution of the radial flow total force (3) is zero. If the axial symmetry of the vortex is broken, then there appears an uncompensated force. Let $\xi < 1$ - be a coefficient characterizing the symmetry breaking. Then uncompensated force can be found from the formula

$$F_{zo} \equiv \left(\int_0^{R/2} \overline{S}_r r \cdot dr - \xi \int_{R/2}^R \overline{S}_r r \cdot dr \right). \quad (4)$$

or

$$F_{zo} \equiv (1 - \xi) \int_{R/2}^R \overline{S}_r r \cdot dr. \quad (5)$$

This force results in the motion of the vortex as a whole. The reason for this distortion (and, as a consequence, the motion of the vortex) is the inertia of the sand particles. Thus, the motion of the vortex is carried out by internal energy (and not by wind force). This we can see on Mars.

Another reason for the motion of vortex (in earth conditions) is air resistance. When vortex is moving it is necessary to take into account the fact that air resistance creates an additional flow, mass current directed against the velocity of the vortex translational motion. In Chapter 4.7 it is shown that this mass current creates a force directed along the velocity of the vortex translational motion (though it may sound strange).

6. Retention of vortex shape

It was shown above that at the boundary of the vortex at $r = R$ radial current $J_r(R) = 0$ and energy flow $\overline{S}_r(R) = 0$.

The energy flow (as shown above) is proportional to the Lorentz force driving the mass current in the direction of the energy flow. In

particular, the radial energy flow affects the radial mass current. From $\overline{S}_r(R)=0$ it follows that there is no radial energy flow at the boundary of the vortex, i.e. dust particles are NOT pushed out beyond the existing radius of the vortex.

Any change in the shape of the vortex must be accompanied by change in internal energy flows. In this case the internal impulses must change - see, for example, (4.2, 5.2). In this case, the sum of the impulses must change. Consequently, the change in shape can be caused only by the external impulse. Thus, in the absence of the external impulse the vortex retains its shape.

Of course, the wind can also affect the shape and motion of the vortex. Our goal was to show that all the metamorphoses of the vortex and its very existence could be caused by internal energy or, more exactly, gravitational energy.

7. Mathematical model of non-cylindrical vortices

The previous statement concerned vortices with cylindrical shape. However, sand vortices often have non-cylindrical and very intricate shape – see Figure 5. In [3], two forms of vortices are considered: cone with rectilinear or curvilinear generatrix with point downwards. It is assumed that these vortices are formed in baroclinic atmosphere where the air density is a function of pressure, temperature, and / or humidity. However, vortices exist both in the barotropic atmosphere and in the absence of the atmosphere [1].

So, our task is to find a mathematical model of vortices with non-cylindrical shape.

We return again to Example 1 in Section 2. The root of the equation $j_r(r)=0$ determined the radius $R = \chi$ of cylindrical vortex. Now we change the value. If the value χ will depend on z , then the radius R will also depend on z . But this very dependence determines the shape of the vortex.

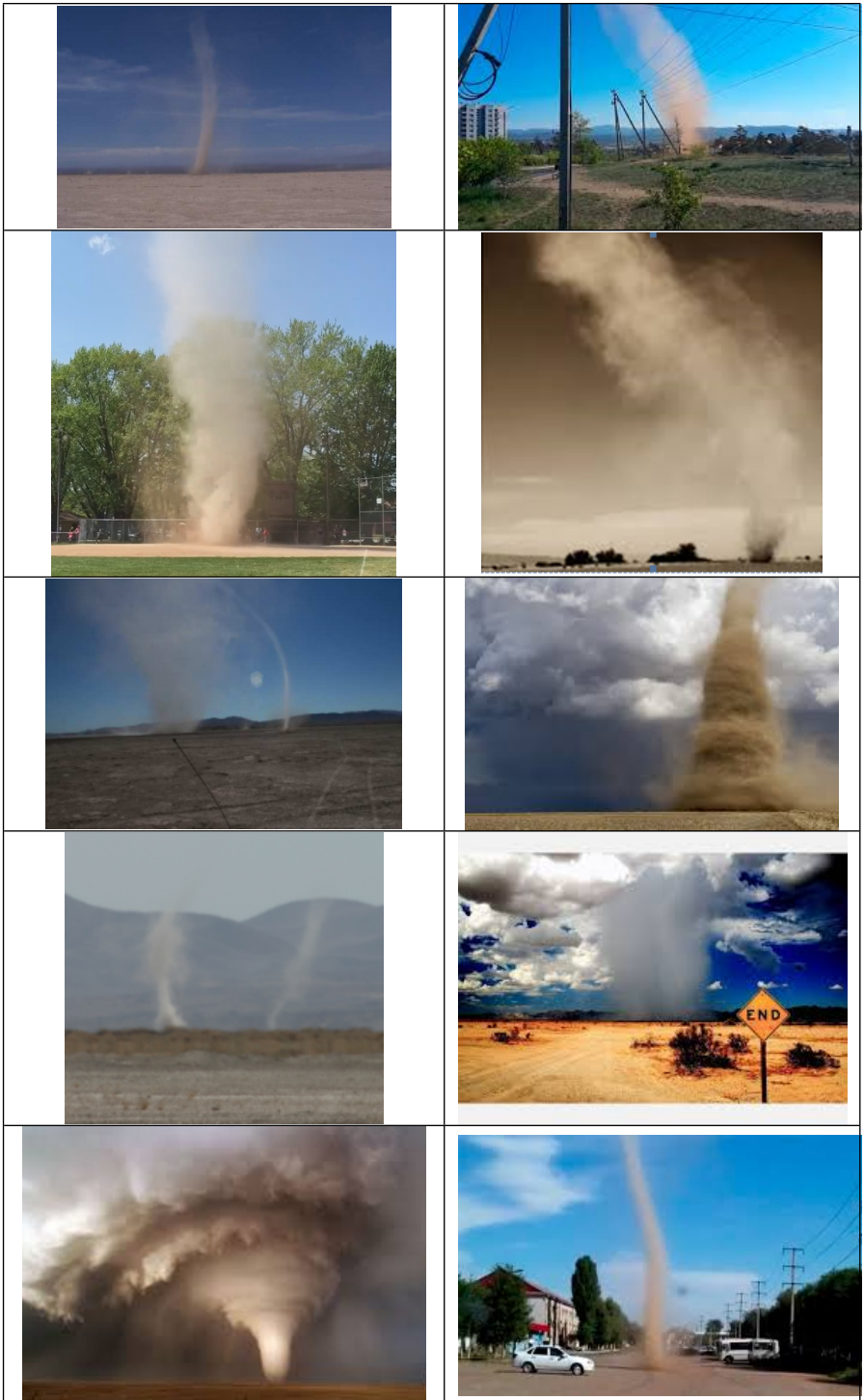


Fig.. 5.

With this in mind consider a mathematical model which differs from the one used above where the functions of currents intensities and densities were determined from (2.9-2.14) in the fact that the function $\chi(z)$ is used instead of constant χ . We rewrite (2.9-2.14) taking this into account:

$$H_{r.} = h_r(r) \cdot \cos(\chi(z)), \quad (1)$$

$$H_{\varphi.} = h_{\varphi}(r) \cdot \sin(\chi(z)), \quad (2)$$

$$H_{z.} = h_z(r) \cdot \sin(\chi(z)), \quad (3)$$

$$J_{r.} = j_r(r) \cdot \cos(\chi(z)), \quad (4)$$

$$J_{\varphi.} = j_{\varphi}(r) \cdot \sin(\chi(z)), \quad (5)$$

$$J_z = j_z(r) \cdot \sin(\chi(z)). \quad (6)$$

The system of equations (1-6) differs from the system (2.9-2.14) only in the fact that the derivative $\chi'(z)$ of function $\chi(z)$ with respect to z is used instead of the constant χ . Consequently, the solution of the system (7-14) will differ from the solution of the system (2.15-2.22) only in the fact that the derivative $\chi'(z)$ is used instead of the constant χ . Thus, the solution in this case will take the following form:

$$j_r = -\chi'(z) \cdot q \cdot r \cdot \sin(\pi \cdot r / \chi'(z)), \quad (7)$$

$$j_{\varphi} = \left[\begin{aligned} & h \cdot \left(\frac{\pi^2}{\chi'(z)R^2} - \chi'(z) \right) \cdot r \cdot \sin(\pi \cdot r / \chi'(z)) + \\ & + \frac{h}{\chi'(z)} \left(2 - \frac{\pi}{\chi'(z)} \right) \cdot \cos(\pi \cdot r / \chi'(z)) \end{aligned} \right], \quad (8)$$

$$j_z = q \left(2 \sin(\pi \cdot r / \chi'(z)) + \frac{\pi \cdot r}{R} \cdot \cos(\pi \cdot r / \chi'(z)) \right), \quad (9)$$

$$h_r = h \cdot r \cdot \sin(\pi \cdot r / \chi'(z)), \quad (10)$$

$$h_{\varphi} = q \cdot r \cdot \sin(\pi \cdot r / \chi'(z)), \quad (11)$$

$$h_z = -\frac{h}{\chi'(z)} \left(2 \sin(\pi \cdot r / \chi'(z)) + \frac{\pi \cdot r}{R} \cos(\pi \cdot r / \chi'(z)) \right). \quad (12)$$

These functions will depend on $\chi'(z)$. When $\chi(z) = \eta z$ equations (7-12) are transformed into equations (2.9-2.14).

References

1. Dust_devil, http://en.wikipedia.org/wiki/Dust_devil.
2. R.P. Feynman, R.B. Leighton, M. Sands. The Feynman Lectures on Physics, volume 2, 1964.
3. M.V. Kurgansky. Simple models of spiral vortices in a baroclinic atmosphere, Institute of Atmospheric Physics named after A.M. Obukhov, Russian Academy of Sciences, Moscow, 2012, http://www.inm.ras.ru/library/seminars/s9-mmgpdp/Moscow_27_09_2012_Kurgansky.pdf (in Russian)
4. Khmelnik S.I. Mathematical Model of Dust Whirl, <http://vixra.org/abs/1505.0087>, 2015-05-11.

Chapter 4.1a. Clouds

First of all, for reader's convenience, we briefly describe the known beliefs about cloud formation, composition and structure [1-5].

Clouds formation is always associated with adiabatic cooling of ascending air [1]. Only adiabatic processes also take place in existing cloud [2]. The cloud consists of drops. Drops have a diameter from 2 to 200 microns. Drops of a larger diameter are raindrops. The drop is formed as a result of steam condensation on the smallest solid particle. In general these are the particles of sea salt availability in the air.

Drops disintegration, coagulation, gravitation and repulsion continuously take place in the cloud (we will not consider the physics of these processes [1-5]). However, in average, there is a distance, calculated in millimeters between drops. Stokes proved that very small spherical bodies with a diameter of less than 0.02 millimeters fall at a very slow velocity. Drops can be held by a weak ascending air (not more than 0.5 meters per second) [2, 5]. But actual pre-raindrops have a size of 0.2 millimeters. Whole cloud can be held by ascending air, if this flow is not low and penetrates into entire air thickness, i.e. per hundreds of meters. But this contradicts the admitted fact that only adiabatic processes take place in the cloud.

So, the cloud is a limited air volume in which the scattered drops move. As all the processes in the cloud are adiabatic, energy does not input into this volume and there is no external air flow.

Our point of interest will be how such a construction made of scattered drops mass exists and does not fall? In fact, internal adiabatic processes cannot create an ascending force for the cloud as a whole, and there is no external air flow.

Another not so evident issue is the detection of that energy source which mixes the thousands of tons of water. That internal energy that appeared in the cloud during its formation when adiabatic cooling of ascending air is apparently insufficient for such work performance.

Absolutely similar issues arise when considering a sand-devil, see Chapter 4.1. There, scattered dust particles form a stable vertical column too. Chapter 4.1 shows that the energy source for sand vortex is the energy of gravitational field, and then a vortex shape retention is explained.

By analogy with sand-devil, cloud model is based on the following assumptions. The cloud consists of material particles - drops. The motion of these particles assimilates to mass currents. Mass currents in gravitational field are described by Maxwell-like gravitational equations. Interaction between the moving masses is described by gravitomagnetic Lorentz forces.

Mass currents arising in the cloud circulate along vortex section and in vertical direction (upward, downward). Kinetic energy of such circulation is consumed for the losses from drops collisions. It comes from a gravitating body - Earth. Potential energy of the cloud does not change and, therefore, isn't consumed. Namely in this case there is no potential energy conversion into kinetic energy and vice versa. However, the gravitating body consumes its energy for mass currents creation and maintenance.

Cloud holdup above the Earth is explained as follows. According to analogy between Maxwell's and Maxwell-like gravitational equations it follows that S gravitational energy flow can exist. Such a flow can exist and **cannot** change in time. A gravitational momentum exists together with the flow. If the body is in gravitational energy flow (and this flow **does not** change in time), then S force $F=S\backslash c$ oppositely directed to flow where c is the light velocity acts on the body. This follows from the law of conservation of momentum [6]. It should be mentioned again that this is a complete analogy between gravitational and electromagnetic field.

So, a constant flow of gravitational energy in time exists together with constant mass currents in a cloud. It is down-directed. In accordance with the above, up-directed force acts on the cloud and holds it at a certain height.

Since such arithmetic model is completely similar to mathematical model of a sand vortex, we will not consider it in more detail.

In conclusion, let turn attention to the similarity during the sand-devil and cloud formation. And in both cases, initial air stratification is necessary: cool stale air - from above, and warm light air - from below. Warm air in this situation begins to rise upward, but it cannot rise from a flat evenly heated surface. For the rise, the irregularity availability is necessary, which can be a hill, a structure, a single tree, a car passing through the field, and a sandhill for sand vortex. These irregularities are called as triggers. Wind twists the air vortex around the trigger. Rotating mass current creates a column of mass current in which the particles rotate, move along radii, and circulate in vertical direction. This follows directly from arithmetic model.

The following pictures illustrate an analogy between the clouds and sand-devils.

References

1. A.M. Borovikov, I.I. Gayvoronsky and others. Physics of clouds. Leningrad: Hydrometeorological Publishing House, 1961. - 248 p. (in Russian)
2. Andreev A.O., Dukalskaya M.V., Golovina E.G. Clouds: origin, classification, recognition. - St. Petersburg: RSHU, 2007. - 228 p. (in Russian)
3. B. Kazhinsky, Rainfall Physics, "Technique - Youth," 1955, No. 1, pp. 28-32. (in Russian)
4. Why there are clouds. Mechanics of clouds.
<http://principact.ru/content/view/262/29/>
5. <https://ru.wikipedia.org/wiki/Облака> (in Russian)
6. R. Feynman, R. Leighton, M. Sands. The Feynman Lectures on Physics, v. 6, Electrodynamics.
7. Khmelnik S.I. Why Don't Clouds Fall?
<http://vixra.org/abs/1701.0605>, 2017-01-25.

| Облака | Пыльные вихри |
|---|--|
|  |  |
|  |  |
|  |  |
|  |  |
|  |  |

Chapter 4.2. Water Soliton

Contents

- 1. Introduction \ 54
- 2. Vertical stability \ 55
- 3. Soliton motion \ 58
- References \ 58

1. Introduction

The study of solitons began with the well-known Russell's observation on water soliton appearance and motion. Ever since, many different soliton mathematical models have appeared, and a water soliton became an insignificant special case of a large group of physical phenomena corresponding to these mathematical models [2-5]. However, to the author's knowledge, these models consider wave processes, and the processes of masses transfer are explicitly observed in water solitons. Sea wave transfers energy, but leaves water on its place - water only fluctuates in a vertical direction. Soliton transfers water - a tsunami that continues to move by land, should be the proof of it. In addition, water transfer in a horizontal direction cannot be explained by mass oscillation in a vertical direction and kinetic energy conversion into potential energy and vice versa. Water transfer in a horizontal direction must be connected with a horizontal flow of kinetic energy, which cannot be obtained from potential energy. We can remember the wind, but even in the first Russell's observation there was no wind. The concept of that the cause of soliton motion is the wind and environment nonlinearity seems unconvincing. It seems that this "device" inside has its own motor, and environmental resistance is only a catalyst, a force that presses on throttle pedal. This issue is discussed in more detail in Chapter 4.7.

It is shown that water soliton, being the "ancestor" of solitons theory, falls out of wave mathematical model of solitons. Therefore, the non-wave mathematical model is considered below, substance and energy flows within the water soliton are considered, energy source is revealed, its shape and causes of soliton shape and motion as a whole are explained. This model is completely similar to sand-devil mathematical model - see Chapter 4.1.

Let us first consider a soliton with cylindrical base. Its mathematical model is similar to sand vortex mathematical model. Flows

of gravitational energy, created by mass currents penetrate the soliton body. Formula dependencies between currents and energy flows are considered in Chapter 4.1. for sand vortex. The same dependencies can be used in this case.

2. Vertical stability

The apparent difference that should be justified is the bell shape of water soliton, in contrast to cylindrical shape of sand vortex. This difference is due to the fact that soliton upper layers press on the lower layers by gravity. Let us consider what this leads to.

In particular, there is an energy flow in soliton body directed vertically, with a density of

$$S_z = -j_\varphi h_\varphi r^2 \frac{\alpha}{2}. \quad (30)$$

This energy flow creates a pressure force acting in each section on the soliton body with R radius,

$$F_{z0} = -\frac{1}{c} \int_0^R S_z 2\pi r \cdot dr = \frac{1}{c} j_\varphi h_\varphi \pi \alpha \int_0^R r^3 \cdot dr = \frac{j_\varphi h_\varphi \pi \alpha R^4}{4c}. \quad (32)$$

As the energy flow (30) is directed downward, the oppositely directed force (32) is directed upward and supports the soliton in a vertical position. Its gravity counteracts and balances it.

Hence it follows that the radius of soliton should decrease upon z increase. Let us estimate the dependence of radius on z , designating it as $R(z)$. So,

$$F_{z0} = \frac{j_\varphi h_\varphi \pi \alpha}{4c} (R(z))^4. \quad (33)$$

The gravity of vortex part located above the level is equal to

$$P(z) = -\int_z^L p \cdot \pi (R(z))^2 dz. \quad (34)$$

where p – water density. Forces (33, 34) are balanced, i.e.

$$\frac{j_\varphi h_\varphi \pi \alpha}{4c} (R(z))^4 = \int_z^L p \cdot \pi (R(z))^2 dz. \quad (35)$$

Differentiating this expression, we obtain:

$$\frac{j_\varphi h_\varphi \pi \alpha}{4c} \cdot \frac{d}{dz} \left((R(z))^4 \right) = -p \cdot \pi (R(z))^2$$

or

$$(R(z)) \frac{d(R(z))}{dz} = -\eta, \tag{36}$$

where

$$\eta = \frac{pc}{j_\varphi h_\varphi \alpha}. \tag{36a}$$

$R(z)$ function is defined as solution of this equation. For this purpose, $R(0)$ initial condition must be specified. $R(z)$ and $R'(z)$ functions when $R(0) = 10$ and $\eta = 2$ - upper curves, $\eta = 3$ - lower curves are shown for illustration on Fig. 3.

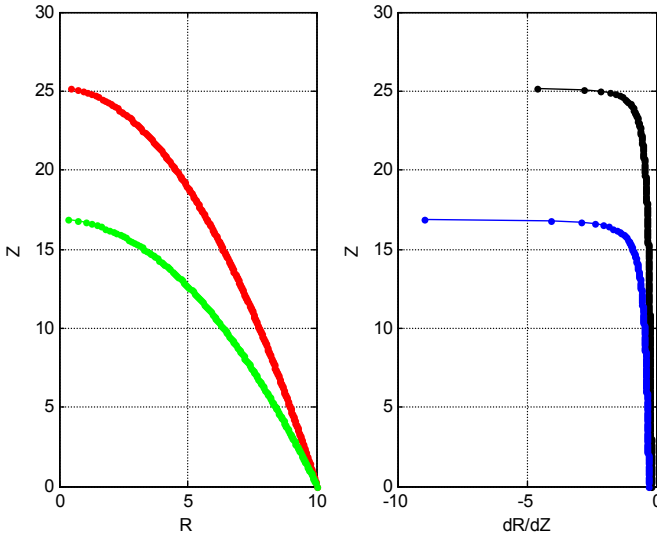


Fig. 3

Under this $R(z)$ we can find from (34) the soliton weight

$$P_o = -p \cdot \pi \int_0^L (R(z))^2 dz, \tag{37}$$

soliton volume

$$V_o = \pi \int_0^L (R(z))^2 \cdot dz \tag{38}$$

and height of soliton center of gravity

$$L_o = \frac{p \cdot \pi}{P_o} \int_0^L (R(z))^2 z \cdot dz. \tag{39}$$

Potential soliton energy

$$W_p = P_o L_o / g \quad (40)$$

where g - acceleration of gravity. Combining (39, 40), we find

$$W_p = \frac{P \cdot \pi}{g} \int_0^L (R(z))^2 z \cdot dz . \quad (41)$$

W_k soliton kinetic energy, in which the mass circulates "up and down" is equal to potential energy (if neglect the losses due to internal friction), i.e.

$$W_k \approx W_p . \quad (42)$$

This energy is the energy of mass currents. Losses of this energy due to internal friction are replenished with the energy of gravity field.

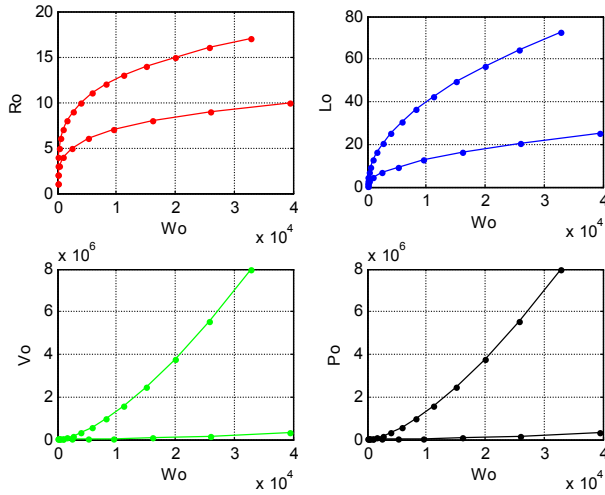


Fig. 4.

At the moment of soliton formation, it receives $W_o \approx W_k \approx W_p$ energy. It follows from (36, 41) that $R_o = R(0)$ initial radius depends on W_o initial energy (at given p, g, η). In turn, soliton height, shape, volume, and weight depend on $R(0)$. Let us consider these dependences when $p=1, g=10, \eta=2$ - see Fig. 4, where the upper curves refer to W_o values, indicated on axis, and the lower ones to $W_o/10$ values.

Fig. 5 shows the dependence of soliton height on $L_o = f(R_o)$ lower radius. The form of this function depends on coefficient to find η . With $L_o = f(R_o)$ function known from observations, we can find the value of coefficient to find η . Fig. 5 shows that coefficient is $\eta = 2, 4, 7$ (upper, middle, lower curves, respectively).

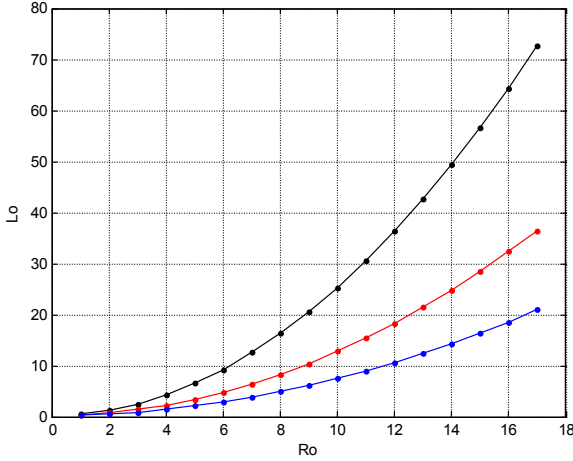


Fig. 5.

3. Soliton motion

Soliton motion path is poorly predictable and this soliton is similar to sand devil - see Section 4.1.5. When moving both the soliton and vortex, we need to take into account the fact that air resistance creates a secondary flow - a mass current directed against the velocity of their translational motion. Chapter 4.7 shows that this mass current creates a force directed by velocity of vortex translational motion (as paradoxical as it may sound).

Gravitational energy in soliton is converted into kinetic energy of internal jets of water, which in turn is converted into thermal frictional energy and into kinetic energy of soliton motion.

References

1. Khmel'nik S.I. Mathematical Model of Dust Whirl, <http://vixra.org/abs/1505.0087>, 2015-05-11.
2. Verin O.G. Soliton and physics, in Russian, <http://www.sciteclibrary.ru/rus/catalog/pages/12297.html>
3. Kudryashchov N.A. Nonlinear waves and solitons, 1997, , in Russian, <http://www.pereplet.ru/obrazovanie/stsoros/265.html>
4. The many-sided soliton, in Russian, <http://ilib.mccme.ru/djvu/bib-kvant/soliton.htm>
5. The theory of solitons. Mathematical description and physical applications, in Russian, http://ksit.psu.ru/dmdocuments/Solitons_auo_book.pdf

Chapter 4.3. Whirlpool

Contents

1. Introduction \ 59
2. Mathematical Model \ 60
3. The Equations of Hydrodynamics for a Whirlpool \ 62
4. The Computational Algorithm \ 63
5. The Analysis of the Whirlpool Equations \ 64
6. Energy Flows \ 66
7. Pressure \ 67
8. Conclusions 68
- Appendix 1 \ 69
- References \ 69

1. Introduction

Recently, there appeared a mathematical model of oceanic whirlpools [1], which is almost identical to the models built for space black holes. The similarity between the whirlpools and black holes is found in the fact that an object that happened to be near these objects becomes involved in them and never returns. Such a distant analogy stresses (in our opinion) the fact that this mathematical model is very far from completion. In the presented paper the author attempts to build such a model. This model, as well as above mentioned one, has the same base – the relativity theory. However, the proposed model is more downlanded (or, if you want, water-landed), because in it we use the equations of hydrodynamics and the consequences of the theory of relativity, which are relevant only in the case of low Earth's gravity.

Another question is also of interest – about the source of energy which enables the whirlpool to be spinning for a long time when surrounded by still waters. This issue becomes even more important due to the fact that the whirlpools (and not the Moon) are energy sources for the tide [2]. In [1] a source of energy whirlpools not analyzed. Below we show that this source is the Earth's gravitational field.

In the below presented mathematical model of the whirlpool we are using a system of MLG-equations of gravitomagnetism, described in Chapter 1. The model is based on the following assumptions: the motion

of water is likened to mass currents; the interaction between moving masses is described by gravity-magnetic Lorentz forces (GL-forces).

Mass currents in the vortex circulate along the horizontal sections of the vortex and along the vertical line. The kinetic energy of such circulation is expended on losses from internal friction. It comes from a gravitating body - the Earth. The potential energy of the vortex does not change and, therefore, is not expended. That is, in this case there is no transformation of the potential energy into kinetic energy and vice versa. However, the gravitating body expends its energy on creating and maintaining mass currents - see Chapter 3.

In the whirlpool the currents create intensities; the currents together with intensities create Lorentz forces; Lorentz forces act on the mass, moving in the current, thereby changing the direction of the currents. All these processes together are described by MLG-equations together, from which the Lorentz force are excluded. However, these processes can be traced consistently and be linked with the MLG-equations – see Chapter 3.

2. Mathematical Model

It would be interesting to compare the presented mathematical model with a real whirlpool – see Fig. 0.



Fig. 0a.



Fig. 0b.

In Chapter 2 shows, that MLG equations for gravity-magnetic intensities H and mass currents densities J for stationary gravity-magnetic field in cylindrical coordinates r , φ , z have the following form

$$\frac{H_r}{r} + \frac{\partial H_r}{\partial r} + \frac{1}{r} \cdot \frac{\partial H_\varphi}{\partial \varphi} + \frac{\partial H_z}{\partial z} = 0, \quad (1)$$

$$\frac{1}{r} \cdot \frac{\partial H_z}{\partial \varphi} - \frac{\partial H_\varphi}{\partial z} = J_r, \quad (2)$$

$$\frac{\partial H_r}{\partial z} - \frac{\partial H_z}{\partial r} = J_\varphi, \quad (3)$$

$$\frac{H_\varphi}{r} + \frac{\partial H_\varphi}{\partial r} - \frac{1}{r} \cdot \frac{\partial H_r}{\partial \varphi} = J_z, \quad (4)$$

$$\frac{J_r}{r} + \frac{\partial J_r}{\partial r} + \frac{1}{r} \cdot \frac{\partial J_\varphi}{\partial \varphi} + \frac{\partial J_z}{\partial z} = 0 \quad (5)$$

These equations describe, in fact, the processes of currents, tensions and Lorentz forces interaction, namely:

1. The intensity of the gravitational field is directed along the axis of whirlpool,

2. It creates a vertical mass flow - a mass current J_z .

3. Vertical mass current J_z generates annular gravity-magnetic field H_φ and radial gravity-magnetic field H_r - see (4).

4. Gravity-magnetic field H_φ deflects by GL-forces vertical mass flow in the radial direction, creating a radial mass flow - radial mass current J_r .

5. Gravity-magnetic field H_φ deflects by GL-forces radial mass flow perpendicular to the radius, creating a vertical mass current J_z .

6. Gravity-magnetic field H_r deflects by GL-forces vertical mass flow perpendicular to the radius, creating an annular mass current J_φ .

7. Gravity-magnetic field H_r deflects the GL-forces annular mass flow is perpendicular to the radius, creating a vertical mass current J_z .

8. The mass current J_r generates a vertical gravity-magnetic field H_z and annular gravity-magnetic field H_φ - see (2).

9. The mass current J_φ generates a vertical gravity-magnetic field H_z and radial gravity-magnetic field H_r - see (3)

10. The mass current J_z generates an annular gravity-magnetic field H_φ and radial gravity-magnetic field H_r - see (4).

GL-forces can be found as follows. Let us transform (1.3):

$$F_L = G \cdot \xi \cdot S_o, \quad (9)$$

where

$$S_o = (J \times H). \quad (10)$$

This vector product in cylindrical coordinates looks as:

$$S_o = \begin{bmatrix} S_{or} \\ S_{o\phi} \\ S_{oz} \end{bmatrix} = \begin{bmatrix} J_\phi H_z - J_z H_\phi \\ J_z H_r - J_r H_z \\ J_r H_\phi - J_\phi H_r \end{bmatrix}. \quad (11)$$

So, for a known solution of equations system (3-6, 8) the GL-forces can be found by (9-11).

3. The Equations of Hydrodynamics for a Whirlpool

Whirlpool, as the movement of water, also satisfies the Navier-Stokes equations for a viscous incompressible fluid. For stationary flow this equation has the following form (see, for instance, [3]):

$$\operatorname{div}(v) = 0, \quad (16)$$

$$\nabla p - \mu \cdot \Delta v + \rho(v \cdot \nabla)v - \rho F_m = 0, \quad (17)$$

where

ρ - permanent water density,

μ - coefficient of internal friction,

p - pressure,

v - the rate of flow in the given point, a vector,

F_m - mass force, a vector.

The mass current and the rate of flow are connected by an obvious relation

$$J = \rho \cdot v. \quad (18)$$

Therefore, the equations (7) and (16) are identical, and the equation (17) can be rewritten as

$$\nabla p - \frac{\mu}{\rho} \cdot \Delta J + \frac{1}{\rho} (J \cdot \nabla)J - \rho \cdot F = 0. \quad (19)$$

The mass forces here are GL-forces F_L and gravity forces P , or taking into account (2.9),

$$F = G \cdot \xi \cdot S_o + P. \quad (20)$$

For known currents and forces the pressure can be found from (19). So, the equations system

$$(2.1-2.5, 2.8.1-2.8.3, 19, 20) \quad (21)$$

is the equation system of whirlpool, permitting to find the distribution of speeds and pressures in the body of the whirlpool.

4. The Computational Algorithm

In Chapter 2 (Section 2) it is shown that for equations (1-5) there exists a solution in the form of functions having the following form:

$$H_{r\cdot} = h_r(r) \cdot \cos(\chi z), \quad (1)$$

$$H_{\varphi\cdot} = h_\varphi(r) \cdot \sin(\chi z), \quad (2)$$

$$H_{z\cdot} = h_z(r) \cdot \sin(\chi z), \quad (3)$$

$$J_{r\cdot} = j_r(r) \cdot \cos(\chi z), \quad (4)$$

$$J_{\varphi\cdot} = j_\varphi(r) \cdot \sin(\chi z), \quad (5)$$

$$J_z = j_z(r) \cdot \sin(\chi z). \quad (6)$$

where χ is a constant, and $h_r(r)$, $h_\varphi(r)$, $h_z(r)$, $j_r(r)$, $j_\varphi(r)$, $j_z(r)$ is a function of the coordinate r ; the derivatives of these functions will be denoted by primes.

In Chapter 2 it is shown that after substituting (9-14) into (1-5), the following system of equations is obtained:

$$h_z = -(h_r/r + h'_r)/\eta, \quad (18)$$

$$j_z = h_\varphi/r + h'_\varphi, \quad (19)$$

$$j_r = -\eta h_\varphi, \quad (20)$$

$$j_\varphi = -\eta h_r - h'_z. \quad (21)$$

In this system of 4-th differential equations with 6-th unknown functions, two functions can be defined arbitrarily. In Appendix 1 it is shown that the solution of this system of equations can have the following form:

$$h_r(r) = -h \cdot e^{br^n}, \quad (22)$$

$$h_\varphi(r) = -q \cdot e^{br^m}, \quad (23)$$

$$h_z(r) = \frac{h \cdot e^{br^n}}{\eta \cdot r} (1 + bnr^n), \quad (24)$$

$$j_r(r) = \eta q \cdot e^{br^m}, \quad (25)$$

$$j_\varphi(r) = -h \cdot e^{br^n} \left(\eta + \frac{1}{\eta r^2} (bn^2 r^n (br^n + n) - 1) \right), \quad (26)$$

$$j_z(r) = -\frac{q \cdot e^{br^m}}{r} (1 + bmr^m). \quad (27)$$

Algorithm of the system (3.21) solution can be, for instance, as follows:

1. determine the intensities and currents $(h_r, h_\varphi, h_z, j_r, j_\varphi, j_z)$ from (2.2-2.7),
2. determine GL-forces from (2.8.1-2.8.3),
3. determine mass forces from Π_0 (3.20),
4. determine the pressures from (3.19).

5. The Analysis of the Whirlpool Equations

Now we shall analyse the solution (4.22-4.27). The origin will be located on the ocean surface, and the axis oz will direct straight up.

Example 1.

In Fig. 1 shows the functions (4.22-4.27) at $q = 1, h = 3, m = 3.5, n = 3.6, b = -0.05, \chi = 1$. The left column shows the functions (h_r, h_φ, h_z) , and in the right column shows the functions (j_r, j_φ, j_z) . It is seen that there is a certain radius $r = R_b$ at which $J_z = 0$. Let us call the radius of "vertical calm": at $r < R_b$ the current $J_z < 0$ directed down, and at $r > R_b$ the current $J_z > 0$ directed up. In this case .

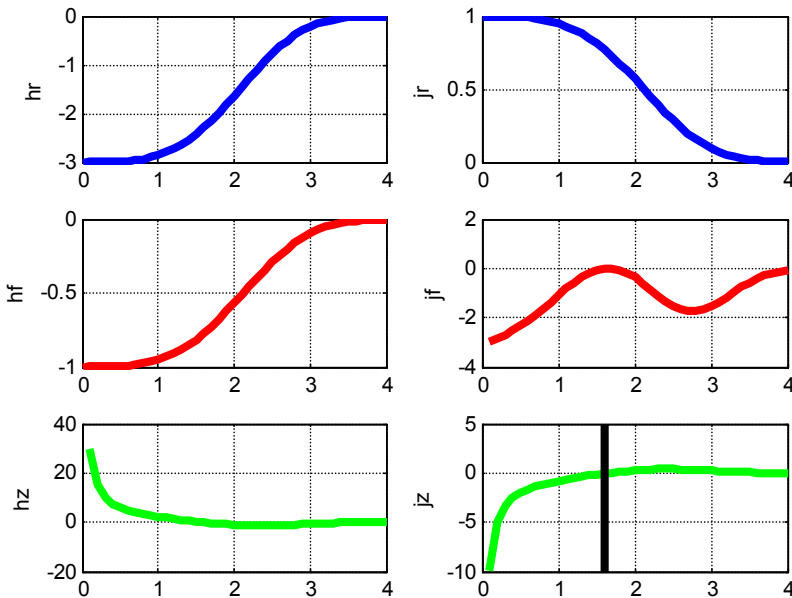


Fig.1. (fig-Vod-1.m)

So, there exists a certain radius of "vertical calm" for which the vertical flow of water is not present ($J_z = 0$), and more close to the

center of whirlpool the water flow is directed down ($J_z < 0$), but with increasing distance from this radius the water begins to rise ($J_z > 0$). And so the water of surrounding ocean pours into the funnel with this radius of "vertical calm".

Let us look now on the vector field of the currents J_r , J_z in the vertical plane of the whirlpool section. The Fig 2 shows fragment of this field for the part of the plane $r = \overline{0, 3}$ and $z = \overline{0, -1.4}$ for the same value of the constants. It shows also "the vertical of calm". One can see that the mass currents (equivalent to the speeds) decrease drastically when the distance to the whirlpool center increases.

So we see that the mass currents in the whirlpool circulate vertically. Wherein in a small central area the mass of water moves down with great speed, and in the distant, but large area the water rises up with low speed. On the free surface of the ocean along the axis a recess is formed and along the borders the elevation is formed - this can be seen in Fig. 2, if you mentally unite the ends of the arrows in the upper horizontal. The water rushes from the elevation to the recess. The kinetic energy of such circulation is expended only on the losses of internal friction. The potential energy does not change. It means that in this case there is no transformation of potential energy into kinetic energy and vice versa. However (as we already indicated) the gravitating body expends its energy for creating and maintaining the mass currents – see Chapter 3.

Now let us consider the vector field of currents J_r , J_φ on the circle in horizontal plane of whirlpool for the same values of constants – see Fig. 4. There the analyzed points located on the "dotted" radii are designated by circles. "Green (light)" short segments show the vectors of currents proportional to the speeds, and the "blue (dark)" segments combine the ends of these vectors. Evidently, the distribution of vectors recalls Fig. 0b. One can see that on small radii the speeds are directed tangentially to the circle, and with increase of the radius the radial components of the overall speed also are increasing, but the overall speed is decreasing.

As shown in the general case, there is a movement along the helix. When $\eta \cdot z$ is a member in formula (4.9-4.14) the helical line is cylindrical, and when function $\chi(z)$ is present instead of $\eta \cdot z$, a conical helical line appears. This case is discussed in detail in Chapter 4.1.

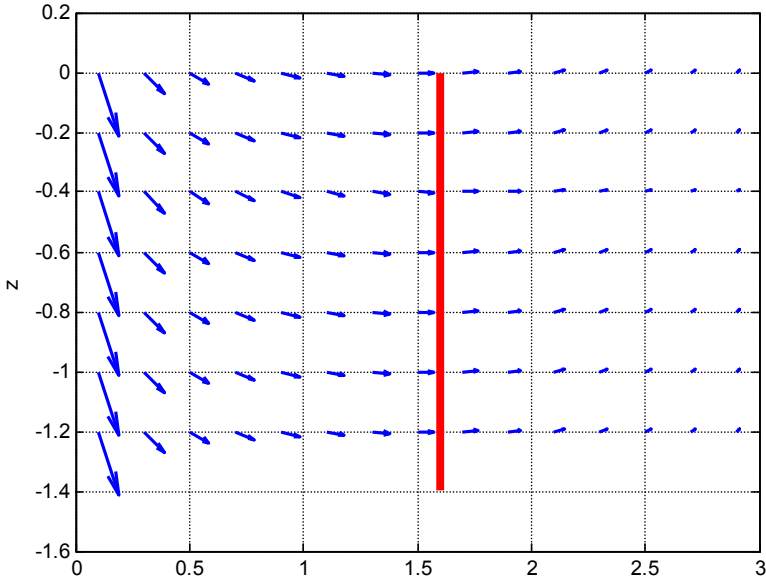


Fig. 2 (Glubina.m)

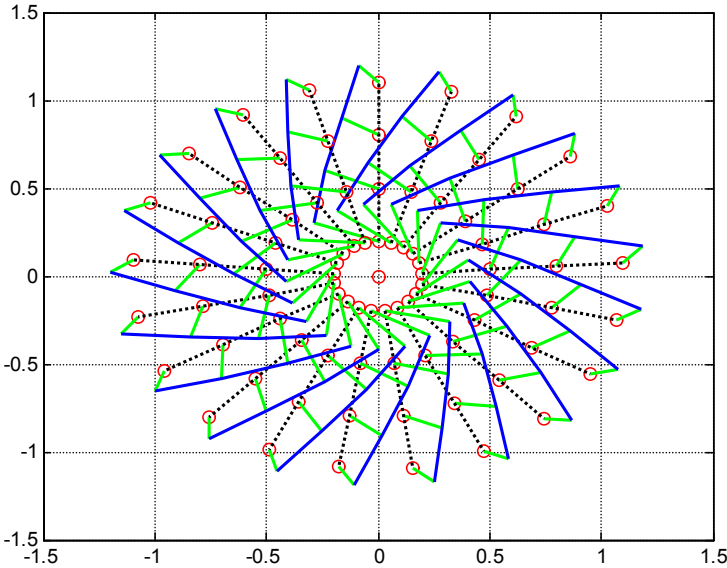


Fig.4 (Volny.m)

6. Energy Flows

Energy flows are described in this case in the same way as in Chapter 4.1. In accordance with (2.11), we consider only the functions, shown in Fig. 5:

$$\begin{bmatrix} \overline{S_r}(r) \\ \overline{S_\varphi}(r) \\ \overline{S_z}(r) \end{bmatrix} = \begin{bmatrix} (j_\varphi h_z - j_z h_\varphi) \\ (j_z h_r - j_r h_z) \\ (j_r h_\varphi - j_\varphi h_r) \end{bmatrix}. \quad (1)$$

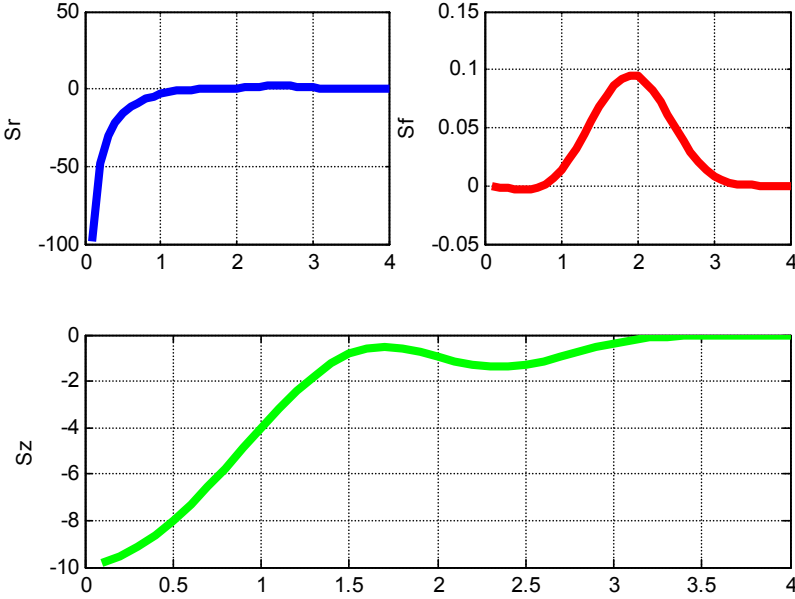


Fig.5. (fig-Vod-1.m)

Just as in Chapter 4.1, it can be shown that, что in a whirlpool the flow of energy circulates vertically. Consequently, the energy of vertical circulation remains constant. The potential energy of the whirlpool also remains constant. Thus, in this case, there is no conversion of potential energy into kinetic energy and vice versa. The energy flux circulates also along the rim. Radial flow of energy is spent on compensation for the losses from internal friction. This energy can come only from the outside - from a gravitating body (as already pointed out (as already indicated - see Chapter 3)).

7. Pressure

In conclusion let us consider the calculation of pressure in the whirlpool with the help of the algorithm described in Section 4. The pressure will be determined by formula (3.19), and the mass forces - by formula (3.20). Thus,

$$\nabla p = \frac{\mu}{\rho} \cdot \Delta J - \frac{1}{\rho} (J \cdot \nabla) J + \rho \cdot G \cdot \xi \cdot S_o + \rho \cdot P. \quad (1)$$

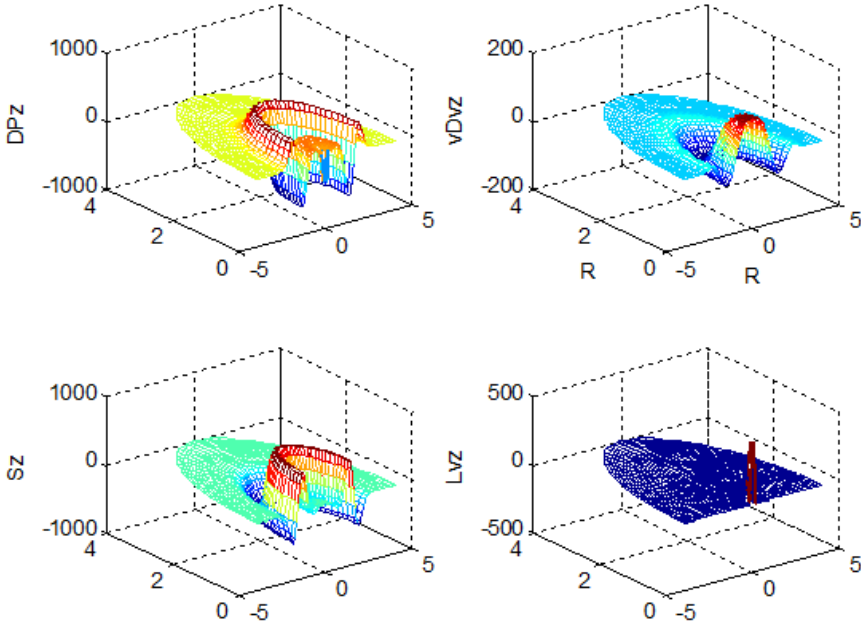


Fig. 6 (VodovorotFig.m)

Fig. 10 shows the values from (1) and calculated for the surface of whirlpool for $z = 0$. In the calculation we have used the previous values of the constants and the following values of constants from (1):

$$\frac{\mu}{\rho} = 10^{-8}, \quad \frac{1}{\rho} = 1, \quad \rho \cdot G \cdot \xi, \quad \rho \cdot P = 1. \quad (2)$$

The windows in Fig. 10 show projections on the axis z for $z = 0$ of the following values:

$$DPz = \nabla p, \quad Lvz = \frac{\mu}{\rho} \Delta J, \quad vDvz = (J \cdot \nabla) J, \quad Sz = S_o. \quad (3)$$

The pressures on the free surface reflect the form of whirlpool's surface.

8. Conclusions

Based on the determined assumptions a system of whirlpool equations was built and one of the possible solutions was found. This solution explains the observed phenomena, namely

- vertical circulation of water: the active fall of water in the center of whirlpool and the rising of water from the depths with low speed, but on a great space.,

- horizontal rotation of water around the circumference with forming linear waves, at an angle to the tangent of the circle,
- form of whirlpool's surface,
- the existence of energy source of whirlpool energy in a calm ocean.

Appendix 1.

Для решения 4-х уравнений (4.18-4.21) с 6-ю неизвестными функциями для дальнейшего мы определим следующие две функции:

$$h_{\varphi}(r) = -q \cdot e^{br^m}, \quad (1)$$

$$h_r(r) = -h \cdot e^{br^n}, \quad (2)$$

где h , q , b , m , n – некоторые константы. Тогда

$$h'_{\varphi}(r) = -q b m r^{m-1} \cdot e^{br^m}, \quad (3)$$

$$h'_r(r) = -h b n r^{n-1} \cdot e^{br^n}. \quad (4)$$

Из (3.20) находим:

$$j_r(r) = \eta q \cdot e^{br^m}. \quad (5)$$

Из (3.18) находим:

$$h_z = \frac{h \cdot e^{br^n}}{\eta \cdot r} (1 + b n r^n). \quad (6)$$

Аналогично, из (3.19) находим:

$$j_z = \frac{h_{\varphi}}{r} + h'_{\varphi}, \quad (7)$$

$$j_z = -\frac{q \cdot e^{br^m}}{r} (1 + b m r^m). \quad (8a)$$

Найдем из (6):

$$h'_z = \frac{h}{\eta} \left(\left(\frac{e^{br^n}}{r} \right)' (1 + b n r^n) + \left(\frac{e^{br^n}}{r} \right) (1 + b n r^n)' \right),$$

$$h'_z = \frac{h}{\eta} \left(\left(\frac{b n r^{n-1} e^{br^n}}{r} - \frac{e^{br^n}}{r^2} \right) (1 + b n r^n) + \left(\frac{e^{br^n}}{r} \right) b n n r^{n-1} \right),$$

$$h'_z = \frac{h}{\eta} e^{br^n} \left(\left(\frac{b n r^n}{r^2} - \frac{1}{r^2} \right) (1 + b n r^n) + \left(\frac{1}{r^2} \right) b n n r^n \right),$$

$$\begin{aligned}
 h'_z &= \frac{h}{\eta} e^{br^n} \frac{1}{r^2} (b^2 r^{2n} n n + b n r^n (n - n + n n) - 1), \\
 h'_z &= \frac{h}{\eta} e^{br^n} \frac{1}{r^2} (b n^2 r^n (b r^n + n) - 1).
 \end{aligned} \tag{9}$$

При известной функции $h'_z(\mathbf{r})$ по (2, 3.21) находим:

$$j_\varphi = -h \cdot e^{br^n} \left(\eta + \frac{1}{\eta r^2} (b n^2 r^n (b r^n + n) - 1) \right). \tag{10}$$

Итак, далее мы будем использовать решение системы (4.18-4.21) в виде функций $(h_r, h_\varphi, h_z, j_r, j_\varphi, j_z)$, определенных по (2, 1, 6, 5, 10, 8) соответственно.

References

1. Francisco J. Beron-Vera, Yan Wang, María J. Olascoaga, Gustavo J. Goni, George Haller, Objective Detection of Oceanic Eddies and the Agulhas Leakage. *J. Phys. Oceanogr.*, 43, 1426–1438, 2013.
2. Khizirow U.S. The ebb and flow - the result of the precession of the whirlpools. «The Papers of Independent Authors», Publisher «DNA», Russia-Israel, Printed in USA, Lulu Inc., catalogue 16537771, vol. 33, 2015, ISBN 978-1-329-02052-8 (in Russian).
3. Khmelnik S.I. Navier-Stokes equations. On the existence and the search method for global solutions. Second edition. Published by “MiC” - Mathematics in Computer Comp., printed in USA, printed in USA, Lulu Inc., ID 9976854, Israel, 2011, ISBN 978-1-4583-2400-9
4. Khmelnik S.I. Mathematical Model of Dust Whirl, <http://vixra.org/abs/1505.0087>, 2015-05-11.
5. Khmelnik S.I. The Equation of Whirlpool, <http://vixra.org/abs/1506.0157>, 2015-06-21.

Chapter 4.4. Saturn's Hexagon

Contents

- 1. Introduction \ 71
- 2. Brief description of the Earth whirlpool mathematical model \ 73
- 3. Brief description of the Earth whirlpool mathematical model \ 74
- 4. Mathematical model of an elliptical whirlpool \ 79
- Appendix 1. Solution of Maxwell's equations in elliptical cylindrical coordinates \ 80
- Appendix 2. Decomposition of a hexagon into ellipses \ 92
- References \ 85

1. Introduction

A giant storm in the form of a hexagon, each side of which is larger than Earth diameter exists at the north pole of Saturn [1, 2, 3]. This hexagon does not move on the planet, it rotates and holds its shape. It has an amazing stability - for more than 30 years. A lot of studies are devoted to such a storm mathematical model construction, but the recognized model is absent [3]. A mathematical model of such a storm, similar to mathematical model of the ocean whirlpool, given in Section 3.1 is proposed below. It is shown that the energy source, allowing the storm to rotate for a long time, is a gravitational field of Saturn.

An external similarity between this storm and the ocean whirlpool is evident - see Fig. 1 and Fig. 2. The main difference relates to surface shape. It can be said, emphasizing this analogy, that there is a hexagon "gas whirlpool" on Saturn, in contrast to round ocean whirlpool on Earth.

Let us also note that hexagon gas whirlpools are also observed under terranean conditions: satellite images analysis has shown the clouds of hexagonal form presence above the anomalous zone in Atlantic Ocean known as the Bermuda Triangle - see Fig. 3 [4].

Firstly, a mathematical model of elliptical whirlpool is constructed. It is constructed by analogy with mathematical model of a circular whirlpool - see Section 4.3.

Then a hexagon gas whirlpool is the sum of elliptical gas whirlpools is shown. Each gas whirlpool is determined by its own initial conditions in Maxwell's equations. When there are several independent

initial conditions, several solutions-elliptical gas whirlpools appear. As the system of Maxwell's equations is linear, then a real solution is the sum of these solutions. The sum has the form of a hexagon whirlpool.

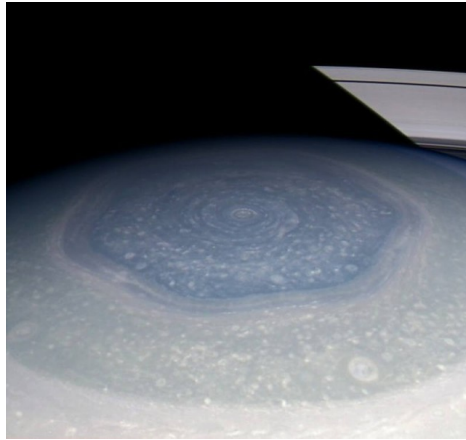


Fig. 1.



Fig. 2.



Fig. 3.

2. Brief description of the Earth whirlpool mathematical model

Whirlpool mathematical model uses the system of Maxwell-like gravitational equations - see Chapter 1. The model is based on the following assumptions. Water movement assimilates to mass currents. Interaction between the moving masses is described by gravitomagnetic Lorentz forces (hereinafter GL-forces), similar to Lorentz forces in electrodynamics, acting between the moving electric charges.

Mass currents in a whirlpool circulate along the helix line, in which the radius varies exponentially (see Fig. 2.8.7). Kinetic energy of such circulation is consumed for the losses from internal friction. It comes from a gravitating body - Earth. Whirlpool potential energy does not change and, therefore, is not consumed. In other words in this case potential energy is not converted into kinetic energy and vice versa. However, a gravitating body consumes its energy for mass currents creation and maintenance, i.e. for whirlpool retention.

The whirlpool as water movement also complies with Navier-Stokes equation for incompressible viscous liquid. Section 4.3 shows that the water pressure in whirlpool can be calculated by Navier-Stokes equation depending on mass currents. It is found that the locus of points with a constant value of vertical pressure component on a free surface is a circle of a given radius. The pressure on free surface reflects the shape of whirlpool surface. Consequently, the concentric protrusions and cavities, corresponding to wave-like pressure dependence on radius should be on the whirlpool surface. On the basis of this, Section 4.3 presents the whirlpool surface pattern - see Fig. 4 (fragment of Fig. 4.3.10).

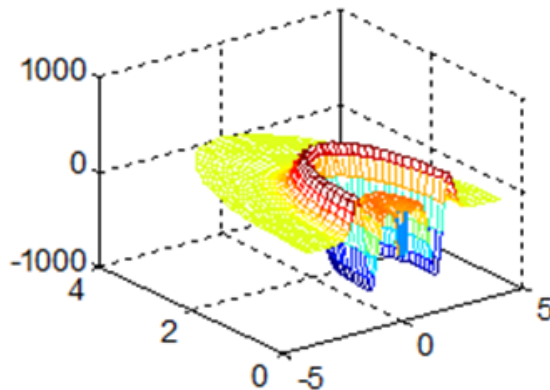


Fig. 4.

A similar approach is used below. It only remains to show that a solution of Maxwell's equations for elliptical whirlpool and, further, for hexagon whirlpool is available.

4. Mathematical model of an elliptical whirlpool

Maxwell's equations for a stationary gravitomagnetic field are the following (see (1.10-1.12) in Chapter 2):

$$\operatorname{div}(H) = 0, \quad (1)$$

$$\operatorname{div}(J) = 0, \quad (2)$$

$$\operatorname{rot}(H) = J, \quad (3)$$

where H - gravitomagnetic tensions, J - densities of mass currents.

Let us consider these equations in ξ , φ , z elliptical coordinates [5, p. 161] - see also Fig. 5:

$$\operatorname{div}(H) = \left(\frac{1}{a\Delta^3} (\operatorname{sh}(\xi)\operatorname{ch}(\xi)H_\xi + \sin(\varphi)\cos(\varphi)H_\varphi) + \frac{1}{a\Delta} \left(\frac{\partial H_\xi}{\partial \xi} + \frac{\partial H_\varphi}{\partial \varphi} \right) + \frac{\partial H_z}{\partial z} \right) = 0, \quad (4)$$

$$\operatorname{rot}_\xi(H) = \left(\frac{1}{a\Delta} \frac{\partial H_z}{\partial \varphi} - \frac{\partial H_\varphi}{\partial z} \right) = J_\xi, \quad (5)$$

$$\operatorname{rot}_\varphi(H) = \left(\frac{\partial H_\xi}{\partial z} - \frac{1}{a\Delta} \frac{\partial H_z}{\partial \xi} \right) = J_\varphi, \quad (6)$$

$$\operatorname{rot}_z(H) = \left(\frac{1}{a\Delta^3} (\operatorname{ch}(\xi)\operatorname{sh}(\xi)H_\varphi - \cos(\varphi)\sin(\varphi)H_\xi) + \frac{1}{a\Delta} \left(\frac{\partial H_\varphi}{\partial \xi} - \frac{\partial H_\xi}{\partial \varphi} \right) \right) = J_z, \quad (7)$$

$$\operatorname{div}(J) = \left(\frac{1}{a\Delta^3} (\operatorname{sh}(\xi)\operatorname{ch}(\xi)J_\xi + \sin(\varphi)\cos(\varphi)J_\varphi) + \frac{1}{a\Delta} \left(\frac{\partial J_\xi}{\partial \xi} + \frac{\partial J_\varphi}{\partial \varphi} \right) + \frac{\partial J_z}{\partial z} \right) = 0, \quad (7a)$$

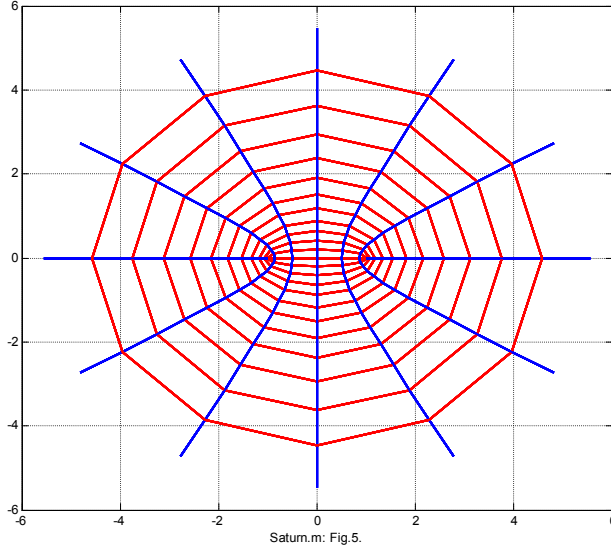
where

$$\Delta = \sqrt{(\operatorname{ch}^2(\xi) - \cos^2(\varphi))}, \quad (7b)$$

a - semi-focal distance,

ξ , φ , z coordinates are related to x , y , z rectangular coordinates by the following formulas

$$x = a\text{ch}(\xi)\cos(\varphi), \quad y = a\text{sh}(\xi)\sin(\varphi), \quad z = z. \quad (7c)$$



For fixed ξ , z , the point describes an ellipse in a horizontal plane. For fixed φ , z , the point describes a hyperbola in a horizontal plane. In particular, Fig. 5 shows the ellipses and hyperbolas constructed according to (7c) when $a = 1$, depending on $0 \leq \xi < 1.2$, $0 \leq \varphi < 2\pi$.

One of the possible solutions of equations (4-7a) is of the following form (as shown in Appendix 1):

$$H_{\xi} = h_{\xi}\Delta^{-2}\sin(\varphi)\cos(\varphi), \quad (8)$$

$$H_{\varphi} = h_{\varphi}\Delta^{-2}\text{sh}(\xi)\text{ch}(\xi), \quad (9)$$

$$H_z = \Delta^{-2}, \quad (10)$$

$$J_{\xi} = \frac{2}{a\Delta^5}\sin(\varphi)\cos(\varphi), \quad (11)$$

$$J_{\varphi} = -\frac{2}{a\Delta^5}\text{sh}(\xi)\text{ch}(\xi), \quad (12)$$

$$J_z = \frac{3}{a\Delta^5}(h_{\varphi}\text{sh}^2(\xi)\text{ch}^2(\xi) - h_{\xi}\sin^2(\varphi)\cos^2(\varphi)), \quad (13)$$

where h_{ξ} , h_{φ} constants are associated with the form correlation

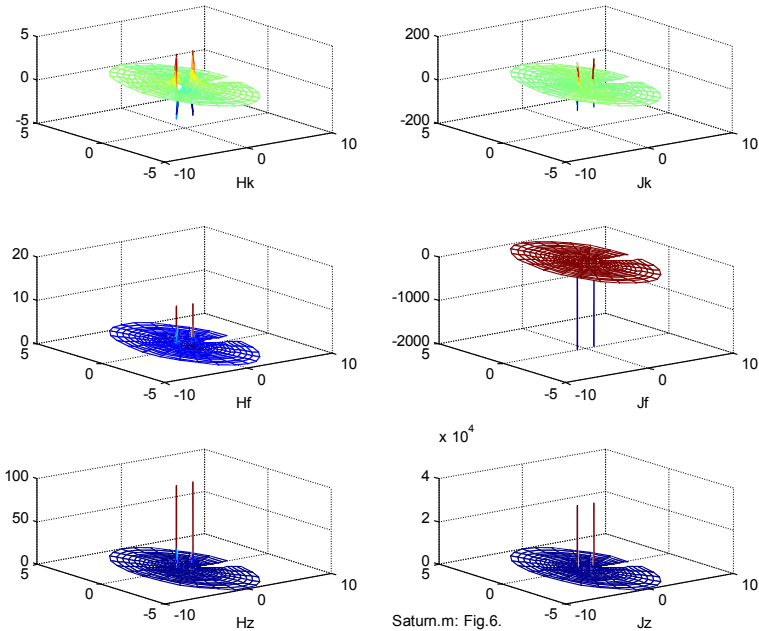
$$h_\xi + h_\varphi = 0. \tag{14}$$

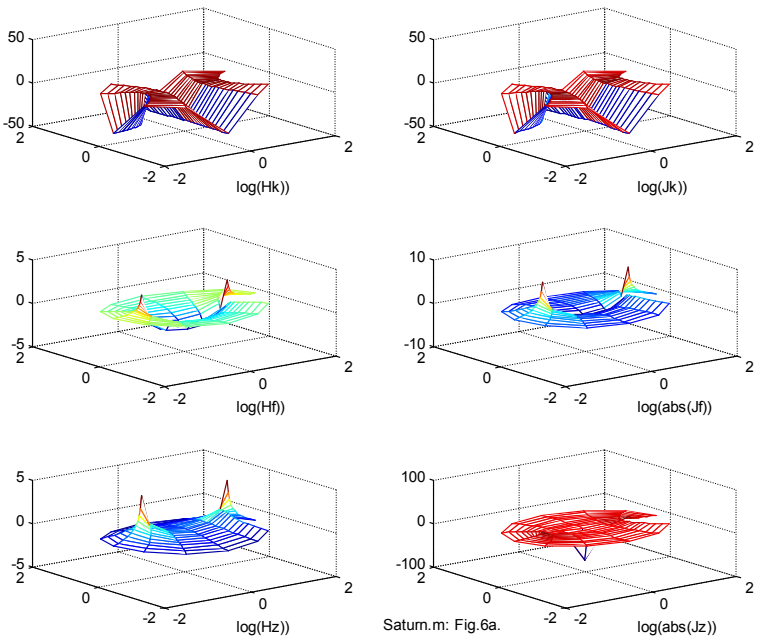
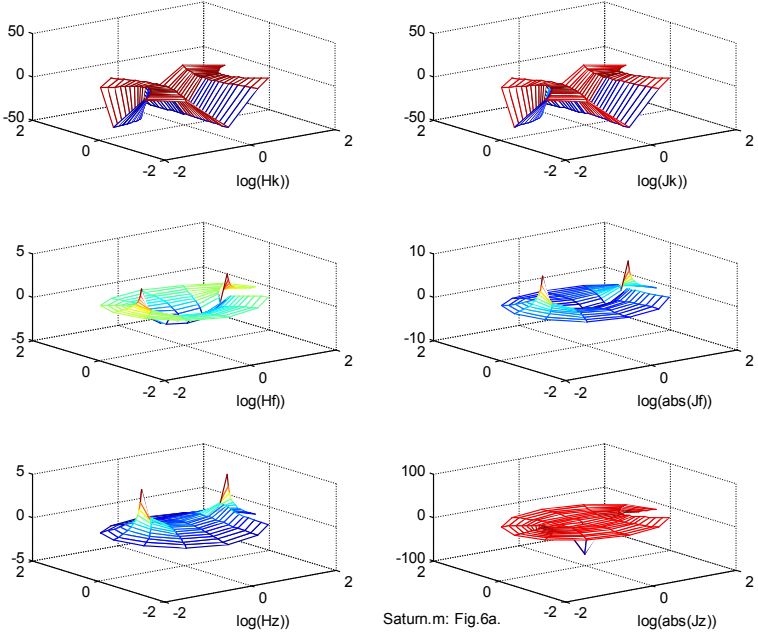
Fig. 6 shows the graphs of functions (8-13) when $a=1$, $h_\xi=1$, $h_\varphi=-1$ on (x, y) plane, where (x, y) are determined by (7c) depending on $0 \leq \xi < \xi_{\max}$, $0 \leq \varphi < 2\pi$. Fig. 6a shows the same graphs, but on a logarithmic scale for illustration purposes.

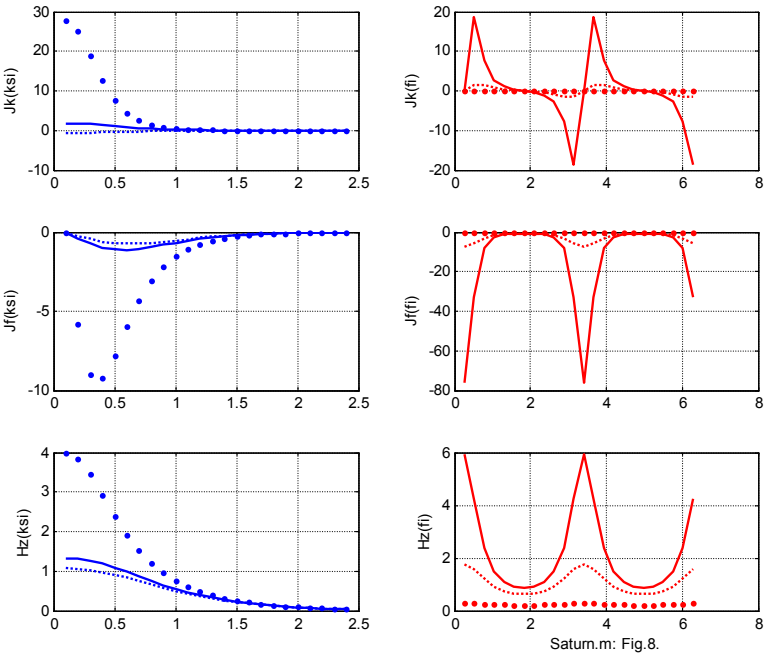
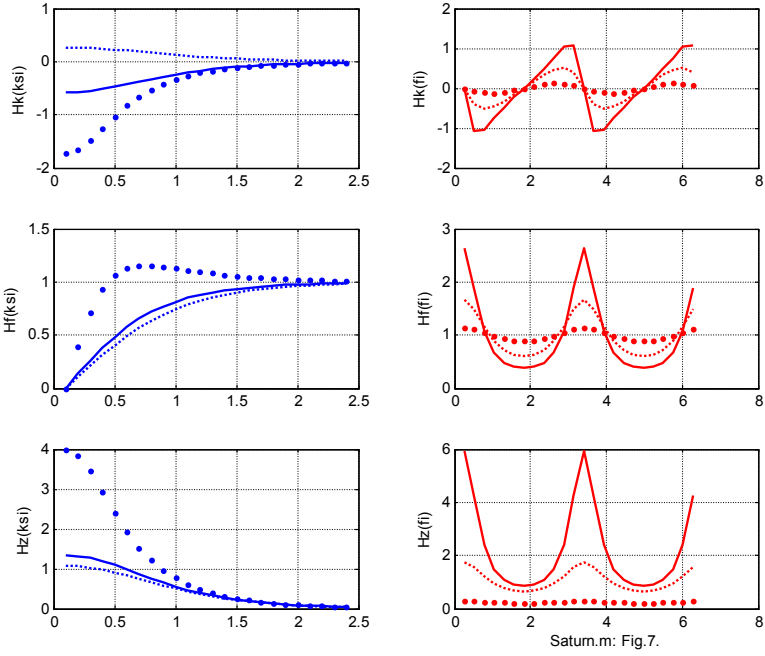
In the left column of Fig. 7 $H_\xi(\xi)$, $H_\varphi(\xi)$, $H_z(\xi)$ functions for a given φ value are shown. In this case, these functions are denoted by the solid line, dots and dashed lines when $\varphi=1.05, 1.83, 3.67$ correspondingly.

In the right column of Fig. 7 $H_\xi(\varphi)$, $H_\varphi(\varphi)$, $H_z(\varphi)$ functions for a given ξ value are shown. In this case, these functions are denoted by the solid line, dots and dashed lines when $\xi=0.4, 0.7, 1.4$ correspondingly.

Finally, Fig. 8 shows $J_\xi(\xi)$, $J_\varphi(\xi)$, $J_z(\xi)$ and $J_\xi(\varphi)$, $J_\varphi(\varphi)$, $J_z(\varphi)$ functions in the same manner.







4. Mathematical model of a hexagon whirlpool

The pattern shown in Fig. 4 is determined by initial conditions - mass currents at the whirlpool base. When there are several groups of independent initial conditions, several solutions of specified type appear. Since the system of Maxwell's equations is linear, then a real solution is the sum of these several solutions. If the group of initial conditions defines a group of elliptical whirlpools with a common center, then the summarized solution will determine a whirlpool with the sum of ellipses configuration.

It can be shown that the sum of ellipses configuration has the form of a closed curve F. This means that the locus of points with a constant value of vertical pressure component on a free surface differs from the circle of a given radius and has the form of a closed curve F. A vertical pressure component value will have the same magnitude on this curve F. Consequently, in this case the concentric curves F should be observed instead of concentric circles on the whirlpool surface.

Any closed convex curve F can be decomposed into the sum of ellipses. For the proof let us note the following. Any such curve can be represented by two functions of φ angle:

$$x = f_x(\varphi), \quad (1)$$

$$y = f_y(\varphi). \quad (2)$$

Discrete functions (1, 2) presented in such manner can be expanded into trigonometric series of the form

$$x = \sum_{n=2}^N x_n, \quad (3)$$

$$y = \sum_{n=2}^N y_n, \quad (4)$$

where

$$x_n = \left(\alpha_n \cos\left(\frac{2\pi(n-1)}{N}\varphi\right) + \beta_n \sin\left(\frac{2\pi(n-1)}{N}\varphi\right) \right), \quad (5)$$

$$y_n = \left(\eta_n \cos\left(\frac{2\pi(n-1)}{N}\varphi\right) + \lambda_n \sin\left(\frac{2\pi(n-1)}{N}\varphi\right) \right). \quad (6)$$

Here, each pair of (x_n, y_n) addends represents an ellipse. Consequently, a curve F is the sum of ellipses.

Appendix 2 describes the decomposition of a hexagon into ellipses. A solution for elliptical whirlpool is shown above. Consequently, a group of initial conditions for hexagon whirlpool formation can exist. Observations on Saturn and the Bermuda Triangle show that the combinations of initial conditions mentioned above can exist.

Appendix 1. Solution of Maxwell's equations in elliptical cylindrical coordinates

Section 3 shows the Maxwell's equations in ξ, φ, z elliptical coordinates (3.4 - 3.7a).

Let us search for the solution of these equations based on assumption that all variables don't change along z axis. Then equations (2, 11-13, 14) will take the form of:

$$\frac{1}{\Delta^2} (\text{sh}(\xi)\text{ch}(\xi)H_\xi + \sin(\varphi)\cos(\varphi)H_\varphi) + \left(\frac{\partial H_\xi}{\partial \xi} + \frac{\partial H_\varphi}{\partial \varphi} \right) = 0, \quad (1)$$

$$\frac{1}{a\Delta} \frac{\partial H_z}{\partial \varphi} = J_\xi, \quad (2)$$

$$-\frac{1}{a\Delta} \frac{\partial H_z}{\partial \xi} = J_\varphi, \quad (3)$$

$$\left(\frac{1}{a\Delta^3} (\text{ch}(\xi)\text{sh}(\xi)H_\varphi - \cos(\varphi)\sin(\varphi)H_\xi) + \frac{1}{a\Delta} \left(\frac{\partial H_\varphi}{\partial \xi} - \frac{\partial H_\xi}{\partial \varphi} \right) \right) = J_z, \quad (4)$$

$$\frac{1}{\Delta^2} (\text{sh}(\xi)\text{ch}(\xi)J_\xi + \sin(\varphi)\cos(\varphi)J_\varphi) + \left(\frac{\partial J_\xi}{\partial \xi} + \frac{\partial J_\varphi}{\partial \varphi} \right) = 0. \quad (5)$$

From (3.7b) we find:

$$\frac{\partial(\Delta^{-2})}{\partial \xi} = \frac{\partial(\text{ch}^2(\xi) - \cos^2(\varphi))^{-1}}{\partial \xi} = 2\Delta^{-4} \text{sh}(\xi)\text{ch}(\xi), \quad (6)$$

$$\frac{\partial(\Delta^{-2})}{\partial \varphi} = \frac{\partial(\text{ch}^2(\xi) - \cos^2(\varphi))^{-1}}{\partial \varphi} = 2\Delta^{-4} \sin(\varphi)\cos(\varphi). \quad (7)$$

Let us assume that

$$H_\xi = h_\xi \Delta^{-2} \sin(\varphi)\cos(\varphi), \quad (8)$$

$$H_\varphi = h_\varphi \Delta^{-2} \text{sh}(\xi)\text{ch}(\xi). \quad (9)$$

Then

$$\frac{\partial H_\xi}{\partial \xi} = h_\xi \sin(\varphi)\cos(\varphi) \frac{\partial(\Delta^{-2})}{\partial \xi} = 2\Delta^{-4} h_\xi \sin(\varphi)\cos(\varphi) \text{sh}(\xi)\text{ch}(\xi), \quad (10)$$

$$\frac{\partial H_\xi}{\partial \varphi} = h_\xi \sin(\varphi) \cos(\varphi) \frac{\partial(\Delta^{-2})}{\partial \varphi} = 2\Delta^{-4} h_\xi \sin^2(\varphi) \cos^2(\varphi), \quad (11)$$

$$\frac{\partial H_\varphi}{\partial \varphi} = h_\varphi \operatorname{sh}(\xi) \operatorname{ch}(\xi) \frac{\partial(\Delta^{-2})}{\partial \varphi} = 2h_\varphi \Delta^{-4} \operatorname{sh}(\xi) \operatorname{ch}(\xi) \sin(\varphi) \cos(\varphi), \quad (12)$$

$$\frac{\partial H_\varphi}{\partial \xi} = h_\varphi \operatorname{sh}(\xi) \operatorname{ch}(\xi) \frac{\partial(\Delta^{-2})}{\partial \xi} = 2\Delta^{-4} h_\varphi \operatorname{sh}^2(\xi) \operatorname{ch}^2(\xi). \quad (13)$$

From (1, 8-13) we find:

$$\frac{1}{\Delta^2} \left(\operatorname{sh}(\xi) \operatorname{ch}(\xi) h_\xi \Delta^{-2} \sin(\varphi) \cos(\varphi) + \right) + \left(\frac{2\Delta^{-4} h_\xi \sin(\varphi) \cos(\varphi) \operatorname{sh}(\xi) \operatorname{ch}(\xi) +}{2\Delta^{-4} h_\varphi \operatorname{sh}(\xi) \operatorname{ch}(\xi) \sin(\varphi) \cos(\varphi)} \right) = 0$$

or

$$3h_\xi \sin(\varphi) \cos(\varphi) \operatorname{sh}(\xi) \operatorname{ch}(\xi) + 3h_\varphi \operatorname{sh}(\xi) \operatorname{ch}(\xi) \sin(\varphi) \cos(\varphi) = 0$$

or

$$h_\xi + h_\varphi = 0. \quad (14)$$

From (4, 8-13) we find:

$$\left(\frac{1}{a\Delta^3} \left(\operatorname{ch}(\xi) \operatorname{sh}(\xi) h_\varphi \Delta^{-2} \operatorname{sh}(\xi) \operatorname{ch}(\xi) - \cos(\varphi) \sin(\varphi) h_\xi \Delta^{-2} \sin(\varphi) \cos(\varphi) \right) + \right. \\ \left. \frac{1}{a\Delta} \left(2\Delta^{-4} h_\varphi \operatorname{sh}^2(\xi) \operatorname{ch}^2(\xi) - 2\Delta^{-4} h_\xi \sin^2(\varphi) \cos^2(\varphi) \right) \right) = J_z$$

or

$$\left(\left(h_\varphi \operatorname{ch}(\xi) \operatorname{sh}(\xi) \operatorname{sh}(\xi) \operatorname{ch}(\xi) - h_\xi \cos(\varphi) \sin(\varphi) \sin(\varphi) \cos(\varphi) \right) + \right. \\ \left. \left(2h_\varphi \operatorname{sh}^2(\xi) \operatorname{ch}^2(\xi) - 2h_\xi \sin^2(\varphi) \cos^2(\varphi) \right) \right) = a\Delta^{-5} J_z$$

or

$$3h_\varphi \operatorname{sh}^2(\xi) \operatorname{ch}^2(\xi) - 3h_\xi \sin^2(\varphi) \cos^2(\varphi) = a\Delta^{-5} J_z$$

or

$$J_z = \frac{3}{a\Delta^5} \left(h_\varphi \operatorname{sh}^2(\xi) \operatorname{ch}^2(\xi) - h_\xi \sin^2(\varphi) \cos^2(\varphi) \right) \quad (15)$$

Let us substitute (2, 3) in (4). Then we obtain

$$\frac{1}{\Delta^2} \left(\operatorname{sh}(\xi) \operatorname{ch}(\xi) \frac{1}{a\Delta} \frac{\partial H_z}{\partial \varphi} - \sin(\varphi) \cos(\varphi) \frac{1}{a\Delta} \frac{\partial H_z}{\partial \xi} \right) + \\ + \left(\frac{1}{a\Delta} \frac{\partial^2 H_z}{\partial \varphi \partial \xi} - \frac{1}{a\Delta} \frac{\partial^2 H_z}{\partial \varphi \partial \xi} \right) = 0$$

or

$$\left(\text{sh}(\xi)\text{ch}(\xi)\frac{\partial H_z}{\partial \varphi} - \sin(\varphi)\cos(\varphi)\frac{\partial H_z}{\partial \xi} \right) = 0. \quad (16)$$

From (6, 7) we find that

$$\left(\text{sh}(\xi)\text{ch}(\xi)\frac{\partial(\Delta^{-2})}{\partial \varphi} - \sin(\varphi)\cos(\varphi)\frac{\partial(\Delta^{-2})}{\partial \xi} \right) = 0. \quad (17)$$

Comparing (16, 17), we see that

$$H_z = \Delta^{-2}. \quad (18)$$

From (2, 3, 18) we obtain:

$$J_\xi = \frac{1}{a\Delta} \frac{\partial(\Delta^{-2})}{\partial \varphi}, \quad (19)$$

$$J_\varphi = -\frac{1}{a\Delta} \frac{\partial(\Delta^{-2})}{\partial \xi}. \quad (20)$$

or, considering (6, 7),

$$J_\xi = \frac{2}{a\Delta^5} \sin(\varphi)\cos(\varphi), \quad (21)$$

$$J_\varphi = -\frac{2}{a\Delta^5} \text{sh}(\xi)\text{ch}(\xi). \quad (22)$$

Thus, if H_ξ and H_φ variables are determined by (8, 9), respectively, then H_z , J_ξ , J_φ , J_z variables are determined by (18, 21, 22, 15), respectively, and the condition (14) is met.

Appendix 2. Decomposition of a hexagon into ellipses

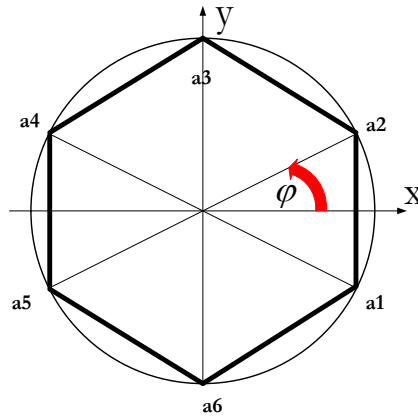


Fig. 1.

Let us consider the hexagon shown in Fig. 1. It can be represented by two functions of φ angle:

$$x = f_x(\varphi), \tag{1}$$

$$y = f_y(\varphi). \tag{2}$$

These functions are shown in Fig. 2. Let us represent these functions by a set of points. In Fig. 2 each segment is represented by three points: $n = 3$, and $[a1, a2]$ is a segment repeated twice. In this case, each function is represented by $N = 7n$ points. The discrete functions (1, 2) represented in such manner can be expanded into trigonometric series of the following form (4.1, 4.2).

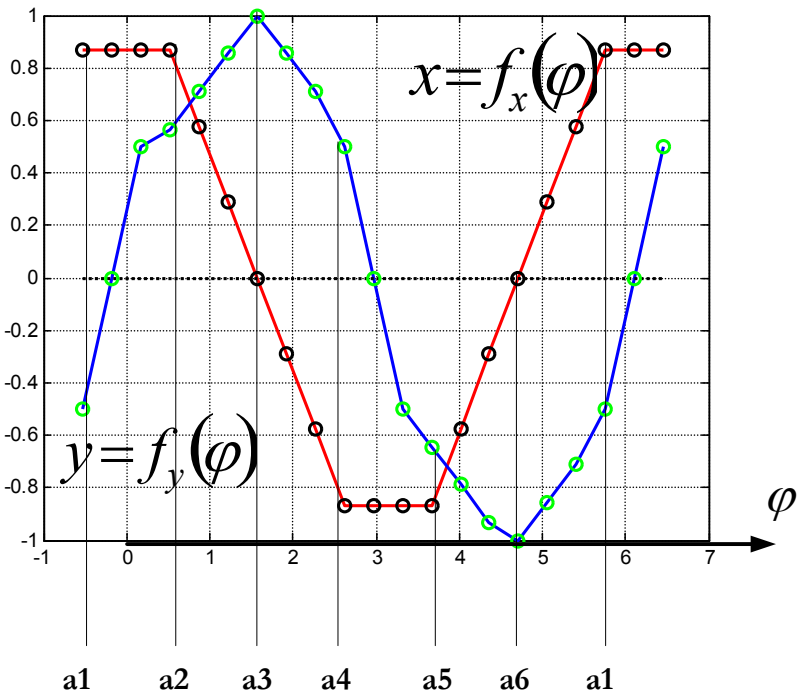
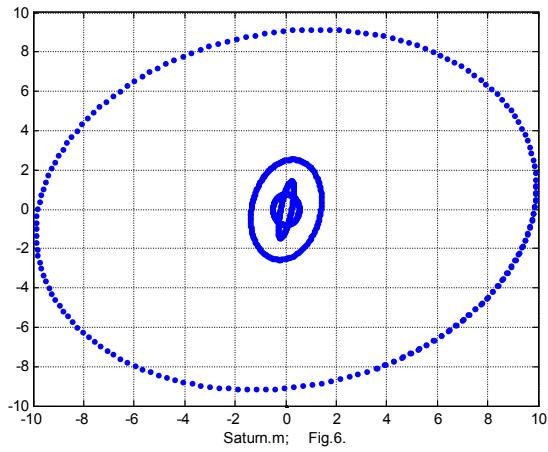
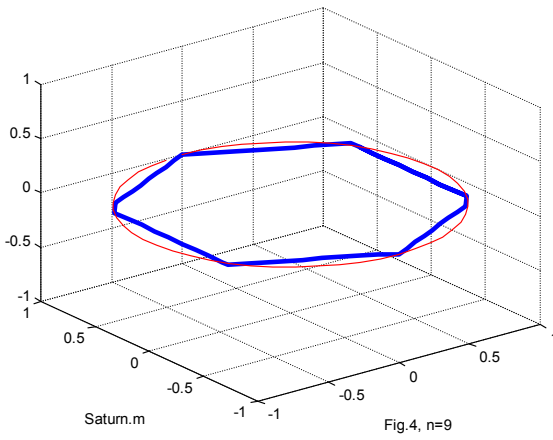
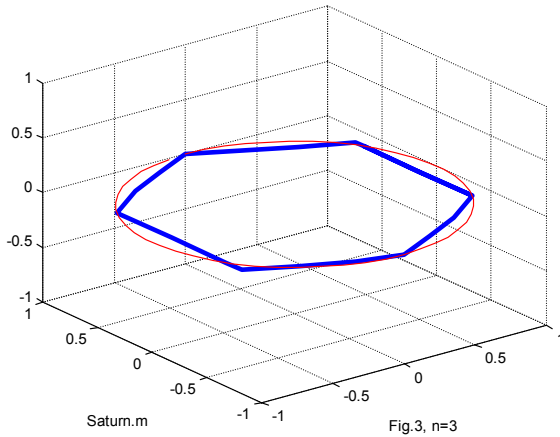


Fig. 2.

The modeling shows that the constant value of addends when $n = 1$ can be neglected. Consequently, the functions (1, 2) in polar and cylindrical coordinates can be approximated by a set of $(N - 1)$ functions describing the **ellipses**. The sum of such functions represents a hexagon. For example, Fig. 3 and 4 show the figures as a result of such approximation when $n = 3$ and $n = 9$, respectively. Fig. 6 shows the first 4 ellipses in decomposition of a hexagon when $n = 3$. The first ellipse is separated by dots.



References

1. Saturn's hexagon, (in Russian),
<http://naucaitechnika.ru/blog/43524663032/10-strannyih-obektov-Solnechnoy-sistemyi,-o-kotoryih-nam-malo-ch>
2. Saturn's hexagon, (in Russian), <http://fishki.net/1592643-krupnye-inoplanetnye-buri-i-uragany.html>
3. Saturn's hexagon,
https://en.wikipedia.org/wiki/Saturn%27s_hexagon
4. It disclosed the secret of the Bermuda Triangle,
<https://lenta.ru/news/2016/10/24/bt/>, (in Russian).
5. Andre Ango. Mathematics for Electrical and Radio Engineers, publ. "Nauka", Moscow, 1964, 772 p. (in Russian).
6. Khmelnik S.I. Hexagonal Storm on Saturn,
<http://vixra.org/abs/1611.0313>, 2016-11-23.

Chapter 4.4a.

Active Field of Honeycombs

Contents

1. Introduction \ 86
 2. Prerequisites \ 87
 3. Geometry of honeycombs \ 88
 4. Gravitational field of honeycombs \ 88
 5. Modeling \ 92
 6. Field effect on biological objects assumption \ 94
- References \ 94

1. Introduction

It is shown that a non-monotonic gravitational field exists in the neighborhood of honeycombs. The structure of this field is considered. It is assumed that this field is the result of honeycombs specific effect on biological objects. A possible action of this field on biological objects is described.

"To date, a lot of observations have accumulated in natural science, indicating the existence of specific effect on bioobjects, structures of cavity-type (pyramids, honey combs and combs similar to them, porous materials, etc.)" [1]. Such effects are mostly shown in honeycombs. For example, in [2] the beekeeper writes: "Cellular structures such as honeycombs create a field that depresses vital function of microbes and even plant roots, so that the nests for wasps and bees are always clean. If to held honeycombs over the head of a man without honey, the fatigue feeling and headache will disappear, blood pressure, sleep will be normalized in a few minutes." In [3, p. 205] other trial subjects note "... a curious phenomenon - the so-called phosphenes: mobile, constantly changing bright colorful designs when closed (and sometimes open) eyes - now flaming auroras, flashes, sparks, flowing waves and spirals, then the most complex geometric constructions of amazing beauty, like nothing natural" - see Fig. 0. Various phenomena near honeycombs are described in [4]. It follows from what has been said that a certain field that is an active source of effects on biological objects exists in the neighborhood of honeycombs. Further, the nature of such an active field is studied.

Note that there are some studies in which various hypotheses about this field nature are considered - see [1] and references to this study, [9-11]. The proposed hypothesis differs in the fact that it allows to obtain some quantitative estimates.



Fig. 0.

2. Prerequisites

The existence of gravitational waves is predicted by the general theory of relativity. From this it follows that, in case of weak gravitational fields and low velocities the gravity is described by Maxwell-like equations. Precisely such conditions exist on the Earth. Consequently, gravitoelectromagnetic effects similar to electromagnetic effects, might be observed.

Let us consider electrostatics equations, which are the following (hereinafter the GHS system is used):

$$\operatorname{div} E = 4\pi\rho, \quad (1)$$

$$\operatorname{rot} E = 0, \quad (2)$$

where

- ρ - density of electric charge $\sqrt{\text{g} \cdot \text{cm}}/\text{cm}^3$;
- q - electric charge $\sqrt{\text{g} \cdot \text{cm}}$;
- E - electric field intensities. $\sqrt{\text{g} \cdot \text{cm}}/\text{sec}^2$

From Chapter 1 it follows that the following gravitostatics equations are applied

$$\operatorname{div} E_g = 4\pi G\rho_g, \quad (3)$$

$$\operatorname{rot} E_g = 0, \quad (4)$$

where

- ρ_g - density of mass [g/cm^3];
- m – mass [g];
- E_g - the intensity of the gravitoelectric field [cm/sec^2];
- G - gravitational constant, $G \approx 7 \cdot 10^{-8}$ [$\text{cm}^3/\text{g} \cdot \text{sec}^2$].

3. Geometry of honeycombs

Honeycombs (see Fig. 1) consist of quite thin, closely-spaced bee cells. The thickness of honeycombs with unsealed brood is about 22 mm. Bee cell is of hexagon shape and is characterized by the following dimensions: depth - 11-12 mm, diameter of inscribed circle - 5.37-5.42 mm, volume - about 0.28 cm^3 . Cell walls have a thickness of approximately 0.1 mm. The deviation from this average value can be not more than 0.002 mm. About four cells are concentrated in 1 cm^2 [6]. Wax density is about 1 g/cm^3 .



Fig. 1 (from [2]).

4. Gravitational field of honeycombs

Fig. 2 shows a fragment of honeycombs in x, y, z Cartesian coordinates and ABCD plane in xOz coordinates, perpendicular to honeycombs plane. We will determine the vectors of E_{gx} , E_{gy} , E_{gz} gravitational intensities created by masses of honeycombs. Thus, it is

necessary to solve equations (2.3, 2.4) under known $\rho_g(x, y, z)$ mass density distribution function in honeycombs. In particular, this mass density distribution function along oy axis when $x = 0$ and $z = 0$ in Fig. 2 - $\rho_g(0, y, 0)$ has the form shown in Fig. 3. Here it is assumed that the honeycombs are sufficiently deep and masses are located, in fact, on a hexagon grid.

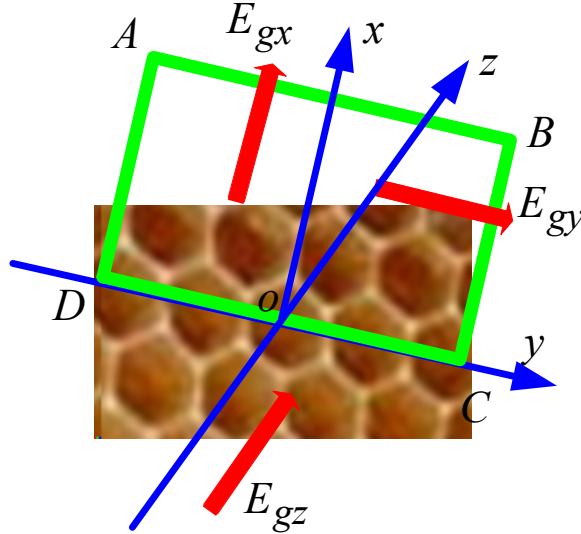


Fig. 2.

Such $\rho_g(0, y, 0)$ function can be approximated by $\text{Ch}(\beta y)$ function, where β is a some coefficient, depending on cell diameter. At that $\rho_g(0, y, 0)$ function as a whole is approximated by $\text{Chd}(\beta y)$ periodic function, composed of $\text{Ch}(\beta y)$ functions, defined on $y \in (-R, R)$ segment, which is equal to cell width. Similarly, $\text{Shd}(\beta y)$ function composed of $\text{Sh}(\beta y)$ functions defined on the same $y \in (-R, R)$ segment can be defined. For the following it is important to note that

$$\frac{d}{dt} \text{Chd}(\beta y) = \text{Shd}(\beta y), \quad \frac{d}{dt} \text{Shd}(\beta y) = \text{Chd}(\beta y). \quad (1)$$

$\rho_g(0,0,z)$ function is defined in a similar way. In this case, the mass density distribution function in honeycombs can be determined by the formula

$$\rho_g(x, y, z) = \frac{\rho_o}{h} \text{Chd}(\beta y) \text{Chd}(\beta z) \delta(x). \quad (2)$$

Here it is assumed that $x = 0$ at the cell bottom, and the function is

$$\delta(x) = \begin{cases} 1, & \text{если } x \leq h, \\ 0, & \text{если } x > h, \end{cases} \quad (3)$$

where

h - cell height,

β - known coefficient (wall thickness in Ch function depends on it - see also Fig. 2),

ρ_o - wax density.

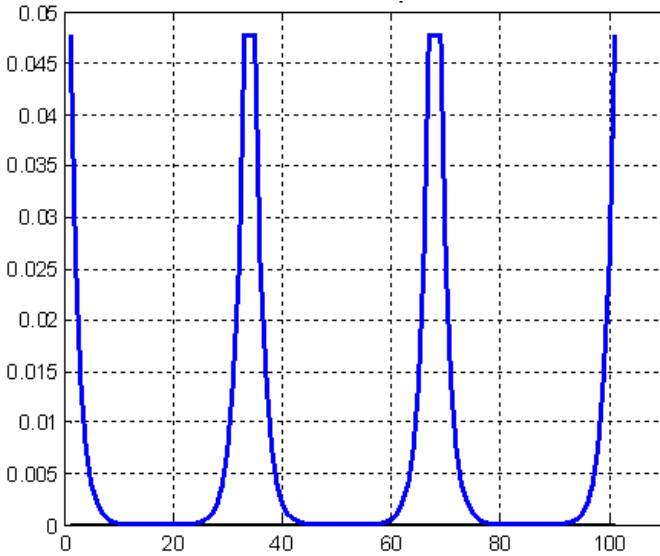


Fig. 3.

In [7, 8] a solution of the following equations (2.1, 2.2) providing the form (2) is given. In consequence of analogy between electrostatics and gravitostatics mentioned in par. 2, this solution can be applied to equations (2.3, 2.4, 2, 3). Then we have:

$$E_{gx}(x, y, z) = e \cdot \text{Chd}(\beta y) \text{Chd}(\beta z) \cos(\beta x), \quad (4)$$

$$E_{gy}(x, y, z) = e \cdot \text{Shd}(\beta y) \text{Chd}(\beta z) \sin(\beta x), \quad (5)$$

$$E_{gz}(x, y, z) = e \cdot \text{Chd}(\beta y) \text{Shd}(\beta z) \sin(\beta x), \quad (6)$$

$$e = 4\pi G \rho_o h. \quad (7)$$

Thus, under these conditions, cells plane forms a field of intensities (4, 5, 6) that harmonically change towards ox . In other words a non-monotonic harmonic field is formed in the direction perpendicular to cells plane.

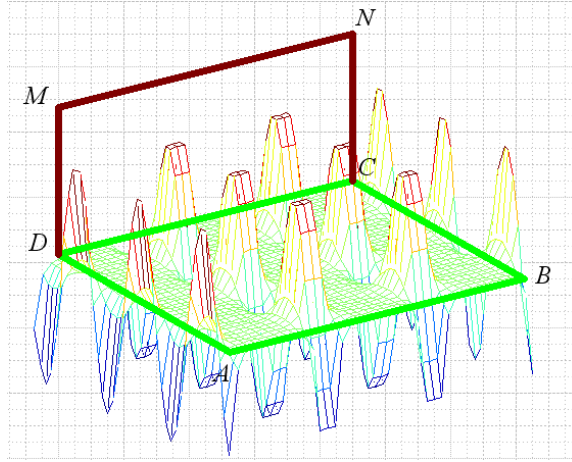


Fig. 4.

As an example Fig. 4 shows $E_{gx}(x, y, z = 0)$ harmonic field of intensities on ABCD plane, perpendicular to ACNM combs plane – compare with Fig. 2. Fig. 4 shows the values of intensities (laid off in a vertical direction). But the vector of this intensities is directed along ABCD plane parallel to CB side. This field is static. Obviously, there should be a period of this field formation and a wave exists in this period. This wave's E_{gx} vector of intensities is directed towards wave propagation - from the honeycombs. Consequently, such a wave is longitudinal.

Example. According to Section 3 it follows that the cell height is $h = 1.2[\text{cm}]$. In accordance with (7) we obtain

$$e = 4\pi G \rho_o h = 4\pi \cdot 7 \cdot 10^{-8} \cdot 1 \cdot 1.2 \approx 10^{-6} [\text{cm/sec}^2].$$

Consequently, at maximum point, the gravitational intensities is $E_{\max} \approx 10^{-6} [\text{cm/sec}^2]$. For comparison, we note that the mass of 1g (which is equal to cell mass) at a distance of $r = 3[\text{cm}]$ creates the following intensities:

$$p = \frac{4\pi G}{r^2} = \frac{4\pi \cdot 7 \cdot 10^{-8}}{9} \approx 10^{-7} \text{ [cm/sec}^2\text{]}.$$

This intensities p is less than intensities E . Besides, intensities p (unlike intensities E) decreases suddenly and monotonically with a distance.

5. Modeling

A solution found in the previous section is correct in a close neighborhood of honeycombs plane, since it doesn't take into account the limitations of this plane and edge effects associated with it.

In [7] a solution of similar task related to electrostatics 1) is given, considering the edge effects and 2) in case of arbitrary charge distribution function along the plane width. Let us apply this solution to our task in a particular case when z coordinate value is fixed. Consider the vector-function

$$E = [E_x(x, y), E_y(x, y)] \tag{8}$$

and functional of the following form

$$F(E) = \iint_{x,y} \left[\frac{1}{2} E_{gy} \cdot \left(\frac{\partial^2 E_{gx}}{\partial y^2} + \frac{\partial^2 E_{gx}}{\partial x \partial y} \right) + \frac{1}{2} E_{gx} \cdot \left(\frac{\partial^2 E_{gy}}{\partial y^2} + \frac{\partial^2 E_{gy}}{\partial x \partial y} \right) \right. \\ \left. + E_{gx} \cdot \left(\frac{\partial^2 E_{gx}}{\partial x^2} + \frac{\partial^2 E_{gx}}{\partial x \partial y} \right) - E_y \cdot \left(\frac{\partial^2 E_{gy}}{\partial x^2} + \frac{\partial^2 E_{gy}}{\partial y^2} \right) \right. \\ \left. + 4\pi G \rho_g \cdot \left(\frac{\partial E_{gx}}{\partial x} + \frac{\partial E_{gx}}{\partial y} \right) \right] dx dy, \tag{9}$$

where $\rho_g(x, y)$ is a known function. This functional gradient has the form of

$$p = \begin{cases} \left(\frac{\partial^2 E_y}{\partial y^2} + \frac{\partial^2 E_y}{\partial x \partial y} + \frac{\partial^2 E_x}{\partial x \partial y} + \frac{\partial^2 E_x}{\partial x^2} + 4\pi G \cdot \left(\frac{\partial \rho}{\partial x} + \frac{\partial \rho}{\partial y} \right) \right), \\ \left(\frac{\partial^2 E_x}{\partial y^2} + \frac{\partial^2 E_x}{\partial x \partial y} - \frac{\partial^2 E_y}{\partial x^2} - \frac{\partial^2 E_y}{\partial x \partial y} \right). \end{cases} \tag{10}$$

When escaping on functional (9) upon gradient (10), there is an optimal value of the function (8) which satisfies the following equation

$$p = 0. \tag{11}$$

As E field doesn't have a constant component, then from (10, 11) it follows that (2.3, 2.4). Thus, escape on functional (9) under gradient (10) at a given $\rho_g(x, y)$ leads to a solution of equations (2.3, 2.4).

In [7] the method of such a solution of these equations software implementation is described. Below we only give the field calculation using this program. Fig. 5 shows the result of $E_{gx}(x, y, z = 0)$ three cells field calculation in the same ABCD plane. In Fig. 6 the same field with a minus sign is shown for illustration purposes.

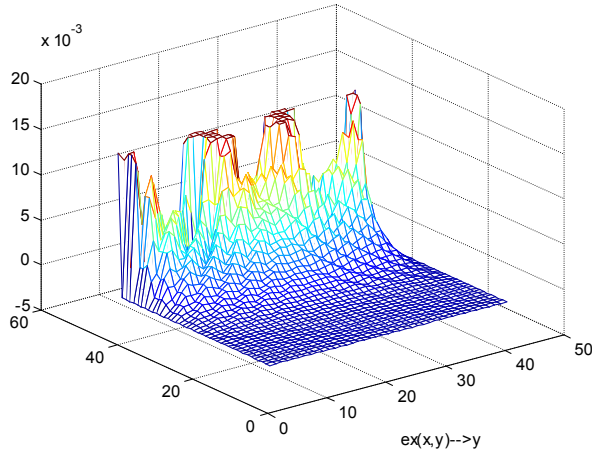


Fig. 5.

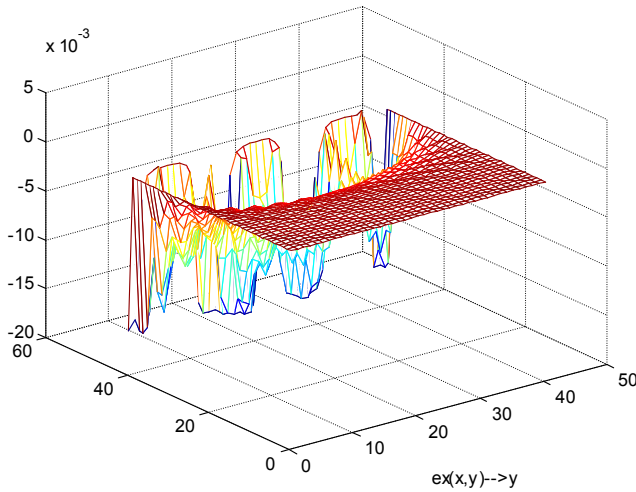


Fig. 6.

6. Field effect on biological objects assumption

The non-monotonic field considered modulates a constant field of Earth's attraction. Therefore, the total field has a non-monotonic gradient. The moving mass that appears in such a field is displaced to the nearest point with zero gradient. If this moving mass, for example, is a microorganism, then its movability becomes limited. Vital function of such disabled microorganism becomes limited and it dies. So in such a way we can explain (noted above) the fact of microorganisms' vital function inhibition in the neighborhood of honeycombs.

Movable particles in a human body under the influence of this field also attempt to be arranged at points with zero gradient. Thus, the harmonic field intensities reduces a thermal chaos of moving particles, creating some order. Apparently, exactly this has a beneficial effect on a human health near the honeycombs.

References

Note: **DNA-№.crp** – The Papers of independent Authors,
ISSN 2225-6717, <http://izdatelstwo.com/>

1. Etkin V.A. The effect of cavity structures, http://samlib.ru/e/etkin_w/effectpolostnyhstruktur.shtml
2. Shishkin A. Miracle effect of honeycombs, <http://amursk.su/2009-11-11-13-22-53/118-2009-12-26-17-14-40.html>
3. Grebennikov V. Secrets of the world of insects, 1990.
4. Grebennikov V. The secret of the bee nest, http://www.matri-x.ru/book_foto.shtml
5. ...
6. Honeycomb. <https://en.wikipedia.org/wiki/Honeycomb>
7. Khmelnik S.I. Calculation of static electric and magnetic fields on the basis of the variational principle. **DNA-19**, 2011
8. Khmelnik S.I. Variational principle of extremum in electromechanical and electrodynamic systems. Publisher by "MiC", printed in USA, fourth edition, Lulu Inc., ID 1769875, Israel, 2012, ISBN 978-0-557-04837-3.
9. Serkov N.V. Cellular structure as an open thermodynamic system, <http://lib.izdatelstwo.com/Papers2/Serkow.pdf>

10. Grebennikov V.S., Zolotarev V.F. The theory of field radiation of multilayer structures,
<http://lib.izdatelstwo.com/Papers2/Grebennikow.pdf>
11. Grebennikov VS, Zolotarev V.F. Rapid processes in the environment of physical vacuum as a source of physical phenomena,
<http://lib.izdatelstwo.com/Papers2/GrebZolot.djvu>

Chapter 4.5. About water flow flowing into the funnel and out of pipe

Contents

- 1. Introduction \ 96
- 2. Mathematical model \ 97
- 3. Jet characteristics \ 100
- 4. Conclusions \ 103
- References \ 103

1. Introduction

To author's knowledge, a strict model of water flow flowing out of a pipe with sufficiently high velocity (created by artificial pressure or gravity) and forming a rotating vortex - funnel has not been constructed yet. The experiments allow us to establish only that the vortex is formed when flow velocity exceeds a certain threshold value [1]. Water twists not only in funnel, but also when escaping out of the hose, in a steep waterfall, when it flows out of the cock under high pressure, etc. Another phenomenon observed when water flows out of the pipe is that water compressed at the outlet from the pipe rather rapidly expands again [2].

Next, we consider water flow flowing out of the pipe into airspace - see Fig. 1 and Fig. 2. It is shown, in particular, that phenomena observed when water flows out of the pipe - rotation of jet and expansion of jet can be explained by significant gravitomagnetic forces availability.



Fig. 1.



Fig. 2.

The following mathematical model uses the system of Maxwell-like gravitational equations - see Chapter 1. The model is based on the following assumptions. Movement of water assimilates to mass currents. Interaction between the moving masses is explained by gravitomagnetic Lorentz forces (GL-forces) existence.

Mass currents create the strengths in water flow; mass currents together with the strengths create Lorentz forces; Lorentz forces effect on masses moving in a current, thereby changing the direction of currents. All these processes are jointly described by Maxwell's equations, in which Lorentz forces are excluded. However, these processes can be followed sequentially and related to Maxwell's equations - see Section 2.2.

2. Mathematical model

Mathematical model of unusual fountain completely coincides with the model of dusty vortex of non-cylindrical shape - see Chapter 4.1, Section 7. In this model, $R(z)$ vortex radius, and in this case - funnel radius is z function in section at z height. Therefore, for any $R(z)$ function a mathematical model can be constructed.

Consequently, it can be argued that gravitomagnetism equations are confirmed by experiment. Whereby, the existence of significant gravitomagnetic forces and gravitomagnetic energy flow is confirmed.

In the following, we consider the dependencies of mass currents and flows densities in stream from z upon linear $R(z)$ function. At that, we will assume that flow parameters are defined as in Example 1 of Chapter 4.1. Fig. 3 shows $R(z)$ и $\chi(z)$ functions - see Section 7 in Chapter 4.1. It is assumed that the source is located at the level of $z = 0$.

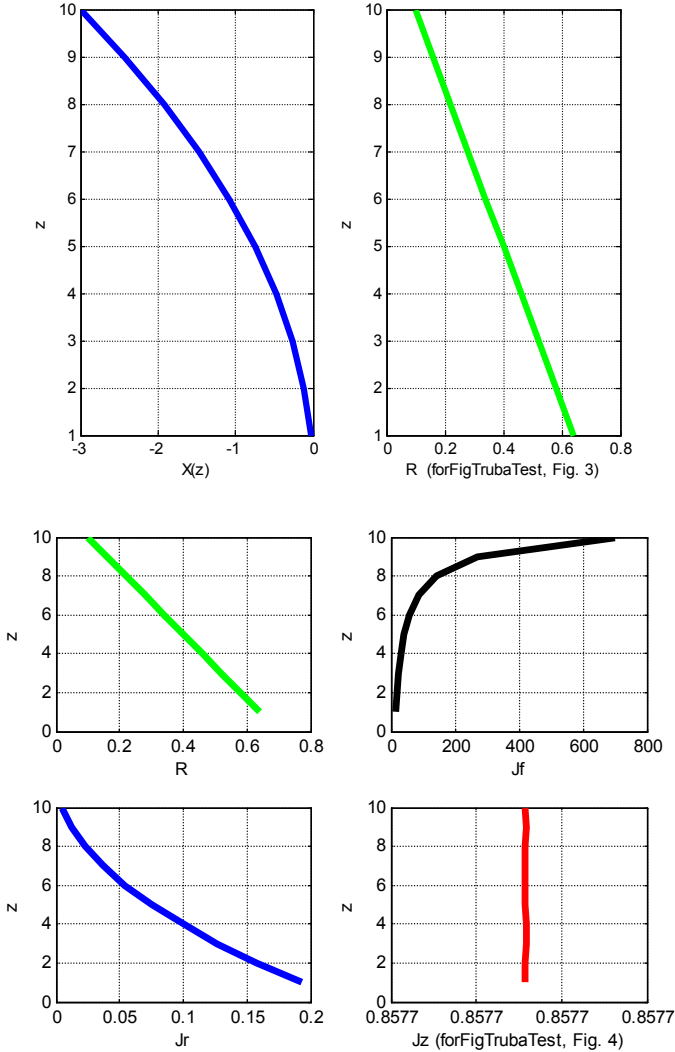
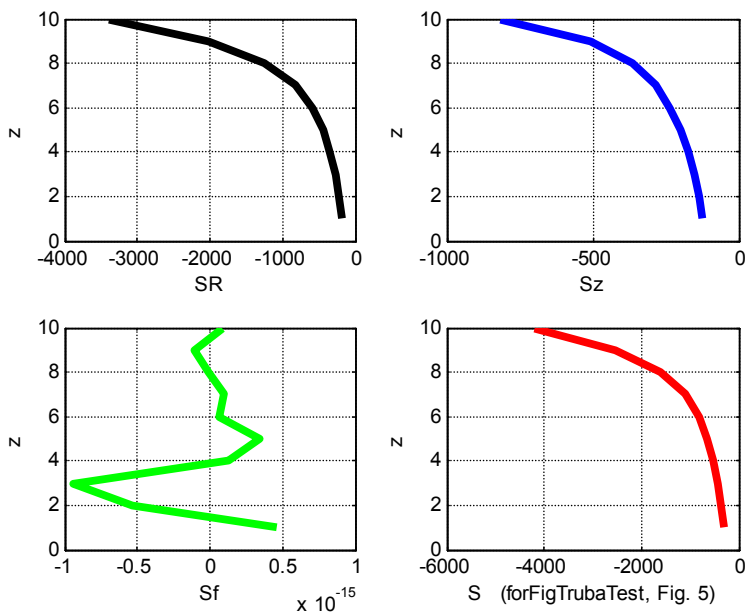


Fig. 4 shows the dependences of the total mass currents in a given section at a height of z - J_r , J_φ , J_z . It can be seen that mass current along the jet remains constant.

Fig. 5 shows the dependences of the total energy flows in a given section at a height of z - S_r , S_φ , S_z , and also their sum is $S = S_r + S_\varphi + S_z$. It can be seen that flow is $S_\varphi = 0$.



Analysis of solution obtained shows the following.

1. Solution doesn't take into account the gravity (thus solution doesn't depend on jet direction).
2. Mass currents and energy flows are present only in a volume limited by $R(z)$ radius. Solution does not take into account the losses of jet substance for radiation from this volume.
3. J_r radial mass current is always directed from the jet center.
4. There are circular J_ϕ and vertical J_z mass currents.
5. S_r radial energy flow is consumed for environment resistance overcoming, which is "expanded" by jet.
6. S_z vertical energy flow is directed along the jet and is consumed for environment resistance overcoming.
7. The method obtained allows finding the energy flows and mass currents at a given jet shape. Inverse problem - jet shape determination at known jet source energy is not currently solved.
8. $S = S_r + S_\phi + S_z$ total energy flow increases with jet length increase and, consequently, jet source cannot be the source of this energy. The source of this energy is gravitational energy of Earth - see Chapter 3.

3. Jet characteristics

Let assume that ρ jet density is constant along the jet section. Since jet mass in section doesn't depend on z , ρ jet density in section at z level is

$$\rho(z) \cdot Q(z) = \rho(z) \cdot \pi R^2(z) = C = \text{const}, \quad (1)$$

or

$$\rho(z) = C / \pi R^2(z), \quad (2)$$

where $Q(z)$, $R(z)$ - area and radius of section, respectively. Denote by $v_z(z)$ - jet velocity. Then mass current with a density (3.5) passing through jet section is defined as

$$\overline{J}_z(z) = \iint_{r, \varphi} J_z(r, \varphi, z) dr \cdot d\varphi. \quad (3)$$

On the other hand, this current is

$$\overline{J}_z(z) = \rho(z) v_z(z), \quad (4)$$

and kinetic energy of this current is

$$W_z(z) = 0.5 \rho(z) v_z^2(z). \quad (5)$$

Combining (2, 4, 5), we can find

$$v_z(z) = \frac{\pi}{C} R^2(z) \overline{J}_z(z), \quad (6)$$

$$W_z(z) = \frac{\pi}{2C} R^2(z) \left(\overline{J}_z \right)^2(z). \quad (7)$$

Density of the mass current passing full circle of r radius with v_φ velocity inside jet is,

$$J_\varphi(r) = \rho(r) v_\varphi(r). \quad (8)$$

But

$$v_\varphi(r) = r \cdot \omega(r). \quad (9)$$

where ω is angular velocity of circumferential mass current. From (2, 8, 9) we obtain:

$$\omega(r, z) = \frac{v_\varphi(r, z)}{r} = \frac{J_\varphi(r, z)}{r \cdot \rho(z)} = \frac{\pi R^2(z) J_\varphi(r, z)}{r \cdot C}. \quad (10)$$

Let us suppose, for example, that $r = 0.5 \cdot R$. Then

$$\omega(r, z) = \frac{2\pi}{C} R(z) J_\varphi(r, z). \quad (11)$$

It is commonly known that kinetic energy density of the ring rotational motion with coordinates (r, z) is equal to

$$W_{\varphi}(r, z) = \frac{1}{2} I(r) \omega^2(r, z), \quad (12)$$

where $I(r)$ - density of ring inertia moment, and

$$I(r) = r^2 \rho_r(z). \quad (13)$$

Here $\rho_r(z)$ - density of jet ring, and

$$\rho(z) = \int_0^R (\pi r^2 \rho_r(z)) dr. \quad (14)$$

If (as mentioned above) $\rho(z)$ jet density is constant across section (does not depend on z), then (14) can be performed only under the condition that

$$W_{\varphi}(r, z) = \frac{1}{2} I(r) \omega^2(r, z), \quad (12)$$

In order to verify, we substitute (15) in (14) and obtain identical equation:

$$I(r) = r^2 \rho_r(z). \quad (13)$$

Here $\rho_r(z)$ is the density of the jet ring, and

$$\rho(z) = \int_0^R (\pi r^2 \rho_r(z)) dr. \quad (14)$$

If (as indicated above) the jet density $\rho(z)$ is constant on the cross-section (does not depend from z), then (14) can be satisfied only under the condition, that

$$\rho_r(z) = \frac{\rho(z)}{r^2 \pi R}. \quad (15)$$

To verify, we substitute (15) in (14) and obtain the identity:

$$\rho(z) = \int_0^R \pi \frac{\rho(z)}{\pi R} dr = \rho(z). \quad (16)$$

From (13, 15, 16) it follows that

$$I(r) = \frac{\rho(z)}{\pi R}, \quad (17)$$

$$W_{\varphi}(r, z) = \frac{\rho(z)}{2\pi R(z)} \omega^2(r, z). \quad (18)$$

Hence, considering (2) under we find:

$$W_{\varphi}(r, z) = \frac{C}{2\pi^2 R^3(z)} \omega^2(r, z), \quad (18)$$

and then taking into account (10) we obtain:

$$W_{\varphi}(r, z) = \frac{C}{2\pi^2 R^3(z)} \frac{\pi^2 R^4(z) J_{\varphi}^2(r, z)}{r^2 \cdot C^2} = \frac{R(z) J_{\varphi}^2(r, z)}{2r^2 \cdot C}. \quad (19)$$

Finally, the total kinetic energy of jet layer rotation at a given level is

$$W_{\varphi z}(z) = \frac{R(z)}{2C} \int_0^{R(z)} \frac{J_{\varphi}^2(r, z)}{r^2} dr. \quad (20)$$

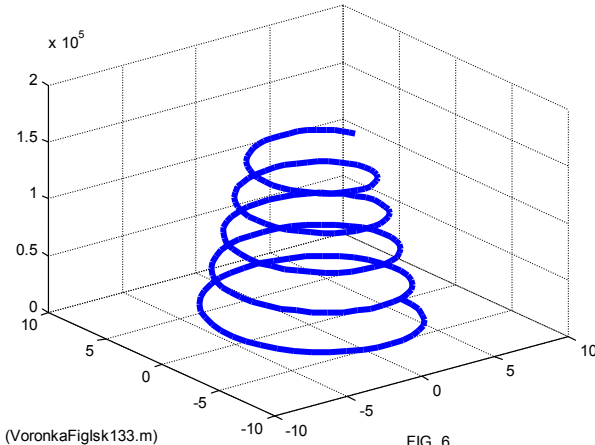
Let us suppose, for example, that $r = 0.5 \cdot R$. Then

$$W_{\varphi z}(r, z) = \frac{2J_{\varphi}^2(r, z)}{R(z) \cdot C}, \quad (21)$$

$$W_{\varphi z}(z) = \frac{2}{C \cdot R(z)} \int_0^{R(z)} J_{\varphi}^2(r, z) dr. \quad (22)$$

Thus, at known density of mass currents in jet according to (6, 7, 10, 20), jet vertical velocity, kinetic energy of jet vertical motion, angular velocity of elementary masses full circle motion, kinetic energy of jet rotational motion can be found. Thus,

- kinetic energy of jet translation and rotation motion increases towards jet,
- jet velocity increases towards jet,
- jet rotation velocity increases towards jet.



Each element of the water jet mass rotates at angular velocity of (10), falls down with velocity of (6) and thus moves along the helix line. Besides, this element moves away from the column central line with $v_r \equiv J_r$ radial velocity, i.e. jet expands downward and at the same time its density decreases - see Fig. 6.

4. Conclusions

Rotation of water flowing into the funnel or flowing out of pipe can be described by Maxwell-like gravitational equations. At the same time, water movement assimilates to mass currents. There is a solution of these equations that agrees with observed motion: the mass of water jet rotates, goes down and thus moves along the helix line; In addition, there is a radial velocity of jet spreading downward and jet density decrease.

Jet energy increases towards the jet direction. This means that this energy source cannot be the source of jet. This energy source is a gravitational energy of Earth - see Chapter 3.

References

1. R. Fernandez-Feria and E. Sanmiguel-Rojas. On the appearance of swirl in a confined sink flow. Universidad de Málaga, E.T.S. Ingenieros Industriales, 29013 Málaga, Spain. Received 3 March 2000; accepted 2 August 2000.
2. Titiens O.N. Hydro and aeromechanics. Volume 2. Movement of liquids with friction and technical applications, http://gidb.ru/book_view.jsp?idn=014100&page=1&format=djvu
3. Khmelnik S.I. About Flow of Water Into the Funnel and from Pipe, The Papers of independent Authors, ISSN 2225-6717, № 38, 2015; and <http://vixra.org/abs/1506.0201>, 2015-06-28 (in Russian).

Chapter 4.6. Sea Currents

Contents

- 1. Introduction \ 104
- 2. Mathematical model \ 106
- 3. Solution analysis \ 108
- 4. Conclusions \ 112
- Appendix 1 \ 112
- References \ 114

1. Introduction

Accepted ideas about the causes of sea currents are badly coherent with closed current trajectories and configuration resistance and current trajectories section form existence. A mathematical model of sea currents is constructed below using equations of gravitomagnetism. It is shown that this model explains internal mass forces existence which creates the flow and forces that ensure the stability of configuration and jet section form.

Three groups of currents, distinguished by the factors that create these currents are given: [1]

- Gradient currents caused by horizontal gradients of hydrostatic pressure,
- Currents caused by wind
- Flood currents,

These factors can be the cause of currents initiation, but they cannot (for centuries) maintain the closed current trajectory existence (since oppositely directed sections of this trajectory should be subjected to oppositely directed influences, and factors specified are monodirectional at all trajectory points). However, the currents are generally closed (as can be seen on maps - see Fig. 1, 2 [1]). Consequently, internal mass forces creating the current should be available.

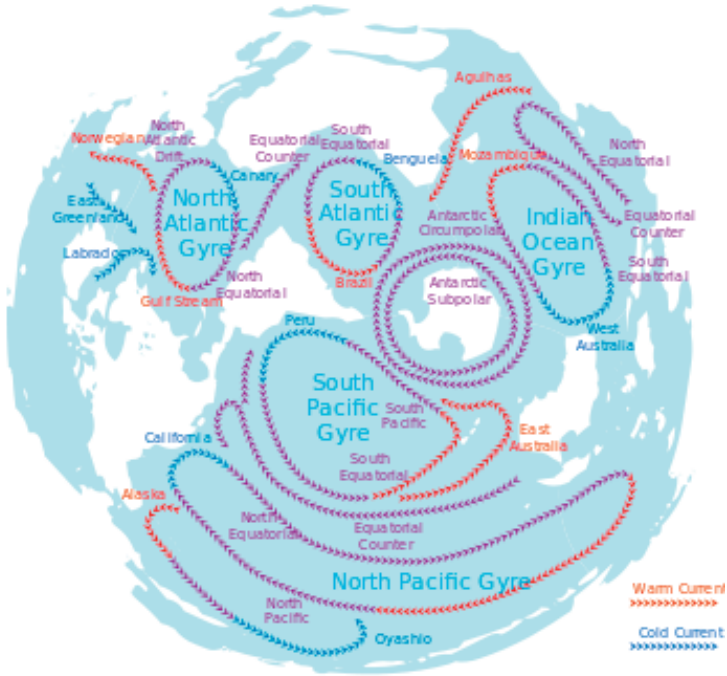


Fig. 1.

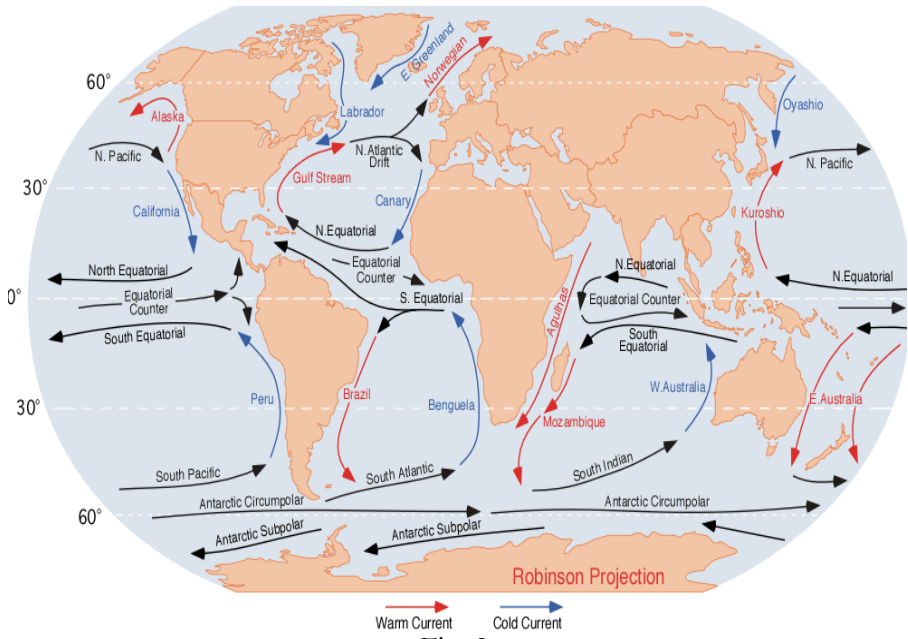


Fig. 2.

Currents retain the configuration of their trajectory and jet section form. In order to explain these phenomena, the differences in jet water and environmental waters composition and properties are usually pointed out. It is more natural (in our opinion) to assume that these differences are the consequence of jet isolation, and not the cause of this isolation. Consequently, the forces that ensure the configuration and jet section form stability should exist.

To the author's knowledge, such questions are not reflected in existing theories and numerical methods of ocean currents calculation - see, for example, [2, 3]. Below a theory explaining internal driving forces and forces that ensure the current stability existence is proposed. A mathematical model of currents is considered. At that, the system of Maxwell-like gravitomagnetism equations described in Chapter 1 is used. Interaction between the moving masses is explained by gravitomagnetic Lorentz forces (GL) existence, which, as shown in Chapter 1, can be significant.

2. Mathematical model

Maxwell-like equations for H gravitomagnetic tensions and J mass currents densities in a stationary gravitomagnetic field are the following (see system B in Chapter 1)

$$\operatorname{div}(H) = 0, \quad (1)$$

$$\operatorname{rot}(H) = J, \quad (2)$$

$$\operatorname{div}(J) = 0, \quad (3)$$

Let us consider the current in the form of parallelepiped, where $a\theta$ is a water-surface elevation, and the axes are located in accordance with Fig. 3. We assume that v current velocity is directed along Ox axis. In Cartesian coordinates, the equations (1, 2, 3) will be the following (see 5.1-5.5 in Chapter 2):

$$\frac{\partial H_z}{\partial y} - \frac{\partial H_y}{\partial z} = J_x, \quad (5)$$

$$\frac{\partial H_x}{\partial z} - \frac{\partial H_z}{\partial x} = J_y, \quad (6)$$

$$\frac{\partial H_y}{\partial x} - \frac{\partial H_x}{\partial y} = J_z, \quad (7)$$

$$\frac{\partial H_x}{\partial x} + \frac{\partial H_y}{\partial y} + \frac{\partial H_z}{\partial z} = 0, \quad (8)$$

$$\frac{\partial J_x}{\partial x} + \frac{\partial J_y}{\partial y} + \frac{\partial J_z}{\partial z} = 0. \quad (9)$$

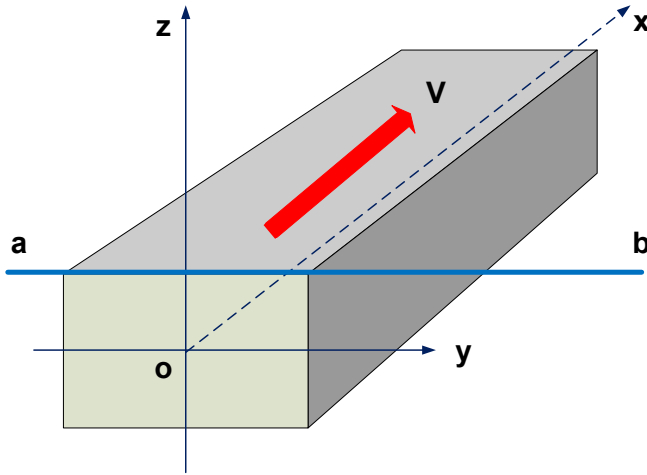


Fig. 3.

From physical considerations it is clear that the field must be homogeneous along OX axis, i.e. the derivatives according to x argument must be absent, and therefore equations (5-9) must be rewritten as follows:

$$\frac{\partial H_z}{\partial y} - \frac{\partial H_y}{\partial z} = J_x, \quad (10)$$

$$\frac{\partial H_x}{\partial z} = J_y, \quad (11)$$

$$-\frac{\partial H_x}{\partial y} = J_z, \quad (12)$$

$$\frac{\partial H_y}{\partial y} + \frac{\partial H_z}{\partial z} = 0, \quad (13)$$

$$\frac{\partial J_y}{\partial y} + \frac{\partial J_z}{\partial z} = 0. \quad (14)$$

In Appendix 1 it is shown that the solution of this system of equations can be the following:

$$H_x = h_x(y) \cdot \exp(\eta \cdot z), \quad (6)$$

$$H_y = h_y(y) \cdot \exp(\eta \cdot z), \quad (7)$$

$$H_z = h_z(y) \cdot \exp(\eta \cdot z), \quad (8)$$

$$J_x = j_x(y) \cdot \exp(\eta \cdot z), \quad (9)$$

$$J_y = j_y(y) \cdot \exp(\eta \cdot z), \quad (10)$$

$$J_z = j_z(y) \cdot \exp(\eta \cdot z), \quad (11)$$

where

η – some constant,

$h_r(y)$, $h_\phi(y)$, $h_z(y)$, $j_r(y)$, $j_\phi(y)$, $j_z(y)$ – functions of coordinate; the derivatives of these functions will be indicated by dashed lines.

At that

$$h_x(y) = \sin(b_3 y) / (b_1 + b_2 y^4), \quad (15)$$

$$h_y(y) = \exp(b_5 |y|) - b_4. \quad (16)$$

$$h_z = -\frac{b_5}{\eta} \exp(b_5 |y|), \quad (17)$$

$$j_x = -\left(\frac{1}{\eta} b_5^2 + \eta \right) \exp(b_5 |y|) + \eta b_4. \quad (18)$$

$$j_y = \eta \sin(b_3 y) / (b_1 + b_2 y^4), \quad (19)$$

$$j_z = \left\{ \begin{array}{l} b_3 \cos(b_3 y) / (b_1 + b_2 y^4) \\ -4b_2 y^3 \sin(b_3 y) / (b_1 + b_2 y^4) \end{array} \right\}, \quad (20)$$

where b_k – some constants.

3. Solution analysis

Next let us consider the indicated functions when

$$\eta = 0.2, \quad b_1 = 3, \quad b_2 = 0.0016, \quad b_3 = 0.06, \quad b_4 = 4, \quad b_5 = -0.1.$$

j_x , j_y , j_z mass currents do not depend on x coordinate, and, depending on y coordinate, are determined from (18-20). $j_x(y)$, $j_y(y)$, $j_z(y)$ functions are shown in Fig. 4.

Fig. 5 shows J_x , J_z mass currents as functions of z coordinate.

The currents for several specified y values are shown. The currents are shown at a scale of 1 in 10.

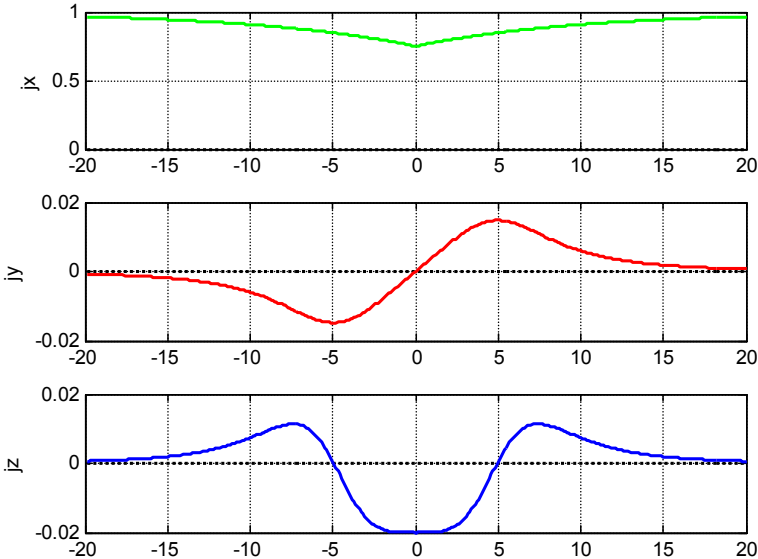


FIG. 4 (Golfstrim.m)

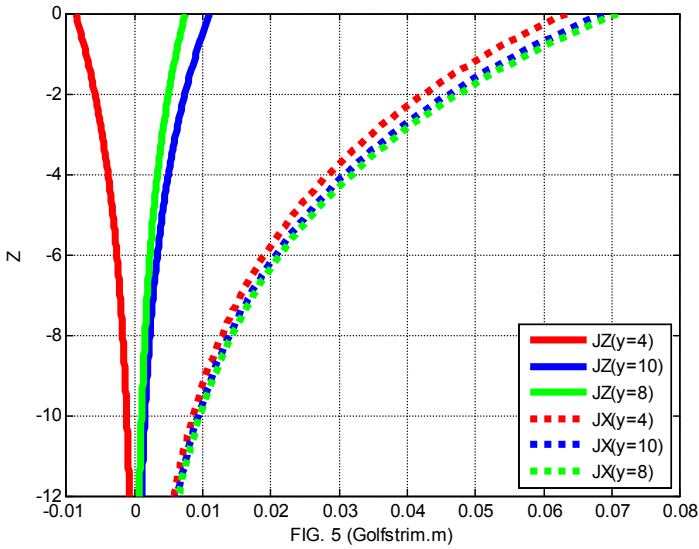


FIG. 5 (Golfstrim.m)

Let us consider a vector field of J_y , J_z currents in the vertical plane of jet section. Fig. 6 shows a fragment of this $y = -15, 15$ field and $z = [0, -2, -4, -6, -8]$. Thus, the mass currents in a jet circulate in a vertical direction. At the same time, in a small central region, the

mass of water descends at a high velocity and in a distant but significant in volume region, it rises at a low velocity. A deepening is formed along the axis on a jet free surface (see AA arc in Fig. 6), and an elevation is formed along the boundaries (see AB arcs in Fig. 6). This is similar to rotary stream surface. Water swoops down from the elevation into the deepening. A kinetic energy of such circulation is consumed only for the losses from internal friction. Rotary stream potential energy doesn't change. In other words in this case there is no potential energy conversion into kinetic energy and vice versa. However (as mentioned in Chapter 3), a gravitating body consumes its energy for mass currents creation and maintenance.

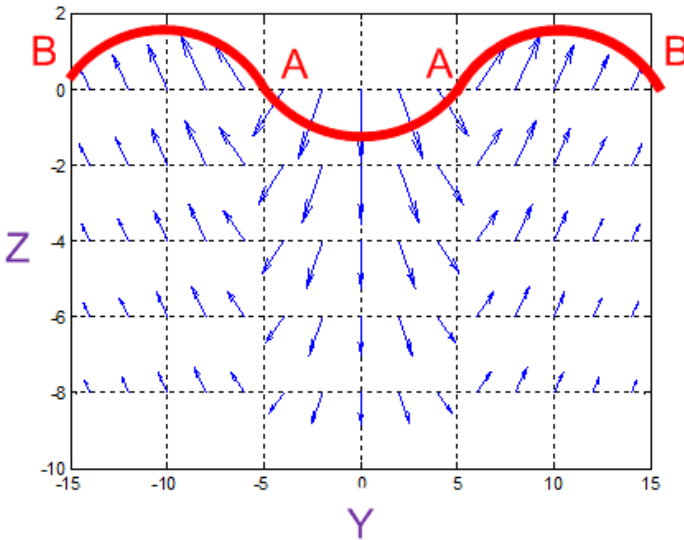


Fig. 6 (Golfstrim.m).

Fig. 7 shows J_x , $-J_x$, J_y , J_z currents in a horizontal plane of jet section. It can be seen that J_y currents directed perpendicular to jet lateral surface are close to zero on lateral surface and are directed from the jet (see also Fig. 4). This means that lateral waters don't enter into jet, and jet waters don't leave the jet, i.e. there is no exchange between jet waters and environmental waters: jet retains its composition!

It can be seen that J_x currents rapidly decrease with the depth. This corresponds, for example, to the Gulf Stream structure [4]. J_z vertical currents also decrease with a depth and we can talk about the vertical size of a current. It is also seen that the mass currents along the flow are approximately 100 times greater than the mass currents in other directions.

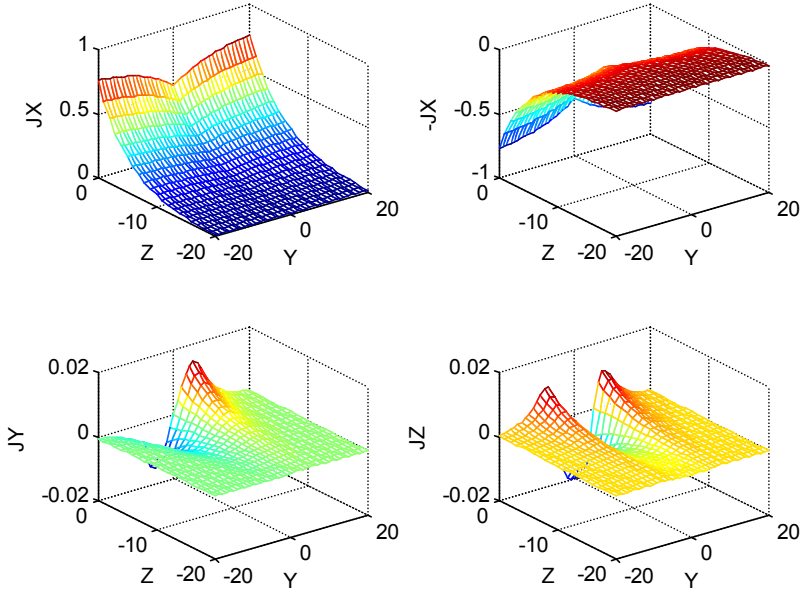


Fig. 7 (Golfstrim.m).

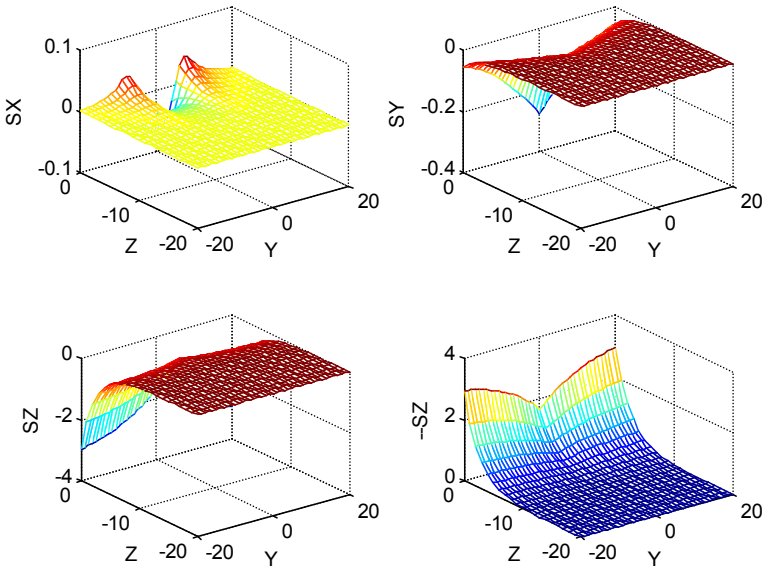


Fig. 8 (Golfstrim.m).

By analogy with (1.8.3) in Chapter 2, we write the following expression for gravitational energy vector density projections:

$$S_{xyz} = \begin{bmatrix} S_x = J_y H_z - J_z H_y \\ S_y = J_z H_x - J_x H_z \\ S_z = J_x H_y - J_y H_x \end{bmatrix} \quad (1)$$

Fig. 8 shows S_x , S_y , S_z , $(-S_z)$ energy flows density in the horizontal plane of jet section.

4. Conclusions

The proposed mathematical model explains

- sea current energy source
- closed current trajectory existence
- current trajectory configuration upload
- current form preservation
- current isolation from environmental waters

Appendix 1

Let us rewrite equations (2.10-2.14):

$$\frac{\partial H_z}{\partial y} - \frac{\partial H_y}{\partial z} = J_x, \quad (1)$$

$$\frac{\partial H_x}{\partial z} = J_y, \quad (2)$$

$$-\frac{\partial H_x}{\partial y} = J_z, \quad (3)$$

$$\frac{\partial H_y}{\partial y} + \frac{\partial H_z}{\partial z} = 0, \quad (4)$$

$$\frac{\partial J_y}{\partial y} + \frac{\partial J_z}{\partial z} = 0. \quad (5)$$

Let us search for the system of equations (1-5) solution in the form of functions that are separable with respect to coordinates. These functions are the following:

$$H_x = h_x(y) \cdot \exp(\eta \cdot z), \quad (6)$$

$$H_y = h_y(y) \cdot \exp(\eta \cdot z), \quad (7)$$

$$H_z = h_z(y) \cdot \exp(\eta \cdot z), \quad (8)$$

$$J_x = j_x(y) \cdot \exp(\eta \cdot z), \quad (9)$$

$$J_y = j_y(y) \cdot \exp(\eta \cdot z), \quad (10)$$

$$J_z = j_z(y) \cdot \exp(\eta \cdot z), \quad (11)$$

where

η – some constant,

$h_r(y)$, $h_\phi(y)$, $h_z(y)$, $j_r(y)$, $j_\phi(y)$, $j_z(y)$ – functions of y coordinate; the derivatives of these functions will be indicated by dashed lines.

Substituting (6-11) in (1-5), we obtain:

$$h'_z - \eta h_y = j_x, \quad (12)$$

$$\eta h_x = j_y, \quad (13)$$

$$-h'_x = j_z, \quad (14)$$

$$h'_y + \eta h_z = 0, \quad (15)$$

$$j'_y + \eta j_z = 0. \quad (16)$$

Let us substitute (13, 14) in (16). Then we obtain:

$$\eta h'_x - \eta h'_x = 0. \quad (17)$$

Expression (17) is an identity of $0 = 0$. Therefore (16) follows from (13, 15) and can be excluded from the system of equations (12, 16). The remaining 4 differential equations (12-15) contain 6 unknown functions. Therefore, any two functions can be defined at random.

For the following we define the following two h_x and h_y functions.

Then we find

$$j_y = \eta h_x, \quad (18)$$

$$j_z = -h'_x, \quad (19)$$

$$h_z = -h'_y / \eta, \quad (20)$$

$$j_x = h'_z - \eta h_y = -h''_y / \eta - \eta h_y. \quad (21)$$

Let us assume that

$$h_x(y) = \sin(b_3 y) / (b_1 + b_2 y^4), \quad (22)$$

$$h_y(y) = \exp(b_5 |y|) - b_4. \quad (23)$$

where b_k – some constants. Then

$$h'_x(y) = \left\{ \begin{array}{l} b_3 \cos(b_3 y) / (b_1 + b_2 y^4) - \\ - 4b_2 y^3 \sin(b_3 y) / (b_1 + b_2 y^4)^2 \end{array} \right\}, \quad (24)$$

$$h'_y(y) = b_5 \exp(b_5 |y|). \quad (25)$$

$$h''_y(y) = b_5^2 \exp(b_5 |y|). \quad (26)$$

$$h_z = -\frac{b_5}{\eta} \exp(b_5 |y|), \quad (27)$$

$$j_x = -\frac{1}{\eta} h_y'' - \eta h_y = -\left(\frac{1}{\eta} b_5^2 + \eta\right) \exp(b_5 |y|) + \eta b_4. \quad (28)$$

$$j_y = \eta \sin(b_3 y) / (b_1 + b_2 y^4), \quad (29)$$

$$j_z = \left\{ \begin{array}{l} b_3 \cos(b_3 y) / (b_1 + b_2 y^4) \\ -4b_2 y^3 \sin(b_3 y) / (b_1 + b_2 y^4) \end{array} \right\}, \quad (30)$$

So, $(h_x, h_y, h_z, j_x, j_y, j_z)$ functions are defined by (22, 23, 27, 28, 29, 30), respectively.

References

1. https://ru.wikipedia.org/wiki/Морские_течения
2. A.S. Monin, G.M. Zhikharev, Ocean vortices, USSR Academy of Sciences, UFN, 1990, vol. 160, no. 5, http://elibrary.lt/resursai/Uzsienio%20leidiniai/Uspechi_Fiz_Nauk/1990/5/r905a.pdf
3. Robert H. Stewart, Introduction To Physical Oceanography, Department of Oceanography, Texas A & M University, 2008, http://oceanworld.tamu.edu/resources/ocng_textbook/PDF_files/book.pdf
4. <https://ru.wikipedia.org/wiki/Гольфстрим>
5. Khmelnik S.I. Sea Currents and Gravitomagnetism. The Papers of independent Authors, ISSN 2225-6717, № 21, 2015; and <http://vixra.org/abs/1507.0113>, 2015-07-15 (in Russian).

Chapter 4.7. Water and sand Tsunami

Contents

1. Introduction \ 115
2. Mathematical model \ 117
3. Energy flows \ 120
4. Vertical stability and motion \ 122
5. Conclusions \ 122
- Appendix 1 \ 122
- Appendix 2 \ 123
- References \ 125

1. Introduction

Water and sand tsunamis are often combined into one class of phenomena with water solitons and sand-devils. Exteriorly they are different in size and shape. Huge sizes of tsunami impress - see Fig. 1-4. As for the shape, then, in contrast to solitons and sand vortexes having a bell or cylindrical shape, the tsunami shape can be approximated by parallelepiped. Therefore, the parallelepiped tsunami shape is used in mathematical model of tsunami.

Let us look once again at Fig. 1-4. The concept of that the cause of this machine motion is the wind and environment nonlinearity seems unconvincing. We cannot avoid the impression that this "device" inside has its own motor, and environment resistance is only a catalyst - a force that presses on throttle pedal.



Fig. 1.



Fig. 2



Fig. 3.



Fig. 4.

2. Mathematical model

Maxwell-like gravitational equations for H gravitomagnetic strengths and densities of J mass currents in a stationary gravitomagnetic field are the following (see system B in Chapter 1)

$$\operatorname{div}(H) = 0, \quad (1)$$

$$\operatorname{rot}(H) = J, \quad (2)$$

$$\operatorname{div}(J) = 0, \quad (3)$$

These equations describe a motionless tsunami. But when the tsunami is moving, it should take into account the fact that air resistance and elementary masses inertia create an additional flow - a mass current directed against tsunami translational motion velocity - see Fig. 4a. It can be assumed that there is some constant current source as $\overline{J}_v \equiv -\overline{v}$. In

Cartesian coordinates, let us assume that a velocity is directed along Ox axis. In this case, equations (1, 2, 3) will be the following:

$$\frac{\partial H_z}{\partial y} - \frac{\partial H_y}{\partial z} = J_x + J_v, \quad (5)$$

$$\frac{\partial H_x}{\partial z} - \frac{\partial H_z}{\partial x} = J_y, \quad (6)$$

$$\frac{\partial H_y}{\partial x} - \frac{\partial H_x}{\partial y} = J_z, \quad (7)$$

$$\frac{\partial H_x}{\partial x} + \frac{\partial H_y}{\partial y} + \frac{\partial H_z}{\partial z} = 0, \quad (8)$$

$$\frac{\partial J_x}{\partial x} + \frac{\partial J_y}{\partial y} + \frac{\partial J_z}{\partial z} = 0. \quad (9)$$

From physical considerations it is clear that the field must be a uniform along vertical axis, i.e. the derivatives according to z argument must be missing, and therefore equations (5-9) must be rewritten as:

$$\frac{\partial H_z}{\partial y} = J_x + J_v \quad (10)$$

$$-\frac{\partial H_z}{\partial x} = J_y \quad (11)$$

$$\frac{\partial H_y}{\partial x} - \frac{\partial H_x}{\partial y} = J_z \quad (12)$$

$$\frac{\partial H_x}{\partial x} + \frac{\partial H_y}{\partial y} = 0 \quad (13)$$

$$\frac{\partial J_x}{\partial x} + \frac{\partial J_y}{\partial y} = 0 \quad (14)$$

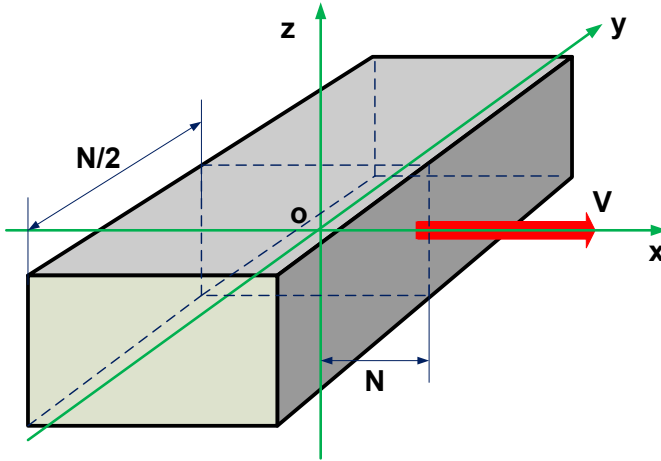


Fig. 4a.

The solution of combined equations (10-14) is found in Appendix 1. It is the following:

$$H_x = h_x \cos(\alpha x) \sin(\beta y), \quad (15)$$

$$H_y = h_y \sin(\alpha x) \cos(\beta y), \quad (16)$$

$$H_z = h_z \sin(\alpha x) \sin(\beta y) + J_z y, \quad (17)$$

$$J_x = j_x \sin(\alpha x) \cos(\beta y) + J_x y, \quad (18)$$

$$J_y = j_y \cos(\alpha x) \sin(\beta y), \quad (19)$$

$$J_z = j_z \cos(\alpha x) \cos(\beta y), \quad (20)$$

where

α, β - constants,

$h_x, h_y, h_z, j_x, j_y, j_z$ - amplitudes of functions.

In Appendix 1 it is shown that under given α, β, j_x, j_z the remaining h_x, h_y, h_z, j_y amplitudes can be found by the following formulas:

$$h_z = \frac{j_x}{\beta}, \quad (21)$$

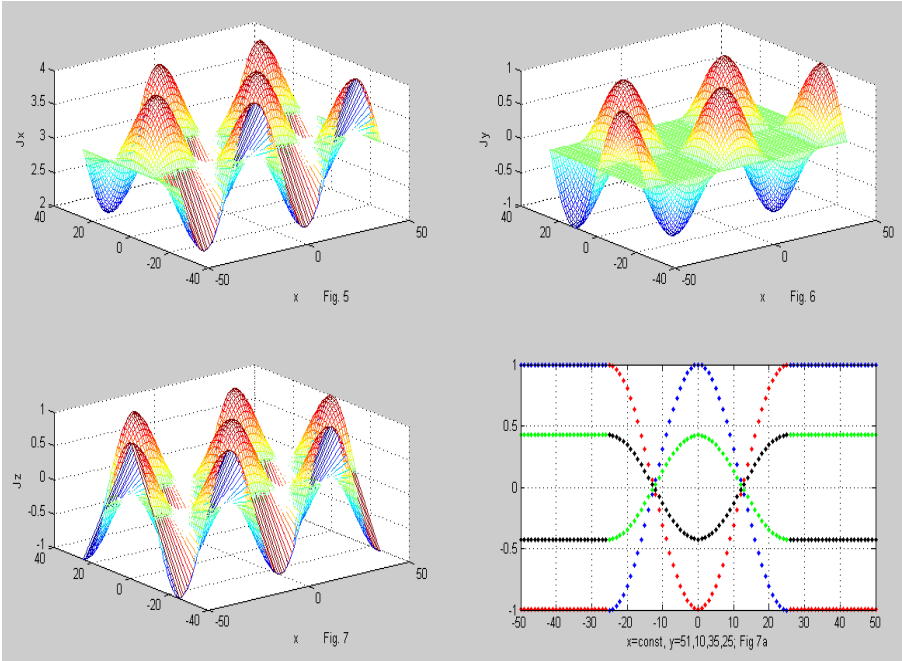
$$j_y = -j_x \frac{\alpha}{\beta}. \tag{22}$$

$$h_y = -h_x \frac{\alpha}{\beta}, \tag{23}$$

$$h_x = -j_z \left(\frac{\alpha^2}{\beta} + \beta \right). \tag{24}$$

Let us suppose that the cross-sectional area is such that

$$-N \leq x \leq N \text{ и } -\frac{N}{2} \leq y \leq \frac{N}{2}.$$



Figures 5, 6, 7 show J_x, J_y, J_z values on (x, y) section plane at $\alpha = 2\pi/N, \beta = 2\pi/N, j_z = 1, j_x = 1, J_y = 3$. Fig. 7a shows the functions (20) at fixed values of y . Thus, under certain values of α, β the sum of vertical currents (20) on each horizontal line and in each section is equal to zero. This means that in each vertical layer of tsunami the counter flows (up-down) exist. Herewith the whole tsunami potential energy remains constant. This is similar to wheel rotation at a constant velocity in vertical plane, when potential and kinetic energies remain constant.

3. Energy flows

In Appendix 2, these projections of gravitational energy density vector in tsunami body are calculated. When $J_v = 0$ they are the following:

$$S_{x_0} = \left(\frac{1}{2} \sin(2\alpha x) (j_y h_z \sin^2(\beta y) - j_z h_y \cos^2(\beta y)) \right), \quad (21)$$

$$S_{y_0} = \left(\frac{1}{2} \sin(2\beta y) (j_x h_z \cos^2(\alpha x) - j_x h_z \sin^2(\alpha x)) \right), \quad (22)$$

$$S_z = \left(\begin{array}{c} j_x h_y \sin^2(\alpha x) \cos^2(\beta y) - j_y h_x \cos^2(\alpha x) \sin^2(\beta y) \\ + J_v h_y \sin(\alpha x) \cos(\beta y) \end{array} \right). \quad (23)$$

When $J_v > 0$ these flows take the form of:

$$S_x = (S_{x_0} + J_v j_y y \cdot \cos(\alpha x) \sin(\beta y)), \quad (24)$$

$$S_y = (S_{y_0} - J_v j_x x \cdot \sin(\alpha x) \cos(\beta y) - J_v h_z \sin(\alpha x) \sin(\beta y) - J_v^2 y), \quad (25)$$

$$S_z = (S_{z_0} + J_v h_y \sin(\alpha x) \cos(\beta y)). \quad (26)$$

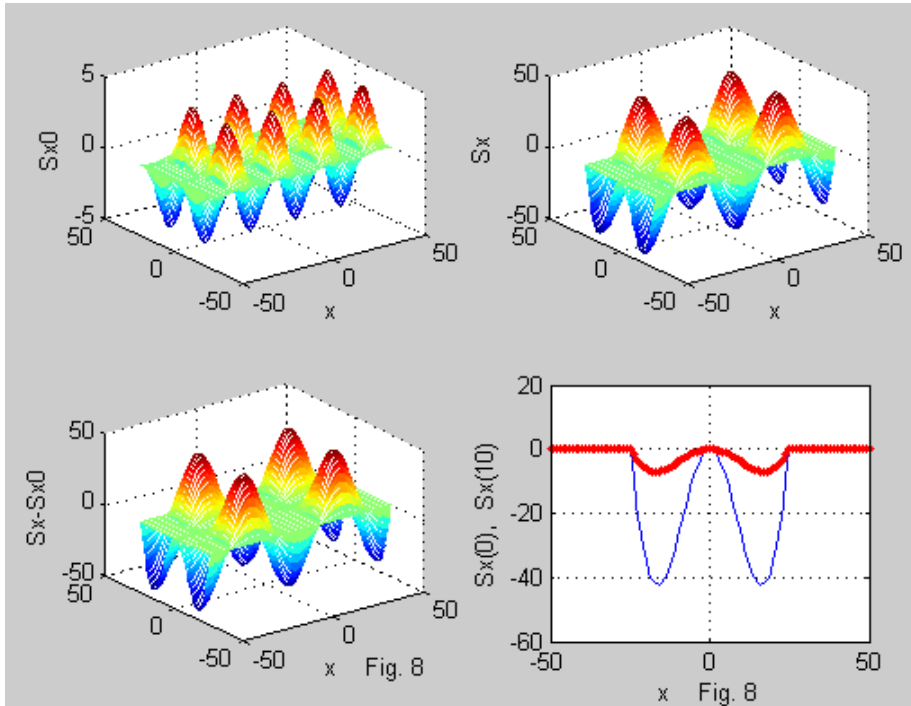


Fig. 8 shows S_{x0} , S_x , $(S_x - S_{x0})$ values on (x, y) section plane when $\alpha = 2\pi/N$, $\beta = 2\pi/N$, $j_z = 1$, $j_x = 1$, $J_y = 3$. The last window shows $S_x(x, y = 0)$ and $S_x(x, y = 10)$ dependencies - see lower and upper curves, respectively. Integration of S_{x0} , S_x values on (x, y) section plane shows that

$$\overline{S_{x0}} = \int_{x,y} S_{x0} dx dy = 0, \quad (27)$$

but

$$\overline{S_x} = \int_{x,y} S_x dx dy < 0. \quad (28)$$

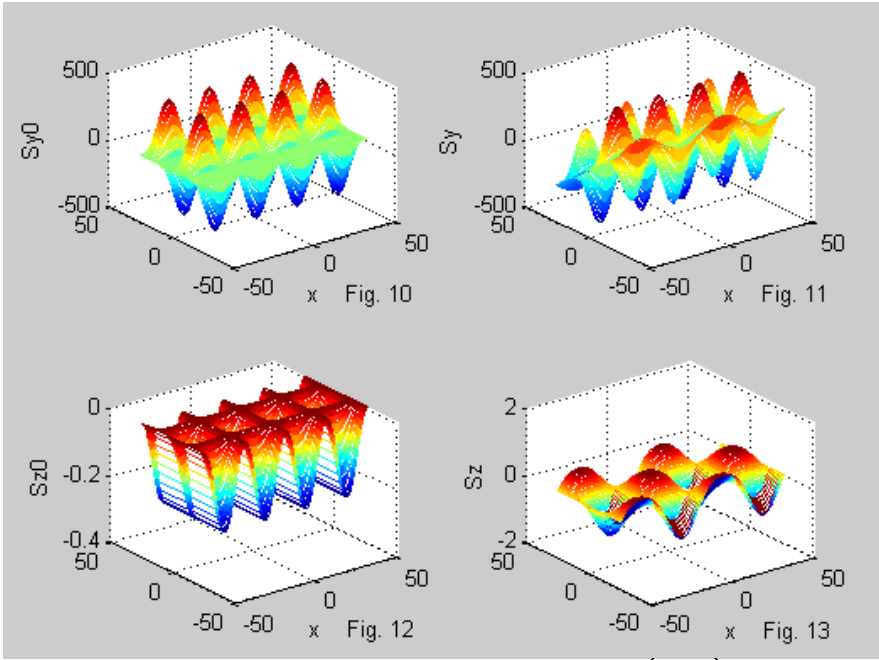


Fig. 10-13 show S_{y0} , S_y , S_z , S_{z0} values on (x, y) section plane at $\alpha = 2\pi/N$, $\beta = 2\pi/N$, $j_z = 1$, $j_x = 1$, $J_y = 3$. It is seen that

$$S_y \approx S_{y0}, \quad (29)$$

$$S_z \approx S_{z0}, \quad (30)$$

where integral values are the following

$$\overline{S_y} = \int_{x,y} S_y dx dy \approx 0, \quad (31)$$

$$\overline{S_z} = \int_{x,y} S_z dx dy < 0, \quad (32)$$

4. Vertical stability and motion

Thus,

1. at any J_v there is a vertical flow of gravitomagnetic energy not depending on J_v

$$\overline{S_z} < 0. \quad (33)$$

2. at $J_v > 0$ there is a horizontal flow of gravitomagnetic energy

$$\overline{S_x} < 0. \quad (34)$$

Simultaneously with these energy flows, $\overline{P_z} < 0$ and $\overline{P_x} < 0$ flows of gravitomagnetic momentum exist. In accordance with the law of momentum conservation, the oppositely directed $\overline{P_{mz}} > 0$ and $\overline{P_{mx}} < 0$ momenta of tsunami mass exist. $\overline{P_{mz}} > 0$ momentum holds the vertical shape of tsunami, and $\overline{P_{mx}} < 0$ momentum moves tsunami in direction opposite to velocity.

Thus, the cause of tsunami motion is air resistance. This air resistance creates an additional mass current directed against v velocity of vortex translational motion. So, there is a positive feedback between tsunami velocity and its mechanical momentum: **after starting the movement, tsunami picks up the velocity.** Gravitomagnetic energy does the work - see Chapter 3.

5. Conclusions

Proposed mathematical model explains the following:

- energy source for tsunami movement
- source of tsunami driving force
- tsunami shape retention

Appendix 1

The solution of combined equations (2.10-2.14) will be sought in the form of:

$$H_x = h_x \cos(\alpha x) \sin(\beta y), \quad (41)$$

$$H_y = h_y \sin(\alpha x) \cos(\beta y), \quad (42)$$

$$H_z = h_z \sin(\alpha x) \sin(\beta y) + J_v y, \quad (43)$$

$$J_x = j_x \sin(\alpha x) \cos(\beta y) + J_v, \quad (44)$$

$$J_y = j_y \cos(\alpha x) \sin(\beta y), \quad (45)$$

$$J_z = j_z \cos(\alpha x) \cos(\beta y), \quad (46)$$

where

$h_x, h_y, h_z, j_x, j_y, j_z$ - amplitudes of functions,

α, β - constants.

Let us differentiate (41-46) and substitute the expression obtained in initial combined equations (2.10-2.14). For example, from (2.10) we obtain:

$$h_z \beta \cdot \sin(\alpha x) \cos(\beta y) + J_y = j_x \sin(\alpha x) \cos(\beta y) + J_y.$$

After reducing by common multipliers, we find:

$$h_z \beta = j_x, \quad (48)$$

Similarly, from (2.11-2.14) we find:

$$-h_z \alpha = j_y, \quad (49)$$

$$h_y \alpha - h_x \beta = j_z, \quad (50)$$

$$h_x \alpha + h_y \beta = 0, \quad (51)$$

$$j_x \alpha + j_y \beta = 0. \quad (52)$$

From (48, 49) we find:

$$h_z = \frac{j_x}{\beta}, \quad (53)$$

$$j_y = -j_x \frac{\alpha}{\beta}. \quad (54)$$

From (50, 51) we find:

$$h_y = -h_x \frac{\alpha}{\beta}, \quad (55)$$

$$h_x = -j_z \left(\frac{\alpha^2}{\beta} + \beta \right). \quad (56)$$

Thus, under given α, β, j_x, j_z the remaining j_y, h_z, h_x, h_y , variables can be found from equations (56, 55, 54, 53), respectively.

Appendix 2

By analogy with (1.8.3) in Chapter 2, we write an expression for gravitational energy density vector projections:

$$S_{xyz} = \begin{bmatrix} S_x = J_y H_z - J_z H_y \\ S_y = J_z H_x - J_x H_z \\ S_z = J_x H_y - J_y H_x \end{bmatrix} \quad (60)$$

Using the formulas (2.15-2.20) of the main text, we find the gravitational energy density vector projections:

$$S_{xyz} = \begin{bmatrix} S_x = j_y \cos(\alpha) \sin(\beta) (h_z \sin(\alpha) \cos(\beta) + J_v y) - \\ \quad - j_z \cos(\alpha) \cos(\beta) h_y \cos(\alpha) \cos(\beta) \\ S_y = j_z \cos(\alpha) \cos(\beta) h_x \cos(\alpha) \sin(\beta) - \\ \quad - (j_x \sin(\alpha) \cos(\beta) + J_v) (h_z \sin(\alpha) \sin(\beta) + J_v y) \\ S_z = (j_x \sin(\alpha) \cos(\beta) + J_v) h_y \sin(\alpha) \cos(\beta) - \\ \quad - j_y \cos(\alpha) \sin(\beta) h_x \cos(\alpha) \sin(\beta) \end{bmatrix} \quad (61)$$

When multiplying, we find:

$$S_{xyz} = \begin{bmatrix} S_x = j_y \cos(\alpha) \sin(\beta) h_z \sin(\alpha) \sin(\beta) + j_y \cos(\alpha) \sin(\beta) J_v y - \\ \quad - j_z \cos(\alpha) \cos(\beta) h_y \sin(\alpha) \cos(\beta) \\ S_y = j_z \cos(\alpha) \cos(\beta) h_x \cos(\alpha) \sin(\beta) - \\ \quad - j_x \sin(\alpha) \cos(\beta) h_z \sin(\alpha) \sin(\beta) - J_v j_x \sin(\alpha) \cos(\beta) \\ \quad - h_z \sin(\alpha) \sin(\beta) J_v - J_v^2 y \\ S_z = j_x \sin(\alpha) \cos(\beta) h_y \sin(\alpha) \cos(\beta) + J_v h_y \sin(\alpha) \cos(\beta) - \\ \quad - j_y \cos(\alpha) \sin(\beta) h_x \cos(\alpha) \sin(\beta) \end{bmatrix} \quad (62)$$

or

$$S_x = \begin{bmatrix} \frac{1}{2} j_y h_z \sin^2(\beta) \sin(2\alpha) + J_v j_y y \cdot \cos(\alpha) \sin(\beta) - \\ \quad - \frac{1}{2} j_z h_y \cos^2(\beta) \sin(2\alpha) \end{bmatrix}, \quad (63)$$

$$S_y = \begin{bmatrix} \frac{1}{2} j_z h_x \cos^2(\alpha) \sin(2\beta) - \frac{1}{2} j_x h_z \sin^2(\alpha) \sin(2\beta) - \\ \quad - J_v j_x y \cdot \sin(\alpha) \cos(\beta) - J_v h_z \sin(\alpha) \sin(\beta) - J_v^2 y \end{bmatrix}, \quad (64)$$

$$S_z = \begin{pmatrix} j_x h_y \sin^2(\alpha x) \cos^2(\beta y) + j_y h_x \sin(\alpha x) \cos(\beta y) - \\ - j_y h_x \cos^2(\alpha x) \sin^2(\beta y) \end{pmatrix}. \quad (65)$$

References

1. Khmel'nik S.I. Mathematical Model of Water and Sand Tsunami. The Papers of independent Authors, ISSN 2225-6717, № 33, 2015, а также <http://vixra.org/abs/1505.0100>, 2015-05-13 (in Russian).

Chapter 4.8. Additional forces of celestial bodies interaction

Contents

- 1. Introduction \ 126
- 2. Gravitomagnetic interaction of moving masses \ 127
- 3. Known experiments \ 129
- 4. Gravitomagnetic interaction of the satellite and Earth \ 131
- 5. Conclusions \ 136
- References \ 137

1. Introduction

In Chapter 1, the Maxwell-like gravitational equations specified based on known experiments are considered, from which it follows that the significant forces of moving masses gravimagnetic interaction in a vacuum can exist. These equations are valid only under conditions of a weak gravitational field at low velocities. Therefore, it should be expected that the gravimagnetic interactions between satellites, asteroids and larger celestial bodies can be observed in space. The calculations of such interactions and some examples are given below.

In Chapter 1 it is shown that Maxwell-like gravitational equations must be supplemented by some empirical coefficient of medium gravitational permeability. This coefficient for vacuum has the size of $\xi \approx 10^{12}$ order and sharply decreases with pressure increase. This explains the absence of visible effects of moving masses gravimagnetic interaction in the air. However, these interactions are clearly demonstrated in a vacuum. The restriction can also be the fact that, as it follows from the basic GR equations, Maxwell-like gravitational equations are valid only under conditions of a weak gravitational field at low velocities. Therefore, it should be expected that such gravimagnetic interactions between satellites, asteroids and larger celestial bodies can be observed in space.

2. Gravitomagnetic interaction of moving masses

Let us consider m_1 and m_2 masses, moving with v_1 and v_2 velocities, respectively. In Appendix 5 of Chapter 1 it is shown that in this case the gravitomagnetic Lorentz forces which are the following (here the unitary vectors of velocity are denoted by dashed lines) arise:

$$\overline{F_{21}} = \sigma \overline{f_{21}}, \quad (1)$$

$$\overline{F_{12}} = \sigma \overline{f_{12}}, \quad (1a)$$

where

$$\overline{f_{21}} = (\overline{v'_1} \times (\overline{v'_2} \times \overline{r'})). \quad (2)$$

$$\overline{f_{12}} = (\overline{v'_2} \times (\overline{v'_1} \times \overline{r'})), \quad (2a)$$

$$\sigma = \frac{\zeta \xi G \cdot m_1 m_2 v_1 v_2}{c^2 r^2}, \quad (3)$$

where $\zeta = 2$, $\xi \approx 10^{12}$.

Let us consider the case when both velocities lie in the same xOy plane. In Appendix 3 of Chapter 1 it is shown (see (2a)) that in this case vector product (2) is the following:

$$\overline{f_{21}} = (v'_{2x} r'_y - v'_{2y} r'_x) \begin{bmatrix} v'_{1y} \\ -v'_{1x} \end{bmatrix}. \quad (4)$$

Thus, in this case

$$\overline{f_{21}} \perp v'_1. \quad (5)$$

In particular, when $r'_y = 0$, i.e. $r' = r'_x$, we have:

$$\overline{f_{21}} = r' \cdot v'_{2y} \begin{bmatrix} -v'_{1y} \\ v'_{1x} \end{bmatrix}. \quad (6)$$

The vectors included in this formula are shown in Fig. 1.

If even $v'_{1x} = 0$, i.e. $v'_1 = v'_{1y}$, then

$$\overline{f_{21}} = -r' \cdot v'_{2y} v'_1. \quad (7)$$

Thus, in this case the force (7) is repelling. Consequently, the force (1) is also repelling. The force of two masses attraction is always attractive and equal to

$$P = \frac{Gm_1m_2}{r^2}. \tag{8}$$

In Appendix 5 of Chapter 1 it is also shown that

$$F = \phi_g P, \tag{9}$$

where

$$\phi_g = \zeta \xi \cdot \frac{v_1 v_2}{c^2}. \tag{10}$$

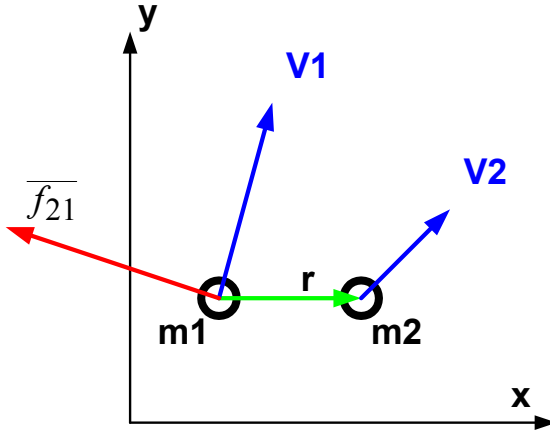


Fig. 1.

Example 1. Let us consider two m_1 and m_2 masses located at $\bar{r} = r_x$ distance. Let their velocities satisfy the following conditions

$$v'_{1x} = 0, \text{ i.e. } v'_1 = v'_{1y},$$

$$v'_{2x} = 0, \text{ i.e. } v'_2 = v'_{2y},$$

i.e. their \bar{v}_2, \bar{v}_1 velocities are parallel to Oy axis. Then from (7) we

find $\bar{f}_{21} = -r' \cdot v'_2 v'_1$. The vector of this force is directed opposite to $\bar{r} = r_x$ vector. At that the module of repelling force is equal to (9). The attractive force is always equal to (8). Consequently, in this position the force of masses interaction will be absent, if $\phi_g = 1$.

We have $c \approx 3 \cdot 10^{10}$ cm/sec., $\zeta = 2$. Let us suppose that $v_1 = v_2 = 10^5$ cm/sec. Then from (10) we have:

$$\phi_g = 1 = \zeta \xi \cdot \frac{v_1 v_2}{c^2}, \text{ from which we find } \xi = \frac{c^2}{\zeta \cdot v_1 v_2} \text{ or}$$

$$\xi = \left(3 \cdot 10^{10} \right) / 2 \cdot \left(10^5 \right) \approx 5 \cdot 10^{10}. \text{ Under these conditions,}$$

the total force will be attractive, if $\xi < 5 \cdot 10^{10}$, and repelling if $\xi > 5 \cdot 10^{10}$.

3. Known experiments

It was mentioned above that the observations of gravimagnetic interactions between satellites, asteroids and larger celestial bodies should be expected in space. The unexplained experiment using Explorer-I satellite (1958) is briefly described below. Then the mathematical model of satellite flight, considering gravimagnetic interaction between the Earth and satellite is considered, and it is shown that the results of such modeling coincide with observations.

In [2] Hoagland describes the Brown's experiment with Explorer-I satellite (1958). The trajectory of this satellite was clearly contrast to calculated trajectory, and no explanation has been found up to now. Investigating this fact, Hoagland doesn't restrain his creative impulse:

1) "... this is a delightful space discovery, which, obviously, being publicly confirmed, would mean the most important result of all the space program! This is a concealment, which continues to this day. "

2) "It seems that immediately after launching, the real trajectory of Explorer-I unequivocally violated two basic physical laws of the twentieth century. And it DID NOT gain any scientific recognition, prizes or discussions... even 50 years after the absolutely unexpected discovery."

3) "...in contrast to public "proves" of Explorer-I anomalous behavior, in private capacity, secretly, he (Brown) was looking for a serious working alternative to Newton and Einstein!"

4) von Braun's intensive world search for working physics to solve this fundamental problem was not something that he did "just out of interest." Obviously, he was the only aware of that if this "violation" of classical mechanics in satellites dynamics was not understood and then somehow taken under control, the impossibility of future satellites placing on the planned orbits will quickly put an end of entire space program!

5) If a space vehicle can not be launched on an accurate, predictable orbit, then scientific missions based on known satellite orbits... could not be successfully carried out. The fly-arounds of designed objectives could not be planned for military purposes.

6) "Radically "non-Newtonian" in-orbit behavior of Explorer-I (and other US satellites) should be considered as the main scientific and political discovery in the early space program, if not in the field of solar system research over the last 50 years! "

Hoagland also points to a number of other unexplained experiments

1) " 34 hours after launching, the first Soviet automatic lunar probe successfully crossed the Moon's orbit, but was found ahead of the Moon by as much as "5.953 km" before remaining on the annual, solar orbit... This was the first independent confirmation of this possibility, because the Soviets in Earth's orbit could always say (and said) that any orbit they achieved was "planned". The Moon miss, and even at a distance greater than the Moon diameter itself (3.475 km), considering a complex system of space navigation availability, was an important evidence that the mysterious "Force" (not Newtonian gravitation) pointedly acting on Von Braun's space vehicle, acted also on the Soviet vehicles!"

2) "Two months later, when it was the Von Braun's turn to carry out another American lunar mission Pioneer 4, his space vehicle was found at a distance of 59.533 km before Moon. Ten times more than a mistake of Russian scientists!"

3) "Open access data consideration revealed the equally unexpected "behavior" of two additional Explorer satellites under Von Braun's military program, as well as similar "mysteriously increased orbits" of three successfully launched US Navy Avangard satellites to such an extent that the latter became the oldest artificial satellites still rotating around the Earth!"

4) "However, as we have noticed, even after 50 years no one noticed or asked deeper questions about this amazing event sequence: repeated violations of Newton's laws and Einstein's relativity theory when launching the first US satellites!"

5) "For a little more than one year and half... Von Braun successfully launched two more Explorer satellites, and US Navy - three (of the planned 11 satellites) Avangard satellites. And they all showed the same kind of "mysterious anomalies of orbits!"

Further Hoagland notes that in the absence of an adequate theory, a need for "the rocket that would have enough fuel to withstand any "non-Newtonian uncertainties" that it would collide on its way... arised"

So, the energy resources of rocket allow the satellite to send some v_p launching velocity. However, the real trajectory is such that, for its existence, the satellite should have acquired $v_r > v_p$ launching velocity. In order to explain this contradiction, Hoagland suggests that rockets somehow acquired additional energy during acceleration.

Hoagland is looking for an explanation of all these facts in the theory of torsional fields. A highly unusual theory [4], based on the fact that gravity distribution velocity is finishing and, consequently, a violation of Newton's third law can be committed is also known. An explanation is justified below.

4. Gravitomagnetic interaction of the satellite and Earth

Further, it is shown that experimental trajectory of Explorer-I satellite coincides with the calculated trajectory, which is obtained by considering gravitomagnetic Lorentz force.

Table 1.

| Path parameter | Calculated values obtained by traditional methods | Experimental values |
|---|---|---------------------|
| 1 | 2 | 3 |
| Apogee (km) [2, p. 5] | $a_1 = 1575$ | $a_2 = 2534$ |
| Perigee (km) [2, p. 5] | $p_1 = 224$ | $p_2 = 360$ |
| Orbital period (min) [2, p. 5] | 105 | 114.7 |
| The same, but calculated in this article under given apogee and perigee | $T_1 = 105$ | $T_2 = 114.3$ |
| Velocity of satellite delivery - velocity at perigee (m/sec) [4] | $v_1 = 8129$ | $v_2 = 8214$ |
| The same, but calculated in this article under given apogee and perigee | $v_1 = 8125$ | $v_2 = 8210$ |
| Semimajor axis (km) [5] | | 7832 |
| Eccentricity [5] | | 0.14 |

Chapter 4.8. Additional forces of celestial bodies interaction

| | | |
|-----------------|------|--------|
| Inclination [5] | | 33,24° |
| Weight (kg) [5] | 21.5 | 21.5 |

In [2, 4, 5] the parameters of Explorer-I satellite trajectory, which are summarized in Table are given. 1. Let us denote by:

$G = 6.67 \cdot 10^{-11}$ - gravitational constant (here and below the SI system is used)

$R = 6.37 \cdot 10^6$ - Earth radius,

$M = 5.97 \cdot 10^{24}$ - Earth mass,

$m = 21.5$ - satellite weight,

p - perigee (see Table 1).

At first, we will simulate the calculated trajectory, choosing a launching velocity so that it could pass through the perigee and apogee points specified and could have a specified duration of turnover. For this, trajectory calculation can be carried out by the following formula

$$g = \frac{d^2 \bar{r}}{dt^2}, \tag{1}$$

where

g - acceleration caused by Earth's attraction,

t - current time,

$\bar{r}(x, y)$ - vector of distance from the Earth to satellite, where the system of plane coordinates is tied to earth center.

Acceleration is calculated, as is known, by the formula [3]

$$g = \frac{G \cdot M \cdot r}{|r|^3}. \tag{2}$$

In this case, the initial values should be as follows:

$$\left. \begin{aligned} x_0 &= r_0 = R + p, \\ y_0 &= 0, \end{aligned} \right\} \tag{3}$$

$$\left. \begin{aligned} (dx/dt)_0 &= 0, \\ (dy/dt)_0 &= v_{yo}, \end{aligned} \right\} \tag{4}$$

where v_{yo} - velocity of satellite at perigee. This calculation can also be carried out by the following analytical formulas [6]:

$$\left. \begin{aligned} r(\varphi) &= \frac{P}{1 - e \cdot \cos(\varphi)}, \\ P &= \frac{r_0^2 v_{y0}^2}{GM}, \\ e &= 1 - \frac{P}{r_0}, \end{aligned} \right\} \quad (4a)$$

where

φ - $r(\varphi)$ vector angle with the abscisse,

P - ellipse parameter (satellite trajectory),

e - ellipse eccentricity.



Fig. 1.

Fig. 1 of [2] shows the trajectories of satellite

- with $p_1 = 0.224 \cdot 10^6$ perigee and $a_1 = 1.575 \cdot 10^6$ apogee,
- with $p_2 = 0.36 \cdot 10^6$ perigee and $a_2 = 2.534 \cdot 10^6$ apogee.

The differences between $\Delta a = 0.959 \cdot 10^6$ perigees and $\Delta p = 0.136 \cdot 10^6$ apogees differ by factor of 7 - see Table. 1.

Fig. 2 shows the calculated satellite trajectories

- with $p_1 = 0.224 \cdot 10^6$ perigee, $a_1 = 1.575 \cdot 10^6$ apogee, $v_1 = 8125$ launching velocity, $T_1 = 105$ min orbiting period for theoretical orbit (tr),
- with $p_2 = 0.36 \cdot 10^6$ perigee, $a_{20} = 2.35 \cdot 10^6$ apogee, $v_2 = 8210$ launching velocity, $T_2 = 114.3$ min orbiting period for experimental orbit (ex),
- Earth radius and circumference (rz, oz, zz).

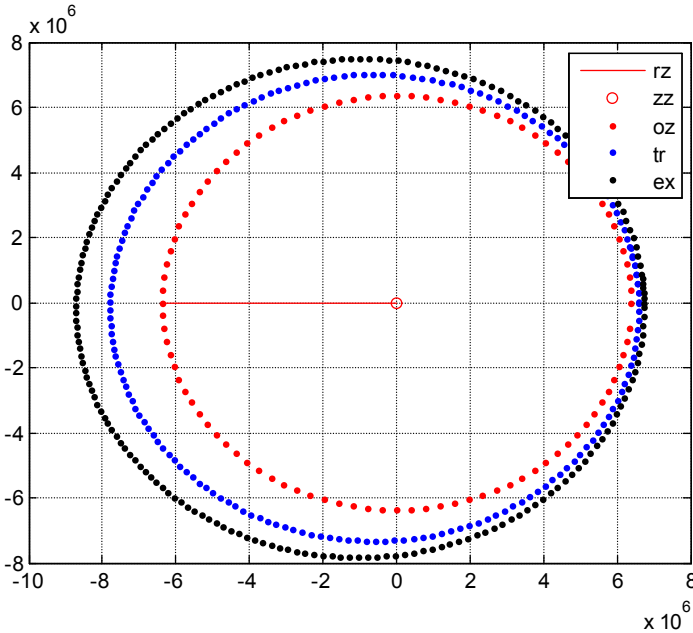


Fig. 2 ('fspunath, mode=7')

As shown above, m_2 moving mass acts on other m_1 moving mass by the following gravitomagnetic Lorentz force:

$$\overline{F}_{21} = \frac{\xi \cdot G m_1 m_2}{c^2 r^3} (\overline{v}_1 \times (\overline{v}_2 \times \overline{r})), \tag{5}$$

where

\bar{r} - vector of distance between masses,

\bar{v}_1, \bar{v}_2 - corresponding velocities,

ξ - coefficient of medium gravitational permeability,

$c = 3 \cdot 10^8$ - light velocity.

In our case, Earth acts on satellite, and satellite's influence on Earth can be neglected. In this case, the acceleration that satellite acquires under gravitomagnetic Lorentz force action from the Earth's side is the following,

$$\bar{L} = \frac{\xi \cdot GM}{c^2 r^3} (\bar{v}_c \times (\bar{v}_3 \times \bar{r})), \quad (6)$$

where \bar{v}_c, \bar{v}_3 - velocity of satellite and Earth, respectively.

The coefficient of ξ gravitational permeability is approximately determined above based on Samokhvalov's experiments. This coefficient nonlinearly depends on air pressure. Satellite trajectory partially passes through the atmosphere in which the pressure varies with elevation, and partially in space with zero pressure. Therefore we cannot strictly consider the influence of this coefficient. Next, we determine an average value of this coefficient on the assumption that it doesn't change throughout the whole trajectory.

Thus, considering the gravitomagnetic Lorentz force, acceleration will be calculated by the following formula:

$$\bar{w} = \bar{g} + \bar{L}. \quad (7)$$

At that, the initial conditions (3, 4) with the following constant values are accepted:

$p_2 = 0.36 \cdot 10^6$ - experimentally found perigee,

$v_1 = 8125$ satellite velocity at perigee, which is achieved in accordance with theoretical calculation.

Thus, it is assumed that engines delivered to satellite that particular launching velocity for which they were designed. But a trajectory was determined considering the Lorentz gravitomagnetic force.

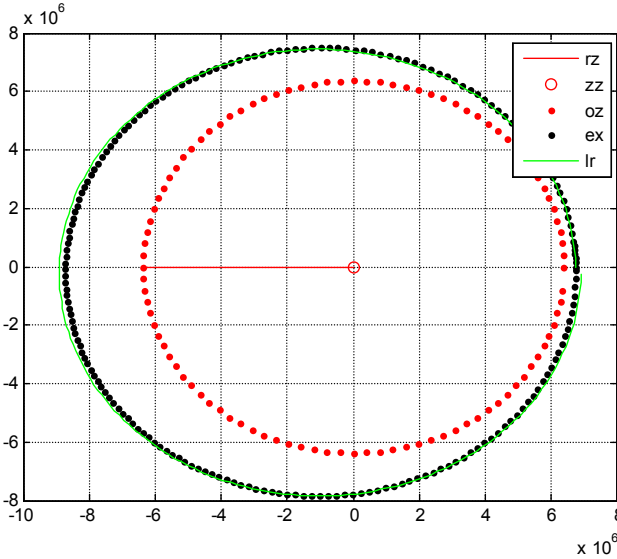


Fig. 3 ('fspunath, mode=10')

Furthermore, the average value of $\xi = 2.65 \cdot 10^6$ medium gravitational permeability coefficient is taken. This value differs from $\xi = 10^{12}$ value for vacuum found above, as the satellite flew in low-density atmosphere.

Fig. 3 shows the calculated trajectories of satellite with $p_2 = 0.36 \cdot 10^6$ perigee:

- satellite trajectory with $v_2 = 8210$ launching velocity, $a_{20} = 2.35 \cdot 10^6$ apogee and $T_2 = 114.3 \text{ min}$ orbiting period for experimental orbit (ex), calculated by traditional method - see also in Fig. 2,
- satellite trajectory with $v_1 = 8125$ launching velocity, $a_2 = 2.53 \cdot 10^6$ apogee and $T_2 = 114.3 \text{ min}$ orbiting period, calculated considering Lorentz gravitomagnetic force (lr),
- Earth radius, circle and centre (rz, zz, oz).

5. Conclusions

Thus, the actual satellite orbit is such that when calculating the known theory it should have $v_2 = 8210$ launching velocity. However,

according to satellite energy reserves it could reach $v_1=8125$ ($v_2 - v_1 = 85$) launching velocity. In order to explain this contradiction, it was assumed that satellite during acceleration received an additional energy (from unknown source) and reached $v_2=8210$ launching velocity. This article shows that the satellite also at $v_1=8125$ launching velocity (without obtaining an additional energy) could have the specified actual orbit.

Thus, the observed trajectory of Explorer-I satellite coincides with the trajectory calculated by proposed theory, i.e. it can be explained without using unknown energy sources, but only taking considering Lorentz gravitomagnetic force. In this case, an energy source is the Earth's gravitational field (just as the energy consumed by electric charges under Lorentz forces action is supplied by current source).

An insignificant difference between perigees mentioned above can be explained as well as the difference between apogees, but for this it is necessary to consider the trajectory of satellite acceleration, that isn't done here.

Moreover, Explorer-I satellite actual trajectory coincidence with calculated trajectory, which is obtained considering Lorentz gravitomagnetic force, is one more confirmation of the fact that Maxwell-like gravitational equations are valid and vacuum (and any other medium) has a gravitational permeability for magnetogravitational interactions between masses transmission.

References

1. Zilberman G.Ye. Electricity and magnetism, Moscow, publ. "Science", 1970.
2. Richard Caulfield of Hoagland. Von Braun's 50-year secret, 2010, http://alexfl.ru/vechnoe/vechnoe_braun.html, http://alexfl.ru/vechnoe/vechnoe_braun1.html
3. P.I. Bakulin, E.V. Kononovich, V.I. Frost. Course of General Astronomy, 1976, <http://www.bibliotekar.ru/astronomia/>
4. O.H. Derevensky. Spillules and fittings of universal gravitation, <http://newfiz.narod.ru/gra-opus.htm>
5. Explorer-1, Wikipedia, <http://ru.wikipedia.org/wiki/Эксплорер-1>
6. O.V. Golubeva. Theoretical mechanics. The Higher School Publishing House, 1976.

7. Khmelnik S.I., Khmelnik M.I. Additional forces of interaction of celestial bodies. The Papers of independent Authors, ISSN 2225-6717, № 21, 2012.
8. Khmelnik S.I., Khmelnik M.I. More on the additional (non-Newtonian) forces of interaction of celestial bodies. The Papers of independent Authors, ISSN 2225-6717, № 24, 2013.

Chapter 4.9. Turbulent flows generating mechanism and method of their calculation

Contents

1. Introduction \ 139
 2. Gravitomagnetic interaction of moving masses \ 140
 3. Gravitomagnetic interaction as the cause of turbulence \ 140
 4. Quantitative estimations \ 142
 5. Example: turbulent water flow in a pipe \ 143
 6. Turbulent flow equations \ 145
- References \ 148

1. Introduction

An explanation of turbulent flows generating mechanism, based on Maxwell-like gravitational equations is proposed below. It is shown that the flowing fluid moving molecules interact with each other similarly to moving electric charges. The forces of such an interaction can be calculated and included in Navier-Stokes equations as mass forces. Navier-Stokes equations supplemented by such forces become the hydrodynamics equations for turbulent flow. In this case the calculation of turbulent flows can be performed using the known methods for Navier-Stokes equations solution.

Chapter 1 shows that Maxwell-like gravitational equations must be supplemented by some medium gravitational permeability empirical coefficient. This coefficient for a vacuum has $\xi \approx 10^{12}$ size of order and sharply decreases with pressure increase. This explains the absence of visible effects of moving masses gravimagnetic interaction in the air. However, these interactions are clearly demonstrated in a vacuum.

The moving molecules in a fluid flow are separated by vacuum. Therefore, their gravitomagnetic interaction forces can be significant and influence on the flow pattern.

It is known that the fluid or gas laminar flow velocity spontaneous increase (without external forces) leads to a turbulent flow [1]. The mechanism of flow spontaneous change from laminar to turbulent is not

found. Obviously, a source of forces perpendicular to flow velocity must be detected.

Further, it is shown that the fluid moving masses gravitomagnetic interaction may be the cause of turbulence.

2. Gravitomagnetic interaction of moving masses

Let us consider two m_1 and m_2 masses, moving with v_1 and v_2 velocities, respectively. In Appendix 5 of Chapter 1 it is shown that in this case gravitomagnetic Lorentz forces arise, which are the following (velocity unitary vectors are denoted by dash lines here):

$$\overline{F_{21}} = \sigma \overline{f_{21}}, \quad (1)$$

$$\overline{F_{12}} = \sigma \overline{f_{12}}, \quad (2)$$

where

$$\overline{f_{21}} = (\overline{v_1'} \times (\overline{v_2'} \times \overline{r'})). \quad (3)$$

$$\overline{f_{12}} = (\overline{v_2'} \times (\overline{v_1'} \times \overline{r'})), \quad (4)$$

$$\sigma = \frac{\zeta \xi G \cdot m_1 m_2 v_1 v_2}{c^2 r^2}, \quad (5)$$

where $\zeta = 2$, $\xi \approx 10^{12}$.

In case of parallel $\overline{v_1} = \overline{v_2}$ speeds and equal $\overline{F_{12}} = -\overline{F_{21}}$ force masses, the laminar flow retains its pattern. However, in general case, when $\overline{v_1} \neq \overline{v_2}$, $\overline{F_{12}} \neq \overline{F_{21}}$ forces arise, i.e. an unbalanced $\overline{\Delta F} = \overline{F_{12}} + \overline{F_{21}}$ force acting on m_1 and m_2 masses and distorting these masses motion trajectories (let us note that in this case Newton's third law isn't observed [2]) arise. From the above formulas it follows that the unbalanced force is directed at an angle to flow velocity, which violates laminarity.

In Appendix 5 of Chapter 1 it is also shown that gravitomagnetic Lorentz forces effectiveness greatly exceeds the effectiveness of electromagnetic Lorentz forces at comparable speeds.

3. Gravitomagnetic interaction as the cause of turbulence

For unbalanced forces appearance, the following conditions must be fulfilled:

1. velocities must have a certain value (at which the forces become significant);
2. reason for velocities local changes must arise, for example,
 - barrier appearance
 - pressure variation while jet flowing out of water.

We can specify a number of reasons for unbalanced forces increase:

- temperature increase at which v_1 and v_2 velocities cease to be parallel due to thermal fluctuations,
- viscosity, i.e. intermolecular attraction forces decrease, which counteract an unbalanced force which expands the molecules.

A number of external factors can be indicated causing the appearance of unbalanced forces due to v_1 and v_2 velocities parallelism external violation and, for example,

- temperature, pressure sudden changes,
- additional fluid or other substances injection.

The local change of a pair of tie molecules equal velocities, caused, for example, by asymmetric impact, inevitably spreads to the whole flow range.

Navier-Stokes equations allow to determine flow velocities encountering or leaving a barrier. While knowing these velocities, the above equations can determine the unbalanced forces. Then these forces, as velocity functions, can be included in Navier-Stokes equations as mass forces.

The kinetic energy of turbulent motion increases with increasing turbulence. This increase occurs due to the action of gravitomagnetic forces of Lorentz. The source of these forces and this additional energy is (as shown above) the gravitational field of the Earth.

There are devices in which this additional energy is used - so-called cavitation heat generators. The first such device was "Apparatus for Heating Fluids" by J. Griggs [6]. In it "*the rotor rides a shaft which is driven by external power means. Fluid injected into the device is subjected to relative motion between the rotor and the device housing, and exits the device at increased pressure and/or temperature*". At present, there are many such devices that differ in the ways of creating turbulent motion - see, for example, [7], where there are also references to many prototypes. Such devices provide efficient, simply, inexpensive and reliable sources of heated water and other fluids for residential and industrial use.

Together with the existence of cavitation heat generators there is no generally accepted theory that reveals the source of additional energy

that appears as a result of the functioning of these cavitation heat generators. In particular, Griggs in [6] points out that his "device is 6 thermodynamically highly efficient, despite the structural and mechanical simplicity of the rotor and other compounds", but does not provide a theoretical justification for this statement. The authors of the following devices also do not consider the reasons for the efficiency of their devices.

All this confirms that the source of the additional energy of the cavitation heat generators is the gravitational field of the Earth

4. Quantitative estimations

Let us consider the formulas (2.1-2.5). From them it follows that:

$$\overline{\Delta F} = \sigma \overline{\Delta f}, \tag{7}$$

where

$$\overline{\Delta F} = \overline{F_{21}} + \overline{F_{12}}, \tag{8}$$

$$\overline{\Delta f} = \overline{f_{21}} + \overline{f_{12}}. \tag{9}$$

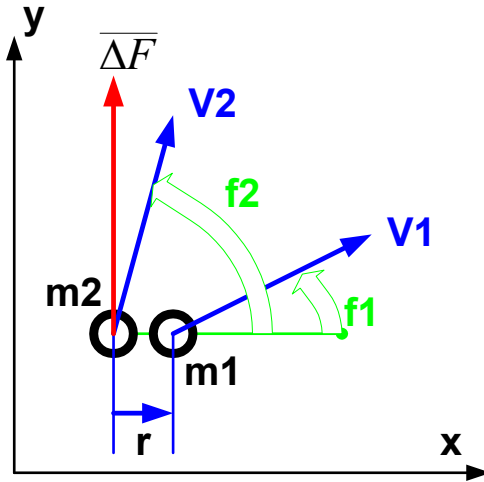


Fig. 1.

Let us consider two adjacent fluid molecules. The distance between fluid molecules remains unchanged. In view of little r distance between them, it can be assumed that \overline{v}_1 , \overline{v}_2 velocity vectors of these molecules are applied to one point and lie in some common xOy plane. Then the vector (9) also lies in this plane. Fig. 1 shows \overline{v}_1 , \overline{v}_2 , \overline{r} vectors geometry.

In Appendix 5 of Chapter 1 (see (6)) it is also shown that vectors value (9, 8) is determined by the following formulas

$$\Delta f = r \sin(\varphi_2 - \varphi_1). \quad (10)$$

$$\Delta F = \sigma \sin(\varphi_2 - \varphi_1). \quad (11)$$

This force occurs when adjacent molecules strike against the barrier at different angles. It can be assumed that the total force is applied to one of molecules. Therefore, it creates dipole torque composed of two molecules,

$$M = r \cdot \Delta F. \quad (12)$$

Each pair of adjacent fluid molecules forms a dipole with a torque (12). Torques increase fluid molecules local velocities, which in turn increase the torques of dipoles specified. Therefore, a turbulence, having begun, continues to develop, spreading in the fluid volume.

A formula (11) determines the forces of fluid molecules gravitomagnetic interaction, as a function of these contacting molecules velocities. These forces can be included in Navier-Stokes equations as mass forces - see below.

5. Example: turbulent water flow in a pipe

Next, we consider the case of fluid jets interaction, assuming that the groups of molecules forming the jet element interact. Let us consider a special case when the jets velocity vectors are equal to $|\mathbf{v}_1| = |\mathbf{v}_2| = v$ and group masses are equal to $m_1 = m_2 = m$. At that, by (4), we find the following force

$$\sigma = \zeta \xi G \left(\frac{mv}{cr} \right)^2. \quad (11)$$

where r – distance between jets. Denote by d the typical size of group (jet diameter) and rewrite (11) in the form of

$$\sigma = \zeta \xi G \left(\frac{\rho \cdot d^3 v}{cr} \right)^2. \quad (11a)$$

where ρ - fluid density and mass of group

$$m = \rho \cdot d^3. \quad (11b)$$

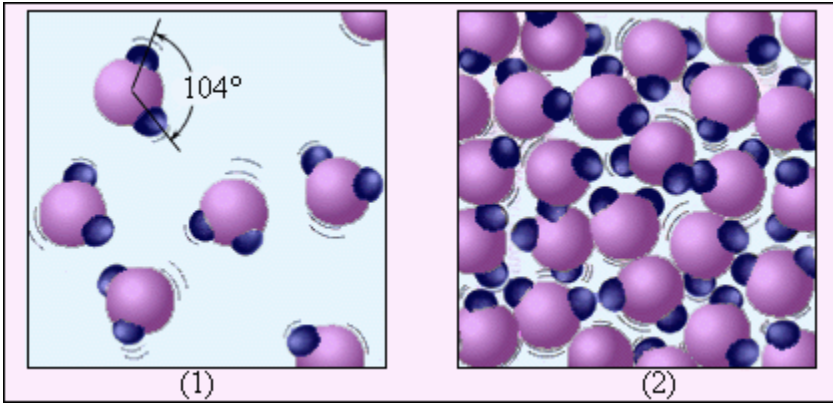


Fig. 2 (from Wikipedia.ru). Water vapor (1) and water (2). The water molecules are increased approximately $5 \cdot 10^7$ times.

A further example relates to water. As molecules in a fluid are located at distances comparable with the size of molecules themselves (see Fig. 2), the distance between molecules must be assumed as equal to molecule diameter, which for water is equal to $r \approx 3 \cdot 10^{-12}$ cm. Water density is $\rho = 1 \text{g/cm}^3$. Let us also find the velocity of water flow at which a turbulence arises. It is known [3] that the condition for turbulence occurrence is determined by Reynolds criterion, which for round pipe is the following

$$\text{Re} = Dv / \eta, \tag{12}$$

where D - pipe diameter, η - kinematic viscosity coefficient. For water $\eta \approx 0.01 \text{cm}^2/\text{f}$ [3]. Let us suppose that $D = 2.5 \text{cm}$. A turbulence occurs if Reynolds number is $\text{Re} > 2300$. In this case, from (12), we find the turbulent flow $v = 10$ cm/sec velocity. Let the diameter of interacting jets is equal to $d \approx 0.1 \text{cm}$. Above it is stated that $\zeta = 2$, $\xi \approx 10^{12}$, $G \approx 7 \cdot 10^{-8}$. Then from (11a) we find

$$\sigma = 2 \cdot 10^{12} \cdot 7 \cdot 10^{-8} \left(0.1^3 \cdot 10 / (6 \cdot 10^{10} \cdot 3 \cdot 10^{-12}) \right) \approx 2000 \text{ dyne} \tag{13}$$

Let us suppose that $\sin(\varphi_2 - \varphi_1) \approx 10^{-2}$. Then we find the force (9):

$$\Delta F \approx 20 \text{ dyne} \tag{14}$$

From (10, 14) we also find a torque:

$$M \approx r \cdot \Delta F \approx 2 \text{ dyne} \cdot \text{cm}. \tag{15}$$

6. Turbulent flow equations

Let us return again to formula (5) from Appendix 5 of Chapter 1:

$$\overline{F}_{21} = \frac{\zeta \xi G m^2}{c^2 r^3} \left(\overline{v}_1 \times \left(\overline{v}_2 \times \overline{r} \right) \right) \left[\text{dyne} = \frac{\text{g} \cdot \text{cm}}{\text{sec}^2} \right]. \quad (1)$$

Similarly to par. 5, we find

$$\overline{\Delta F} = \mathcal{G} \cdot \overline{\Delta f}, \quad (2)$$

where

$$\mathcal{G} = \frac{\zeta \xi G m^2}{c^2 r^3} \left[\frac{\text{g}}{\text{cm}^2} \right], \quad (3)$$

$$\overline{\Delta f} = \mathcal{G} \left(\left(\overline{v}_1 \times \left(\overline{v}_2 \times \overline{r} \right) \right) - \left(\overline{v}_2 \times \left(\overline{v}_1 \times \overline{r} \right) \right) \right). \quad (4)$$

Considering (11b), we rewrite (3) in the form of

$$\mathcal{G} = \frac{\zeta \xi G \rho^2 d^6}{c^2 r^3} \left[\frac{\text{g}}{\text{cm}^2} \right]. \quad (4a)$$

Next, the forces causing a turbulence will be denoted by T. In Appendix 3 of Chapter 1 it is shown (see also Fig. 1) that if all the vectors lie in one plane, then (4) is equivalent to formula

$$T_y = \mathcal{G} \cdot R_x \left(v_{2x} v_{1y} - v_{2y} v_{1x} \right), \quad (5)$$

where

T_y - force acting on mass moving with v_2 velocity

R_x - distance between mass centers.

Let two adjacent groups of molecules be located on ox axis. Denote by:

$$R_x = dx, \quad (6a)$$

$$v_2 = v, \quad v_1 = v + dv. \quad (6b)$$

Then

$$T_y = \mathcal{G} \cdot dx \left(v_x \left(v_y + dv_y \right) - v_y \left(v_x + dv_x \right) \right) \quad (7)$$

or

$$T_y = \mathcal{G} \cdot dx \left(v_x dv_y - v_y dv_x \right). \quad (8)$$

Similarly, for the right coordinate system, we have:

$$T_z = \mathcal{G} \cdot dy \left(v_y dv_z - v_z dv_y \right), \quad (9)$$

$$T_x = \mathcal{G} \cdot dz \left(v_z dv_x - v_x dv_z \right). \quad (10)$$

Let us consider the operator (which hereinafter for brevity sake will be called as turbulean)

$$\Omega(\mathbf{v}) = \begin{vmatrix} v_z \frac{dv_x}{dz} - v_x \frac{dv_z}{dz} \\ v_x \frac{dv_y}{dx} - v_y \frac{dv_x}{dx} \\ v_y \frac{dv_z}{dy} - v_z \frac{dv_y}{dy} \end{vmatrix} \left[\frac{\text{cm}}{\text{sec}^2} \right]. \quad (11)$$

Example 1. Consider the ideal laminar flow in which $v_x \neq 0$, $v_y = 0$, $v_z = 0$. Obviously, in this case, $\Omega(\mathbf{v}) = \mathbf{0}$ i.e. a laminar flow cannot spontaneously pass into the turbulent flow.

In accordance with (6a) we have

$$R = dx = dy = dz \quad (12)$$

From (10-12) the following expression follows

$$T = R^2 \mathcal{G} \cdot \Omega(\mathbf{v}) \left[\text{cm}^2 \frac{\text{g}}{\text{cm}^2} \cdot \frac{\text{cm}}{\text{sec}^2} = \frac{\text{g} \cdot \text{cm}}{\text{sec}^2} = \text{dyne} \right]. \quad (13)$$

or

$$T = \mathcal{G}_1 \cdot \Omega(\mathbf{v}) [\text{dyne}], \quad (14)$$

where

$$\mathcal{G}_1 = R^2 \mathcal{G} = \frac{R^2 \zeta \xi G \rho^2 d^6}{c^2 r^3} [\text{g}]. \quad (15)$$

An expression (14) defines the force acting on a group of molecules on the part of three adjacent groups of molecules located in front of it on coordinate axes, if coordinate differentials are equal to distance between molecules (12). This force acts on the four groups of molecules volume, i.e. on $4d^3$ volume. Therefore, the force acting on a unit volume is,

$$T_m = \rho_m \Omega(\mathbf{v}) \left[\frac{\text{dyne}}{\text{cm}^3} = \frac{\text{g}}{\text{sec}^2 \text{cm}^2} \right], \quad (16)$$

where

$$\rho_m = \frac{\mathcal{G}_1}{4d^3} = \frac{R^2 \zeta \xi G \rho^2 d^3}{4c^2 r^3} \left[\frac{\text{g}}{\text{cm}^3} \right]$$

or

$$\rho_m = \frac{\zeta \xi G \rho^2 d^8}{4c^2 r^3} \left[\frac{\text{g}}{\text{cm}^3} \right], \quad (17)$$

as $R \approx d$.

Let us note for comparison that the mass force dimensionality in hydrodynamics equations is $F_m \left[\frac{\text{dyne}}{\text{g}} = \frac{\text{cm}}{\text{sec}^2} \right]$, and the dimensionality of force acting on unit volume is $\rho F_m \left[\frac{\text{dyne}}{\text{g}} \frac{\text{g}}{\text{cm}^3} = \frac{\text{dyne}}{\text{cm}^3} = \frac{\text{g}}{\text{sec}^2 \text{cm}^2} \right]$. And the force has exactly this dimensionality(16). At that the coefficient (17) has the density dimensionality and can be called as the turbulent density of a given fluid.

Example 2. Let us find ρ_m turbulent density of water. We have:

$\rho = 1\text{g/cm}^3$, $d \approx 0.1\text{cm}$, $c \approx 3 \cdot 10^{10} \text{cm/sec}$, $\zeta = 2$, $\xi \approx 10^{12}$. Let the diameter of jet is equal to $d \approx 0.1\text{cm}$ and a distance between jets is $r \approx 10^{-8} \text{cm}$. Then

$$\rho_m = \frac{\zeta \xi G \rho^2 d^8}{4c^2 r^3} = \frac{2 \cdot 10^{12} \cdot 7 \cdot 10^{-8} \cdot 10^{-8}}{4 \cdot (3 \cdot 10^{10})^2 (10^{-8})^3}$$

or $\rho_m \approx 0.4 \left[\frac{\text{g}}{\text{cm}^3} \right]$.

Forces (16) can be included in Navier-Stokes equations. Navier-Stokes equations supplemented by such forces become hydrodynamics equations for turbulent flow.

A turbulean (11) structurally is similar to expression

$$(\mathbf{v} \cdot \nabla) \mathbf{v} = \begin{bmatrix} v_x \frac{\partial v_x}{\partial x} + v_y \frac{\partial v_x}{\partial y} + v_z \frac{\partial v_x}{\partial z} \\ v_x \frac{\partial v_y}{\partial x} + v_y \frac{\partial v_y}{\partial y} + v_z \frac{\partial v_y}{\partial z} \\ v_x \frac{\partial v_z}{\partial x} + v_y \frac{\partial v_z}{\partial y} + v_z \frac{\partial v_z}{\partial z} \end{bmatrix}, \quad (18)$$

included in Navier-Stokes equations. Therefore, in order to calculate turbulent flows, it is necessary to use the known methods for Navier-Stokes equations solving and, in particular, the method proposed in [4].

An expression (18) is included in Navier-Stokes equations with ρ factor. Consequently, a turbulean (11) will influence on equation solution if a coefficient (17) will have $\rho_m \approx \rho$ value.

References

1. Ivanov B.N. World of physical hydrodynamics. From the problems of turbulence to the physics of the cosmos. Ed. 2nd. - Moscow: Editorial URSS, 2010 (in Russian)
2. Zilberman G.E. Electricity and Magnetism, Moscow. "Science", 1970 (in Russian)
3. Wilner J.M. etc. Handbook of hydraulics and hydraulic drives, ed. "High School", 1976 (in Russian)
4. Khmelnik S.I. Navier-Stokes equations. On the existence and the search method for global solutions (second edition). Published by "MiC" - Mathematics in Computer Comp., printed in USA, printed in USA, Lulu Inc., ID 9976854, Israel, 2010, ISBN 978-1-4583-2400-9.
5. Khmelnik S.I. The Emergence Mechanism and Calculation Method of Turbulent Flows. The Papers of independent Authors, ISSN 2225-6717, № 22, 2014; and <http://vixra.org/abs/1311.0025>, 2013-11-04.
6. James L. Griggs. Apparatus for Heating Fluids, United States Patent, 5188090, 1993, <http://www.rexresearch.com/griggs/griggs.htm>
7. Petrakov AD, Pleshkan SN, Radchenko S.M. Rotary, cavitation, vortex pump, <http://www.freepatent.ru/patents/2393391>

Chapter 5. Experiments

There are experiments that, without regard, are attributed to perpetuum mobile, just because there are no acceptable explanations. Meanwhile, some of them can be explained by the assumption of a significant magnitude of the gravitomagnetic forces. More such experiments and their mathematical models are described below.

Chapter 5.1. Samokhvalov's Experiments

Contents

- 1. Introduction \ 150
- 2. First Experiment \ 150
- 3. Second Experiment \ 153
- 4. The Role of Gravito-magnetic Lorentz Forces \ 155
- 5. Some experimental estimates \ 158
- References \ 159

1. Introduction

Samokhvalov had conceived and carried out a series of unexpected and surprising experiments, which presumably can be explained by interaction of irregular mass currents [4-8]. For the author, these experiments served as an incentive for the development of this topic. Analyzing these experiments, it could be assumed that they correspond to the Maxwell equations for gravity. It could be seen, then irregular mass currents J_g create variable gravito-electrical intensity E_g and gravito-magnetic induction B_g . At the interaction of this induction with the masses m , moving with speed v there arises gravito-magnetic Lorentz force.

It is important to note that the effect are so significant, that in order to explain them within the said Maxwell-similar equations these equations should be supplemented by a certain empirical coefficient ξ . Further it is shown that with such modification the results of experiments are in good agreement with Maxwell's equations for gravity, which we agreed above to call MGM-equations.

It should be noted that Samokhvalov did not accept such an explanation of his experiments.

2. First Experiment

Consider the Samokhvalov experiment described in [1]. Two disks are placed into a vacuum chamber; they are misbalanced (by skewed axes)

and are rotating in one direction. Both disks are overheated. Technical parameters of the setup are as follows:

- Material of the disks aluminum
- Pressure in the chamber $1Pa$
- Density of aluminum $\rho \approx 2.7g/cm^3$
- Thickness of the disks $h \approx 0.09cm$
- Diameter of the disks $2R = 16.5cm$
- Gap between the disks $d \approx 0.3cm$
- Beating on the sides $0.05cm$
- Number of revolutions $f \approx 50/sec$
- Temperature of overheating (in [4] is written that the temperature rise measured after some minutes was $50K$).

Let us consider the disk's rotation as mass current. We can assume that this current is formed by the mass's motion in the circle of the upper band of the disk of radius $R \approx 7sm$ and the cross-section

$$S \approx 0.3 \cdot 2.5cm^2 \approx 7.5cm^2 . \quad (1)$$

The speed of this mass is

$$v = 2\pi R \cdot f \approx 2\pi \cdot 7 \cdot 50 \approx 2200sm/sec . \quad (2)$$

So, the mass current is

$$J_g = S\rho v \approx 7.5 \cdot 2.7 \cdot 2200 = 4400g/sec . \quad (3)$$

This current is variable because the beating of the disks. In accordance with (1.2.4) this current causes a variable axial induction (along the ox axis of the disk) average on the circle area of radius R ,

$$B_g = \frac{2\xi G J_g}{cR} \quad (4)$$

or

$$B_g = \frac{2 \cdot \xi \cdot 7 \cdot 10^{-8} \cdot 4400}{3 \cdot 10^{10} \cdot 7} \approx 3\xi \cdot 10^{-15} . \quad (5)$$

This induction is variable in time because of the disks. We shall assume that the circular frequency of this induction is

$$\omega \approx 2\pi f = 314 . \quad (6)$$

In accordance with (1.2.9), the strength of vortex electric current created by variable gravito-magnetic flow, is

$$J_{ge} = \frac{\eta}{cR_e} \cdot \frac{d\Phi_g}{dt} \quad (7)$$

or

$$J_{ge} = \frac{\eta\omega}{cR_e} \cdot \Phi_g \quad (8)$$

In our case

$$\Phi_g = \beta\pi R^2 B_g = \beta\pi R^2 \cdot 3 \cdot 10^{-15}, \quad (9)$$

where β – is the coefficient of induction weakening on the level of the driven disk (because of the gap). So,

$$J_{ge} = \frac{\eta\omega}{cR_e} \cdot \beta\pi R^2 B_g \quad (10)$$

or

$$J_{ge} = \frac{1.8 \cdot 10^{14} \cdot 314}{3 \cdot 10^{10} R_e} \cdot \beta\pi 8.25^2 \cdot 3 \cdot \xi 10^{-15} = \frac{\xi\beta}{R_e} 10^{-6} \quad (10a)$$

This electric current raises the disk temperature. In the experiment it was shown that the disk's temperature has increased by $\Delta T \approx 100$ grades. Let us consider the equivalent voltage

$$E_e = J_{ge} R_e \quad (11)$$

And assume that such increase of the disk temperature may be due to the voltage E_e . From (10a, 11) we find

$$E_e = \xi\beta 10^{-6}. \quad (12)$$

Let us assume that such equivalent voltage is $E_e = 200$. Then we find

$$\xi\beta \approx 2 \cdot 10^8. \quad (13)$$

Here ξ depends on the pressure, and β depends on the gap. Assuming that $\beta \approx 1/d^2$ and knowing that $d \approx 0.3sm$, we find $\beta \approx 0.01$. Thus, based on Samokhvalov's experiment we can now assume that for the indicated conditions the gravitational permeability coefficient with the pressure of 0.1 atm is equal to

$$\xi_p(0.1) \approx 2 \cdot 10^{10}. \quad (14)$$

3. Second Experiment

Let us now consider the experiments of Samokhvalov described in [5]. Two disks are placed into a vacuum chamber, misbalanced by skewed axes. The first of them rotates forcibly, and the second disk begins rotation due to the impact of the first one. The speed f_2 of the second disk's rotation (if the rotation speed of the first one is constant) depends on the gap between the disks d and on the pressure in vacuum chamber p . We may assume that the rotation speed of the driven disk is

$$f_2(p, d) = f_{2p}(p) \cdot f_{2d}(d). \quad (1)$$

This experiment explores these two dependences.

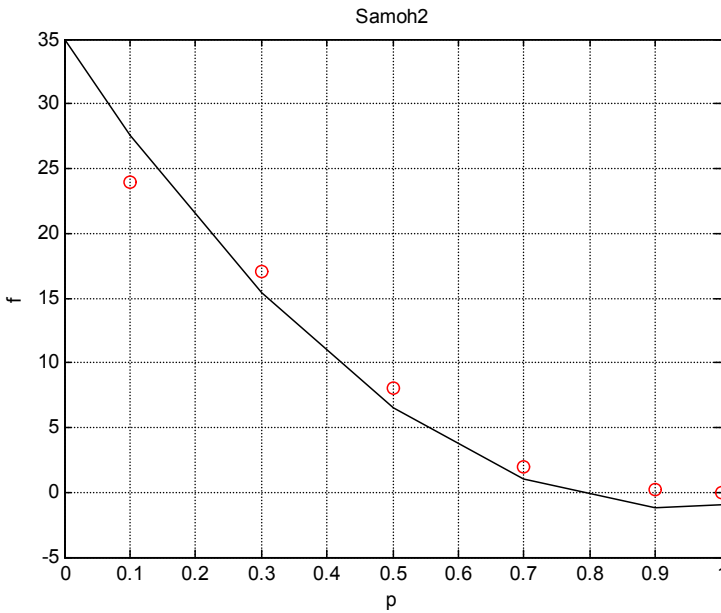


Fig. 1.

The dependence of rotation speed on the pressure is given in [2] on Fig 2, from which we find

$$p = [0.1, 0.3, 0.5, 0.7, 0.9, 1] \text{ (atm)},$$

$$f = [24, 17, 8, 2, 0.2, \varepsilon],$$

where ε is a small value that it is impossible to find from the experiment results.

Fig. 1 shows this experimental dependence (by circles) and (by full line) – the approximating function in the form of a polynomial with 5 members. We assume that,

$$f_2(p, d = 0.2) = f_{2p}(p) \cdot f_{2d}(0.2) \tag{2}$$

In particular, by approximating function we find:

$$f_2(0.1, 0.2) = 25, \quad f_2(0, 0.2) \approx 35. \tag{2a}$$

The dependence of rotation speed on the distance

is given in [5, Fig. 3], from which we find:

$$d = [0.15, 0.2, 0.25, 0.3] \text{ (sm)},$$

$$f_1 = [24, 17, 6, 5] \text{ при } p = 1 \text{ atm},$$

$$f_{102} = [30, 25, 12, 10] \text{ при } p = 1.02 \text{ atm}.$$

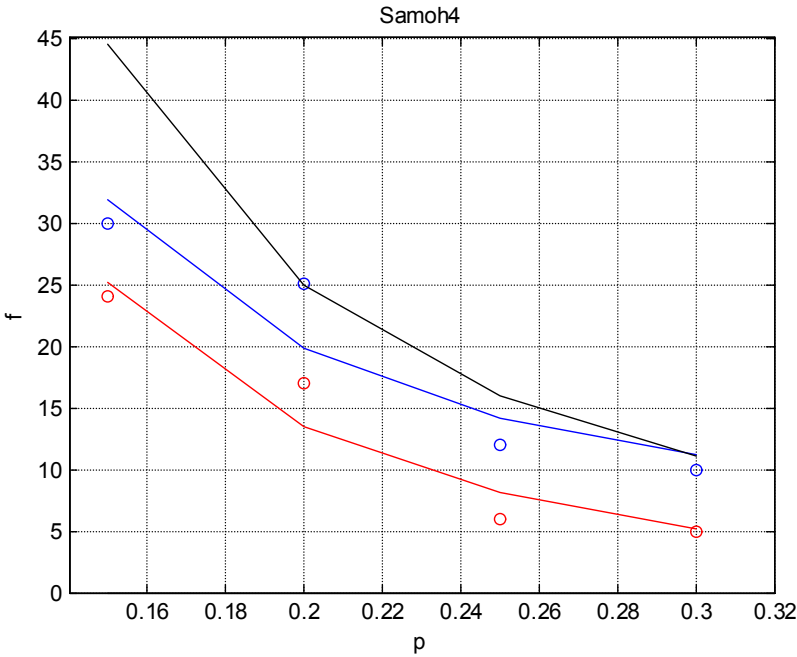


Fig. 2.

Fig. 2 shows this experimental dependence (by circles) and the approximating function (by full line) – in the form of $a + b/d^2$, and the function

$$f_{2d}(d) = 1/d^2. \tag{3}$$

To a first approximation further we shall use the function (2). In particular, for $d = 0.2$ (cm) we have

$$f_{2d}(0.2) \approx 25. \tag{3a}$$

Analysis of the functions $f_{2p}(p)$ and $f_{2d}(d)$

Taking into account (2, 3a), we find:

$$f_{2p}(p) = f_2(p, 0.2) / f_{2d}(0.2) = 0.04 f_2(p, 0.2). \quad (4)$$

In particular from (2a) we find:

$$f_{2p}(0) = 0.04 f_2(0, 0.2) = 0.04 \cdot 35 \approx 1.5, \quad (6)$$

Below in (p.3.7) it will be shown that

$$f_{2p}(p) = \vartheta \cdot \xi_p^2(p). \quad (8)$$

Thus,

$$\xi_p(p) \approx \sqrt{\frac{f_{2p}(p)}{\vartheta}}, \quad (9)$$

From (9) it follows that

$$\frac{\xi_p(0)}{\xi_p(p)} \approx \sqrt{\frac{f_{2p}(0)}{f_{2p}(p)}}, \quad (10)$$

In experiment 1 it was shown, that

$$\xi_p(0.1) \approx 2 \cdot 10^{10}. \quad (11)$$

Combining (5, 6, 10, 11), we get

$$\xi_p(0) \approx \xi_p(0.1) \sqrt{\frac{f_{2p}(0)}{f_{2p}(0.1)}} \approx 2 \cdot 10^{10} \sqrt{\frac{1.5}{1}} \approx 2.5 \cdot 10^{10}.$$

From this we can find a crude estimate of the gravitational permeability of vacuum:

$$\xi \approx 10^{10}. \quad (13)$$

4. The Role of Gravito-magnetic Lorentz Forces

In Samokhvalov's experiments the driving disk drags the driven disk. Now we shall present the explanation of this phenomenon. Samokhvalov notes that first there occurs the vibration of the driving disk, and then begins the rotation of the driven disk – then see Fig. 3.

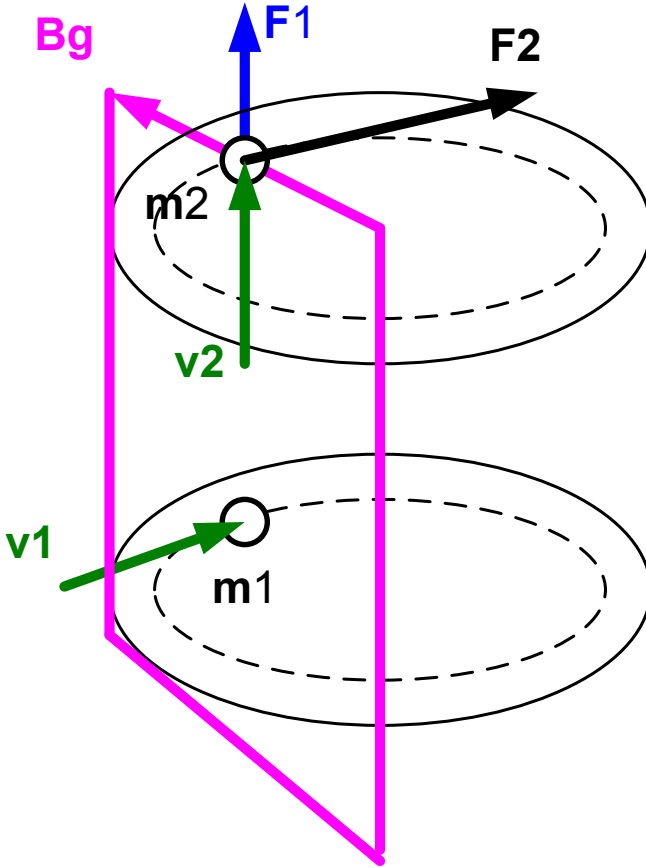


Fig. 3.

The disks' vibration is explained in the following way - see Fig. 3. Above, analyzing the Experiment 1, it was shown that the driving disk is variable mass current (2.3) with circular frequency (2.6). This current mass m_1 , moving with speed v_1 , creates a variable gravito-magnetic induction (2.4), which is perpendicular to the mass current of drive disc, ie radially and parallel to the disc plane – see a closed curve on Fig. 3. This induction vector at the slave drive moves with a speed v_1 relative to the mass m_2 of the driven disc. This raises gravito-magnetic Lorentz force, acting on the mass m_2 and directed vertically and having the form

$$F_1 = m_2 v_1 B_g \frac{c}{c} \tag{1}$$

Above, when analyzing the experiment 1, we have showed that the masses m_1 , m_2 are the mass of a circle of higher band of the disk with radius $R \approx 7\text{cm}$ and cross-section (2.1). This mass is equal to

$$m_1 = m_2 = 2\pi R S \rho. \quad (2)$$

The force F_1 is directed perpendicularly to the disk plane and varies with the frequency $f \approx 50/\text{sec}$, causing the vibration of the driven disk. Evidently, the speed v_2 of this vibration is proportional to the force F_1 , i.e.

$$v_2 = \alpha F_1, \quad (3)$$

where α is a certain constant.

This force may explain the "oscillatory" character of the process of repulsion of the screen with the increase of the oscillations amplitude (angle of the frame's deviation) after steadying of the disk rotation speed", which is reflected in the Samokhvalov's experiments described in [5].

Rotating force acting on the driven disk is explained as follows – see Fig. 3. The foregoing gravito-magnetic induction B_g (2.4), created by the driving disk is directed perpendicularly to the mass current of the driving disk, i.e. along the disk's radius and parallel to its plane. This induction acts on the vertically vibrating mass m_2 of the driven disk by gravito-magnetic Lorentz force (1.1.1):

$$F_2 = m_2 v_2 B_g \frac{c}{c}. \quad (4)$$

This force is tangential to the circumference of the disc, because perpendicular to the direction of induction (which is directed along the radius of the disk) and the speed (which is perpendicular to the plane of the disk). Due to the fact, that the speed of vibration v_2 and the induction B_g are changing synchronously, the vector of this force doesn't change direction. Apparently, the rotation speed of the driven disk is proportional to the force F_2 , i.e. the number of its revolutions is

$$f_2 = \gamma F_2, \quad (5)$$

where γ – a certain constant. Combining (1-5) we get

$$\begin{aligned}
 f_2 &= \gamma m_2 v_2 B_g \frac{\xi}{c} = \gamma m_2 B_g \frac{\xi}{c} \alpha F_1 = \\
 &= \gamma m_2 B_g \frac{\xi}{c} \alpha m_2 v_1 B_g \frac{\xi}{c} = \alpha \gamma \left(m_2 \frac{\xi}{c} B_g \right)^2.
 \end{aligned} \tag{6}$$

Because gravito-magnetic induction B_g proportional gravito-magnetic permeability ξ (which follows from (2.4, 2.5)), the number of revolutions of the slave drive is

$$f_2 = \mathcal{G} \cdot \xi^2. \tag{7}$$

Which is proportional to ξ^2 with a certain proportionality factor \mathcal{G} . This ratio is used in the above analysis of the Experiment 2 – see (3.8).

5. Some experimental estimates

The analysis of Samokhvalov's experiments considered above makes it possible to obtain a rough estimate of the gravitational permeability coefficient ξ :

$$\xi \approx 10^{10}. \tag{1}$$

This value can be greatly underestimated, since the experiments were performed with an average vacuum, but ξ increases with decreasing of pressure. At atmospheric pressure $\xi \Rightarrow 0$, that explains the absence of visible effects of gravitational interaction of moving masses.

The gravitational permeability of the medium is now introduced into the equation for the gravitomagnetic induction rotor in the same way as the magnetic permeability of the medium is introduced into the equation for the magnetic induction rotor.

In order to discover the phenomenon of the decrease in the air gravitational permeability compared to vacuum gravitational permeability we should point out that the magnetic permeability of electrically conductive materials sharply decreases with increasing of current frequency which forms the magnetic field (due to the appearance of Foucault currents shielding the magnetic induction). It can be assumed that being influenced by alternating gravimagnetic field the moving air molecules behave similarly to free electrons in a conductor under the action of an alternating magnetic field – “Foucault mass currents” screening the gravimagnetic induction arise in the air. In this case, it can be assumed that at low velocity of mass motion the significant effects can be observed even in the atmosphere.

References

Note: **DNA-№.crp** – The Papers of independent Authors,
ISSN 2225-6717, <http://izdatelstwo.com/>

1. Samokhvalov V.N. Mass-dynamic and Mass-variational interaction of moving masses. **DNA-13**, 2009 – C. 110-159.
2. Samokhvalov V.N. Quadrupole radiation of the rotating masses. **DNA-14**, 2010 – C. 112-145.
3. Samokhvalov V.N. Forceful action of mass-variational radiation on solids. **DNA-15**, 2010 – C. 175-195.
4. Samokhvalov V.N. The study of the forceful action and reflection of rotating mass quadrupole radiation from solids. **DNA-18**, 2011 – C. 165-187.
5. Samokhvalov V.N. Force effects at mass-dynamic interaction on the average vacuum. **DNA-19**, 2011 – C. 170-181.
- 6 Samokhvalov V.N. Investigation and measurement of force effects during mass-dynamic interaction. **DNA-24**, 2013 - C. 113-131.
7. Khmelnik S. I. More on Experimental Clarification of Maxwell-similar Gravitation Equations. **DNA-28**, 2014 – C. 104-124; and <http://vixra.org/abs/1311.0023>, 2013-11-04.

Chapter 5.2. Aldo Costa's Gravity Motor

“My small work will bring them (perpetual motion seekers) advantage: they will not have to flee from the kings and rulers without fulfilling their promises”

Leonardo Da Vinci

Contents

1. Introduction \ 161
2. Did not Flee... \ 162
3. Unbalanced Wheels \ 162
4. The Main Idea \ 164
5. The Definition of Gravimagnetic Lorentz Force \ 164
6. The Mathematical Model of Aldo Costa's Wheel \ 166
7. Quantitative Estimates \ 169
8. Some Comparisons \ 170
9. Technology \ 171
- Appendix 1. Circumferential Body Movement by Force of Gravity \ 171
 1. Ball Movement within a Tubular Circle \ 171
 2. Movement of a Ball within a Deformed Tubular Circleference \ 173
 3. The Dynamics of Ball Movement within a Deformed Tubular Circleference \ 175
 4. The momentum of force for Movement of Ball within a Deformed Tubular Circleference \ 176
- Appendix 2. Movement of Load on Vertical Step \ 177
- References \ 180

1. Introduction

It is known that the work of gravity for a body displacement along a closed pass is equal to zero.

In [1] one may read: After having reformed many efforts of building a perpetual motion machine, "Leonardo, after trying to comprehend, why such

motion machines of different systems do not work, claims the inevitability of the existence of inherent effects disrupting the work of such machines. His followers, based on his authority, use the principle of the impossibility of perpetual motion as an already firmly established law of nature. The Academy of Paris, basing on the views of these followers, had not presented a rigorous proof of the impossibility of the existence of a perpetual motion machine. Academy of Paris "meant well", when saying: "such work (of the creators of perpetual motion) is too wasteful, it has destroyed a lot of families. Often happens that a talented mechanic, who could take his rightful place, had squandered in that way his reputation, time and talent."

But the mechanics can not get calm down, because principle of the impossibility of perpetual motion is **not** firmly established as the law of nature. Repeated attempts to build a perpetual motion machine have been taken for centuries [2] and are continued now. But they only allow, as Leonardo wrote, to assert the inevitability of the existence of some interfering factors. There is no proof of the existence of such reasons, and the law of energy conservation has nothing to do with it.

2. Did not Flee...

There is a known history of Orferius's successful test of perpetual motion machine [3]. This work has been financed by Count Karl, who also led the "selection committee" including famous scientists. Count Karl was also considered one of the leading scientists of his time. Hard to imagine that Orferius undertook to deceive such a man. It seems to me less likely than a successful test. Orferius did not have to flee from the Count due to not having fulfilled his promises.

3. Unbalanced Wheels

Among the projects of perpetual motion the so-called unbalanced wheels are rather common. As described in [3] "the first design of unbalanced wheels was described by Marquis Worchester. From the description, it follows that it was a wheel with two rims - one within the other. To the rims weights are attached by means of strings so that when they are moved downward they are displaced towards the outer rim, and at movement upwards - towards the internal. "The author was unable to find a description of the wheel, but in [4] descriptions of several such devices are provided.

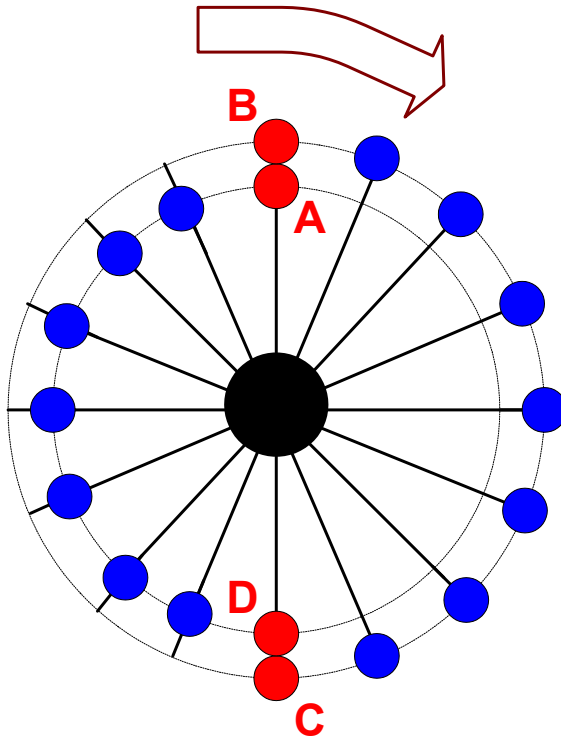


Fig. 1.

We shall consider the most impressive of them. In [5] the gravitational motor of Aldo Costa is described. Its design can be summarized as follows - see Fig. 1. The loads attached to the spokes revolve around a common axis. At the points A and C the loads move along the spoke in the points B and D respectively. Thus, if you move down (right) the loads rotate along the radius R_1 and moving up (right) loads rotate along the radius $R_2 < R_1$ - this is similar to what was proposed by the Marquis of Worcester - see above.

The wheel is mounted vertically, has a diameter of 18 m and contains 236 complex mechanisms for switching the position of loads - see Fig. 2. Machine parts are described in detail in the patent [9]). Several videos of the device are given in [10].

Note that here, as well as in the work of Marquis Worcester, there is a "wheel with two rims - one within the other. ... The weights are attached to the rim so, that during the downward movement they are displaced towards the outer rim and at movement upwards - towards the internal rim."

Another device of this type Dmitriev suggested [11]. Detailed description of the device and a few videos of his work presented in [12].



Fig. 2.

4. The Main Idea

Chapter 3 shows that the force of gravity can do work. At the same time, the author solemnly declares that he admits the energy conservation law (realizing, however, that this will not help author). Further, it is shown that this law does not contradict the possibility of constructing an eternal engine using the forces of gravity. In this case it is natural that the kinetic energy of the Earth decreases, but the author ignores this problem (in the same way as hydroelectric plants designers ignore it).

5. The Definition of Gravimagnetic Lorentz Force

In Chapter1 it is shown that gravimagnetic Lorentz force, acting from mass m_1 on mass m_2 , is determined by an expression of the form (here and further the CGS system is used)

$$\overline{F_{12}} = \frac{k_g m_1 m_2}{r^3} \left[\overline{v_2} \times \left[\overline{v_1} \times \overline{r} \right] \right], \quad (1)$$

where

- coefficient $k_g = \frac{\xi G}{c^2}$, (2)
- $G \approx 7 \cdot 10^{-8}$ - gravitational constant,
- $c \approx 3 \cdot 10^{10}$ - the speed of light in vacuum,
- ξ - gravimagnetic permeability of the medium,
- \overline{r} - a vector directed from point m_1 to point m_2 ,
- $\overline{v_1}$, $\overline{v_2}$ - speeds of masses m_1 and m_2 accordingly

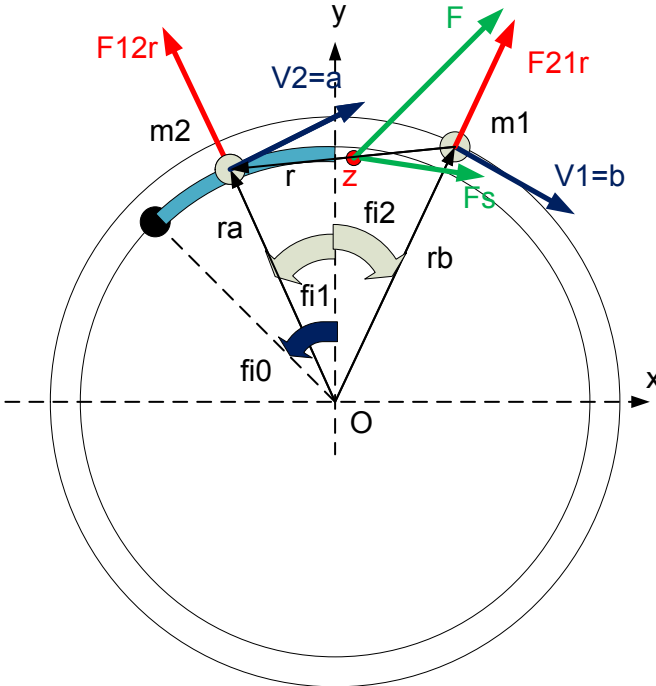


Fig. 3.

It is important to note that the effects in the above experiments are so significant that to explain them within the Maxwell-like gravitational equations it is necessary to enter gravimagnetic coefficient of permeability of the medium ξ (the same as the coefficient of permeability

of the medium μ in electromagnetism). However, the value of coefficient ζ in these experiments may be estimated only very roughly.

6. The Mathematical Model of Aldo Costa's Wheel

Consider Fig. 3, which shows the two weights on the wheel Aldo Costa. In our case the velocities in the formula (1) - are the linear speed of loads rotation. We shall select in the formula (1), the expression

$$\overline{f}_{12} = (\overline{a} \times (\overline{b} \times \overline{r})), \quad (3)$$

where

$$\overline{a} = \overline{v}_2, \quad \overline{b} = \overline{v}_1.$$

In the right Cartesian coordinate system, this expression takes the form

$$\overline{f}_{12} = \begin{bmatrix} a_y(b_x r_y - b_y r_x) - a_z(b_z r_x - b_x r_z) \\ a_z(b_y r_z - b_z r_y) - a_x(b_x r_y - b_y r_x) \\ a_x(b_z r_x - b_x r_z) - a_y(b_y r_z - b_z r_y) \end{bmatrix}. \quad (4)$$

The loads rotate at the same speed and in opposite directions. So

$$|a| = \omega R_2, \quad |b| = \omega R_1, \quad (5)$$

where R_2, R_1 are the radii of the semicircles, - angular velocity. We shall further denote radius vectors of loads m_1 and m_2 as r_b and r_a , respectively. Then

$$\overline{r} = r_a - r_b. \quad (6)$$

As the loads rotate in one plane, so

$$r_z = 0, \quad a_z = 0, \quad b_z = 0. \quad (7)$$

With this in mind, we obtain:

$$\overline{f}_{12} = \begin{bmatrix} a_y(b_x r_y - b_y r_x) \\ -a_x(b_x r_y - b_y r_x) \\ 0 \end{bmatrix}$$

or

$$\overline{f}_{12} = D [a_y, -a_x] \quad D = (b_x r_y - b_y r_x) \quad (8)$$

Similarly,

$$\overline{f}_{21} = D_2 [b_y, -b_x] \quad D_2 = -(a_x r_y - a_y r_x) \quad (8.1)$$

Now we shall find

$$\Delta f = \overline{f_{12}} - \overline{f_{21}} = \begin{bmatrix} Da_y - D_2b_y \\ -Da_x + D_2b_x \end{bmatrix} \quad (9)$$

From Fig. 3 it follows

$$\angle AOm_2 = \varphi_1, \quad \angle AOm_1 = \varphi_2$$

$$a_x = \omega R_1 \cos \varphi_1, b_x = \omega R_2 \cos \varphi_2,$$

$$a_y = \omega R_1 \sin \varphi_1, b_y = -\omega R_2 \sin \varphi_2,$$

$$r_a = R_1 \begin{bmatrix} -\sin \varphi_1, \cos \varphi_1 \end{bmatrix},$$

$$r_b = R_2 \begin{bmatrix} \sin \varphi_2, \cos \varphi_2 \end{bmatrix} \quad (10)$$

$$r = r_a - r_b. \quad (11)$$

Let us denote

$$\Delta f_L = \Delta f / |r|^3. \quad (16)$$

From (1, 3) it follows that

$$\Delta F = k_g m_1 m_2 \Delta f_L, \quad (17)$$

One can assume that the force acts on a pair of **rigidly** connected (through rim and spoked of wheels) masses and is applied to the center of the segment r - see the point in Fig. 3. The radius vector of this point

$$\overline{r_z} = \left(\overline{r_a} + \overline{r_b} \right) 2. \quad (20)$$

Let us find the projection ΔF_s of the force ΔF on the tangent to the circle of radius r_z . It is equal to the scalar product of this force on the unit K_w of vector perpendicular to the radius $\overline{r_z}$, i.e.

$$\Delta F_s = \overline{\Delta F} \otimes K_w. \quad (21)$$

If

$$r_z = \begin{bmatrix} r_{zx}, r_{zy} \end{bmatrix} \quad (22)$$

then

$$K_w = \begin{bmatrix} -r_{zy}, r_{zx} \end{bmatrix} / |r_z|. \quad (23)$$

In such way we may find the force (21). It creates a torque

$$M_s = \Delta F_s |r_z|. \quad (24)$$

Taking into account (21-23), we get

$$M_s = \overline{\Delta F} \otimes \begin{bmatrix} -r_{zy}, r_{zx} \end{bmatrix}. \quad (25)$$

Mass m_2 moves along the arc φ_o of radius R_1 - see Fig. 3. In this it interacts with the mass m_1 , which also moves along the arc φ_o of radius R_2 . The distance between them remains constant: $|r| = const$. The length of vector OZ also remains constant: $|r_z| = const$. The torque (25) also remains constant: $M_s = const$ - see further. In the highest point m_2 switches to a circle of radius R_2 ("top jump"), i.e. assumes the role of the mass m_1 . At this point the mass moving on a circle of radius R_1 after the former mass, assumes the role of the mass m_2 , etc.

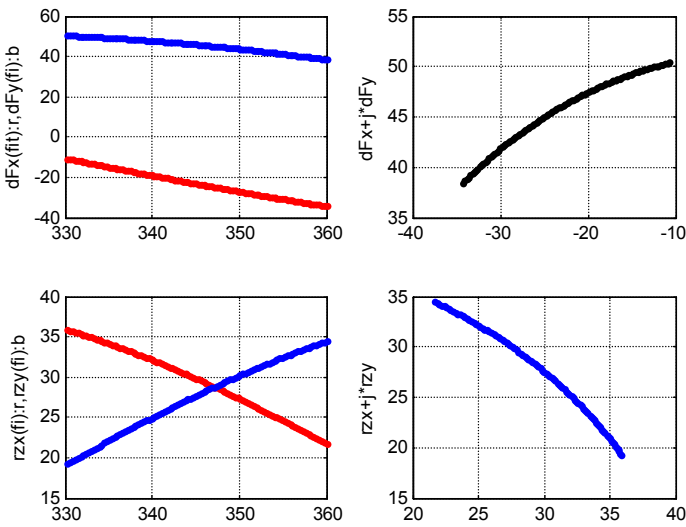


Fig. 4.

Counting moment (25), we can show can be shown that on the bottom of the wheel a similar torque of opposite sign is created. Thus in a real device the “bottom jump” must be excluded.

It can be shown that on the bottom wheel (where occurs the "lower jump") create the same momentum and with the same sign

Fig. 4 shows the results of the overall calculation. Thus:

- The first window shows projections of vector (21): ΔF_{sy} - above, ΔF_{sx} - below.
- The second window shows hodograph of vector (21) in the form $\Delta F_s = \Delta F_{sx} + j \cdot \Delta F_{sy}$.

- The third window shows projections of vector (22): r_{zx} - above, r_{zy} - below.
- The fourth window shows hodograph of vector (22) in the form $r_z = r_{zx} + j \cdot r_{zy}$.

Similarly, we can consider the forces involved in the movement of loads vertically - see Appendix 2.

7. Quantitative Estimates

In the example $|r| \approx 48$, $|r_z| \approx 41$ for $R_1 = 45$, $R_1 = 50$ (in CGS system), and the forces and forces torques are calculated in the conditions

$$K_{gm} = k_g m_1 m_2 = 1. \quad (31)$$

The torques are equal to: above - $M_s \approx 2000$ and below - $M_s \approx -2000$.

The torque acts in the time period $T_1 \approx 0.05$. Consequently, in the highest point the structure is affected by the torque

$$(F\Delta t)_o = K_{gm} M_s T_1 / R_1 \approx 2K_{gm}, \quad (32)$$

where the coefficient K_{gm} needs determination. In Appendix 1.4 it is shown that each load in such structure for continuous rotation needs to get a force impulse

$$(F\Delta t)_1 \approx 2500. \quad (33)$$

Consequently, to obtain continuous rotation by the Lorentz forces a following condition should be observed:

$$(F\Delta t)_o = 2(F\Delta t)_1 \quad (34)$$

or

$$K_{gm} = 2500. \quad (35)$$

Let us estimate for this case the value of coefficient ξ . Let the masses be $m_1 = m_2 = 500\Gamma$. Then from conditions (31, 35) we shall find

$$2500 = k_g 500^2 \quad (36)$$

or

$$k_g = 0.01.$$

Further from (2) we find

$$\xi = k_g c^2 / G = \frac{0.01(3 \cdot 10^{10})^2}{7 \cdot 10^{-8}} = 10^{26}. \quad (37)$$

This value coincides with that obtained in the analysis of Tolchin's inertioid [8]. With this value of ξ (in order of magnitude) the presented explanation is legitimate.

In this example, the angle $\varphi_o = \pi/6$. Consequently, in one revolution of the masses 12 pairs interact and we can assume that the torque $M_s \approx 2000$ is acting permanently. Thus, **a structure is possible in which the motion is due to the energy of the gravitational field.**

8. Some Comparisons

However, similar to the described problem of gravitational mass movement, we can consider exactly the same problem of the heavy electric charges motion, where there is no question about the legality of Maxwell-like gravitational equations and the value of the coefficient of gravimagnetic permeability of medium

Let us compare the Lorentz force in the interaction of mass and charge. Above we have described the Lorentz force acting from the first body to the second, in the form

$$F_{Lg} = k_g \frac{m^2}{r^3} \cdot \left[\vec{v}_2 \times \left[\vec{v}_1 \times \vec{r} \right] \right],$$

where $k_g = \frac{\xi G}{c^2}$. Similarly the Lorentz force acting from the first charge to the second has the form:

$$F_{Le} = k_e \frac{q^2}{r^3} \cdot \left[\vec{v}_2 \times \left[\vec{v}_1 \times \vec{r} \right] \right],$$

where $k_e = \frac{\mu}{c^2}$. So, the Lorentz force F_{Le} , acting on the charges, relates to Lorentz force F_{Lg} , acting on the masses (for the same speeds and distances), as

$$\frac{F_{Le}}{F_{Lg}} = \frac{k_e q^2}{k_g m^2} = \frac{\mu}{k_g c^2} \left(\frac{q}{m} \right)^2.$$

Assuming that $\mu = 1$ and $k_g = 0.01$ (as was shown above), we find:

$$\frac{F_{Le}}{F_{Lg}} = 10^{-19} \left(\frac{q}{m} \right)^2.$$

Let us compare this with ratio of attraction forces:

$$\frac{F_{Pe}}{F_{Pg}} = \frac{(1/\varepsilon)q^2}{Gm^2}.$$

For $\varepsilon = 1$ and $G \approx 7 \cdot 10^{-8}$ we find that:

$$\frac{F_{Pe}}{F_{Pg}} \approx 10^7 \left(\frac{q}{m} \right)^2$$

If $F_{Le} = F_{Pe}$, then $F_{Lg} 10^{19} = F_{Pg} 10^{-7}$ or $F_{Lg} = F_{Pg} 10^{26}$. Thus, if for $k_g = 0.01$ the conditions (distance and speed) are such that for two charges the Lorentz force is equal to the attractive force, then for two masses the Lorentz force is 10^{26} times stronger than the attractive force. This means that the structure using the energy of gravitation field and based on gravitomagnetic Lorentz forces is significantly more effective than the same design based on magnetic Lorentz forces – and so, the latter is not worth to try implementing.

9. Technology

Those 18 m, which Aldo Costa demonstrates, may be explained, apparently, by the size of switches - they are complex, and therefore large. Furthermore, they are complex and therefore require constant adjustment, which complicates operation.

The author can offer much less complex and compact structure. Investment is needed and any other assistance in advancing the project.

Appendix 1. Circumferential Body Movement by Force of Gravity

Here we consider some idealized design, equivalent wheel Aldo Costa. For this construction, we can strict construct a mathematical model.

1. Ball Movement within a Tubular Circle

Let us consider a globular body of weight P, moving along a rigid tube coiled in a circle – see Fig. 1. The circle is located on vertical plane.

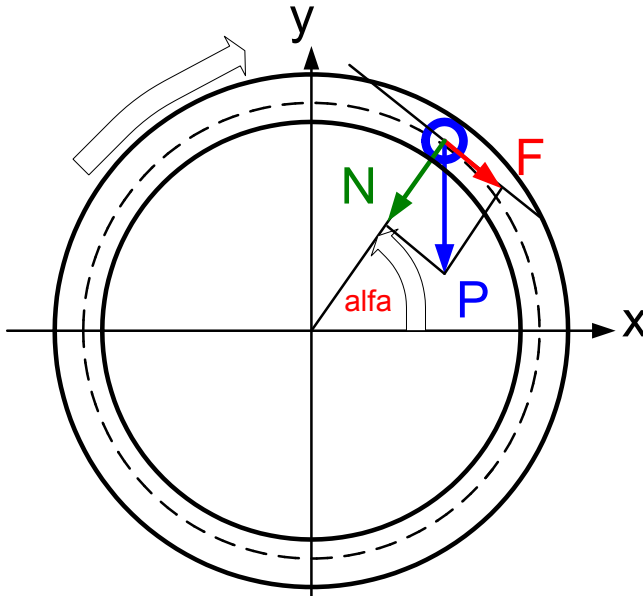


Fig. 1.

Find the force F , acting on the body along a tangent

$$F = P \cos \alpha = xP / R .$$

The force torque is

$$M_F = FR = xP .$$

Let us take a moment to be positive if it is directed clockwise. Find the pressure force N , acting on the circle along the radius:

$$N = P \sin \alpha = -yP / R .$$

The body's friction force along the circle is

$$T = kN = -kyP / R .$$

where k - friction coefficient. The torque of this force is:

$$M_T = TR = -kyP .$$

The Table 1 shows formulas for these forces and torques in the 4 quadrants.

Table 1.

| | 1 | 2 | 3 | 4 |
|--|----------------|---------------|---------------|----------------|
| | $F = xP / R$ | $F = xP / R$ | $F = xP / R$ | $F = xP / R$ |
| | $M_F = xP$ | $M_F = xP$ | $M_F = xP$ | $M_F = xP$ |
| | $T = -kyP / R$ | $T = kyP / R$ | $T = kyP / R$ | $T = -kyP / R$ |
| | $M_T = -kyP$ | $M_T = kyP$ | $M_T = kyP$ | $M_T = -kyP$ |

2. Movement of a Ball within a Deformed Tubular Circumference

Now let us assume that the ball is moving within a tube shown on Fig. 2. The Figure shows only the axis line of the tube and several positions of the ball. Shows only the upper half of the tube. This tube consists of three parts: arc 'ad' of radius R_1 , arc 'bc' with radius R_2 and segment AB ("the step"), located at an angle φ to the horizontal.

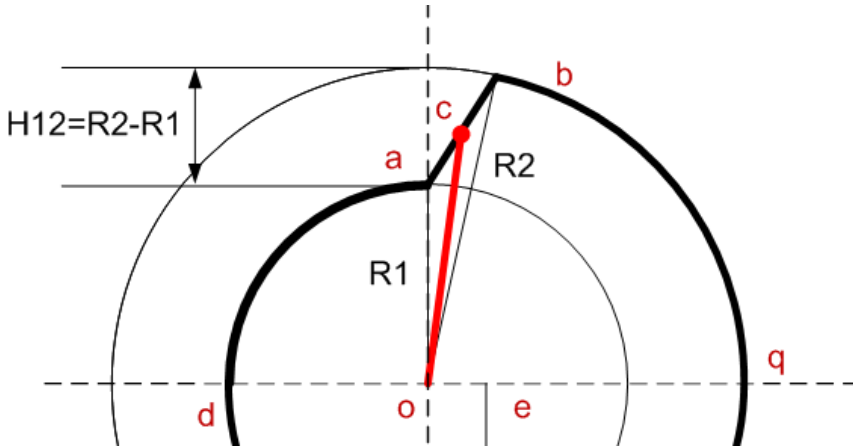


Fig. 2.

Table 2 shows formulas for the forces named above and their torques in the 4 quadrants for such deformed tube.

Table 2.

| | 1 | 2 | 3 | 4 |
|--|---|--|---|--|
| | $\varphi = \left(\frac{\pi}{2}, 0\right)$ | $\varphi = \left(0, -\frac{\pi}{2}\right)$ | $\varphi = \left(-\frac{\pi}{2}, -\pi\right)$ | $\varphi = \left(-\pi, \frac{\pi}{2}\right)$ |
| | $F = xP / R_2$ | $F = xP / R_2$ | $F = xP / R_1$ | $F = xP / R_1$ |
| | $M_F = xP$ | $M_F = xP$ | $M_F = xP$ | $M_F = xP$ |
| | $T = -kyP / R_2$ | $T = -kyP / R_2$ | $T = -kyP / R_1$ | $T = -kyP / R_1$ |
| | $M_T = -kyP$ | $M_T = kyP$ | $M_T = kyP$ | $M_T = -kyP$ |
| | $A_1 = (1 - k)PR_2$ | $A_2 = (1 - k)PR_2$ | $A_3 =$ $(-1 - k)PR_1$ | $A_4 =$ $(-1 - k)PR_1$ |

| | | | |
|---|---|---|--|
| $dv_1 = g \cdot \left(\begin{array}{c} \cos \varphi \\ -k \sin \varphi \end{array} \right) \frac{d\varphi}{v_1}$ | $dv_2 = g \cdot \left(\begin{array}{c} \cos \varphi \\ +k \sin \varphi \end{array} \right) \frac{d\varphi}{v_2}$ | $dv_3 = g \cdot \left(\begin{array}{c} \cos \varphi \\ +k \sin \varphi \end{array} \right) \frac{d\varphi}{v_3}$ | $dv_4 = g \cdot \left(\begin{array}{c} -\cos \varphi \\ -k \sin \varphi \end{array} \right) \frac{d\varphi}{v_4}$ |
| $\frac{v_{1k}^2 - v_{1o}^2}{2} = gR_2(1-k)$ | $\frac{v_{2k}^2 - v_{2o}^2}{2} = gR_2(1-k)$ | $\frac{v_{3k}^2 - v_{3o}^2}{2} = gR_1(-1-k)$ | $\frac{v_{4k}^2 - v_{4o}^2}{2} = gR_1(-1-k)$ |

The summary work of gravity force done by the torques acting on the ball moving along quadrant 1, is equal to

$$A_1 = \int_{\pi/2}^0 (M_F + M_T) d\varphi =$$

$$P \int_{\pi/2}^0 (x - ky) d\varphi = P \int_{\pi/2}^0 \left(x - k\sqrt{R_2^2 - x^2} \right) d\varphi$$

$$A_1 = PR_2 \int_{\pi/2}^0 \left(\begin{array}{c} \cos \varphi - \\ k \sin \varphi \end{array} \right) d\varphi = PR_2 \left[\begin{array}{c} -\sin \varphi - \\ k \cos \varphi \end{array} \right]_{\pi/2}^0$$

$$A_1 = PR_2(1 - k)$$

The work done in quadrants 2, 3, 4 is calculated similarly – see Table 2. All work performed on the semicircle is:

$$A_o = A_1 + A_2 + A_3 + A_4$$

$$A_o = 2P((R_2 - R_1) - 2k(R_1 + R_2))$$

The work performed on the step is:

$$A_s = (-1 - k)P(R_2 - R_1) / \sin \varphi.$$

Summary work performed by gravity force is:

$$A = A_o + 2A_s$$

Note the following. The sliding friction coefficient is $k = 0.1$; $0.5 \approx 0.25$. The rolling friction coefficient of a roll of radius r is $k = f/r$, where $f \approx 0.5mm$ when rolling steel on steel [6] If $r = 20mm$, then $k \approx 0.025$.

3. The Dynamics of Ball Movement within a Deformed Tubular Circleference

Let us find the ball's speed change on an element of length ds of the circle in the first quadrant due to the forces F_1 , T_1 . We have:

$$dv_1 = adt = \frac{F_1 + T_1}{m} dt = \frac{F_1 + T_1}{m} \frac{ds}{v} = \frac{F_1 + T_1}{m} \cdot \frac{R_1}{v_1} d\alpha.$$

Considering Table 2, we get

$$dv_1 = \frac{xP/R_2 - kyP/R_2}{m} \cdot \frac{R_2}{v_1} d\alpha = g \frac{x - ky}{v_1} \cdot d\alpha,$$

$$dv_1 = g \frac{x - ky}{v_1} \cdot d\alpha,$$

$$dv_1 = g \left(x - k\sqrt{R_2^2 - x^2} \right) \frac{d\varphi}{v_1},$$

$$dv_1 = g(\cos \varphi - k \sin \varphi) \frac{d\varphi}{v_1}, \text{ причём } \varphi = \left(\frac{\pi}{2}, 0 \right).$$

Similarly we may calculate the velocity increment on quadrants 2, 3, 4 - see Table. 2. In two steps, we have

$$dv_s = -\frac{kP \cos(\varphi)}{m} \cdot dt,$$

$$dv_s = -kg \cos(\varphi) \frac{dh}{v_s}, \text{ причём } h = \left(0, R_2 - R_1 \right)$$

where φ -is step angle to the horizontal.

We shall integrate the expression for the first quadrant:

$$\int_{v_{1o}}^{v_{1k}} v_1 dv_1 = \int_{\pi/2}^0 gR_2 (\cos \varphi - k \sin \varphi) d\varphi,$$

$$\left| \frac{v_1^2}{2} \right|_{v_{1o}}^{v_{1k}} = gR_2 \left| (-\sin \varphi - k \cos \varphi) \right|_{\pi/2}^0,$$

$$\frac{v_{1k}^2 - v_{1o}^2}{2} = gR_2(1 - k).$$

Similarly we may calculate kinetic energy increment on quadrants 2, 3, 4 - see Table. 2. On the steps we have:

$$\int_{v_{so}}^{v_{sk}} v_s dv_s = \frac{-kg}{\sin \varphi} \int_0^{R_2-R_1} dh, \quad \left| \frac{v_s^2}{2} = \frac{-kg}{\sin \varphi} h \right|_0^{R_2-R_1}$$

$$\frac{v_{sk}^2 - v_{so}^2}{2} = \frac{-kg}{\sin \varphi} (R_2 - R_1).$$

In these formulas, the assumption is made that the step does not change the length of the semicircle.

Since the ultimate speed in a certain segment coincides with the initial velocity in the next section, from the preceding formulas we may find the change in velocity across the tube in one revolution Δv . The loss of kinetic energy then is equal to

$$\Delta W = \frac{v_b^2 - (v_b - \Delta v_b)^2}{2}.$$

4. The momentum of force for Movement of Ball within a Deformed Tubular Circleference

In wheel Aldo Costa all weights (in our scheme - balls) rotate with angular speed ω around the point 'o'. Above the change in kinetic energy ΔW has been found. In our case, to preserve the kinetic energy of the ball, an external energy source must add value ΔW for each revolution of the ball. We assume that this energy is brought by application of force torque $F \cdot \Delta t$ on a certain time interval. This torque increases the angular speed. When the torque is applied to the ball in the point 'b', then

$$F \cdot \Delta t = m \cdot \Delta v_b, \tag{1}$$

where

$$\Delta v_b = R_2 \cdot \Delta \omega_b. \tag{2}$$

This value can be calculated for a given W by the following formula:

$$\Delta W = \left((v_b + \Delta v_b)^2 - v_b^2 \right) / 2 \tag{3}$$

or

$$2 \frac{\Delta W}{R_2^2} = (\omega_b + \Delta \omega_b)^2 - \omega_b^2 \tag{4}$$

or

$$\Delta \omega_b = \sqrt{\omega_b^2 + 2\Delta W / R_2^2} - \omega_b. \tag{5}$$

From (20, 21, 24) we find:

$$F \cdot \Delta t = mR_2 \left(\sqrt{\omega_b^2 + 2\Delta W / R_2^2} - \omega_b \right); \tag{6}$$

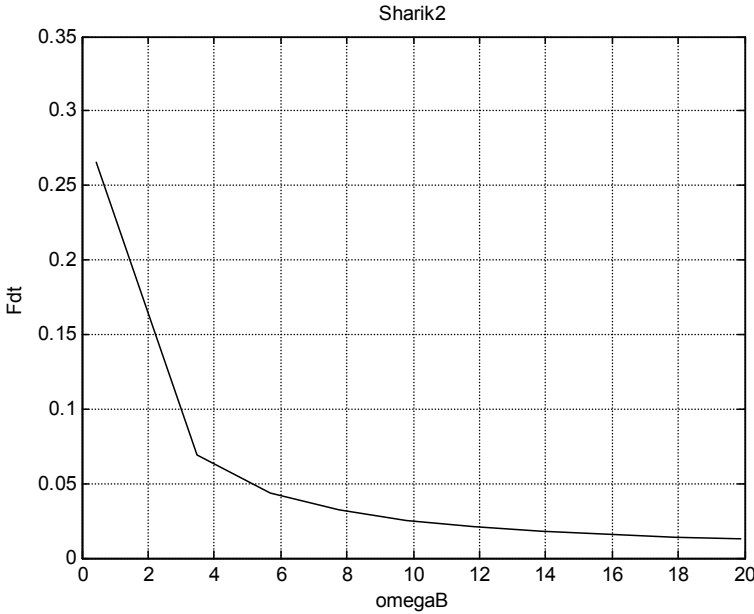


Fig. 3.

If the torque exceeds the specified value, the angular velocity will increase and if the torque is less than the specified value, the angular velocity will decrease and in a certain moment the ball stops. Fig. 3 shows the relationship - $F \cdot \Delta t = f(\omega_b)$. When calculating assumed that in the CGS system

$$P = 5 \cdot 10^5, R_1 = 44, R_2 = 50, \omega = 10, k = 0.025$$

In this the momentum of force must be equal

$$F \cdot \Delta t \approx 2500 \text{ (dyne * s)}$$

Appendix 2. Movement of Load on Vertical Step

Let us consider the case when load m_2 rotates with angular speed ω , and load m_1 moves vertically with the speed v_1 . Then

$$|a| = \omega R_2, \quad b = [0, v_1, 0], \tag{1}$$

As the loads are moving in one plane, then

$$r_z = 0, \quad a_z = 0, \quad b_z = 0. \tag{2}$$

Considering this, from (4) – see section 6), we get:

$$\overline{f_{12}} = \begin{bmatrix} a_y(-v_1 r_x) \\ -a_x(-v_1 r_x) \\ 0 \end{bmatrix} \quad (3)$$

or

$$\overline{f_{12}} = D \begin{bmatrix} a_y \\ a_x \end{bmatrix} \quad D = v_1 r_x. \quad (4)$$

So, from m_1 to m_2 the force (4) is acting. Similarly, let us consider the case, when load m_1 rotates with angular speed ω , and load m_2 moves vertically with the speed v_2 . Then

$$|b| = \omega R_1, \quad a = [0, v_2, 0], \quad (5)$$

and from ((4) – see sector 6), we get

$$\overline{f_{21}} = - \begin{bmatrix} v_1 (b_x r_y - b_y r_x) \\ 0 \\ 0 \end{bmatrix}. \quad (6)$$

So, the force (6) is directed horizontally from m_2 to m_1 and has no influence of the vertical movement.

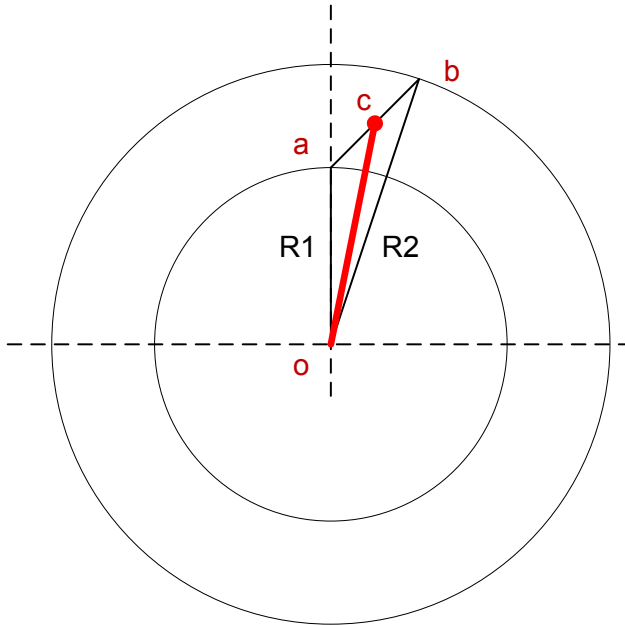


Рис. 4.

Chapter 5.2. Aldo Costa's Gravity Motor

Above the assumption was made, that the speed of motion on the step is constant. In fact, this speed varies even with constant angular speed. Let us consider this question in detail - see Fig. 4. Find the speed of the body on the segment "as". Denote:

$$\gamma = \angle aob, \quad \gamma_2 = \angle aoc, \quad u_1 = \angle u_1' = \angle bao,$$

$$u_2 = \angle u_2' = \angle abo, \quad u_{22} = \angle u_{22}' = \angle aco.$$

Solving the triangle "oab", we find:

$$d = \sqrt{R_1^2 + R_2^2 - 2R_1 R_2 \cos(\gamma)}$$

$$\sin(u_2) = \sin(\gamma),$$

$$u_1 = \pi - \gamma - u_2.$$

Radius "oc" rotates with angular speed ω . Thus

$$\gamma_2 = \omega t.$$

Solving the triangle "oac", we find

$$u_{22} = \pi - \gamma_2 - u_1,$$

$$d_2 = R_1 \sin(\gamma_2) / \sin(u_{22}),$$

$$R_{22} = R_1 \sin(u_1) / \sin(u_{22}).$$

The body's speed on segment "ab"

$$v = \frac{d(d_2)}{dt}.$$

Speed of approach of the body to this segment along a circle of radius R_1 is equal to $v_a = \omega R_1$, and the rate of removal from it along a circle of radius R_2 is equal to $v_a = \omega R_1$. At the points "a" and "b" the speeds change their values as a result of elastic collision, i.e. without energy loss.

Fig. 5 shows functions of time γ_2 , d_2 , R_{22} , v (in windows 1-4, respectively).

Speed of the body along a segment "ab" is substantially higher than circular speed. Therefore, above we examined the interaction of the body rising vertically with the speed v , and the body moving in a circle with the speed $v_a = \omega R_1$ or $v_b = \omega R_1$.

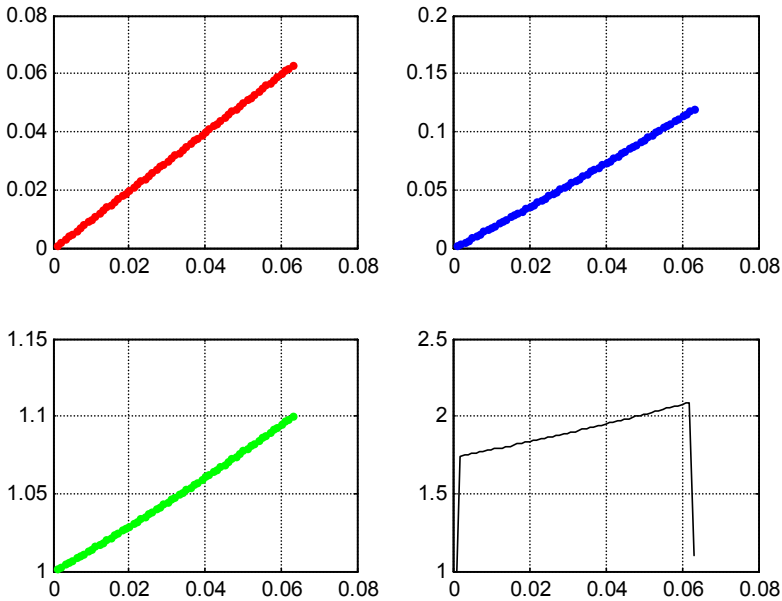


Fig. 5.

References

1. Mogilevsky M. Leonardo da Vinci ... and the principle of impossibility of perpetual motion, "Quantum", № 5, 1999 (in Russian), <http://kvant.mccme.ru/pdf/1999/05/kv0599mogilevsky.pdf>
2. Krasnov A.I. Is it possible to a perpetual motion machine? Moscow, 1956 (in Russian).
3. Is Orffyreus created a perpetual motion machine? (in Russian) <http://www.ortopax.ru/2010/11/dejstvitelno-li-orffyreus-sozdal-vechnyj-dvigatel/>
4. Work gravitational potential field (in Russian) http://fictionbook.ru/author/aleksandr_frolov/novyie_istochniki_je_nergii/read_online.html?page=3
5. Aldo Costa's Gravity Motor, http://peswiki.com/index.php/Directory:Aldo_Costa%27s_Gravity_Motor
6. http://en.wikipedia.org/wiki/Rolling_resistance
7. Aldo Costa. Movement Perpetual. Patent FR 2745857A1, 1995.
8. Vlasov V.N. The greatest revolution in Mechanics, 6, in Russian, <http://vitanar.narod.ru/revolucio/revolucio6/revolucio6.html>
9. Dmitriev M.F. Torque Amplifier, WO 2010/062207, 2010.

Chapter 5.2. Aldo Costa's Gravity Motor

10. Vlasow V.N. The greatest revolution in Mechanics, 5, in Russian, <http://vitanar.narod.ru/revolucio/revolucio5/revolucio5.html>
11. Khmelnik S.I. GTR and Perpetuum Mobile Rehabilitation. The Papers of independent Authors, ISSN 2225-6717, № 28, 2014; and <http://vixra.org/abs/1403.0086>, 2014-03-12.

Chapter 5.3. Tolchin's Inertioid

Contents

- 1. Introduction \ 182
- 2. Mathematical model of Tolchin's experiments \ 183
- 3. Quantitative estimations \ 187
- 4. Possible modifications \ 190
- 5. Conclusions \ 192
- References \ 194

1. Introduction

The secret of Tolchin's inertioid exists for almost a century. Below it is shown that it can be solved using the general relativity theory. A technique for inertioid calculation is given. Structural variations are proposed.

The term "inertioid" and its structure were invented by V.N. Tolchin in the 1930 years. In [1] a detailed description of inertioid and experiments with it are given. Inertioid demonstrates an unsupported movement. The recognized physical model explains this phenomenon by friction forces. However, numerous experiments not confirming this explanation are known [2, 7].

Different theories for this phenomenon explanation are proposed [3]. But they are rejected by modern science due to the fact that unsupported movement is usually considered as impossible because it violates Newton's third law and law of conservation of momentum that follows from it (in mechanics). The latter is a more general physical law. In electrodynamics, this law also considers electromagnetic momentum and therefore momentas of material bodies interacting with wave in total are not equal to zero [4]. For example, in [5] the interaction of electric charges is considered, and it is proved that in this case the law of conservation of momentum can be violated in mechanics. In [6] the conceptual experiments based on it and which demonstrate an unsupported movement are described. This movement is possible due to Lorentz forces availability. Such forces are absent in mechanics and therefore Newton third law follows from the law of conservation of momentum in mechanics.

In Chapter 1 the Maxwell-like gravitational equations are considered. From the basic general relativity equations it follows that, Maxwell-like equations are used to describe the gravitational interactions in a weak gravitational field at low velocities, i.e. on Earth. This means that there are gravitational waves having a gravitoelectric component with E_g tension and a gravitomagnetic component with B_g induction. The gravitomagnetic Lorentz force acts on m mass moving in a gravimagnetic field with velocity (known Lorentz force analogy). It follows that Newton third law can be violated in the Earth's gravitational field (as well as in electromagnetic field).

Below it is shown that Tolchin's inertioid operation is easily explained when considering gravitomagnetic Lorentz force. In addition, Tolchin's experiments allow to refine ξ coefficient value, and this theory allows to offer useful inertioid modifications.

2. Mathematical model of Tolchin's experiments

An inertioid consists of two m_1 and m_2 loads and on the levers mounted on a movable platform - see Fig. 1. Loads rotate towards each other with varying angular velocity (which is provided by actuating mechanism). Inertioid motor is powered on in CA section (from 330 to 360 degrees), and inertioid brake is powered on in DB section (from 150 to 180 degrees). In this case, the loads velocity is maximal when they are located near A point, and is minimal when they are located near B point.

According to author's assumption, the cause of acceleration is that the moving loads interact by gravitomagnetic Lorentz forces. The Lorentz force is inversely proportional to squared distance between the loads. Therefore, this force possesses an essential value only at A and B points, where the distance between loads is minimal. In addition, the Lorentz force is proportional to loads velocities product. Therefore, the Lorentz force at A point (where the velocities are large) is much greater than the Lorentz force at B point (where the velocities are small). Further, the Lorentz force direction depends on whether the loads come close or move away. It should also be noted that the total momentum of Lorentz forces acting from the right and left of these points would be equal to zero at uniform velocity of loads movement near A and B points. But Tolchin provided an abrupt acceleration change precisely at these points that creates a non-zero total Lorentz force momentum. As a result the inertioid motion becomes intermittent - a strong jump to A

Chapter 5.3. Tolchin's Inertioid

point and a weak, reverse-directed jump to B point. These processes are then analyzed quantitatively.

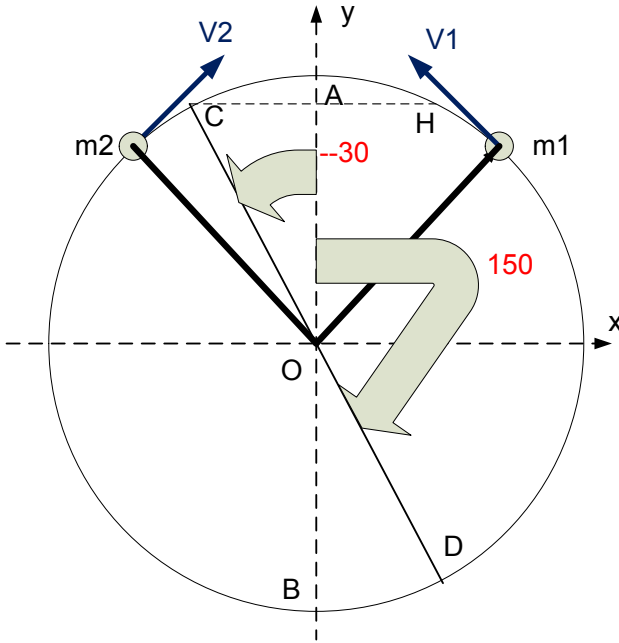


Fig. 1 (Г1.vsd)

Chapter 1 shows that the Lorentz force acting from m_1 mass, on m_2 mass, is defined by the following expression (hereinafter the GHS system is used)

- $$\overline{F}_{12} = \frac{k_g m_1 m_2}{r^3} [\overline{v}_2 \times [\overline{v}_1 \times \overline{r}]] \text{ [dyne]}, \tag{1}$$

where

- $k_g = \frac{\xi G}{c^2}$ is coefficient, (2)
- $G \approx 7 \cdot 10^{-8} \left[\frac{\text{dyne} \cdot \text{sm}^2}{\text{g}^2} = \frac{\text{sm}^3}{\text{g} \cdot \text{sec}^2} \right]$ is the gravitational constant,
- $c \approx 3 \cdot 10^{10} \text{ [sm/sec]}$ is the speed of light in a vacuum,
- ξ is gravimagnetic permeability of the medium,
- \overline{r} is a vector directed from point m_1 to point m_2 ,
- $\overline{v}_1, \overline{v}_2$ is velocities of mass m_1 and m_2 , accordingly.

$\overline{v}_1, \overline{v}_2$ velocities are the velocities of masses relative motion, not dependent on system velocity with which the masses are connected. In our case, these are the linear velocities of loads rotation on the platform, not depending on platform velocity - see Fig. 1.

Let us select in formula (1) the following expression

$$\overline{f} = (\overline{a} \times (\overline{b} \times \overline{r})), \quad (3)$$

where

$$\overline{a} = \overline{v}_2, \quad \overline{b} = \overline{v}_1.$$

In the right cartesian coordinate system, this expression takes the form of

$$\overline{f} = \begin{bmatrix} a_y(b_x r_y - b_y r_x) - a_z(b_z r_x - b_x r_z) \\ a_z(b_y r_z - b_z r_y) - a_x(b_x r_y - b_y r_x) \\ a_x(b_z r_x - b_x r_z) - a_y(b_y r_z - b_z r_y) \end{bmatrix}. \quad (4)$$

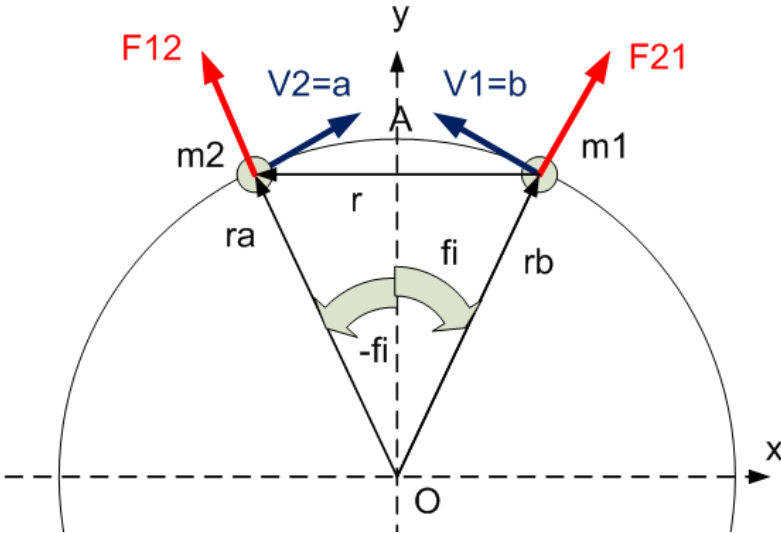


Fig. 2 (I2.vsd)

Loads rotate at the same velocity in opposite directions. Therefore

$$|a| = \omega R, \quad |b| = \omega R, \quad (5)$$

where R - lever length, ω - angular velocity. Let us also denote m_1 and m_2 loads' radius-vectors as r_b and r_a respectively. Then

$$r = r_a - r_b. \quad (6)$$

Chapter 5.3. Tolchin's Inertioid

As loads rotate in parallel planes, between which d distance is kept, and the angles of deviation of masses from vertical line are equal, then

$$r_y = 0, r_z = d, a_z = 0, b_z = 0. \quad (7)$$

Accordingly, we obtain:

$$\bar{f} = -b_y r_x \begin{bmatrix} a_y \\ -a_x \\ d \end{bmatrix}. \quad (8)$$

We will be interested in vertical component of this force

$$f_y = b_y r_x a_x. \quad (9)$$

From Fig. 1 it follows that

$$\begin{aligned} \angle AOm_2 &= -\varphi, \quad \angle AOm_1 = \varphi \\ a_x &= \omega R \cos \varphi, b_x = -\omega R \cos \varphi, \\ a_y &= \omega R \sin \varphi, b_y = \omega R \sin \varphi, \\ r_a &= R \left[-\sin \varphi, \cos \varphi, 0 \right], \\ r_b &= R \left[\sin \varphi, \cos \varphi, 0 \right]. \end{aligned} \quad (10)$$

Consequently,

$$r = r_a - r_b = \left[-2R \sin \varphi, 0, d \right], \quad (11)$$

$$|r| = \sqrt{\left[(2R \sin \varphi)^2 + d^2 \right]} \quad (12)$$

From (9-11) we find:

$$f_y = -\omega R \cos \varphi 2\omega R^2 \sin^2 \varphi = -2\omega^2 R^3 \cos \varphi \sin^2 \varphi, \quad (13)$$

$$f_{yr} = f_y / |r|^3 = 2\omega^2 R^3 \cos \varphi \sin^2 \varphi / |r|^3. \quad (14)$$

From (1, 3) it follows that the force vertical projection is (1)

$$F_{12y} = k_g m_1 m_2 f_{yr}. \quad (15)$$

By virtue of symmetry, two such forces from two loads act on the platform, i.e. the following force acts on the platform along its axis, when loads rotate towards each other

$$F_1 = 2k_g m_1 m_2 f_{yr}, \quad (16)$$

which is calculated for the fourth quadrant (where C point is located). Analogously, in case of loads "scattered" rotation, the force acts

$$F_2 = -2k_g m_1 m_2 f_{yr}, \quad (17)$$

which is calculated for the first quadrant (where H point is located).

The total momentum of these forces is equal to zero at equal velocities of "counter" and "scattered" rotation. This rule is also observed for nonuniform rotation. However, if these "counter" and "scattered" velocities are different, then their total momentum isn't equal to zero and the platform will move (forward or backward). This movement is unsupported, as the Lorentz force has no counteractive force.

3. Quantitative estimations

Let us consider the diagram of m_2 load angular velocities, which is represented by Tolchin's structure [1] - see Fig. 3. Here an involute of circle from Fig. 1 is shown with the same points designations and angles indication. In CA section, a motor accelerates the loads from ω_1 angular velocity to ω_2 angular velocity, and a brake is powered on in DB section.

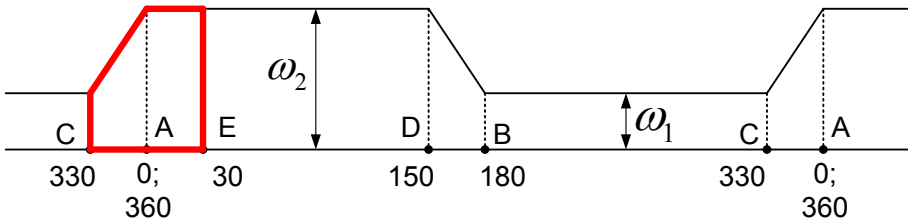


Fig. 3 (T3.vsd)

Let us consider a selected CAE section in Fig. 3. In CA section, m_2 load accelerates from ω_1 to ω_2 velocity with ε acceleration at $t = \overline{0, T_1}$ time interval, and in AE section - moves at ω_2 constant velocity at $t = \overline{T_1, T_2}$ time interval. In Fig. 4 and Fig. 5 the results of this process modeling are shown- the following functions are shown

$$\omega(t) = \omega_1 + \varepsilon \cdot t,$$

$$\varphi(t) = \varphi_0 + \varepsilon \cdot t^2 / 2,$$

$$\left[F_2(\varphi), F_1(\varphi) \right] - \text{see formulas (14, 15, 16),}$$

$F(t)$ - function which is equal to $F_1(\varphi)$ at $t = \overline{0, T_1}$ time interval, and is equal to $F_2(\varphi)$ at $t = \overline{T_1, T_2}$ time interval; only vertical projections of these forces are shown.

In this case T_1, T_2 intervals are defined by the formulas:

$$\varepsilon \cdot T_1^2 / 2 + \omega_1 T_1 = 2\pi - \varphi_0,$$

$$\omega_2 T_2 = 2\pi - \varphi_0.$$

Chapter 5.3. Tolchin's Inertoid

In the first three diagrams, $t = \overline{0, T_1}$ time interval corresponds to the movement in CA section, and $t = \overline{T_1, T_2}$ time interval corresponds to the movement in AE section.

It is seen that $F_1(t)$ and $F_2(t)$ forces directed in the opposite direction (see window 3) and $|F_2(\varphi)| \geq |F_1(\varphi)|$ (see window 4). However, the interval is $\overline{T_1, T_2} < \overline{0, T_1}$. The sum of $F_2(t)$ and $F_1(t)$ momenta is equal to value

$$\Delta S = \int_0^{T_1} F_1(t) dt + \int_{T_1}^{T_2} F_2(t) dt > 0$$

and acts on a bound pair of m_1 and m_2 loads changing the platform velocity. Or, rather,

$$\Delta S = M \cdot \Delta v,$$

where M – platform with loads weight, Δv - its velocity increase due to ΔS momentum. This momentum has a projection on 'oy' axis. Later, the platform in DE section moves at a velocity changed by this momentum.

Table 1.

| Variants: | 1 | 2 | 3 | 4 |
|---------------|-----------|-----------|-----------|-----------|
| | Fig. 4 | Fig. 5 | Fig. 7 | Fig. 8 |
| m | 100 | 500 | 500 | 500 |
| M | 500 | 5000 | 5000 | 5000 |
| d | 0.5 | 1 | 1 | 1 |
| R | 30 | 30 | 30 | 30 |
| φ_0 | 330 | 330 | 330 | 330 |
| ω_1 | 3 | 1 | 1 | 2.7 |
| ε | 100 | 3 | 3 | -3 |
| ξ | 10^{23} | 10^{23} | 10^{23} | 10^{23} |
| T_1 | 0.08 | 0.35 | 0.35 | 0.22 |
| T_2 | 0.05 | 0.26 | 0.22 | 0.35 |
| ω_2 | 11 | 2 | 2.7 | 1 |
| ΔS_1 | 8.7 | 1.37 | 1.37 | 1.73 |
| ΔS_2 | 10.1 | 1.57 | 1.73 | 1.38 |
| ΔS | -1.4 | -0.2 | -0.36 | 0.35 |
| oS | 0.9 | 0.87 | 0.79 | 1.26 |
| Δv | -4.3 | -39 | -71 | 69 |

Thus, it is possible to determine Δv platform velocity momentum at each load rotation under given $m_1, m_2, \omega_1, \varepsilon, R, M, d$ inertioid parameters and air gravimagnetic permeability under ξ_b atmospheric pressure. In this case, momenta are calculated by the following formulas

$$\Delta S_1 = \int_0^{T_1} F_1(t)dt, \quad \Delta S_2 = \int_{T_1}^{T_2} F_2(t)dt, \quad \Delta S = \Delta S_1 + \Delta S_2, \quad oS = \Delta S_1 / \Delta S_2.$$

The results of solution are summarized in Table. 1.

Analogously, we can investigate inertioid behavior at point B. But loads velocities near B point are much less than loads velocities near A point. Therefore, the Lorentz forces at B point are much less than the Lorentz forces at A points - the inertioid receives a large momentum at A point and a small oppositely directed momentum at B point.

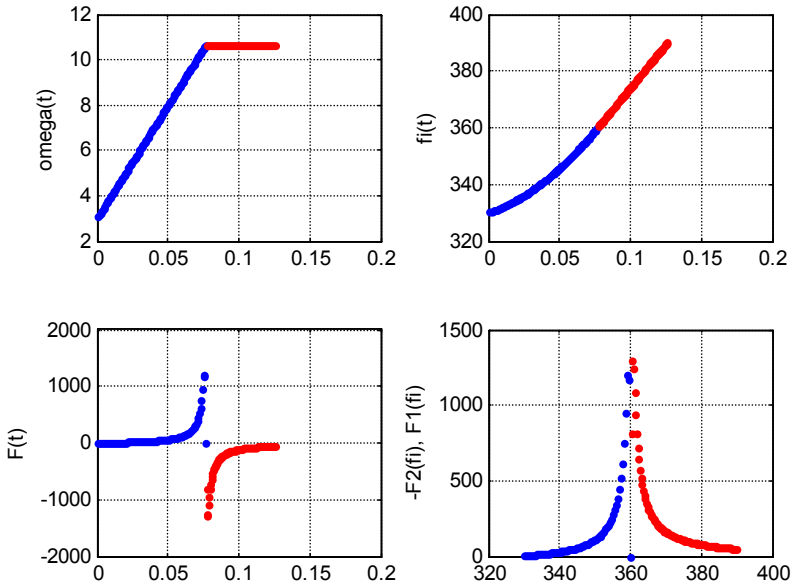


Fig. 4 (subaldo5.m, mode=9)

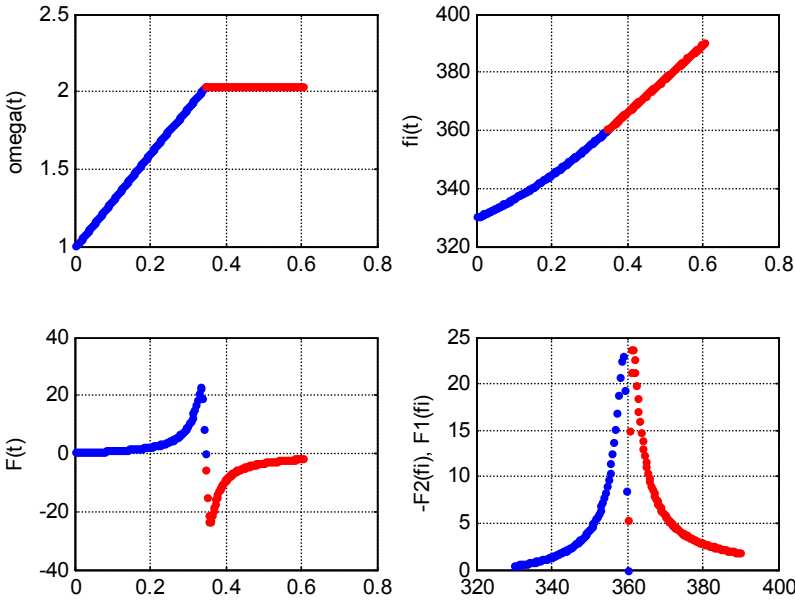


Fig. 5 (subaldo5.m, mode=10)

4. Possible modifications

In inertioid description it is declared that the motor is powered off at A point - see Fig. 1-3. Let us now consider inertioid behavior when the motor is powered off at E point - compare Fig. 3 and Fig. 6. In Fig. 7 are given and in Table. 1 the results of solution are shown. In this case, loads rotate with \mathcal{E} constant acceleration, gaining velocity from $\omega_A = \omega_1$ at A point to $\omega_E = \omega_2$ at E point. Comparison of 2 and 3 variants shows that a momentum in latter case is much higher than a momentum in version 2.

Let us also consider inertioid behavior, if the loads rotate with a constant $(-\mathcal{E})$ slowing down, decreasing the velocity from $\omega_A = \omega_2$ at A point to $\omega_E = \omega_1$ at E point. In this variant 4, a momentum has the same value but an opposite sign as compared to momentum in variant 3 - Fig. 8 and Tab. 1.

Considering the above, we can propose the following diagram of motor power-on - see Fig. 9. The loads are accelerated in CE section with \mathcal{E} acceleration and are braked in DF section with $(-\mathcal{E})$ slowing

down. In this case, the loads at A and B points generate the unidirectional pmomenta (directed along AB - see Fig. 1), i.e. loads generate a useful momentum at both points of A and B approach.

Thus, if the proposed theory is correct, then inertioid efficiency can be substantially increased by the motor power-on time diagram change.

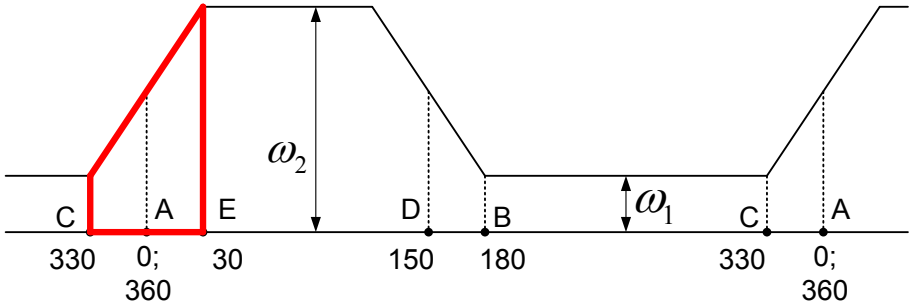


Fig. 6 (Г6.vsd)

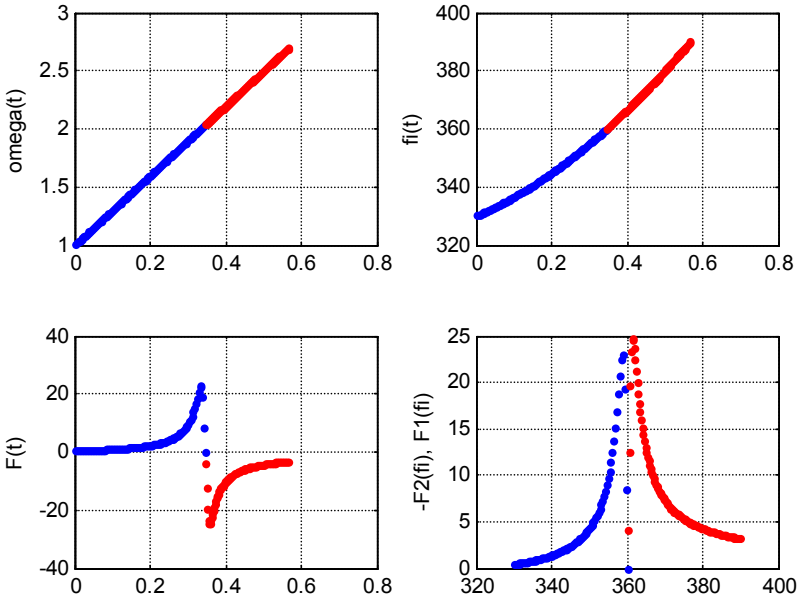


Fig. 7 (subaldo5.m, mode=12)

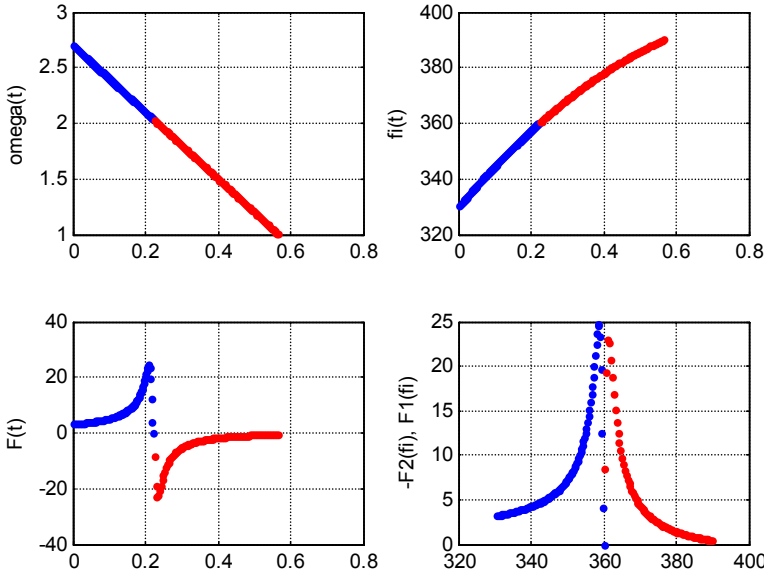


Fig. 8 (subaldo5.m, mode=22)

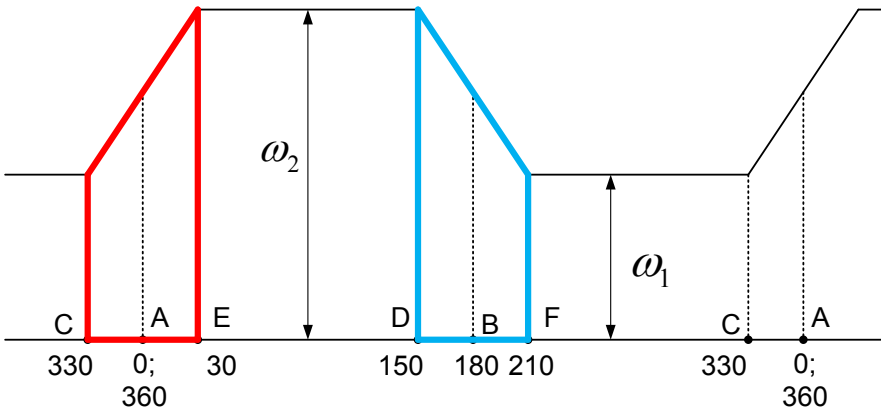


Fig. 9 (I9.vsd)

5. Conclusions

Thus, Tolchin's inertioid can perform an unsupported movement under gravitomagnetic Lorentz forces action (which was discussed in introduction section). However, for this, certain relations must be observed between rotation velocities at different sections of rotation circle. Tolchin was able to find these relations and implement them in its design.

The proposed theory allows to calculate these relations in advance. This fact can be used for theory proving: if inertioid moves/doesn't move exactly in accordance with calculation, then this can be a proof of the theory validity. In addition, this theory allows to provide inertioid useful modifications. This possibility verification will allow to verify the theory validity.

An exact ξ_b value is not yet known. But with inertioid acting, it is possible to solve an inverse problem and find ξ_b and then design other inertioids.

Lorentz forces, as we know, don't perform the work. However, the influence of gravitomagnetic Lorentz forces leads to that the kinetic energy of platform appears. Obviously, this energy source is the energy of inner motor. This is similar to that the electrical energy is a source of additional energy under conductor motion with a current in magnetic field (under Ampère force action, which is a consequence of Lorentz force).

An inertioid moves by inertia periodically receiving a momentum of Lorentz forces. Therefore, it can still be called as inertioid (although inertial forces aren't the driving forces). It should also be called as an inertioid, since this name was kept about a century.

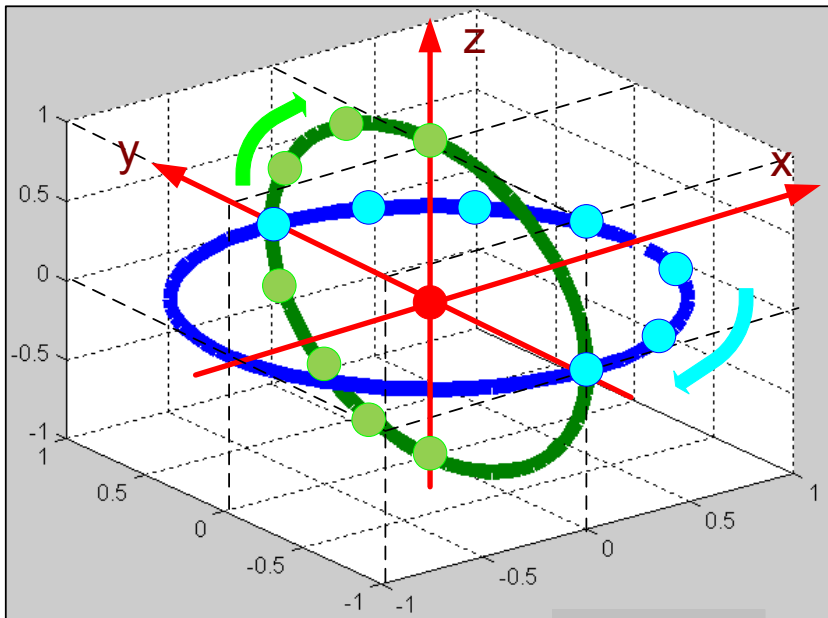


Fig. 10 (DwePoluokrugnostiZaradow.vsd)

However, similar to mass motion gravitational problem considered, it is possible to consider the same problem of electric charges motion (where there is no question about energy source and unsupported motion possibility). In [6], a more complicated design with rotating electric charges is considered. With a view to above, it is possible to replace the electric charges by masses in it - see Fig. 10. These masses rotate continuously and evenly. Then we can obtain a construction which, in contrast to Tolchin's inertioid (where the loads move in the plane) can be called as three-dimensional inertioid.

References

1. Tolchin V.N. Inertsoid. Perm, Perm Publishing House, 1977.
2. Zhigalov V.A. Some urgent issues of unsupported movement, http://second-physics.ru/lib/articles/zhigalov_issues.pdf
3. Inertsoids, <http://ru.wikipedia.org/wiki/Инерционы>
4. R.P. Feynman, R.B. Leighton, M. Sands. The Feynman Lectures on Physics, volume 2, 1964.
5. Zilberman G.E. Electricity and magnetism, Moscow, publ. "Science", 1970.
6. Khmelnik S.I. Non-support motion without violating physical laws, The Papers of independent Authors, ISSN 2225-6717, № 21, 2012.
7. G. Shipov. A quarter of a century of struggle for a new space engine. 3, October, 2008, <http://blog.kob.spb.su/2008/10/03/168/>
8. Samokhvalov V.N. Papers in journals «The Papers of independent Authors», ISSN 2225-6717: 2009, №13; 2010, №14; 2010, №15; 2011, №18; 2011, №19; 2013, №24.
9. Golubeva O.V. Theoretical mechanics. The Higher School Publishing House, 1976.
10. Khmelnik S.I. Tolchin's Inertioid and general theory of relativity. The Papers of independent Authors, ISSN 2225-6717, № 25, 2014; and <http://vixra.org/abs/1404.0429>, 2014-04-19.

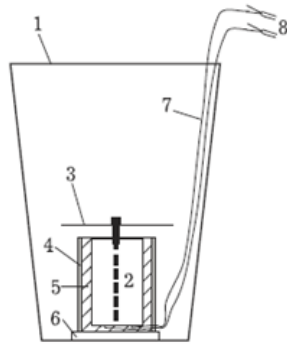
Chapter 5.4. Unusual Fountain

An unusual fountain [1] is installed in England, which constitutes a vortex within a transparent cylinder – the Charybdis vortex fountain – see fig. 1. There is also an article [2] about another artificial vortex, less impressive, but structurally more transparent. The fig. 2 shows this vortex in a glass with presentation of its structure. Fig. 3 shows the process of formation of this whirlpool. In [2] it is described that in the whirlpool a surface layer is absorbed - plastic balls or oil film. We may also indicate a natural phenomenon resembling the unusual fountain [3] – see fig. 4.



Fig. 1.

To the author's knowledge such phenomena have no strict mathematical description. Chapter 4.5 proposes a mathematical model of the flow of water into the funnel and from the pipe. In this case, the MGM equations were used. The interaction between the moving masses of water was described by GL-forces. Further arguments are similar to those given in Chapter 4.5.



- 1. Tumbler
- 2. Micromotor
- 3. Tin plate
- 4. Plastic tube
- 5. Silicone
- 6. Cold welding
- 7. Wires
- 8. Terminals

Fig. 2.



a



b



c



d

Fig. 3: a - a glass with fresh water, b - engine connection and the appearance of a vortex funnel, c - an incomplete vortex funnel, d - a full vortex funnel



Fig. 4.

The mathematical model of an unusual fountain completely coincides with the model of a dusty vortex of noncylindrical form - see Chapter 4.1, Section 7. In this model $R(z)$ is radius of a vortex, and in this case $R(z)$ is radius of an unusual fountain is a function of cross-section at altitude z . Therefore, for any function $R(z)$ mathematical model can be constructed.

Consequently, it can be argued that the equations of gravitomagnetism are confirmed experimentally. This confirms the existence of significant gravitomagnetic forces and gravitomagnetic energy flux.

References

1. <http://www.mirkrasiv.ru/articles/fontan-vodovorot-haribda-charybdis-sanderlend-velikobritanija.html>
2. Bondarov M.N., Savitchev V.I. Artificial maelstrom and its application,
http://bond1958.narod.ru/publikacii/pot_11_2010.pdf
3. <https://www.youtube.com/watch?v=fmMVGil0sXg>
4. Khmelnik S.I. Unusual Fountain and Gravitomagnetism. The Papers of independent Authors, ISSN 2225-6717, № 38, 2015 (in Russian); end <http://vixra.org/abs/1509.0042>, 2015-09-03.

Chapter 5.5. Taylor Vortex

Contents

- 1. Introduction \ 198
- 2. Mathematical model \ 199
- Appendix 1 \ 205
- References \ 204

1. Introduction

The theoretical justification for Taylor vortex is considered below. The proposed mathematical model allows constructing a flow structure between cylinders where correctly alternating vortices with right and left rotation and axes parallel to peripheral velocity of rotating cylinder direction.

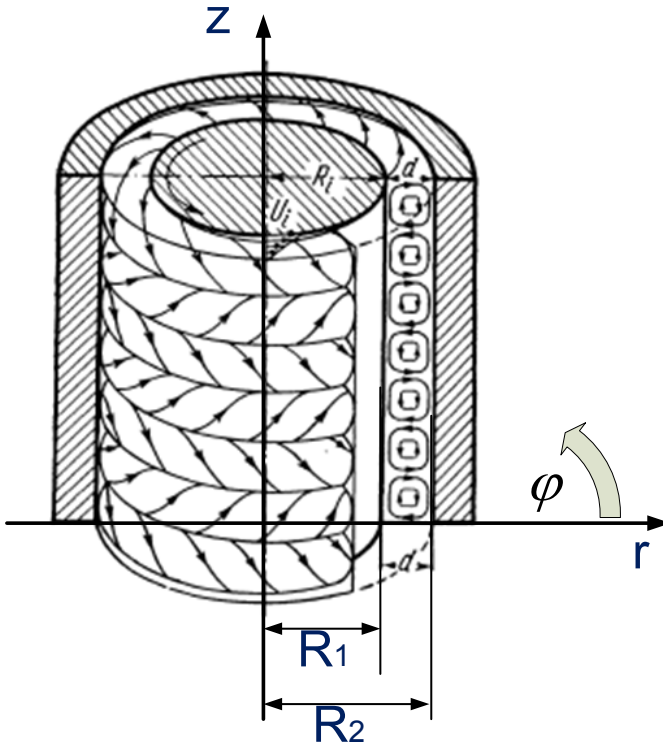


Fig. 1.

In [1] the classical Taylor experiment is described - see Fig. 1, where two cylinders and viscous fluid in the gap between them are shown. The outer cylinder with a radius of $R_2 = R_i + d$ is fixed, and inner cylinder with a radius of $R_1 = R_i$ rotates and thereby creates U_i basic flow.

At a certain rotation velocity in the gap "between cylinders the correctly alternating vortices with right and left rotation and axes parallel to peripheral velocity of rotating cylinder direction arise." These vortices roll full-circle and don't change between two circles. In [1] various experimental studies of such a flow are described, but its mathematical model is absent. Apparently, it cannot be constructed on the basis of known equations of hydrodynamics. A mathematical model of such a flow, constructed based on assumption that, in addition to known mass forces, gravitomagnetic forces appear in flowing fluid, which depend substantially on motion speed is suggested below.

2. Mathematical model

Taylor's design has the massive currents. Let us denote their densities as J_r , J_φ , J_z . These mass currents create such gravitomagnetic tensions as H_r , H_φ , H_z . Densities of mass currents and gravitomagnetic tensions should comply with Maxwell-like gravitational equations for the standard case, happened in our task. These equations for in r , φ , z cylindrical coordinates have the form (see (2.6.1-2.6.5) in Chapter 2) of:

$$\frac{H_r}{r} + \frac{\partial H_r}{\partial r} + \frac{1}{r} \cdot \frac{\partial H_\varphi}{\partial \varphi} + \frac{\partial H_z}{\partial z} = 0, \quad (4)$$

$$\frac{1}{r} \cdot \frac{\partial H_z}{\partial \varphi} - \frac{\partial H_\varphi}{\partial z} = J_r, \quad (5)$$

$$\frac{\partial H_r}{\partial z} - \frac{\partial H_z}{\partial r} = J_\varphi, \quad (6)$$

$$\frac{H_\varphi}{r} + \frac{\partial H_\varphi}{\partial r} - \frac{1}{r} \cdot \frac{\partial H_r}{\partial \varphi} = J_z + J_o, \quad (7)$$

$$\frac{J_r}{r} + \frac{\partial J_r}{\partial r} + \frac{1}{r} \cdot \frac{\partial J_\varphi}{\partial \varphi} + \frac{\partial J_z}{\partial z} = 0. \quad (8)$$

In order to shorten the record, we will use the following designations:

$$co = \cos(\alpha\varphi + \chi z), \quad (9)$$

$$si = \sin(\alpha\varphi + \chi z), \quad (10)$$

where α , χ - some constants. Appendix 1 shows that there is a solution which has the following form:

$$J_r = j_r(r) \mathbf{e}_0, \quad (11)$$

$$J_\varphi = j_\varphi(r) \mathbf{e}_1, \quad (12)$$

$$J_z = j_z(r) \mathbf{e}_1, \quad (13)$$

$$H_r = h_r(r) \mathbf{e}_0, \quad (14)$$

$$H_\varphi = h_\varphi(r) \mathbf{e}_1, \quad (15)$$

$$H_z = h_z(r) \mathbf{e}_1, \quad (16)$$

where $j(r)$, $h(r)$ - some functions of r coordinate. In Appendix 1 it is shown that this solution of 5 equations (4-8) with 6 $j(r)$, $h(r)$ unknown functions can be found at a given $j_\varphi(r)$ function.

Function $j_\varphi(r)$ describes the mass currents. These currents arise in a given construction due to viscous forces. These forces are distributed full circle and this distribution depends on that which of cylinders rotates, dragging the nearby layers of water by viscous friction. Obviously, the rotation speed will decrease towards fixed cylinder.

We will not analyze these relationships, but suppose that in general $j_\varphi(r)$ function has the following form:

$$j_\varphi(r) = a + br, \quad (17)$$

where a , b - known coefficients.

Example 1.

Fig. 2 (mode = 4) shows the graphs of $j_r(r)$, $j_\varphi(r)$, $j_z(r)$, $h_r(r)$, $h_\varphi(r)$, $h_z(r)$ functions in design gap. These functions are calculated iteratively under given $\alpha = 4$, $\chi = 63$, $R_1 = 0.9$, $R_2 = 1$ wire radius and $j_\varphi(r) = -0.3 + r$ function. The first column shows $h_r(r)$, $h_\varphi(r)$, $h_z(r)$ functions, and the second column shows $j_r(r)$, $j_\varphi(r)$, $j_z(r)$ functions. Together with $j_z(r)$ function, the following function is dotted

$$j_{zt} = 2 \sin(\chi r), \quad (18)$$

and together with $j_r(r)$ function, the following function is dotted

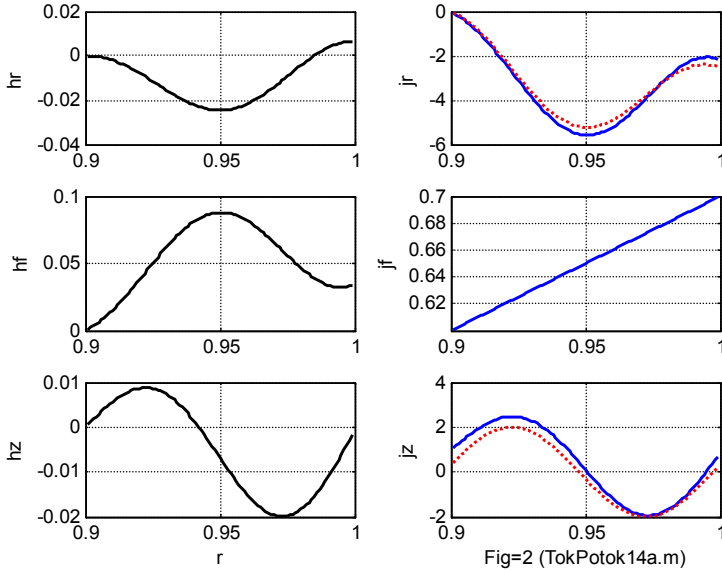
$$j_{rt} = (-2 \cdot (1 - \cos(\chi r)) - 25 \cdot (r - 0.9)). \quad (19)$$

It is seen that, $j_r(r) \approx j_{rt}(r)$, $j_z(r) \approx j_{zt}(r)$. Consequently, there is a solution of equations (4-8), wherein

$$J_r(z) \approx j_{rt}(r) \cos(\alpha\varphi + \chi z), \quad (20)$$

$$J_z(r) \approx j_{zt}(r) \sin(\alpha\varphi + \chi z). \quad (21)$$

- see also (9-12).



Example 2.

In Fig. 3, under conditions of Example 1, $(\overline{J_r(r)} + \overline{J_z(r)})$ field of currents in vertical section of construction gap is shown. Vortices correctly alternating with right and left rotation are seen. This follows from (20, 21). From Fig. 3 it follows that the mass currents, i.e. fluid streams make circular motions in the gap.

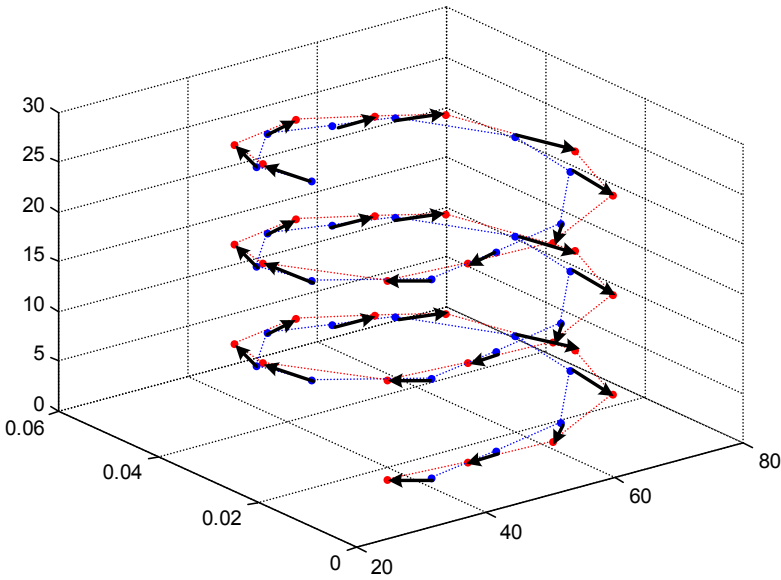
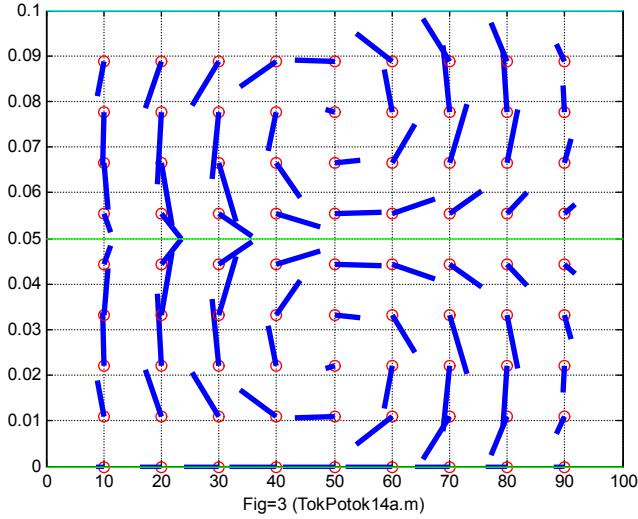


Fig. 4.

Example 3.

Basic current U_i converts fluid circular motions into the spiral motion with an axis - a circle passing along the central line of circular gap. Fig. 4 shows $(\overline{J_r(r)} + \overline{J_z(r)})$ vector field of currents in a segment of

such a spiral. This segment corresponds to the section of toroidal helix in Fig. 1. Vector field is shown only for one radius of this torus. Blue dashed line represents a torus with this radius, and red dashed line unites $(\overline{J_r(r)} + \overline{J_z(r)})$ vectors' ends coming from the blue line.

The nature of motions considered corresponds to motions observed in experiments - see Fig. 1. Consequently, it can be argued that Taylor vortices are explained by gravitomagnetism. The influence of gravitomagnetic forces increases with motion speed increase. Therefore, a laminar flow is observed at low speeds, but with speed increase, the gravitomagnetic forces become very important. The turbulence appears. With further velocity increase, these forces begin to prevail and organized vortices arise.

Appendix 1

A solution of equations (3.4-3.8) in the form of functions (3.11-3.16) is considered. Further, the derivatives of r will be indicated by line marks.

From (3.4) we find:

$$\frac{j_r(r)}{r}co + j'_r(r)co + \frac{j_\varphi(r)}{r}\alpha \cdot co + j_z(r)\chi \cdot co = 0 \quad (1)$$

or

$$\frac{j_r(r)}{r} + j'_r(r) + \frac{j_\varphi(r)}{r}\alpha + j_z(r)\chi = 0. \quad (2)$$

From (3.5, 3.6, 3.7) we find:

$$\frac{h_r(r)}{r} + h'_r(r) + \frac{h_\varphi(r)}{r}\alpha + \chi \cdot h_z(r) = 0, \quad (3)$$

$$\frac{1}{r} \cdot h_z(r)\alpha - h_\varphi(r)\chi = j_r(r), \quad (4)$$

$$-h_r(r)\chi - h'_z(r) = j_\varphi(r). \quad (5)$$

From (3.8) we find:

$$\frac{h_\varphi(r)}{r} + h'_\varphi(r) + \frac{1}{r} \cdot h_r(r)\chi = j_z(r). \quad (6)$$

Thus, we have obtained 5 equations (2-6) with 6 $j(r)$, $h(r)$ unknown functions. Therefore one of the functions can be defined arbitrarily. We define $j_\varphi(r)$ function. In this case, an algorithm for solving these equations is as follows:

1. Set the initial (at $r = 0$) zero values of functions listed above, except for $j_\varphi(r)$.

2. Define $j_\varphi(r)$ function.

3. From (2) we find:

$$j_r'(r) = -\frac{j_r(r)}{r} - \frac{j_\varphi(r)}{r} \alpha - j_z(r) \chi = 0. \quad (7)$$

$$j_r = j_{r\text{old}} + j_r' \cdot dr. \quad (8)$$

5 From (5) we find:

$$h_z'(r) = -j_\varphi(r) - h_r(r) \chi. \quad (11)$$

$$h_z = h_{z\text{old}} + h_z' \cdot dr. \quad (12)$$

6. From (4) we find:

$$h_\varphi(r) = (h_z(r) \alpha / r - j_r(r)) / \chi. \quad (13)$$

$$h_\varphi'(r) = (h_z'(r) \alpha / r - j_r'(r)) / \chi. \quad (14)$$

7. From (6) we find:

$$j_z(r) = h_\varphi'(r) + \frac{h_\varphi(r)}{r} + \frac{1}{r} \cdot h_r(r) \alpha. \quad (15)$$

8. Go to p. 2 with the new value of r variable.

References

1. G. Schlichting. Boundary layer theory. Ed. "Science", Moscow, 1974 (see page 480).
2. Khmelnik S.I. Mathematical Model of the Taylor Vortices. The Papers of independent Authors, ISSN 2225-6717, № 36, 2015; and <http://vixra.org/abs/1511.0248>, 2015-11-25.

Chapter 5.6. Ranque Effect

Contents

- 1. Introduction \ 207
- 2. Maxwell-like gravitational equations of Ranque pipe \ 206
- 3. Pipe section with a swirler \ 208
- 4. Smooth pipe section \ 209
- 6. Energy flows \ 209
- Appendix 1 \ 214
- References \ 213

1. Introduction

Instead of introduction, we raise several very brief quotes from introduction to Hutsol's article [1], which concisely characterize the situation with scientific justification for this effect.

Ranque effect, which lies in the fact that in vortex tubes of sufficient common geometry the gas flow separation into two occurs, one of which is peripheral - has a temperature above original gas temperature and the second is central with a lower temperature accordingly is known. This effect seems even stranger if it is remembered that ... Archimede's buoyant forces would have to lead to hotter gas "floating" in the vortex center. Gases temperature separation effect was discovered by Ranque in 1932.... An intensive experimental and theoretical study of this effect ... continues to the present day. Effect technical simplicity stimulated the activity of inventers.... The range of designed and used devices ... is extremely wide, and their capabilities are impressive.... As for attempts to find an irrefutable scientific explanation for the effect itself, publications on this topic continue to the present day. Thus, over the last 15 years ... (further Hutsol refers to 21 publications - articles, theses, books). ... Apparently, such explanation for the Ranque effect, which would be recognized as indisputable isn't found. Ranque effect is an "unexpected phenomenon", the nature of which "still seems mysterious," according to leading experts in aerodynamics of vortex flows.

Further, Hutsol [1] considers the existing theories, shows their "inherent defects and contradictions in experimental data description," and then offers his own theory. However, another anonym in [2] notes the shortfalls of this theory, as well as several others.

The author doesn't begin to discuss the above statements and cites them only to confirm the **need** to find a new theoretical justification of

Ranque effect. And offer (as usual) his theory, explaining the Ranque effect including a completely different area of physics.

The same anonym in [3] formulates a very profound observation:

Traditional hydrodynamics tacitly based on axiom that the true mode of fluids and gases motion is a laminar current, and turbulence is regarded as its violation caused by a particular restriction of its "freedom". However, based on the fact that the current that was laminar in a relatively narrow channel, when removing the walls that limit it and remaining the previous velocity begins to swirl, it is logical to conclude that exactly vortex flow is a "natural" mode of fluids and gases motion, and it becomes forcedly laminar - just under the influence of environmental constraints! It is enough to look at Reynolds number formula - generally accepted criterion of flow laminarity or turbulence - in case of constant flow rate it increases proportionally to pipe diameter, which means that the current becomes more turbulent. A fluid whirling at a high velocity in a narrow tube is laminar, and even slow currents in the limitless ocean are accompanied by rotary streams and vortices - the same slow, low-observable and safe as flows that have generated them.

This statement about "the priority of turbulent motion" will also be justified in proposed theory.

2. Maxwell-like gravitational equations of Ranque pipe

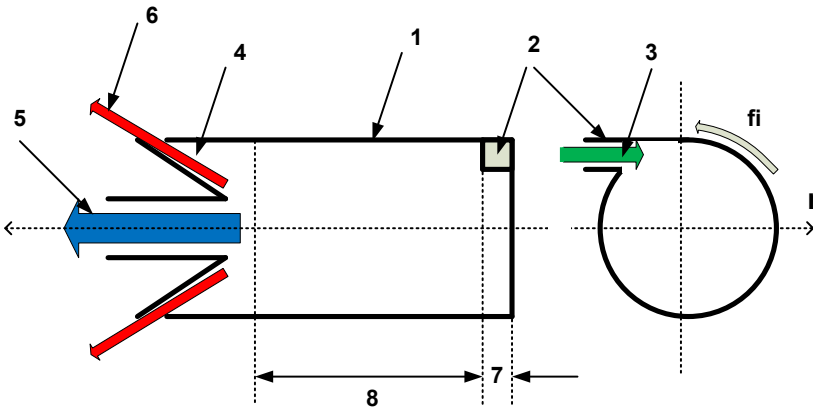


Fig. 1.

Here we consider only the direct-flow Ranque pipe - see Fig. 1 [1], where

1 – cylindrical pipe,

2 – swirler for fluid or gas feeding tangentially to pipe circumference,

3 – input flow,

- 4 – choke dividing the total flow into the central flow 5 and external flow 6,
 7 – pipe section with swirler 2,
 8 – smooth cylindrical pipe section (smooth area)
 r, φ, z – cylindrical coordinates.

The main task is to explain why the internal energy of central flow 5 is much less than the internal energy of external flow 6.

The mass currents exist in pipe. Let us denote their densities as J_r, J_φ, J_z . These mass currents generate H_r, H_φ, H_z magnetogravitational tensions. Mass currents and tensions densities should comply with Maxwell-like gravitational equations. For the stationary case, which takes place in our task, these equations in r, φ, z cylindrical coordinates are the following (see (2.2.1-2.2.5) in Chapter 2):

$$\frac{H_r}{r} + \frac{\partial H_r}{\partial r} + \frac{1}{r} \cdot \frac{\partial H_\varphi}{\partial \varphi} + \frac{\partial H_z}{\partial z} = 0, \quad (3)$$

$$\frac{1}{r} \cdot \frac{\partial H_z}{\partial \varphi} - \frac{\partial H_\varphi}{\partial z} = J_r, \quad (4)$$

$$\frac{\partial H_r}{\partial z} - \frac{\partial H_z}{\partial r} = J_\varphi, \quad (5)$$

$$\frac{H_\varphi}{r} + \frac{\partial H_\varphi}{\partial r} - \frac{1}{r} \cdot \frac{\partial H_r}{\partial \varphi} = J_z. \quad (6)$$

$$\frac{J_r}{r} + \frac{\partial J_r}{\partial r} + \frac{1}{r} \cdot \frac{\partial J_\varphi}{\partial \varphi} + \frac{\partial J_z}{\partial z} = 0. \quad (8)$$

It can be assumed that the field is uniform along OZ vertical axis. In Appendix 1 it is shown that in this case the system of equations (3-6, 8) can have the following solution:

$$J_r = -\frac{\alpha}{2} j_\varphi r \cos(\alpha\varphi) - \frac{1}{2} J_{\varphi\varphi} r, \quad (9)$$

$$J_\varphi = j_\varphi r \sin(\alpha\varphi) + J_{\varphi\varphi} r, \quad (10)$$

$$J_z = h_\varphi \left(1 - \frac{\alpha^2}{2}\right) \cos(\alpha\varphi) + J_{oz}, \quad (11)$$

$$H_r = \frac{\alpha}{2} h_\varphi r \sin(\alpha\varphi), \quad (12)$$

$$H_{\varphi} = h_{\varphi} r \cos(\alpha\varphi) + \frac{J_{z0} r}{2}, \tag{13}$$

$$H_z = -\frac{1}{2} j_{\varphi} r^2 \sin(\alpha\varphi) - \frac{1}{2} J_{\varphi0} r^2. \tag{14}$$

where α , j_{φ} , h_{φ} , $J_{\varphi0}$, J_{z0} - some constants determined by design and input flow.

3. Pipe section with a swirler

$J_{\varphi0}$ mass current can be defined in this section as a value proportional to input flow 3. J_{z0} mass current can be defined as a value proportional to $J_{\varphi0}$ mass current and a constant along the length of this section (because this length is small). Finally, for a given J_{z0} by (3.11), we can find J_z . So, without getting into details of calculations, it is fair to say that there is a mass current (3.11) directed along OZ axis at this section output.

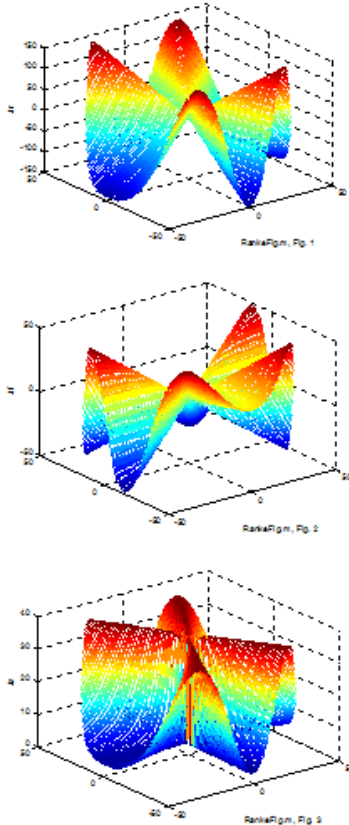


Fig. 2

4. Smooth pipe section

So, at the input of smooth section there is a mass current (3.11) directed along OZ axis, and a mass current with $J_{\varphi 0}$ density is absent ($J_{\varphi 0} = 0$). At that, by (3.9, 3.10, 3.11-3.14) we can find $J_r, J_\varphi, H_r, H_\varphi, H_z$, since from (3.11) $J_z = \alpha, h_\varphi, J_{oz}$ are known. Assuming that j_φ constant is also known, let us consider the solution obtained. Fig. 2 shows the graphs of functions - J_r, J_φ, J_z respectively, when $\alpha = 6, j_\varphi = 1, h_\varphi = 1, J_{\varphi 0} = 0, J_{z0} = 20$.

5. Energy flows

The density of gravitomagnetic energy flow is a gravitomagnetic Poynting vector

$$S = E \times H, \quad (1)$$

where E gravitational intensity is associated with mass current density, as well as electrical intensity is associated with electric current density, i.e.

$$E = \rho \cdot J, \quad (2)$$

where ρ - resistance to mass flow caused by fluid viscosity. Combining (1, 2), we obtain:

$$S = \rho J \times H. \quad (3)$$

Vector product (3) in cylindrical coordinates is the following:

$$S' = \frac{S}{\rho} = J \times H = \begin{bmatrix} S'_r \\ S'_\varphi \\ S'_z \end{bmatrix} = \begin{bmatrix} J_\varphi H_z - J_z H_\varphi \\ J_z H_r - J_r H_z \\ J_r H_\varphi - J_\varphi H_r \end{bmatrix}. \quad (4)$$

Under known J, H , we can find S' . Fig. 3 shows the graphs of functions (4) when $\alpha = 2$. Fig. 4-6 show the graphs of $[S'_r, S'_\varphi, S'_z]$ functions, respectively, when $\alpha = 6, j_\varphi = 1, h_\varphi = 1, J_{\varphi 0} = 0, J_{z0} = 20$.

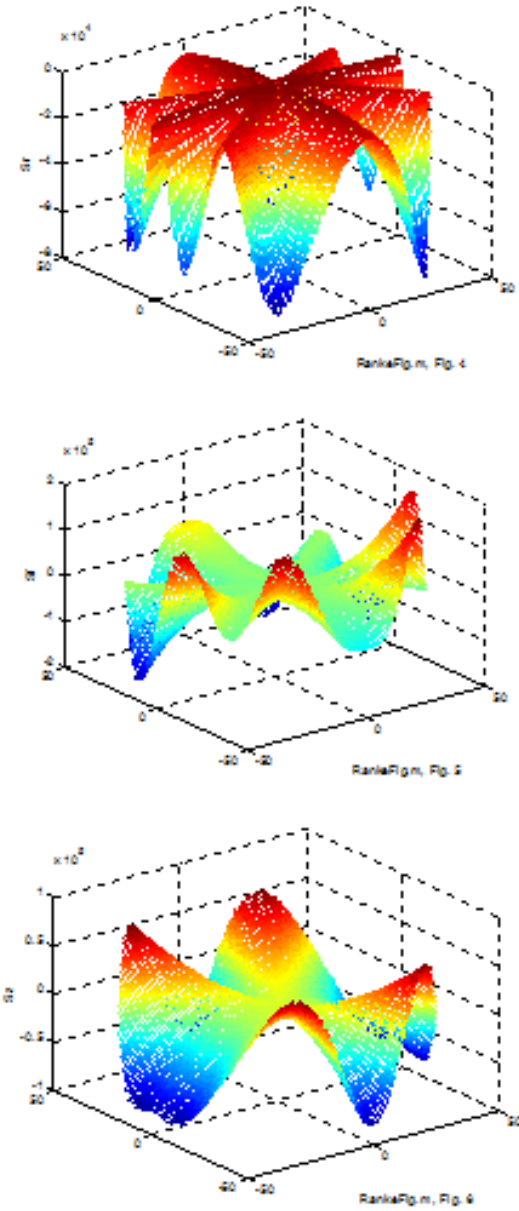


Fig. 3.

The average density of energy flow for each circle can be denoted as $[S'_{rmid}, S'_{\varphi mid}, S'_{zmid}]$. Fig. 4 shows the graphs of $[S'_{rmid}, S'_{\varphi mid}, S'_{zmid}]$ functions depending on radius when $\alpha = 6$, $j_\varphi = 1$, $h_\varphi = 1$, $J_{\varphi 0} = 0$, $J_{z0} = 20$.

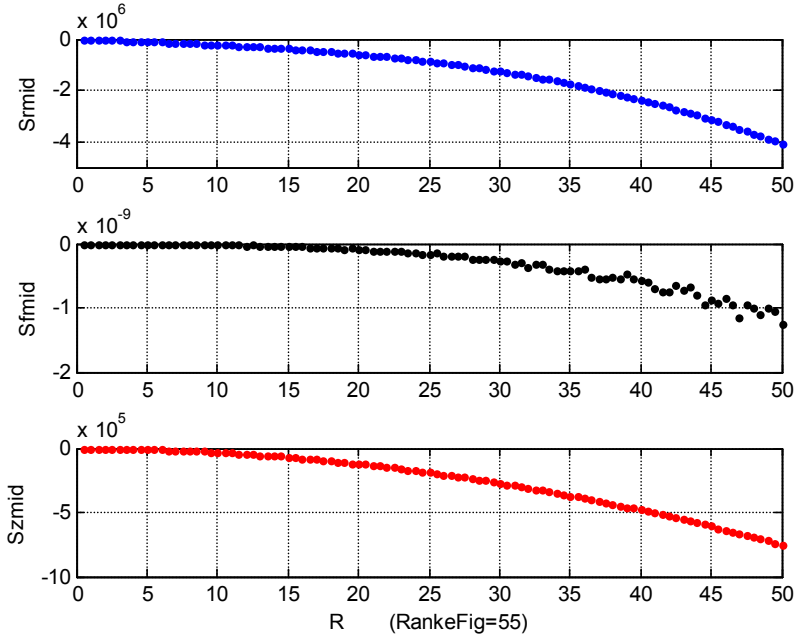


Fig. 4.

From these graphs it follows that energy flows in the central section (at small radii) are close to zero. S_{rmid} and S_{fmid} energy flows are consumed for the thermal losses in ρ resistance, i.e. for viscous friction. These losses determine the temperature of central and external flows. It follows that

internal energy of the central flow 5 is substantially smaller than internal energy of the external flow 6.

Appendix 1.

The solution of equations (3.3-3.6, 3.8) is considered. From physical considerations it is clear that the field must be uniform along the vertical axis, i.e. the derivatives according to z argument must be absent, and therefore equations (3.3-3.6, 3.8) should be rewritten as follows:

$$\frac{H_r}{r} + \frac{\partial H_r}{\partial r} + \frac{1}{r} \cdot \frac{\partial H_\varphi}{\partial \varphi} = 0, \quad (1)$$

$$\frac{1}{r} \cdot \frac{\partial H_z}{\partial \varphi} = J_r, \quad (2)$$

$$-\frac{\partial H_z}{\partial r} = J_\varphi, \quad (3)$$

$$\frac{H_\varphi}{r} + \frac{\partial H_\varphi}{\partial r} - \frac{1}{r} \cdot \frac{\partial H_r}{\partial \varphi} = J_z, \quad (4)$$

$$\frac{J_r}{r} + \frac{\partial J_r}{\partial r} + \frac{1}{r} \cdot \frac{\partial J_\varphi}{\partial \varphi} = 0 \quad (5)$$

Let us suppose that

$$H_{r.} = h_r r \sin(\alpha\varphi) \quad (6)$$

$$H_{\varphi.} = h_\varphi r \cos(\alpha\varphi) + H_{\varphi 0} r \quad (7)$$

From (1, 6, 7) it follows that:

$$\frac{h_r r \sin(\alpha\varphi)}{r} + h_r \sin(\alpha\varphi) - h_\varphi \alpha \sin(\alpha\varphi) = 0, \quad (8)$$

Consequently,

$$h_r = h_\varphi \alpha / 2. \quad (9)$$

From (4, 6, 7) it follows that:

$$\cdot \quad (10)$$

From (9, 10) it follows that:

$$J_z = h_\varphi (1 - \alpha^2 / 2) \cos(\alpha\varphi) + J_{z0}, \quad (11)$$

$$J_{z0} = 2H_{\varphi 0}. \quad (11a)$$

Let us suppose now that

$$J_{r.} = j_r r \cos(\alpha\varphi) + J_{r0} r, \quad (12)$$

$$J_{\varphi.} = j_\varphi r \sin(\alpha\varphi) + J_{\varphi 0} r. \quad (13)$$

From (5, 11, 12) it follows that:

$$\frac{j_r r \cos(\alpha\varphi)}{r} + j_r \cos(\alpha\varphi) + 2J_{r0} + j_\varphi \alpha \cos(\alpha\varphi) + J_{\varphi 0} = 0, \quad (14)$$

Consequently,

$$j_r = -j_\varphi \alpha / 2. \quad (15)$$

$$J_{r0} = -J_{\varphi 0} / 2. \quad (15a)$$

Let us suppose that

$$H_z = -\frac{1}{2} j_\varphi r^2 \sin(\alpha\varphi) - \frac{1}{2} J_{\varphi 0} r^2. \quad (16)$$

From (12, 15, 15a) it follows that the conditions (2, 3) are met which take the form of:

$$\frac{\partial H_z}{\partial \varphi} = -\frac{\alpha}{2} j_\varphi r^2 \cos(\alpha\varphi), \quad (17)$$

$$\frac{\partial H_z}{\partial r} = -j_\varphi r \sin(\alpha\varphi) - J_{\varphi 0} r, \quad (18)$$

Thus,

$$J_{r\cdot} = -\frac{\alpha}{2} j_{\varphi} r \cos(\alpha\varphi) - \frac{1}{2} J_{\varphi 0} r, \quad (12)$$

$$J_{\varphi\cdot} = j_{\varphi} r \sin(\alpha\varphi) + J_{\varphi 0} r, \quad (13)$$

$$J_z = h_{\varphi} \left(1 - \frac{\alpha^2}{2}\right) \cos(\alpha\varphi) + J_{oz}, \quad (11)$$

$$H_{r\cdot} = \frac{\alpha}{2} h_{\varphi} r \sin(\alpha\varphi), \quad (6)$$

$$H_{\varphi\cdot} = h_{\varphi} r \cos(\alpha\varphi) + \frac{J_{z0} r}{2}, \quad (7)$$

$$H_z = -\frac{1}{2} j_{\varphi} r^2 \sin(\alpha\varphi) - \frac{1}{2} J_{\varphi 0} r^2. \quad (16)$$

References

1. A.Gutsol. The Rank effect. Progress in Physical Sciences, Vol 167, No. 6, 1997
2. Devices on the Rank effect,
<http://khd2.narod.ru/whirl/ranque.htm>
3. Turbulence and complex vortex motion,
<http://khd2.narod.ru/whirl/whirldyn.htm>
4. Khmelnik S.I. About the Theoretical Rationale of the Ranque Effect. The Papers of independent Authors, ISSN 2225-6717, № 36, 2015; and <http://vixra.org/abs/1511.0078>, 2015-11-10.

Chapter 5.7. Sound and Gravity

Contents

1. Facts \ 214
2. Electrotechnical experiments \ 216
 - 2.1. Ring with a current above the plane \ 216
 - 2.2. Two planes \ 219
3. Gravitomagnetic analogies \ 220
 - 3.0. Introduction \ 220
 - 3.1. Ring with a mass current above the plane \ 221
 - 3.2. Two planes \ 222
- Reference \ 223

1. Facts

There are several facts which present the sound influence on gravity force. There are also the theories explaining these facts, but all of them are out of existing physical paradigm. An explanation of these facts using Maxwell-like gravitational equations is proposed below.

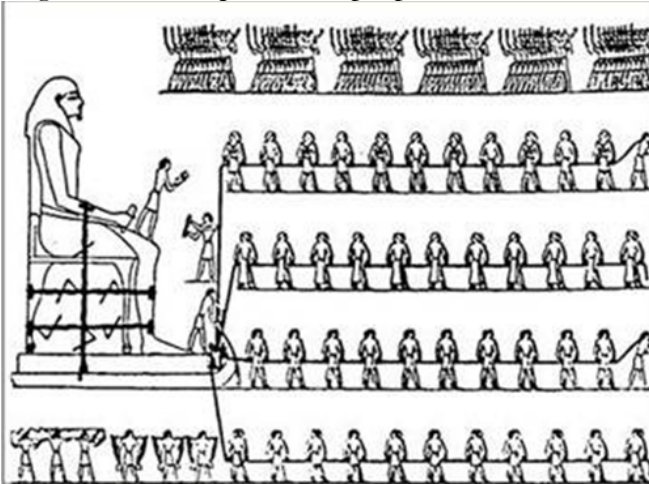


Fig. 1.

1.1. Stone sculptures moving in Ancient Egypt

[1]. "To this day, the drawings of Egyptian hieratic structures with images of large stone sculptures moving have been preserved. From the above-mentioned (see Fig.1) - it can be seen that a small part of people

are pulling the platform on which the sculpture of the Pharaoh is installed, and they support it from overturning, while the other part of people stand apart with sound instruments in their hands which are necessary for Platform levitation with sculpture. ... the platform with its skids just lightly touched the ground, facilitating its transportation. "

1.2. The **coral castle** - a complex of huge structures with a total weight of 1100 tons exist in California. The author and castle builder Edward Lidskalinsh built it manually, with no use of machines, arguing that he discovered the secret of pyramids builders. Neighbors, who sometimes could observe the construction progress, say that Edward moved huge blocks over the air with a wet finger and sang songs to his stones [2].

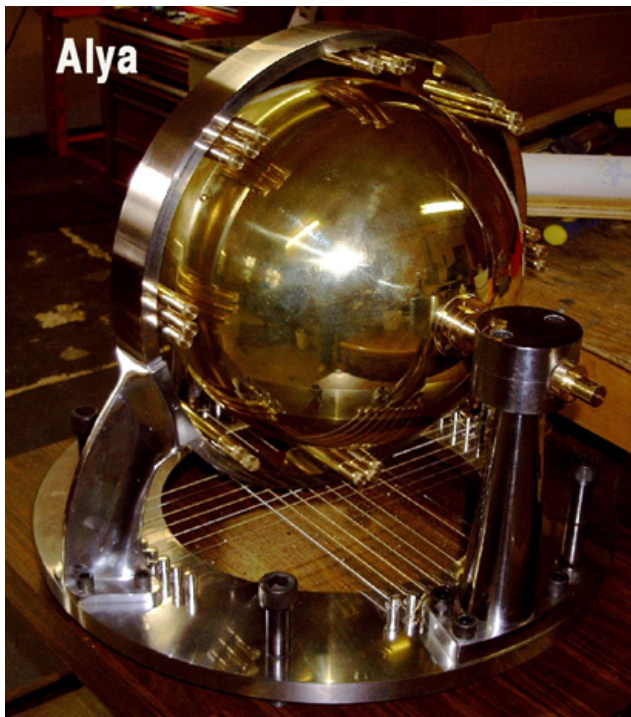


Fig. 2.

1.3. The so-called **perpetual motion machine of John Keely** [3] is known. Schematically it can be represented as follows. There is some structure, which called by the author as sympathetic transmitting device, and containing a lot of tuning forks. "A cylindrical glass vessel with a height of more than one meter, filled with water is located near it. The vessel lid, also made of metal, is connected to sphere by a thick wire made of gold, silver and platinum. Three metal balls, each weighing about

a kilogram lie at the bottom of vessel". "The inventor comes to sympathetic transmitting device, and tuning forks begin to vibrate, arms begin to turn round... Suddenly, a trumpet sounds briefly, and a ball on the bottom of vessel begins to wiggle, then slowly breaks away from the bottom and uprushes through water column. Then it strikes against the lid, rebounds, rises up again and, finally, calms down, tightly snuggling to it." Keely built many other elegant and expensive structures the mechanical motions in which are excited by certain melodies-see, for example, Fig.2.

1.4. Levitation in Tibet. In [4] the following case is described. "250 meters from the rock, opposite to cave, a polished stone flag with rounded cavity was located. A stone block 1*1*1.5 meters in size was submerged into cavity by a group of monks with the help of yaks." Monks with 19 musical instruments, among which there were 13 drums and 5 trumpets, got into arc of 90 degrees before the stone. ... All the drums were opened from one end, fixed on columns and oriented to stone. The monks beaten the drums with large leather beats. The monks also strung behind the instruments. They began to sing and play musical instruments. After about 4 minutes, when the sound reached a certain level, a large stone located in arc focus moved up stately and floated in the air upward to the rock where other monks took the stone. The flight took about 3 minutes. And it was not the only case. Monks continued to do this trick with velocity of 5 or 6 stones per hour. One of the stones is destroyed, which shows that sound resonance effect can cause a destruction. Another interesting aspect of this levitation is the small amount of energy necessary for this - ... we can calculate that a power of about 0.01 watts acts on the stone, ... and a stone weight is over 4 tons. A power of about 52 kilowatts is required for stone rise for 3 minutes."

2. Electrotechnical experiments

2.1. Ring with a current above the plane

At first let us consider the first electrotechnical experiment - see Fig. 3, which shows A conductor ring with U ac voltage source and $CDEF$ metal board the plane of which is parallel to ring plane. J_1 alternating current passing through A ring induces J_2 induction current in $CDEF$ board. In the first approximation, at sufficiently small d distance between the ring and board, it can be assumed that J_2 current flows along the annular closed B circuit, and R radii of A and

B rings coincide. J_1 and J_2 currents are opposite in direction (phase-shifted by $\pi/2$) and therefore repelled with some F force. If board is massive, it remains stationary, and A ring rises by this force over the board.

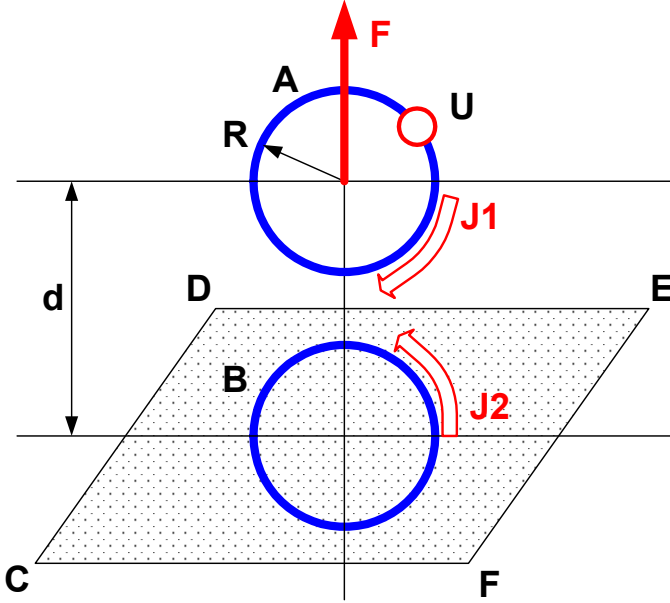


Fig. 3.

This experiment can be more strictly described as follows (hereinafter the GHS system is used). Φ magnetic flow passing through A turn area, along which J_1 alternating electric current flows is,

$$\Phi = \frac{2\pi R J_1}{c}. \quad (2)$$

Electromotive force generated by Φ magnetic flow in B circuit is,

$$\varepsilon = \frac{1}{c} \cdot \frac{d\Phi}{dt}, \quad (3)$$

The strength of inductive electric current in B closed circuit is

$$J_2 = \varepsilon / \rho \quad (4)$$

or

$$J_2 = \frac{1}{c\rho} \cdot \frac{d\Phi}{dt} \quad (5)$$

or, finally,

$$J_2 = \frac{\omega \cdot \Phi}{c\rho}, \quad (6)$$

where ρ - B loop resistance, ω - J_1 current circular frequency. When calculating the force of two rings of R radius attraction, in order to simplify the task, we replace them by two squares with R half-side. Then in a vacuum and when $R \gg d$ we obtain [5]:

$$F = \frac{16J_1J_2R}{c^2d}. \quad (7)$$

Combining (2, 6, 7), we obtain

$$F = \frac{32\pi\omega J_1^2 R^2}{c^4\rho \cdot d} \approx \frac{100\omega J_1^2 R^2}{c^4\rho \cdot d}. \quad (8)$$

Example 1. It will be recalled that this formula refers to GHS system. At that

$$1[\text{Om}] = \frac{10^9}{c^2}[\text{GHS}], \quad 1[\text{A}] = \frac{c}{10}[\text{GHS}].$$

Then from (8) we find:

$$F \approx \frac{100\omega \cdot J_1^2 R^2}{c^4\rho \cdot d} \approx \frac{\omega \cdot J_1^2 R^2}{10^9\rho \cdot d}, \quad (9)$$

where the currents and resistances measured respectively in amperes and ohms. Let us assume that

$$\omega = 1000, \quad R = 100[\text{cm}], \quad d = 10[\text{cm}],$$

$$\rho = 0.01[\text{Om}], \quad J_1 = 100[\text{A}].$$

Then from (9) we find:

$$F \approx \frac{\omega \cdot J_1^2 R^2}{10^9\rho \cdot d} \approx \frac{1000 \cdot 100^2 \cdot 100^2}{10^9 \cdot 10 \cdot 0.01} \approx 1000[\text{dyne}].$$

If A and B rings' resistances are equal, then the heat losses power in A ring is

$$p = J_1^2 \rho. \quad (10)$$

Then, as follows from (8),

$$F = \alpha \cdot p, \quad (11)$$

where

$$\alpha \approx \frac{100\omega \cdot R^2}{c^4 d \rho^2}. \quad (12)$$

Thus, A ring lifting force is proportional to heat power released in this ring.

Example 2. Let us find α , under conditions of Example 1. In this example

$$\rho = 0.01[\text{Om}] = \frac{0.01 \cdot 10^9}{c^2} [\text{GHS}].$$

We have $c = 3 \cdot 10^{10}$. Then

$$\rho = \frac{0.01 \cdot 10^9}{3^2 10^{20}} [\text{GHS}] \approx 10^{-14} [\text{GHS}].$$

From (12) we find

$$\alpha \approx \frac{100 \omega R^2}{c^4 \rho^2 d} = \frac{100 \cdot 1000 \cdot 100^2}{3^4 10^{40} 10^{-28} 10} \approx 10^{-6}.$$

Consequently, $F[\text{dyne}] = \alpha \cdot (p[\text{erg/sec}])$ or $F[\text{dyne}] = \alpha \cdot (10^7 p[W])$. Thus, in this example $F[\text{dyne}] = 10 \cdot (p[W])$. Indeed, in example 1 $P = J_1^2 \rho = 100[W]$ and $F = 1000[\text{dyne}]$.

2.2. Two planes

Let us now consider an electrotechnical experiment (see Fig. 4), in which there are two metal boards 1 and 2. Metal board 1 is penetrated by ψ external variable magnetic flow. In this board, the eddy currents flow. It is extracted from the trajectories of such a current as A ring. The current in this ring induces a current in B ring of the metal board 2. It was demonstrated above that, in this case, A ring experiences a lifting force (11), depending on heat power consumed in this ring. The board 1 contains a set of A rings. Consequently, the board 1 experiences a lifting force (11) proportional to the total heat power consumed by all eddy currents flowing in the board 1. In this case the proportionality factor (12) depends on R mid-radius of eddy current paths.

Example 3. Let us find α , under conditions of Example 2. In this example $\rho = 0.01 \cdot 10^9 / c^2 [\text{GHS}]$. We have $c = 3 \cdot 10^{10}$. Then

$$\rho \approx 10^{-14} [\text{GHS}]. \text{ From (12) we find } \alpha \approx \frac{100 \omega R^2}{c^4 \rho^2 d} = \frac{100 \cdot 1000 \cdot 100^2}{3^4 10^{40} 10^{-28} 10} \approx 10^{-6}.$$

Consequently, $F[\text{dyne}] = \alpha \cdot (p[\text{erg/sec}])$ or $F[\text{dyne}] = \alpha \cdot (10^7 p[W])$. Thus, in this example or $F[\text{dyne}] = 10 \cdot (p[W])$. Indeed, in example 1 $P = J_1^2 \rho = 100[W]$ and $F = 1000[\text{dyne}]$.

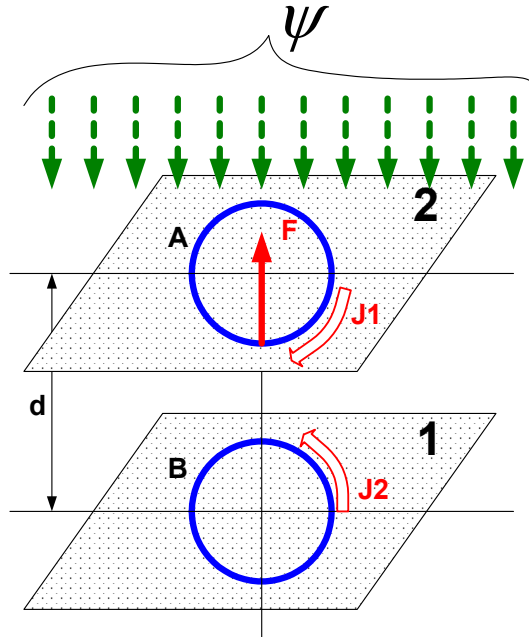


Fig. 4.

3. Gravitomagnetic analogies

3.0. Introduction

In Section 2, some electromagnetic phenomena (which aren't beyond the scope of the classical theory) are considered, and in Chapter 1 an analogy of electromagnetism and gravitoelectromagnetism is considered. On the basis of this, it is shown below that similar phenomena in the field of gravitoelectromagnetism can exist. In particular, it is shown that

- 1) acoustic waves in a rigid body generate an alternating mass current much as alternating magnetic flow generates the eddy currents in metal;
- 2) alternating mass current in one rigid body excites the gravitomagnetic waves that induce an alternating mass current in another rigid body;
- 3) mass currents of two bodies generate the forces of these bodies repelling, similar to forces of two conductors with an electric current repelling.

These phenomena allow to explain the above facts in that sound waves in a rigid body generate the lifting forces. Indeed, sound waves in a rigid body are related to body particles vibrations and can therefore be considered as a mass current (much as charged particles vibrations is an

electric current). This current frequency is a sound frequency. Sound waves velocity in a rigid body can reach significant values, and their intensity can be amplified when a sound resonance of material occurs-for example, at a sound resonance of steel, the sound waves velocity reaches $6 \cdot 10^5 [cm/sec]$ values [6]. Thus, air sound vibrations can create an intensive mass current in a rigid body. Let us also note that sound waves in a rigid body increase the bode temperature, i.e. sound waves mass current releases the energy similar to energy release when an electric current passes through electrical resistance. In this regard, we can talk about the "mass" resistance of rigid body material.

3.1. Ring with a mass current above the plane

Let us now suppose that Fig. 3 shows the mass currents. J_{g1} alternating mass current flows along A ring. In Chapter 1 it is shown that in this case the gravitomagnetic flow passes through the ring A area

$$\Phi_g = \frac{2\pi R G J_{g1}}{c}, \quad (13)$$

where $G \approx 7 \cdot 10^{-8} \left[\frac{\text{dyne} \cdot \text{cm}^2}{\text{g}^2} \right]$ - gravitational constant. This formula

differs from the similar formula (2) by G coefficient in electrodynamics. A gravitomagnetic flow in B circuit generates the following gravitomoving force

$$\varepsilon_g = \frac{\xi}{c} \cdot \frac{d\Phi_g}{dt}, \quad (14)$$

where ξ - gravitational permeability. This formula differs from the similar formula (3) by ξ coefficient in electrodynamics. In vacuum, $\xi \approx 10^{12}$ coefficient, but with pressure increase, sharply decreases. Further similar to previous one we have:

$$J_{g2} = \varepsilon_g / \rho_g \quad (15)$$

or

$$J_{g2} = \frac{\xi}{c\rho_g} \cdot \frac{d\Phi_g}{dt} \quad (16)$$

or, finally,

$$J_{g2} = \frac{\omega \cdot \xi \cdot \Phi_g}{c\rho_g}. \quad (17)$$

Using the formula (7), by analogy we obtain

$$F_g = \frac{16J_{g1}J_{g2}R}{c^2d}. \quad (18)$$

Combining (14, 15, 18), we obtain

$$F_g = \frac{32\pi\omega\xi \cdot GJ_{g1}^2R^2}{c^4\rho_g \cdot d} \approx \frac{100\omega\xi \cdot GJ_{g1}^2R^2}{c^4\rho_g \cdot d}. \quad (19)$$

Reasoning as before, we find the following heat losses power in A ring

$$p_g = J_{g1}^2\rho_g \quad (20)$$

and a force

$$F_g = \alpha_g \cdot p_g. \quad (21)$$

where

$$\alpha_g \approx \frac{100\omega \cdot \xi \cdot GR^2}{c^4\rho_g^2d}. \quad (22)$$

Thus, a lifting force of A ring, through which an alternating mass current flows, is proportional to heat power generated in this ring.

So, a lifting force acts on a tubular ring with pulsating mass current, located above the massive plane. An alternating mass current can be generated through passing a portion of liquid with a certain frequency along the ring. Another ring construction with a mass current is described in Chapter 6.1. Here the ring is considered as a fragment of plane - see below.

3.2. Two planes

Let us now consider Fig. 4, where (contrary to previous one) two solid boards 1 and 2 are shown. The board 1 is penetrated by ψ alternating current of sound waves. In this board, the mass currents, analogous to eddy currents arise in electrical engineering. Reasoning as before, it can be argued that these mass currents induce the mass currents in the board 2. Consequently, the board 1 experiences a lifting force (21), proportional to the total heat power, consumed by all mass currents flowing in the board 1. The proportionality coefficient (22) in this case depends on R mid-radius of these mass currents paths.

Comparing (12) and (22), we note that in case of equal $p_g = p$ heat powers and equal $p_g = p$ resistances, the forces developed in gravitotechnical and electrotechnical structures are related as $\beta = \xi \cdot G$.

Example 4. Let us find α , under conditions of Example 3. In this example $\rho_g \approx 10^{-14}[GHS]$. For vacuum

$$\beta = \xi \cdot G = 10^{12} \cdot 7 \cdot 10^{-8} = 7 \cdot 10^4. \text{ From (22) we find}$$

$$\alpha_g \approx \alpha\beta \approx 10^{-6} \cdot 7 \cdot 10^4 \approx 0.1. \text{ Consequently,}$$

$F_g[\text{dyne}] = \alpha_g \cdot (p_g[\text{erg/sec}])$ or $F_g[\text{dyne}] = \alpha_g \cdot (10^7 p_g[W])$. Thus, in this example or $F_g[\text{dyne}] = 10^6 \cdot (p[W])$ or $F_g[N] = 10 \cdot (p[W])$. If (as in example 1), $p_g = p = 100[W]$, then $F_g = 1000[N]$.

This example shows that the lifting force can be very significant. However, here it is necessary to make two remarks.

- 1) Resistance to mass current is currently unknown. Perhaps it essentially (in one or another direction) differs from the resistance to electric current.
- 2) Gravitational permeability rate under normal pressure ratings is much lower than accepted in example for vacuum. But it can be assumed that a gravitational permeability of air for a gravitomagnetic wave increases substantially if air fluctuates at a frequency of this wave (what is valid in facts under discussion).

Thus, a lifting force acts on a massive plane 1 arranged above the other massive plane massive 2, if this plane 2 is exposed to radiation by intensive sound wave from below.

Reference

1. Moving stone sculptures in ancient Egypt, http://www.74rif.ru/zamok_levitacia.html
2. Coral Castle, <http://bibliotekar.ru/0korall.htm>
3. Dmitry Zakharov. The perpetual motion machine of John Keely, http://www.manwb.ru/articles/science/natural_science/JhonKili_DmZah/
4. Davidson D. Free energy, gravity and ether, http://svitk.ru/004_book_book/13b/3031_devidson-svobodnaya_energiya_gravitaciya_efir.php
5. Yavorsky B.M., Detlaf A.A. Handbook of Physics. "Fizmatgiz", Moscow, 1963.
7. Viktorov I.A. Sound surface waves in solids. Ed. "Science," 1981.
8. Khmelnik S.I. Sound and gravity. The Papers of independent Authors, ISSN 2225-6717, № 21, 2012.

Chapter 6. Experiment Projects

Based on the above-said, we propose the projects of some experiments which can confirm (or confute) the proposed theory. The experiments, which can be a prototype of industrial technical device, are also proposed.

Author would participate in such experiments with pleasure. You are welcome with your suggestions at:

solik@netvision.net.il

Chapter 6.1. Gravitomagnetic induction detection

Contents

- 1. Porous charged ring rotation \ 225
- 2. Massive disk rotation \ 226
- 3. Experiments \ 227
 - 3.1. Gravitomagnetic induction measurement \ 227
 - 3.2. Gravitational permeability measurement \ 229
- References \ 230

1. Porous charged ring rotation

In [1], a rotating charged disk exciting a magnetic field is considered. Eichenwald designates these rotating charges as convection current. His experiment allows to state that a normal electric current, convection current, a rotating electric field and a rotating charged disk uniformly excite the magnetic field.

With a view to Eichenwald experiment, let us consider the porous metal and electrically charged ring with R average radius. Obviously, the charges are located on pores surfaces. It can be approximately assumed that charge distribution density along the ring circumference is described by the following function

$$\rho(\varphi) \approx \rho_0 \cdot (1 + \sin(\lambda\varphi)), \quad (1)$$

where

ρ_0 - constant,

φ - angular coordinate,

λ - "wave" length, depending on the average distance between pores.

If to put ring in rotation with a certain ω angular velocity, then $\varphi(t) = \omega t$ density of charges distribution along ring circumference becomes a function of t time in the form of

$$\rho(t) \approx \rho_0 \cdot (1 + \sin(\lambda\omega t)), \quad (2)$$

A current flowing through the ring is

$$J(t) = \frac{d\rho(t)}{dt} \approx \rho_o \cdot \lambda\omega \cdot \cos(\lambda\omega t). \quad (3)$$

This current generates a magnetic flow perpendicular to ring plane. The average magnetic induction of this flow in terms of ring area is determined in CGS system by the following formula

$$B(t) = \frac{2\mu J(t)}{c \cdot R}, \quad (4)$$

Consequently, the average magnetic induction of rotating charged porous ring in terms of ring area is

$$B(t) \approx 2\rho_o\omega\lambda \cdot \cos(\lambda\omega t)/(cR). \quad (5)$$

2. Massive disk rotation

By analogy, it is fair to say that a rotating porous ring creates a mass current

$$J_g(t) = \frac{dm(t)}{dt} \approx m_o \cdot \lambda\omega \cdot \cos(\lambda\omega t). \quad (6)$$

The average gravitomagnetic induction of this flow in terms of ring area is determined in CGS system by the following formula (see formula (1.2.4) in Chapter 1):

$$B_g = \frac{2G\xi J_g}{cR}. \quad (7)$$

Then from (7) we find that this current creates a variable gravitomagnetic induction

$$B_g \approx 2m_o\xi G\omega\lambda \cdot \cos(\lambda\omega t)/(cR). \quad (8)$$

In Chapter 1 it is shown that in this case a gravitomagnetic flow passes through A ring area - see (1.2.1.4a):

$$\Phi_g = \frac{2\pi R G J_g}{c}, \quad (8a)$$

Consequently, it is fair to say that a rotating porous ring creates the gravitomagnetic induction (8) and gravitomagnetic flow (8a).

Obviously, a rotating solid disc made of porous material also creates a gravitomagnetic induction. Thus, **the rotating porous disk generates a gravitomagnetic induction**. This statement is equivalent to the following:

the rotating porous disk is a constant gravitomagnet

Hence it follows that rotating porous disks, being gravitomagnets, should be attracted or repelled.

As any material isn't solid, then this statement can be extended to any disk. However, its gravitomagnetic properties will be weakly expressed. Hence it follows that rotating disks, being gravitomagnets, should be attracted or repelled. Such phenomena are observed. The question of rotating bodies interaction was considered in detail by Etkin in [2, 3], where a theory that explains this phenomenon in other ways is also proposed.

Let us accentuate once again that effect of rotating discs attraction/repulsion should be the most manifested if the discs are **porous** or, more generally, discontinuous. Discontinuity can be created by nonplanar disk configuration. Exactly such discontinuity of disks was realized in Samokhvalov's experiments - see Chapter 5.1.

Finally, the effect of rotating disks attraction/repellency should be much greater in a vacuum, since gravitomagnetic induction is proportional to ξ gravitomagnetic permeability, which increases sharply with atmospheric pressure decrease - see Chapter 5.1.

3. Experiments

Based on the above, we can perform experiments that will allow to

- calculate the gravitomagnetic induction of various disks depending on rotation speed and pressure,
- calculate ξ gravitomagnetic permeability depending on pressure.

First of all, note that there is a wide variety of porous materials for porous discs production - see, for example, [4]. Wooden discs are also porous, and the most porous is the oak disc. Another way of porous discs production is to make a package of identical thin discs perforated with many holes. In a package such disks should be shifted relative to each other for some small angle. The porous disk, made in one or another way, becomes a constant **gravitomagnet** when rotating.

3.1. Gravitomagnetic induction measurement

Fig. 1 shows the measuring apparatus, where 1 - disk, 2 - electric motor, 3, 4 - tube, 5 - hinge, 6 - pump, 7 - tank, and 8 - water.

Disc 1, rotated by electric motor 2, is a gravitomagnet with B_g gravitomagnetic induction. Pump 6 pumps water 8 from the tank 7 through the tube 3, thereby creating J_g mass current.

Chapter 6.1. Gravitomagnetic induction detection

A gravitomagnetic Ampere force acts on a conductor-tube 3 with J_g mass current in a gravitomagnetic field with B_g gravitomagnetic induction (see (1.2.20) in SI system):

$$F_{ag} = \frac{1}{c} J_g B_g, \quad (9)$$

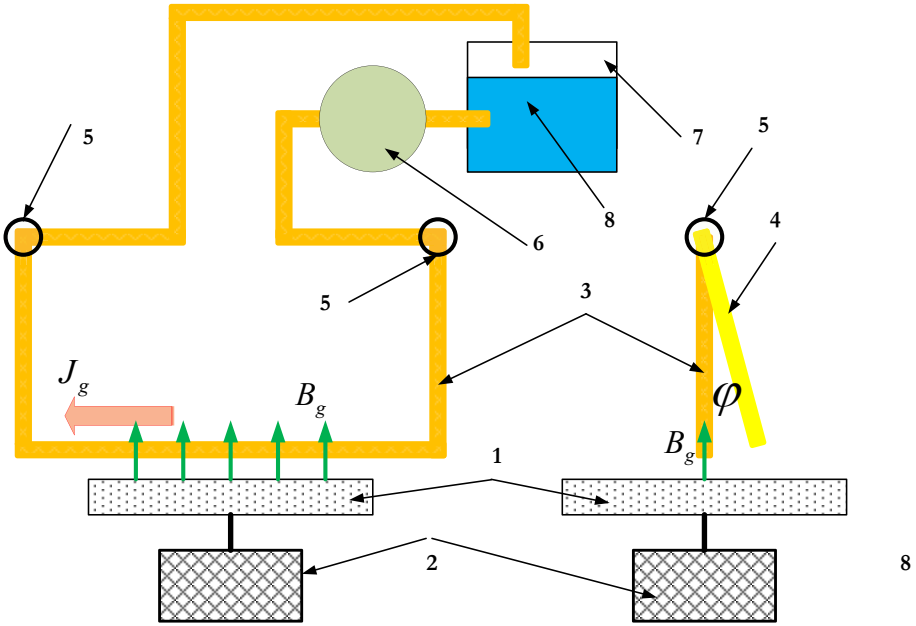


Fig. 1.

This force acts on the length of tube 3 located above the disk 1. Hinges 5 allow a tube 3 to slant off into position 4. φ deflection angle allows to determine F_{ag} force intensity.

J_g mass current in this experiment is also known. Therefore, F_{ag} force measured in such way allows finding the following gravitomagnetic induction

$$B_g = c \cdot F_{ag} / J_g, \quad (10)$$

3.2. Gravitational permeability measurement

Fig. 2 shows the measuring apparatus, where 1, 2 - disks, 3, 4 - electric motors, 5 - spring, 6 - housing.

Disc 1 with electric motor 3 is a gravitomagnet A, and disc 2 with electric motor 4 is a gravitomagnet B. Gravitomagnet A is fixed on the

bottom of housing 6, and gravitomagnet B is suspended on spring 5 to housing cover 6.

When switching-on the gravitomagnets they are attracted or repelled depending on disks rotation direction. The force of attraction/repellency is calculated depending on L length of spring 5 or Z distance between disks 1 and 2.

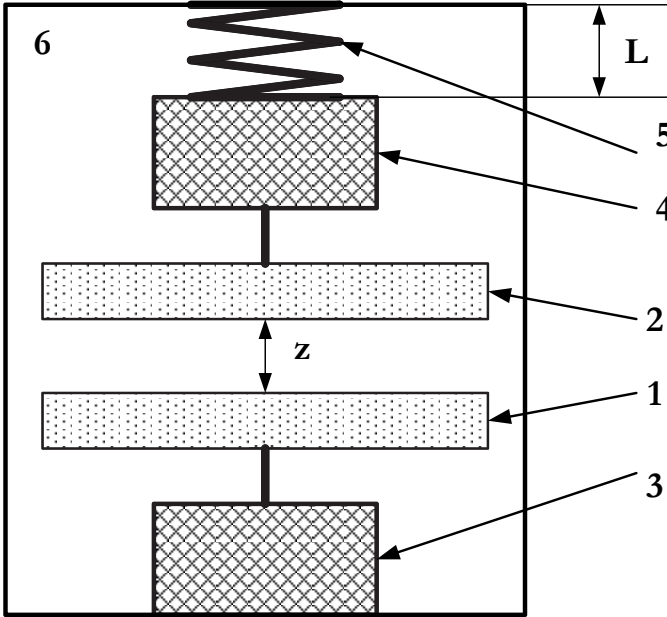


Fig. 2.

F force measured in this way is proportional to dB_g/dz derivative, i.e.

$$F(z) = k \frac{dB_g}{dz}, \quad (11)$$

where k is some coefficient. As B_g gravitomagnetic induction can be measured in experiment 3.1, then k coefficient can be found by the formula (11), i.e.

$$k = F(z) \Big/ \frac{dB_g}{dz}, \quad (12)$$

ξ gravitomagnetic permeability is proportional to B_g gravitomagnetic induction, i.e.

$$\xi = qB_g, \quad (13)$$

where q coefficient is determined by the disk size. For example, for the ring this coefficient can be found from (7). From (11, 13) it follows that

$$F(z) = kq \frac{d\xi(z)}{dz}, \quad (13a)$$

Consequently, the experiment will allow finding the dependence of

$$\xi(z) = \frac{1}{kq} \int_0^z F(z) \cdot dz. \quad (14)$$

An actual gravitational permeability at p given pressure is

$$\xi(p) = \lim_{z \rightarrow 0} \left(\frac{1}{kq} \int_0^z F(z) \cdot dz \right). \quad (15)$$

A gravitational permeability of vacuum is

$$\xi(0) = \lim_{p \rightarrow 0} (\xi(p)). \quad (16)$$

References

1. A. Eichenwald. Electricity, M.L. 1933, paragraph 282, <http://lib.izdatelstwo.com/Papers2/Eyhenvald.djvu>
2. V.A. Etkin. The question of the interaction of rotating bodies, <http://www.etkin.iri-as.org/napravlenn/06vzaimod/O%20vzaim%20vrash%20tel.pdf>
3. V.A. Etkin. On new types of interaction, <http://vixra.org/abs/1307.0149>.
4. S.V. Belov and others. Porous permeable materials. Directory. Moscow, ed. Metallurgy, 1987.

Chapter 6.2. Gravitational Wheel

Contents

1. Introduction \ 231
2. Schematic diagram \ 231
3. Experiment execution \ 233
4. Actual designs \ 234
5. Lorentz gravimagnetic force \ 236
6. Design \ 236
7. Mathematical model \ 238
8. Mathematical modeling \ 240

1. Introduction

In Chapter 3 it is proved that the source of gravitational forces can perform work and this doesn't contradict the physical laws. Many of long proposed designs can be explained from these positions. However, they are not continuously operating machines for the simple reason that incoming gravitational energy is less than friction forces work.

In Chapter 5.2, a substantiation of Aldo Costa's wheel performance and its calculation are given. The large dimensions of device, which Aldo Costa shows, are apparently explained by the size of switches - they are complex, and hence large. In addition, they are complex, and therefore require a constant fine adjustment, which complicates operation.

Below a much less complex and compact design is proposed.

2. Schematic diagram

Wheel schematic diagram can be represented in the form shown in Fig. 1. It is a tube in which the loads are moving. These loads are threaded on spokes, and these spokes are fixed on sleeve so that the angles between each pair of spokes are equal to each other. The tube has a slot that allows the spokes to rotate full-circle.

Lorentz forces arise between loads m_1 and m_2 , moving at different velocity full circle and along the "step". The resultant of these forces rotates the weight m_1 - see Fig. 2.

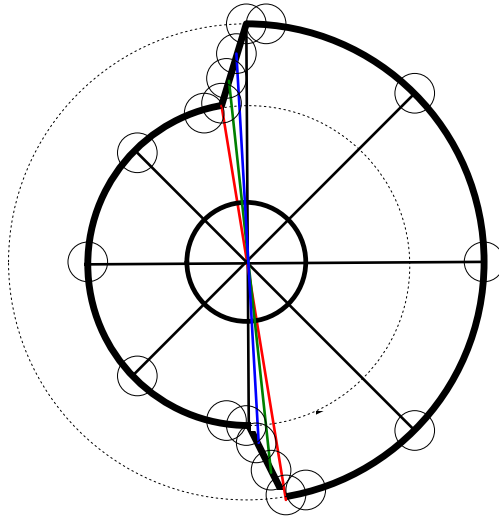


Fig. 1 (Aldo3.vsd (2)).

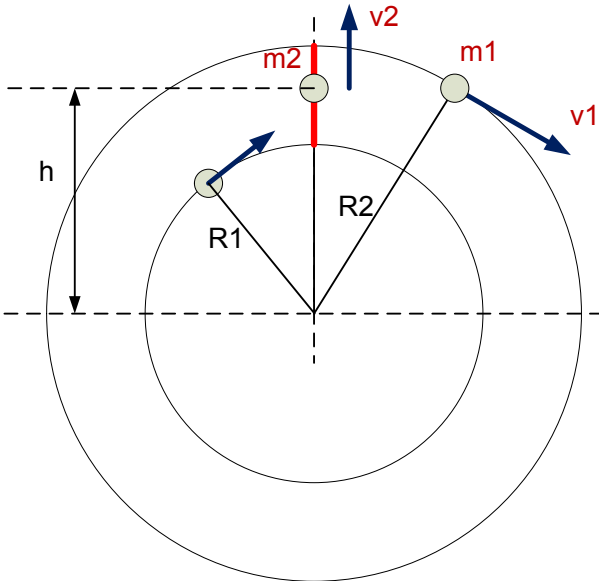


Fig. 2 (Aldo7.vsd).

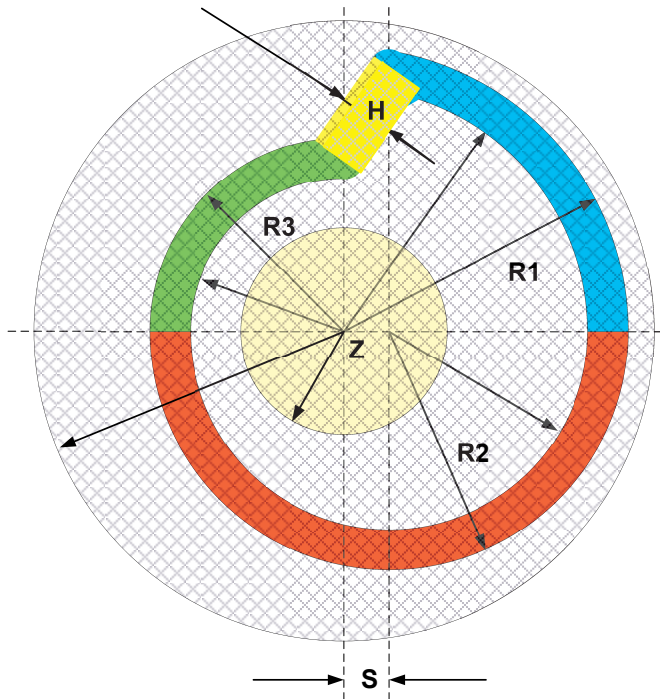


Fig. 3 (Aldo8.vsd).

Less complicated tube configuration is shown in more detail in Fig. 3. It can be seen that it consists of three circle parts and linear conjugation. This variant differs by the fact that there is no lower linear "jump" in it.

There are calculating formulas, but for their application it is necessary to perform, at least one experiment in order to obtain a reference point.

3. Experiment execution

Approximate design dimensions (in cm):

$$R1=100, R2=90, R1=80, H=5, S=5$$

Load weight is determined by the tube diameter

Number of spokes - maximum possible

Center of spokes rotation – p. Z

Rotation velocity - maximum permissible under strength conditions

Design should untwist by reversible machine of direct current in motor mode. After reaching a certain velocity, machine must switch to

generator mode and connect to electric load. The amount of kinetic energy E_1 accumulated by the time of switching (according to electrical engineering laws) can be determined by operation time in generator mode and load rate. The same amount can be determined based on rotation velocity by the time of switching (according to laws of motion) E_2 . If to neglect friction, then, according to energy conservation law, there must be $E_2 = E_1$. If, as a result of experiment it will be found that $E_2 < E_1$, then this will mean that an additional source of energy is available.

Certainly, the continuously operating machine cannot be created on the first try! But such measurements will allow understanding whether there is a hope. It should also be expected that the more this additional energy source will be stronger, the more high will be rotation velocity, what can also be checked with specified experiment organization.

It is important to note that the effect should increase many times in a vacuum (or just in a chamber with reduced pressure).

4. Actual designs

The tube is difficult to make. We can offer a different design - see Fig. 4.

The design is shown in Fig. 4. There are two boards with a slit (see the slit) as shown above in Fig. 3. Each of them has an inner part 2 and 4, in which the axis 5 rotates, and "suspended" part on the bearings of this axis. There is an outer part 1 and 3, covering a slit, and attached to general housing by the brackets 6 (eight skewed brackets 6 are shown in Fig.4). The boards are moved apart a distance of A (see clearance). Loads are the balls 7, through which a spoke 9 is threaded, fixed on axis 5. They can rotate around the spoke 9 and slide along it. Their diameter is $D > A$. Therefore, they do not fall between the boards, but slide along slit edges. Design sectional view on BB is shown below. The slit and brackets 6 are visible. The same sectional view with balls 7 is shown more below. A hole 8 for spoke 9 is shown on a ball.

A ball 7 on a spoke 9 rigidly fixed on the axis 5 is shown in the section. A hole 8 in which the spoke 9 slides can be seen.

Instead of boards the curved stripes attached to fixed spokes can be made.

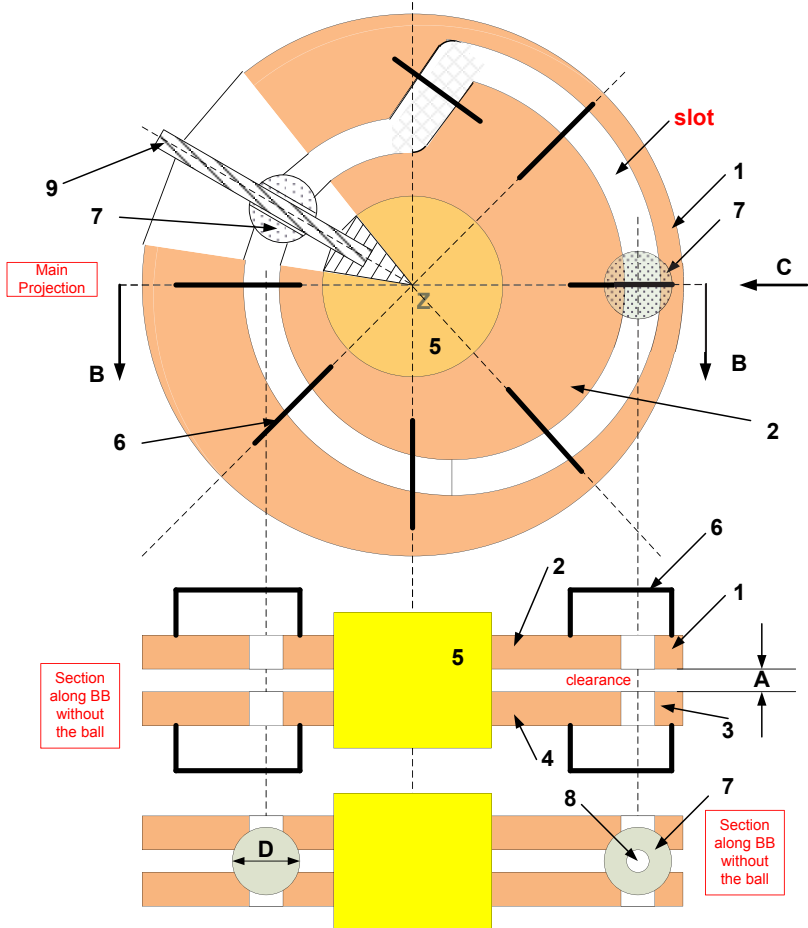


Fig. 4 (Aldo9.vsd).

Another variant of design is a strip, also of the shape shown in Fig. 3. The loads attached to spoke ends (also fixed on the sleeve). However, in this case the loads don't move over the spoke, and spokes move inside the sleeve (along its radius). Centrifugal forces press the loads to strip. In this case, they move as well as inside the tube. In order to reduce frictional forces, the loads are made in the form of a ball-bearing fixed at spoke's forked end.

A design calculation is considered below.

5. Lorentz gravimagnetic force

In Chapter 1 it is shown that Lorentz gravimagnetic force, acting from m_1 mass on m_2 mass, is determined by expression in the form (GHS and SI systems are used here) of

$$\overline{F}_{12} = \frac{k_g m_1 m_2}{r^3} \left[\overline{v}_2 \times \left[\overline{v}_1 \times \overline{r} \right] \right] \tag{1}$$

{ [dyne = g · cm \ sec²] in GHS; [N = kg · m \ sec²], in SI; 1 dyne = 10⁻⁵ N}, where

- $G \approx 7 \cdot 10^{-8} \left[\frac{\text{dyne} \cdot \text{cm}^2}{\text{g}^2} = \frac{\text{cm}^3}{\text{g} \cdot \text{sec}^2} \right] = 7 \cdot 10^{-11} \left[\frac{\text{N} \cdot \text{m}^2}{\text{kg}^2} = \frac{\text{m}^3}{\text{kg} \cdot \text{sec}^2} \right]$ is gravitational constant,
- $c \approx 3 \cdot 10^{10}$ [cm/sek] = $3 \cdot 10^8$ [m/sec] is speed of light in a vacuum,
- ξ is gravimagnetic permeability of the medium,
- \overline{r} is a vector directed from point m_1 to point m_2 ,
- $\overline{v}_1, \overline{v}_2$ is velocities of mass m_1 and m_2 accordingly,
- coefficient

$$k_g = \frac{\xi G}{c^2} \left[\frac{\text{cm}}{\text{g}} \right] \approx 10^{-27} \xi \left[\frac{\text{m}}{\text{kg}} \right]. \tag{2}$$

It is important to note that the effects described in Samohvalov's experiments (see Chapter 5.1) are so significant that in order to explain them within Maxwell-like gravity equations, it is necessary to introduce ξ environment gravimagnetic permeability coefficient (similar to μ environment magnetic permeability coefficient in electromagnetism). However, ξ coefficient value based on these experiments can be estimated very approximately.

6. Design

The wheel is shown in Fig. 3. It is a tube in which the loads are moving. These loads are threaded on spokes, and these spokes are fixed on sleeve so that the angles between each pair of spokes are equal to each other. The tube has some slots that allow the spokes to rotate full-circle.

Upper part of this wheel is shown in Fig. 5, and Fig. 6 shows a part of this fragment.

Masses in this construction act on each other by Lorentz gravimagnetic forces. Force interaction of rotating masses is such that the forces are directed perpendicular to velocity vector. Therefore, masses moving full-circle prove the forces directed along the radius. These forces don't influence on rotation velocity. An exception is a case when mass jumps upward the step. The forces acting on it are perpendicular to step and directly influence on rotation velocity.

As jump is carried out at a high velocity in a short time, other masses have no time to significantly change their position on a circle. Therefore, it can be assumed (in calculations) that the mass stepping up experiences the forces from two other masses shifted as regard to given mass for φ angle and which don't change their position - see Fig. 5. In this case, the force pushing it perpendicular to step can be ignored.

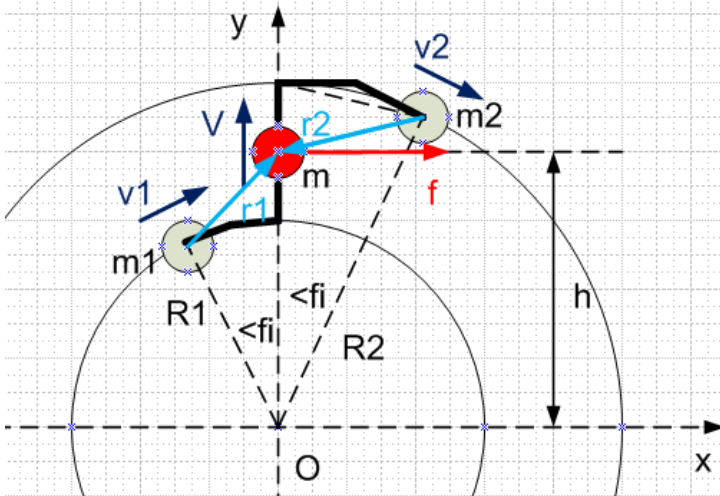


Fig. 5 (AldoMy1.vsd)

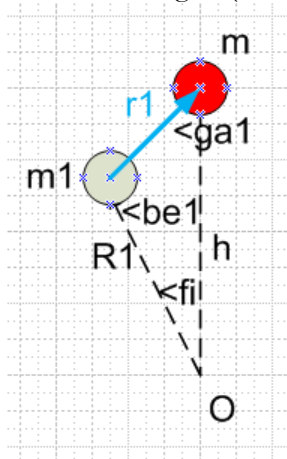


Fig. 6 (AldoMy2.vsd)

7. Mathematical model

The force acting from m_1 mass on m mass is determined by the formula (1), which in this case takes the form of

$$\overline{F}_1 = \frac{k_g m^2}{|r_1|^3} \overline{V} \times \left[\overline{v}_1 \times \overline{r}_1 \right], \quad (3)$$

Here (see also Fig. 6 (AldoMy2.vsd))

$$v_1 = \omega R_1, \quad (4)$$

$$v_{1x} = v_1 \cos(\varphi), \quad (5)$$

$$v_{1y} = v_1 \sin(\varphi), \quad (6)$$

$$|r_1| = \sqrt{h^2 + R_1^2 - 2hR_1 \cos(\varphi)}, \quad (7)$$

$$r_{1x} = r_1 \sin(\gamma_1) \quad (8)$$

$$r_{1y} = h - R_1 \cos(\varphi_1) \quad (9)$$

$$\cos(\beta_1) = \frac{-R_1^2 + r_1^2 + h^2}{2R_1 r_1}, \quad (10)$$

$$\cos(\gamma_1) = \frac{R_1^2 + r_1^2 - h^2}{2r_1 h}. \quad (11)$$

Let us select in formula (3) the following expression

$$\overline{f}_1 = \overline{V} \times \left[\overline{v}_1 \times \overline{r}_1 \right], \quad (12)$$

In the right Cartesian coordinate system, this expression takes the form of

$$\overline{f}_1 = \begin{bmatrix} V_y (v_{1x} r_{1y} - v_{1y} r_{1x}) - V_z (v_{1z} r_{1x} - v_{1x} r_{1z}) \\ V_z (v_{1y} r_{1z} - v_{1z} r_{1y}) - V_x (v_{1x} r_{1y} - v_{1y} r_{1x}) \\ V_x (v_{1z} r_{1x} - v_{1x} r_{1z}) - V_y (v_{1y} r_{1z} - v_{1z} r_{1y}) \end{bmatrix}.$$

As loads move in the same plane, then

$$\overline{f}_1 = \begin{bmatrix} V (v_{1x} r_{1y} - v_{1y} r_{1x}) \\ 0 \\ 0 \end{bmatrix}$$

or

$$\overline{f}_1 = f_{1x} = V (v_{1x} r_{1y} - v_{1y} r_{1x}). \quad (13)$$

We denote the force

$$f_{10} = f_{1x} / (r_1)^3. \quad (14)$$

In order to determine the velocity, let us find jump duration

$$\Delta t = \Delta \varphi / \omega, \quad (15)$$

where $\Delta \varphi \ll \varphi$ is a step slope angle. Body moves along the step with a length of $(R_2 - R_1)$ with the following constant acceleration

$$a = \frac{2(R_2 - R_1)}{\Delta t^2}. \quad (16)$$

Consequently, body velocity at h height is equal to

$$V = \sqrt{2(h - R_1)a}. \quad (17)$$

The force (14) at (17) is calculated in program `aldonew2.m`. On dh length element dh the force $(f_{10} \cdot dh)$, creating the torque $(h \cdot f_{10} \cdot dh)$ acts. When turning to angle $\Delta \varphi$ this torque does the work $(\Delta \varphi \cdot h \cdot f_{10} \cdot dh)$. Consequently, the total force work acting on body during the movement along the step is

$$A_1 = \Delta \varphi \int_{R_1}^{R_2} (f_{10} \cdot h \cdot dh). \quad (18)$$

Similarly, A_2 work of f_{20} force is calculated on the same step. Works A_1 , A_2 , $A = (A_1 + A_2)$ are calculated in program `aldonew3.m`.

Considering (3) together with (14), we note that actual work differs from calculated values by coefficient

$$k_a = k_g m^2. \quad (20)$$

Therefore, the total work of these forces for all loads per revolution is

$$A_o = k_a N (A_1 + A_2). \quad (21)$$

Consequently, device power is

$$P = A_o \omega = k_a N \omega (A_1 + A_2). \quad (22)$$

k_a coefficient in GHS system, as follows from (2) has the following dimension of work

$$k_a = k_g m^2 = 10^{-28} \xi \cdot m^2 [\text{g} \cdot \text{cm}]. \quad (23)$$

and in SI system it is

$$k_a = k_g m^2 = 10^{-27} \xi \cdot m^2 [\text{kg} \cdot \text{m}]. \quad (24)$$

In this case, A_1 , A_2 , $A = (A_1 + A_2)$ values are dimensionless, but when calculating them, the lengths and velocities must be represented in the same measurement system.

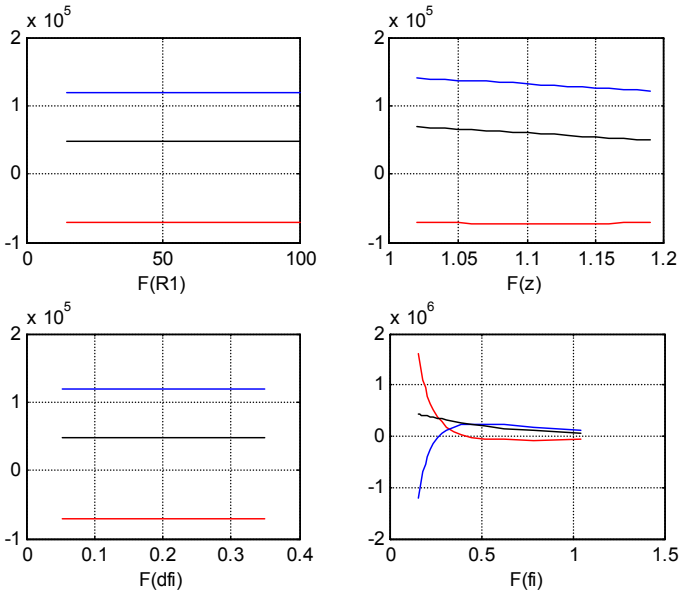


Fig. 7 (aldonew.m)

8. Mathematical modeling

Modeling is performed in program **aldonew3.m**.

Example 1.

Let us estimate the value of ξ coefficient. Based on modeling it follows that $A = (A_1 + A_2) \approx 10^5$ when $N = 6$ and $\omega = 100$. In order that power is equal to 1000 W, a coefficient should be the following

$$k_a = \frac{P}{A \cdot N \omega} = \frac{1000}{6 \cdot 10^5 \cdot 100} \approx 2 \cdot 10^{-4}$$

When $m = 1 \text{ kg}$ из (24) we find: $\xi \approx 2 \cdot 10^{23}$. This value is comparable to that obtained in Tolchin's inertoid analysis - see Chapter 5.3. With this ξ meaning, an assumption of proposed design operability is justified.

In order to increase design economic feasibility, it should be placed in a vacuum chamber. Samokhvalov's experiments (see Chapter 5.1) show that in a vacuum $\xi \approx 2 \cdot 10^{10}$

Example 2.

For Aldo wheel the calculation is carried out in program **aldonew.m**. There when

```
N=236;  
R1=9;  
z=1.05;  
fi=2*pi/N;  
dfi=fi/10;  
omega=0.1;  
m=100;  
ksi=10^25;
```

obtained

```
F=1.6  
ka=10^-27*ksi*m^2=1  
P=ka*N*F/omega=3786 Watt
```

Chapter 6.3. Gravitational waves detection

Contents

1. Introduction \ 242
 2. Lorentz force analogue in gravitational field \ 242
 3. Gravitational radiation measurement \ 243
- Appendix 1. The rate of copper atoms thermal motion \ 244
References \ 251

1. Introduction

Below the costly gravitational radiation detection experiments, which have no effect until now are shown. It is shown that known theories predict the possibility of Lorentz gravitational forces finding on the Earth. It points to known experiments in which these forces are discovered. Based on this the assumption that gravitational radiation of space objects can be detected on the Earth, as Lorentz gravitational forces manifestation is made. The construction of gravitational antenna designed for gravitational waves detection is proposed. It is shown that such a construction is much simpler than that of known gravitational antennas and telescopes.

2. Lorentz force analogue in gravitational field

Chapter 1 shows that it is possible to use Maxwell's equations of gravitomagnetism or Maxwell-like gravitational equations in the weak gravitational field of the Earth for describing the gravitational interactions. This means that there are gravitational waves having a gravitoelectric component with E_g strength and a gravitomagnetic component with B_g induction. A gravitomagnetic Lorentz force (known Lorentz force analogue) of type (in CGS system) acts on the mass m moving in magnetic field with a velocity of v .

$$F_g = \xi \frac{m}{c} [\mathbf{v} \times \mathbf{B}_g] \quad (1)$$

where ξ is a gravitational permeability, and also in vacuum.

$$\xi \approx 10^{12}. \quad (2)$$

Thus, gravitational waves having a gravitoelectric component with E_g strength and a gravitomagnetic component with B_g induction exist in a weak gravitational field of the Earth. These waves can be formed by uneven mass currents (for example, turbulent liquid flows) and act on moving masses by Lorentz forces.

3. Gravitational radiation measurement

The costly gravitational radiation detection experiments, which have no effect until now are known [1]. Detection is based on the fact that gravitational waves must change the body size or distance between two proofmasses.

In the first method, the so-called gravitational antenna - a metal cylinder with a weight of about 2 tons and a length of about 2 meters, suspended so that it can oscillate under weak forces influences is produced. Cylinder length is measured by piezosensors with a sensitivity of 10^{-16} m. Cylinder length varies with a frequency of gravitational wave and, if this frequency coincides with fundamental frequency of gravitational antenna oscillations, then there is a hope to detect this wave. The measurements are refracted by thermal noise and therefore gravitational antenna is installed in a vacuum chamber with cooling up to several degrees.

In the second method, the so-called *gravitational telescope* is a vacuum tunnel with a length of about 2 km. Two proofmasses are placed in this tunnel, and the distance between them is measured by laser interferometer. This distance varies with a frequency of gravitational wave and there is a hope to detect this wave.

Based on above-mentioned, another design of gravitational antenna can be proposed. A massive body is placed in heat-insulated chamber (as in the first method). However, the chamber doesn't get cool. Moreover, a heater must be built in the body of gravitational antenna.

Atoms of our antenna make thermal vibrations. Below in Appendix 2 it is shown that the average velocity of atomic motion in such vibrations at room temperature has, for example, for copper a value of $V_T \approx 3000 \text{ cm/sec}$. Let us denote the atom velocity vector as $\overline{V_T}$ and we will hereafter call it as "thermal" velocity vector. It can also be assumed

that thermal motion takes place under the influence of a certain "thermal" force, which is $\overline{F_T}$ vector, that (as shown in Appendix 2) varies with a frequency of $f \approx 5 \cdot 10^{12} \text{ Hz}$ and with a period of $\tau \approx 0.2 \cdot 10^{-12} \text{ sec.}$ changes direction to the opposite. Under the influence of Lorentz gravitational force $\overline{F_g} \equiv \overline{V_T} \times \overline{B_g}$ such atoms must move on $\overline{V_g}$ "gravitational" velocity vector, directed along $\overline{F_g}$ vector. Thus, the total force acting on an atom is $\overline{F} = \overline{F_T} + \overline{F_g}$. This force doesn't change atom thermal energy (since Lorentz force doesn't perform an operation).

When there is no Lorentz force, thermal radiation of our antenna spreads uniformly in all directions - we can say that in this case antenna directional pattern is a sphere. When Lorentz force appears, the radiation of our antenna becomes asymmetric and directional pattern becomes an ellipsoid, the major axis of which is directed on vector of $\overline{B_g}$ magnetogravitational induction.

Consequently, antenna directional pattern must be deformed under $\overline{B_g}$ induction with a frequency of gravitational wave of f_g , and deformation limit should be determined by B_g induction value. This phenomenon can be detected, as at the present time very sensitive meters of terahertz radiation are available [2].

So, the proposed gravitational antenna should be a solid body (maybe with internal well-stabilized heater), placed in thermally insulated chamber and surrounded by receivers of terahertz radiation. An additional heater is required in order to increase thermal velocity and Lorentz force depending on it, and, eventually, gravitational antenna sensitivity.

Appendix 1. The rate of copper atoms thermal motion

At first, let us consider some constants for copper [3]:

$C_V = 0,385 \text{ kJ/kg} \cdot \text{K}$ is the heat capacity,

$\eta = 16.7 \text{ K}^{-1}$ is coefficient of linear thermal expansion,

$\rho = 9 \text{ g/cm}^3$ is the density,

$m = 10^{-22} \text{ g}$ is mass of the atom,

$a = 2.3 \cdot 10^{-8} \text{ cm}$ is interatomic distance,

$\chi = 7.3 \cdot 10^{-13}$ is compressibility,

$\alpha \approx 3a/\chi = 10^5$ is coefficient of elasticity,

$s_o \approx \sqrt{\frac{kT}{\alpha}} = 0.4 \cdot 10^{-10} \sqrt{T} = 6 \cdot 10^{-10} \text{ cm}$ is the average value of the amplitude of the oscillations of the atom,

$\omega \approx \sqrt{\frac{\alpha}{m}} = \sqrt{\frac{3a}{\chi m}} = 3 \cdot 10^{13} \text{ rad/sec}$ is frequency of the vibrations of the atoms,

$f = \frac{\omega}{2\pi} \approx 4.8 \cdot 10^{12} \text{ sec}^{-1}$ is frequency of vibrations of atoms,

$\lambda = c/f \approx 0.06 \text{ MM}$ is wavelength of thermal terahertz radiation,

$\tau = 1/f \approx 0.2 \cdot 10^{-12} \text{ sec}$ is period of oscillations of the atoms.

Depending on temperature, the average rate of copper atom thermal motions is determined by formula of the following type

$$V_T = \frac{s_o}{\tau} \approx 200 \sqrt{T} \text{ cm/cek}.$$

In particular, when $T = 230 \text{ K}$ we obtain: $V_T = 3000 \text{ sm/sec}$.

References

1. The detector of gravitational waves. Wikipedia.
2. Terahertz radiation. Wikipedia.
3. Berkeley's course of physics. Volume 5. F. Reif. Statistical physics, p. 243; http://alexandr4784.narod.ru/bkurs5/bkurs5_gl6_7.pdf
4. Khmelnik S.I. Detection of gravitational waves. The Papers of independent Authors, ISSN 2225-6717, № 20, 2012.

Chapter 6.4. The theory of dowsing

The magic wand works only in a sensitive hand.

I.V. Goethe

Contents

1. Introduction \ 246
 2. Prerequisites \ 246
 3. Gravitational waves \ 247
 4. The mechanism of system operation \ 248
 5. Some quantitative estim \ 249
 6. Possible experiments \ 251
- References \ 252

1. Introduction

A dowsing physical mechanism is described and an attempt to explain it using the theory of gravitoelectromagnetism is made.

Dowsing is a highly diverse field of human activity. But here the author will analyze only the search for flow water. The reader will not see here a review of publications in this field - their fulness. Science didn't find an explanation for this phenomenon - only general ideas about how it can work are available. These representations are a little supplement what Goethe said, but they should be formulated more rigorously for a reasoned presentation. So, the mechanism of system operation can be the following:

1. flowing water emits some waves (electromagnetic, gravitational, ...),
2. these waves generate some currents in a person,
3. these currents are amplified and transmitted to a dowsing rod in a body sensitive to them;
4. the currents of dowsing rods interact with radiation (see par. 1), which causes the dowsing rod movement.

2. Prerequisites

A dowsing rod (or metal frame - hereinafter such a note will not be repeated) in the hands of a person standing under the power transmission line (PTL), rotates. An explanation can be as follows. PTL is

a source of alternating magnetic field, a magnetic induction vector of which is directed along the earth's surface. The person with a dowsing rod forms a closed current-conducting circuit "a dowsing rod (fresh, current-conducting)" - "a person (in whose body the electrolytic liquids flow - blood, lymph)" - "earth" - "a capacitance between the dowsing rod and earth" for an alternating current. An alternating magnetic field, penetrating a current-conducting circuit, brings it in rotation. An arrangement of a single-phase asynchronous motor is based exactly on this principle. In order to start the operation of such a motor, a starting torque must be applied to it. In our case, an involuntary movement of the hand can be the starting torque.

A current-conducting circuit resistance under weak magnetic field must be small. This can be achieved by the fact that a circuit containing the inductance and capacitance is tuned to resonance with a frequency of alternating magnetic field. Another way could lie in the fact that an element is included in a circuit which converts a magnetic alternating induction into variable electromotive force. It is not known which of these ways is performed in the human body. But the fact is that a dowsing rod rotates under PTL and, therefore, the person (at least some of people) creates a circuit of our "asynchronous motor" rotating under the influence of a weak alternating magnetic field.

3. Gravitational waves

In Chapter 1 it is shown that a gravity is described by Maxwell-like equations (hereinafter, MLG-equations) at weak gravitational fields and low velocities. Exactly such conditions exist on Earth. Consequently, the gravitational effects similar to electromagnetic effects should be observed. In Chapter 1 it is shown that the strength of these effects is determined by gravitomagnetic permeability coefficient. It has a very large value in a vacuum, but is practically equal to zero under air pressure. The main result is that a time-varying particles flow with a mass, is an alternating mass current, which excites gravitomagnetic waves. These waves are very rapidly damped out in the air.

However, if gravitomagnetic waves are damped out, then their energy must flow into another energy. The author suggests that this energy is the energy of a standing magnetic wave. It should be noted that such waves (arisen for another reason) were observed in experiments [1]. In [2] it is shown that such waves can exist for a long time, because there is an exchange of thermal and magnetic energies in the area of this wave existence in the air (similar to magnetic energy conversion into electric energy in a traveling electromagnetic wave). A reverse conversion of

thermal energy into magnetic energy is also available. In addition, this area of existence expands. This process is accompanied by the temperature decrease of the wave region, which is also observed experimentally in [1] and is explained in [2]. Let us also note that a standing wave can exist even after the source of its generation disappearance. This probably explains the fact why some dowzers can detect the regions where such a source was available.

So, a variable mass current excites a gravitomagnetic wave, which is converted into a magnetic standing wave in the air. Both the current and gravitomagnetic standing wave have the same frequency.

A magnetic alternating induction of a standing wave affects the circuit of "asynchronous motor" described above, which rotates the dowsing rod.

4. The mechanism of system operation

Based on it, the following explanation of the mechanism of system operation is proposed - see Fig. 1.

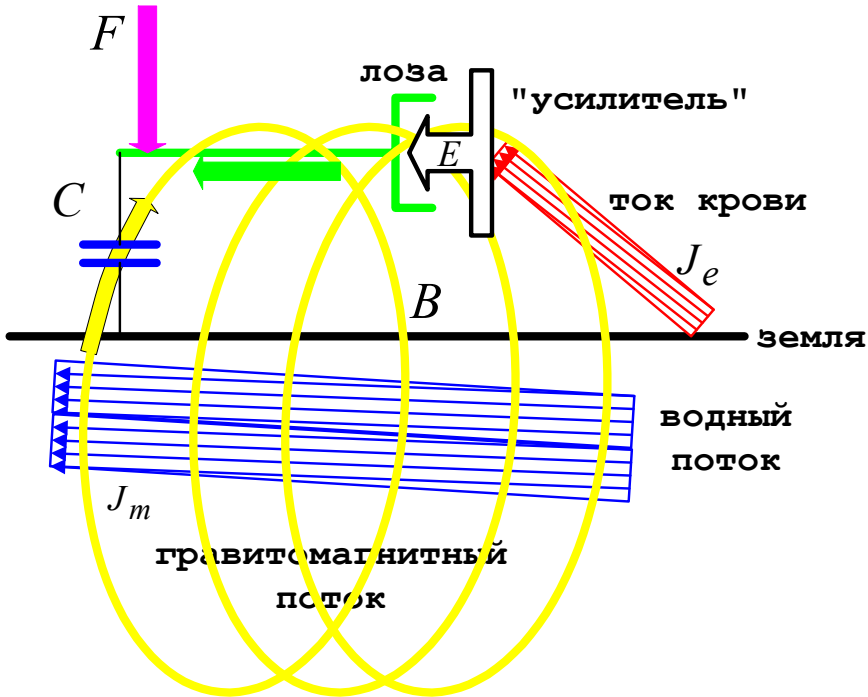


Fig. 1.

Underground water flow is a variable mass current. But this statement is valid only if this flow is turbulent – see Chapter 4.9. Thus, a turbulent water flow is equivalent to J_m variable mass current with a certain f base frequency. A laminar flow is not a variable mass current. A turbulence occurs only at significant fluid flow rates. The well-known Sydney dowsing testing experiment of 1980 [3] was unsuccessful, perhaps because the water velocity in pipes was insufficient to excite the mass current.

J_m variable mass current generates Φ_g alternating gravitomagnetic flow with the same f frequency. The water flow emits exactly this current. During Φ_g gravitomagnetic flow expanding in the air, it forms a magnetic standing wave with B induction and transfers its energy to it. This B induction interacts with K current-conducting circuit "dowsing rod" - "blood flow" - "earth" - " C capacitance". J_e induction electric current arises in K circuit. J_e current is imposed on the principle fluids current flow in the human body in the form of a weak variable component. Some people in their bodies has, apparently, E "amplifier" of such current flows, the input signal of which is this current itself or B induction. The author must directly state that he has no idea how this "amplifier" can be arranged. Besides, the body tunes into resonance with f frequency of B induction, changing its inductance and capacitance in such a way that K circuit resonant frequency becomes equal to f . As a result, J_e current acquires a sufficient value for A "asynchronous motor" effect demonstration - F force of K "asynchronous motor" arises, which induces the dowsing rod rotation in a vertical direction. Thus, a person generate the energy for a dowsing rod rotation.

So, the person is a receiver of induction, created by water turbulent flow, an amplifier and a converter of the currents into rotating force directed by it in the system under consideration.

5. Some quantitative estimations

It is known that the density of electromagnetic wave energy (hereinafter the GHS system is used) is

$$W = \frac{B^2}{8\pi} \left[\frac{\text{g}}{\text{cm} \cdot \text{sec}^2} \right], \quad (1)$$

where B - magnetic induction of this wave. In Chapter 1, it is shown that the density of gravitoelectromagnetic wave energy is

$$W_g = \frac{(\xi B_g)}{8\pi G}, \quad (2)$$

where

B_g is gravitomagnetic induction of this wave $\left[\frac{\text{cm}}{\text{sec}^2} \right]$;

G is gravitational constant, $G \approx 7 \cdot 10^{-8} \left[\frac{\text{cm}^3}{\text{g} \cdot \text{sec}^2} \right]$;

ξ is gravity permeability of vacuum.

If a gravitomagnetic wave transfers its energy to a standing magnetic wave (as specified above), then in accordance with the energy conservation law it follows that

$$W = W_g. \quad (3)$$

From (1-3) we find

$$B = \frac{\xi B_g}{\sqrt{G}} \left[\frac{1}{\text{sec}} \sqrt{\frac{\text{g}}{\text{cm}}} \right]. \quad (4)$$

A gravitational permeability of vacuum, rather than air is considered here, as gravitomagnetic induction converts into magnetic induction with no expansion.

B_g gravitomagnetic induction of a continued conductor with mass current $J_g \left[\frac{\text{g}}{\text{cm}} \right]$ (which is the turbulent water flow) is determined by the following formula (see Chapter 1)

$$B_g = 2GJ_g / (ch), \quad (5)$$

where h - distance from the flow to induction measuring point (in our case - the distance from the flow to dowsing rod). Combining (4, 5), we obtain:

$$B = 2\xi\sqrt{G}J_g / (ch). \quad (6)$$

or

$$B = \frac{2\xi\sqrt{G}}{c} \cdot \frac{J_g}{h} \approx \frac{2 \cdot \xi \cdot \sqrt{7 \cdot 10^{-8}}}{3 \cdot 10^{10}} \cdot \frac{J_g}{h} \approx 2 \cdot \xi \cdot 10^{-14} \frac{J_g}{h}. \quad (7)$$

Let us now find J_g mass current. It is determined by the formula

$$J_g = \alpha S \rho v [g / sec], \quad (8)$$

where

$v [cm \cdot sec^{-1}]$ - water flow rate;

$\rho \approx 1 [g \cdot cm^{-3}]$ - water density;

$S [cm^2]$ - water flow area;

α - coefficient which indicates what turbulent flow oscillates; we will accept $\alpha \approx 0.1$ for further estimations.

Thus, for water

$$J_g = 0.1 S v [g \setminus sec], \quad (9)$$

Combining (7, 9) we finally find the magnetic induction, generated by the turbulent water flow:

$$B \approx 2 \cdot 10^{-15} \cdot \frac{\xi \cdot S \cdot v}{h} [Gs]. \quad (10)$$

Example. In Chapter 1 a rough estimate of $\xi \approx 10^{12}$ vacuum gravitational permeability is given. Let us suppose, further, that $S = 5 [cm^2]$, $v = 10 [cm \cdot sec^{-1}]$, $h = 200 [cm]$. Then, $J_g = 1000 [g \setminus sec]$ and a magnetic alternating induction amplitude is $B \approx 2 \cdot 10^{-15} \cdot 10^{12} \cdot \frac{5 \cdot 10}{200} \approx 10^{-3} [Gs]$. A magnetic induction under PTL also has $B \approx 10^{-3} [Gs]$ size of order. A dowsing rod rotates under the power transmission line. Consequently, $B \approx 10^{-3} [Gs]$ induction obtained in the example can be detected by means of the dowsing rod.

6. Possible experiments

The proposed hypothesis can be proved experimentally. With a good tool base and the experimentator's ability, J_e current, B induction, f frequency and F force can be detected and measured. S , v , h slow characteristics can be simply measured. It is important to note that S , v must satisfy Reynolds criterion for turbulence occurrence. It is known [4] that this condition for the round pipe has the form of

$$Re = Dv / \eta, \quad (12)$$

where D - pipe diameter, η - kinematic viscosity coefficient. For water $\eta \approx 0.01 cm^2/sec$ [4]. A turbulence occurs when Reynolds number is $Re > 2300$. Let us suppose, for example, that $D = 2.5 cm$ and

$S = 5\text{cm}^2$. In this case, from (12), we find $v = 10$ cm/sec velocity of the turbulent flow.

References

1. Roshchin V.V., Godin S. M. Experimental Investigation of Physical Effects in Dynamic Magnetic System. Letters to Journal of Theoretical Physics, 2000, volume 26, iss. 24_(in Russian).
<http://www.ioffe.rssi.ru/journals/pjtf/2000/24/p70-75.pdf>
2. Khmelnik S.I. Energy Processes in Fuel-free Electromagnetic Generators. Publisher by "MiC", printed in USA, Lulu Inc., ID 10292524, Израиль, 2011, Fourth Edition, ISBN 978-1-257-05555-5.
3. Dowsing. Wikipedia.
4. Vilner J.M. and other. Reference manual for hydraulics, hydraulic machines and hydraulic drives, ed. "High School", 1976.

Chapter 6.5. Projects of experiments, considered in previous chapters

1. The lifting force acts on a tubular ring with pulsating mass current, located above the massive plane - see Section 3.1 in Chapter 5.7.
2. The lifting force acts on a massive plane 1 located above another massive plane 2, if plane 2 is exposed to radiation from below by intensive sound wave - see Section 3.2 in Chapter 5.7.
3. Detection of the physical mechanism of dowsing based on gravitoelectromagnetism - see Section 6 in Chapter 6.4.
4. Gravitational waves detection – see Chapter 6.3.

